



HAL
open science

Intérêt du facteur Willebrand comme biomarqueur ou cible thérapeutique : nouveaux concepts dans l'assistance circulatoire et l'infection à COVID-19

Antoine Rauch

► **To cite this version:**

Antoine Rauch. Intérêt du facteur Willebrand comme biomarqueur ou cible thérapeutique : nouveaux concepts dans l'assistance circulatoire et l'infection à COVID-19. Sciences du Vivant [q-bio]. Université Lille, 2021. tel-04467340

HAL Id: tel-04467340

<https://inserm.hal.science/tel-04467340>

Submitted on 20 Feb 2024

HAL is a multi-disciplinary open access archive for the deposit and dissemination of scientific research documents, whether they are published or not. The documents may come from teaching and research institutions in France or abroad, or from public or private research centers.

L'archive ouverte pluridisciplinaire **HAL**, est destinée au dépôt et à la diffusion de documents scientifiques de niveau recherche, publiés ou non, émanant des établissements d'enseignement et de recherche français ou étrangers, des laboratoires publics ou privés.



HABILITATION A DIRIGER DES RECHERCHES

Intérêt du facteur Willebrand comme biomarqueur ou cible thérapeutique :
nouveaux concepts dans les cardiopathies à forces de cisaillement élevées
et la COVID-19

soutenue le 15 juin 2021

Dr Antoine RAUCH

MCU-PH en Hématologie

Unité de recherche : UMR 1011 INSERM, équipe 2,

Etablissement de soutenance : Université de Lille, Ecole doctorale Biologie Santé (446)

Garant : Pr Sophie Susen (CHU Lille, INSERM U1011)

Président du jury : Pr Bart Staels (INSERM U1011)

Rapporteurs :

Pr Philippe Vermersch (CHU Lille, Inserm U1172, Université de Lille)

Pr Chloé James (CHU Bordeaux, INSERM U1034)

Dr Aurélien Lebreton (CHU Clermont-Ferrand, INRA, Unité de Nutrition Humaine
Université Clermont Auvergne)

Membres du jury :

Pr Eric Kipnis (CHU Lille, U1019-UMR9017)

Pr Pierre-Emmanuel Morange (CHU Marseille, INSERM 1263)

Pr Eric Van Belle (CHU Lille, INSERM U1011)

Remerciements

Cette Habilitation à Diriger les Recherches est l'occasion de remercier les nombreuses personnes qui m'ont permis de présenter aujourd'hui ces travaux et perspectives.

Je souhaiterais tout d'abord remercier le Pr Sophie Susen et le Pr Eric Van Belle pour m'avoir accueilli au sein de leur équipe et la qualité de leur encadrement. Merci également aux autres membres de l'équipe 2 en particulier à Annabelle Dupont, Delphine Corseaux, Mickaël Rosa avec qui j'ai pris beaucoup de plaisir à travailler y compris sur la COVID-19.

Je remercie également nos amis de l'U1176 : Cécile Denis et Peter Lenting de m'avoir accueilli au sein de leur laboratoire lors de ma thèse et de leur engagement dans les différentes collaborations qui ont suivies, ainsi que Caterina Casari et Olivier Christophe.

Merci à mes collègues du service d'Hémostase clinique de m'avoir permis de mener de front mes projets de recherche et mon activité médicale ainsi qu'aux biologistes, techniciens et attachés de recherche clinique qui se sont impliqués dans ces différents projets en particulier Emmanuelle Jeanpierre, Claudine Caron, Bertrand et Florence Vaast, Alexandre Ung , Sylvie Hermoire. Bénédicte Pradines et Laureline Bourgeois.

Merci au Pr Alain Duhamel et au Dr Julien Labreuche pour leur temps et leur aide précieuse pour le montage des projets et le traitement statistique des données.

Je terminerai en remerciant l'ensemble des étudiants qui ont permis de faire avancer ces projets notamment Flavien Vincent et Maximilien Desvages qui se sont pris au jeu et avec qui j'aurai beaucoup de plaisir à continuer à travailler.

Sommaire

Curriculum vitae.....	4
Exposé des travaux de recherche.....	8
Travaux de thèse d'Université	11
Travaux post-doctoraux	21
Recherche clinique	35
Activités d'encadrement	39
Perspectives de recherche	40
Liste des publications	48
Tirés à part des principales publications	51

Curriculum vitae

Antoine Rauch, 40 ans (31/07/1980)

Pacsé, 3 enfants

Adresse Professionnelle :

Service d'Hémostase clinique

4^e étage, aile Est, Institut Cardio Pneumologique, CHU Lille

Boulevard du Professeur Jules Leclercq - 59037 Lille Cedex

Tél. : 03 20 44 48 42

antoine.rauch@chru.lille.fr

Numéro d'ordre : 59/22104

RPPS : 10100416030

TITRE ET FONCTIONS

Titres hospitaliers et universitaires

Au sein du Laboratoire d'hématologie, CHU Lille, Université de Lille, labellisé Centre de Ressources et de Compétences Maladies Hémostatiques Constitutionnelles et Centre de Référence Maladie de Willebrand au sein de la filière Maladies Hémostatiques (MHEMO)

- | | |
|-------------------------------------|-----------|
| - MCU-PH | 2017- |
| - Praticien Hospitalier contractuel | 2015-2017 |
| - Assistant Hospitalo-Universitaire | 2012-2015 |
| - Interne en Biologie médicale | 2007-2012 |

Diplômes universitaires

- | | |
|--|------|
| - D.U. enseignement et pédagogie par la simulation en santé | 2018 |
| - Thèse d'université (Ecole doctorale Biologie et Santé, Université Lille 2) | 2014 |
| - D.E.S.C d'Hémobiologie Transfusion (Faculté de Médecine Waremburg, Université Lille 2) | 2013 |
| - D.E.S. de Biologie Médicale (Faculté de Médecine Waremburg, Université Lille 2) | 2012 |
| - Doctorat en Médecine (Faculté de Médecine Waremburg, Université Lille 2) | 2012 |
| - D.I.U. d'Hémostase et Thrombose clinique (Université Lyon 1) | 2012 |
| - Master 2 (Université Paris Diderot) | 2011 |
| - Master 1 (Université Lille 2) | 2009 |

ACTIVITE DE RECHERCHE

Parcours recherche

- | | |
|---|------|
| - Master 1 Biologie et Santé (EDBSL, Université Lille 2) | 2009 |
| - Master 2 Biologie cellulaire, Physiologie et Pathologie (Université Paris Diderot)
Laboratoire d'accueil : EA 2693 « Interface sang-vaisseaux & réparation cardiovasculaire » (Pr Jude)
Direction : Dr Susen | 2011 |
| - Thèse d'Université option recherche clinique, innovation technologique, santé publique (EDBSL, Université Lille 2)
Laboratoire d'accueil : EA 2693 « Interface sang-vaisseaux & réparation cardiovasculaire » (Pr Jude)
Travail de recherche : Protéolyse du facteur Willebrand et cardiopathies à forces de cisaillement élevées. Direction : Pr Susen | 2014 |

Unités d'appartenance

- EA 2693 : « Interface sang-vaisseaux et réparation cardiovasculaire » (Pr Jude) 2011-2015
- INSERM UMR 1011, dirigée par le Pr Staels) 2015-
Equipe 2 Equipe 2 « Heart disease, flow disturbances and haemostasis »
codirigée par les Pr Susen et Van Belle)

PRIX ET BOURSES

- Lauréat de l'appel à projet « Aide à l'émergence, CHU Lille » 2020
- Lauréat de l'appel à projet GIRCI Nord-Ouest « Mobilité internationale » 2020
- Lauréat de l'appel à projet Recherche de l'Association Française des Hémophiles 2020
- Lauréat de l'appel à projet GIRCI Nord-Ouest « Aide à l'émergence » 2019
- Prix du Fonds de dotation CSL Behring pour la recherche 2017

INDICES BIBLIOMETRIQUES

- 39 publications dont 10 en (co)premier auteur (IF>3)
- Score SIGAPS : 506 points
- 700 citations, h-index : 12 (sampra)

Répartition par catégorie et par année

Période 2013-2021								
Année	A	B	C	D	E	NC	Total	Score
2013	0	0	0	0	0	1	1	4
2014	0	1	0	0	0	0	1	24
2015	2	0	2	0	0	0	4	56
2016	4	3	1	0	0	0	8	112
2017	0	0	3	0	1	0	4	16
2018	4	1	1	0	0	0	6	90
2019	3	1	2	0	0	0	6	64
2020	2	5	0	0	0	0	7	118
2021	0	2	1	0	0	0	3	46
Total	15	12	10	0	1	1	39	506

Répartition par catégorie et par position

Période 2013-2021							
Position	Total	A	B	C	D	E	NC
1	7	1	5	0	0	0	1
2	8	6	2	0	0	0	0
3	3	2	0	0	0	1	0
Inv	3	2	0	1	0	0	0
k	17	3	5	9	0	0	0
ADA	1	1	0	0	0	0	0
Total	39	15	12	10	0	1	1

Principales publications

1. Dupont A*, **Rauch A***, Staessens S, Moussa M, Rosa M, Corseaux D, Jeanpierre E, Goutay J, Caplan M, Varlet P, Lefevre G, Lassalle F, Bauters A, Faure K, Lambert M, Duhamel A, Labreuche J, Garrigue D, De Meyer SF, Staels B, Vincent F, Rousse N, Kipnis E, Lenting P, Poissy J, Susen S; Lille Covid Research Network (LICORNE). Vascular Endothelial Damage in the Pathogenesis of Organ Injury in Severe COVID-19. *Arterioscler Thromb Vasc Biol.* 2021 Feb 25:ATVBAHA120315595 (sous presse) (IF: 6,604) *coauteurs
2. **Rauch A**, Paris C, Repesse Y, Branche J, D'Oiron R, Harroche A, Ternisien C, Castet SM, Lebreton A, Pan-Petes B, Volot F, Claeysens S, Chamouni P, Gay V, Berger C, Desprez D, Falaise C, Biron Andreani C, Marichez C, Pradines B, Zawadzki C, Itzhar Baikian N, Borel-Derlon A, Goudemand J, Gerard R, Susen S; French Reference Center on von Willebrand Disease. Gastrointestinal bleeding from angiodysplasia in von Willebrand disease: Improved diagnosis and outcome prediction using videocapsule on top of conventional endoscopy. *J Thromb Haemost.* 2021;19(2):380-386. (IF: 4,157)
3. **Rauch A***, Dupont A*, Goutay J, Caplan M, Staessens S, Moussa M, Jeanpierre E, Corseaux D, Lefevre G, Lassalle F, Faure K, Lambert M, Duhamel A, Labreuche J, Garrigue D, De Meyer SF, Staels B, Van Belle E, Vincent F, Kipnis E, Lenting PJ, Poissy J, Susen S; Lille COVID Research Network (LICORNE); Members of the LICORNE Scientific Committee. Endotheliopathy Is Induced by Plasma From Critically ill Patients and Associated With Organ Failure in Severe COVID-19. *Circulation.* 2020;142(19):1881-1884. (IF: 23,603) *coauteurs
4. **Rauch A**, Labreuche J, Lassalle F, Goutay J, Caplan M, Charbonnier L, Rohn A, Jeanpierre E, Dupont A, Duhamel A, Faure K, Lambert M, Kipnis E, Garrigue D, Lenting PJ, Poissy J, Susen S. Coagulation biomarkers are independent predictors of increased oxygen requirements in COVID-19. *J Thromb Haemost.* 2020;18(11):2942-2953. (IF: 4,157)
5. **Rauch A**, Susen S, Zieger B. Acquired von Willebrand Syndrome in Patients With Ventricular Assist Device. *Front Med (Lausanne).* 2019;6:7. (IF: 3,9)
6. Vincent F*, **Rauch A***, Loobuyck V, Robin E, Nix C, Vincentelli A, Smadja DM, Leprince P, Amour J, Lemesle G, Spillemaeker H, Debry N, Latremouille C, Jansen P, Capel A, Moussa M, Rousse N, Schurtz G, Delhaye C, Paris C, Jeanpierre E, Dupont A, Corseaux D, Rosa M, Sottejeau Y, Barth S, Mourran C, Gomane V, Coisne A, Richardson M, Caron C, Preda C, Ung A, Carpentier A, Hubert T, Denis C, Staels B, Lenting PJ, Van Belle E, Susen S. Arterial Pulsatility and Circulating von Willebrand Factor in Patients on Mechanical Circulatory Support. *J Am Coll Cardiol.* 2018;71(19):2106-2118. (IF : 18,639) *coauteurs
7. Van Belle E*, **Rauch A***, Vincent F, Robin E, Kibler M, Labreuche J, Jeanpierre E, Levade M, Hurt C, Rousse N, Dally JB, Debry N, Dallongeville J, Vincentelli A, Delhaye C, Auffray JL, Juthier F, Schurtz G, Lemesle G, Caspar F, Morel O, Dumontel N, Duhamel A, Paris C, Dupont-Prado A, Legendre P, Mouquet F, Marchant B, Hermoire S, Corseaux D, Moussa K, Manchuelle A, Bauchart JJ, Loobuyck V, Caron C, Zawadzki C, Leroy F, Bodart JC, Staels B, Goudemand J, Lenting PJ, Susen S. Von Willebrand Factor Multimers during Transcatheter Aortic Valve Replacement. *N Engl J Med.* 2016; 375(4):335-44. (IF: 72,406) *coauteurs
8. **Rauch A**, Caron C, Vincent F, Jeanpierre E, Ternisien C, Boisseau P, Zawadzki C, Fressinaud E, Borel-Derlon A, Hermoire S, Paris C, Lavenu-Bombled C, Veyradier A, Ung A, Vincentelli A, van Belle E, Lenting PJ, Goudemand J, Susen S. A novel ELISA-based diagnosis of acquired VWD with increased VWF proteolysis. *Thromb Haemost.* 2016; 115(5):950-9. (IF : 5,627)
9. Van Belle E*, **Rauch A***, Vincentelli A, Jeanpierre E, Legendre P, Juthier F, Hurt C, Banfi C, Rousse N, Godier A, Caron C, Elkalioubie A, Corseaux D, Dupont A, Zawadzki C, Delhaye C, Mouquet F, Schurtz G, Deplanque D, Chinetti G, Staels B, Goudemand J, Jude B, Lenting PJ, Susen S. Von Willebrand Factor As A Biological Sensor Of Blood Flow To Monitor Percutaneous Aortic Valve Interventions. *Circ Res.*2015; 116(7):1193-201 (IF: 11,551). *coauteurs
10. **Rauch A**, Legendre P, Christophe OD, Goudemand J, van Belle E, Vincentelli A, Denis CV, Susen S, Lenting PJ. Antibody-based prevention of von Willebrand factor degradation mediated by circulatory assist devices. *Thromb Haemost.* 2014; 112(5):1014-23. (IF: 4,984)

Abréviations

ACE2 : Récepteur de l'enzyme de conversion de l'angiotensine 2

ACM : Assistance circulatoire mécanique

ACM-FC: ACM à flux continu

ACM-FP: ACM à flux pulsatile

ADAMTS13 : A Disintegrin And Metalloprotease with ThromboSpondin domains13

BHK : Baby Hamster Kidney

CMH : Cardiomyopathie hypertrophique

COVID-19: Maladie à coronavirus 2019

CRMW : Centre national de Référence Maladie de Willebrand

ECMO : Extra Corporeal Membrane Oxygenation

EDTA : Acide éthylènediaminetétraacétique

ETO : Echographie trans-oesophagienne

GPIb α : Glycoprotéine plaquettaire Ib α

HPMVEC : Human pulmonary microvascular endothelial cells

MHC : Micro hémorragies cérébrales

MW : Maladie de Willebrand

NETs : Neutrophil extracellular traps

PFA : Platelet Function Analyser

PSPC : Programme de soutien aux pôles de compétitivité

PPP : Plasma pauvre en plaquettes

PTT : Purpura thrombotique thrombocytopénique

RAo : Rétrécissement aortique

SARS-CoV-2 : Severe Acute Respiratory Syndrome COronaVirus 2

SDRA : Syndrome de détresse respiratoire aigüe

TAVI : Transcatheter Aortic Valve Implantation

TO-ADP : Temps d'occlusion plaquettaire mesuré en PFA sur la cartouche ADP

VWF: Facteur Willebrand (von Willebrand factor)

VWFpp : Propeptide du VWF (VWFpp)

VWF-HPM : Multimères de haut poids moléculaire du VWF

VWF-THPM : Multimères de très haut poids moléculaire du VWF

Exposé des travaux de recherche

Mes travaux de recherche ont jusqu'ici été focalisés sur l'étude des anomalies du facteur von Willebrand (VWF) secondaires aux modifications de flux sanguin induites par le rétrécissement aortique (RAo) ou l'assistance circulatoire mécanique à flux continu (ACM-FC).

Ces travaux ont d'abord été menés au sein de l'équipe d'accueil (EA) 2693, dirigée alors par le Pr Jude, puis au sein de l'unité INSERM UMR-1011 (directeur Pr Staels) à laquelle l'EA2693 a été rattachée en 2015 pour constituer l'équipe 2 (ARTEMIS : « heART disease, flow disturbances and haemostasis »). L'équipe 2 de l'UMR-1011 codirigée par le Pr Sophie Susen (PU-PH Hématologie) et par le Pr Eric Van Belle (PU-PH Cardiologie) et implantée sur le campus hospitalo-universitaire de Lille, rassemble des hématologues-biologistes spécialistes du facteur tissulaire, du VWF et en biologie cellulaire (monocytes/macrophages, VIC, cellules musculaires lisses et adipocytes), des cardiologues spécialistes de l'athérosclérose, du RAo et du syndrome métabolique, et des chirurgiens cardiaques spécialistes des valvulopathies. L'expertise pluridisciplinaire de l'équipe a permis de développer des projets transversaux conjuguant approches cliniques et expérimentales à l'interface de l'hématologie et de la cardiologie sur 2 thématiques principales: la valvulopathie aortique et les cardiopathies ou dispositifs cardiaques à forces de cisaillement élevées. Mes travaux ont essentiellement porté sur cette deuxième thématique qui s'est beaucoup développée depuis le rattachement de notre équipe d'accueil à l'UMR-1011.

Le VWF est une glycoprotéine multimérique d'origine endothéliale qui agit comme un médiateur de l'adhésion et l'agrégation plaquettaire particulièrement dans des conditions de forces de cisaillement élevées. Il existe en effet au niveau de chaque monomère du VWF différents domaines fonctionnels permettant l'interaction du VWF avec les glycoprotéines plaquettaires membranaires GPIIb/IIIa et α IIb β 3. Le VWF est synthétisé puis stocké au niveau endothélial dans les corps de Weibel-Palade sous une forme très multimérisée dite de très hauts poids moléculaire (VWF-THPM). Lors de la sécrétion endothéliale du VWF dans le plasma, ces VWF-THPM sont immédiatement clivés par une protéase plasmatique, l'ADAMTS13 (A Disintegrin And Metalloprotease with Thrombospondin domain), en multimères de poids moléculaire variable, dont les plus fonctionnels sur le plan hémostatique sont les multimères de hauts poids moléculaire (VWF-HPM). Ces VWF-HPM ont comme particularité d'avoir une conformation très sensible aux contraintes hydrodynamiques dites « forces de cisaillement » résultant des modalités d'écoulement du flux. Ils adoptent spontanément en l'absence de forces de cisaillement une conformation globulaire insensible à l'action protéolytique de l'ADAMTS13. Cependant, ils peuvent adopter une conformation de

type chaîne étendue en présence de forces de cisaillement élevées¹ induisant l'exposition au niveau du domaine A2 de différents monomères des sites de clivage par l'ADAMTS13 ce qui favorise alors leur protéolyse^{2,3}.

Mon travail de master 2 s'était inscrit dans la continuité de travaux de l'EA2693 qui avaient mis en évidence que les contraintes hydrodynamiques générées par certaines valvulopathies cardiaques pouvaient retentir sur la structure et la fonction du VWF circulant. Deux travaux de l'EA2693 avaient ainsi permis de préciser la prévalence, la physiopathologie et l'évolution des syndromes de Willebrand acquis associés au RAO sévère ou à la cardiomyopathie hypertrophique (CMH) avec bourgeon septal. L'EA2693 avait ainsi décrit la présence quasi-systématique d'un déficit plasmatique en VWF-HPM chez les patients atteints d'un RAO sévère ainsi que des manifestations hémorragiques cutanéomuqueuses chez un quart des patients étudiés, soulignant ainsi la pertinence de l'association entre RAO et hémorragies digestives établie par un interniste américain en 1958 (syndrome de Heyde). Il existait également chez ces patients une corrélation inverse entre le niveau des forces de cisaillement trans-aortiques secondaires au RAO et l'intensité du déficit plasmatique en VWF-HPM, suggérant un rôle causal de ces anomalies rhéologiques dans la physiopathologie du syndrome de Willebrand acquis⁴. L'EA2693 avait aussi identifié une association similaire entre forces de cisaillement et déficit plasmatique en VWF-HPM dans la CMH avec bourgeon septal⁵. Enfin, l'EA2693 avait mis en évidence le caractère réversible des anomalies de multimérisation du VWF après correction chirurgicale du RAO, excepté en présence d'un mismatch valve prothétique/anneau aortique induisant la persistance de forces de cisaillement trans-aortiques élevées en post-opératoire⁴. Ces différentes observations rendaient concevable l'hypothèse d'un rôle causal des forces de cisaillement dans l'apparition des anomalies de multimérisation du VWF.

Malgré l'observation d'une normalisation du déficit plasmatique en VWF-HPM dès le lendemain de la chirurgie de remplacement valvulaire aortique, l'EA2693 n'avait pas pu caractériser précisément *in vivo* la cinétique de correction du syndrome de Willebrand acquis en raison de l'effet confondant de la circulation extracorporelle en chirurgie cardiaque. Mon travail de master 2 a permis grâce au développement d'un modèle animal de sténose aortique aiguë et réversible de : 1) confirmer expérimentalement le lien de causalité entre l'induction ou la réversion de forces de cisaillement intracardiaques élevées et l'apparition ou la correction du déficit plasmatique en VWF-HPM; 2) et de caractériser *in vivo* la cinétique d'apparition et de correction de ces anomalies du VWF. Mes travaux de thèse et de post-doctorat se sont ensuite poursuivis sur cette thématique de syndrome de Willebrand acquis par anomalies de flux intracardiaques dans deux modèles pathologiques : le RAO et l'ACM-FC.

En parallèle, j'ai poursuivi mon activité hospitalière au sein du service d'Hémostase clinique du CHU de Lille où j'ai pu participer ou conduire des travaux de recherche clinique portant essentiellement sur la maladie de Willebrand. Dans le contexte de pandémie COVID-19, j'ai pu également participer ou conduire des travaux de recherche clinique ou fondamentale soulignant l'importance de l'endothéliopathie et de la dérégulation immunitaire dans la physiopathologie des complications macro- et micro-thrombotiques présentes dans les formes sévères de COVID-19.

Les principaux résultats de ces travaux sont détaillés ci-dessous et les publications en rapport sont présentées en fin de manuscrit.

Travaux de thèse d'Université

Syndrome de Willebrand acquis et cardiopathies à forces de cisaillement élevées

Contexte :

Mon travail de thèse s'est effectué sous la codirection du Pr Susen et du Dr Peter Lenting dans le cadre d'une collaboration entre l'EA2693 et l'unité Inserm U770 dirigée par le Dr Cécile Denis qui nous a fait bénéficier d'approches complémentaires sur le VWF.

Le premier versant de ce travail de thèse s'est inscrit dans la continuité de mon master 2 qui avait confirmé le lien de causalité entre forces de cisaillement intracardiaques et l'apparition d'anomalies de multimérisation du VWF dans le RAo et souligné le caractère dynamique des cinétiques d'apparition et de correction des anomalies de multimérisation du VWF en parallèle des modifications de flux intracardiaques. Nous avons alors souhaité évaluer si ces résultats obtenus dans un modèle animal étaient transposable à l'homme dans deux modèles pathologiques distincts associés à des modifications aiguës des forces de cisaillement intracardiaques : i) à l'initiation d'une ACM-FC s'apparentant à un modèle d'induction aiguë de forces de cisaillement intracardiaques élevées), ii) et lors du traitement percutané du RAo par la procédure de cardiologie interventionnelle TAVI (Transcatheter Aortic Valve Implantation) s'apparentant à un modèle de réversion aiguë de forces de cisaillement intracardiaques élevées. Ce travail a fait émerger le concept innovant d'utiliser le VWF comme biomarqueur de la qualité de l'implantation valvulaire par TAVI en alternative à l'échographie cardiaque.

Dans l'intervalle, l'avènement de l'assistance mono-ventriculaire gauche à demeure chez les patients en insuffisance cardiaque terminale inéligible à la transplantation cardiaque et l'essor des indications d'ECMO a mis en lumière de façon aiguë la problématique du syndrome de Willebrand acquis secondaire à l'ACM-FC. Le second versant de ma thèse a ainsi porté sur la caractérisation du mécanisme de dégradation du VWF sous ACM-FC et le développement de nouveaux outils diagnostiques et thérapeutiques dans ce cadre.

1) le VWF comme biomarqueur d'anomalies de flux intracardiaques dans les valvulopathies cardiaques à forces de cisaillement élevées

Le RAo représente la plus fréquente des valvulopathies de l'adulte. Il s'agit d'une maladie le plus souvent dégénérative affectant 3 à 5% de la population de plus de 60 ans. Une alternative au remplacement valvulaire aortique par sternotomie existe désormais: il s'agit de l'implantation d'une bioprothèse par cathétérisme interventionnel (TAVI : Transcatheter Aortic Valve Implantation). Développé en 2002⁶, le TAVI s'est progressivement imposée comme le

traitement de référence du RAO sévère pour les patients les plus âgés ou avec des comorbidités à haut risque opératoire⁷. Un déficit plasmatique acquis en VWF-HPM est associé au RAO et aux ACM-FC. Ces deux conditions ont un commun de générer des forces de cisaillement élevées qui favorisent l'élongation et la protéolyse des VWF-HPM lors de leur passage au sein de la valve sténosée ou de la pompe d'ACM-FC. Les cinétiques précises d'apparition et de réversion de ces anomalies qualitatives du VWF, respectivement lors de l'initiation de l'ACM-FC ou de la correction du RAO n'étaient pas décrites. Bien que des données expérimentales *in vitro* suggéraient le caractère extrêmement dynamique de telles cinétiques², cet aspect n'avait pas jusqu'ici fait l'objet d'une étude *in vivo*.

Nous avons ainsi étudié l'impact sur la multimérisation du VWF de variations aiguës des forces de cisaillement intracardiaques dans 3 modèles *in vivo* : i) un modèle lapin de sténose aiguë et réversible de l'aorte ascendante (travail de master 2), ii) à l'initiation d'une assistance mono-ventriculaire gauche à flux continu de type HeartMate-II® chez des patients en insuffisance cardiaque terminale, iii) après correction partielle ou complète d'un RAO sévère chez des patients bénéficiant respectivement d'une valvuloplastie aortique (BAV) ou d'un TAVI. L'étude de la multimérisation du VWF a reposé sur 2 approches : i) la technique de référence du Centre national de Référence Maladie de Willebrand (CRMW) reposant sur une électrophorèse sur gel d'agarose, examen le plus sensible pour mettre en évidence des anomalies de multimérisation du VWF mais très chronophage et de réalisation complexe; ii) une mesure automatisée du temps d'occlusion plaquettaire sur la cartouche épinéphrine/ADP (TO-ADP) avec comme hypothèse que ce paramètre biologique, en raison de sa sensibilité à détecter un déficit plasmatique en VWF-HPM dans la maladie de Willebrand constitutionnelle⁸, pouvait constituer un reflet indirect de l'évolution cinétique des anomalies de multimérisation du VWF induite par des variations aiguës d'intensité des forces de cisaillement intracardiaques

Résultats

Dans le modèle lapin dit de « banding aortique » permettant une sténose aiguë et réversible de l'aorte ascendante, nous avons observé une perte significative des VWF-HPM dans le plasma à cinq et trente minutes après induction de la sténose (Figure 1). Chez des patients en insuffisance cardiaque terminale, nous avons observé une cinétique similaire d'apparition d'un déficit plasmatique en VWF-HPM dès l'initiation d'une ACM-FC de type HeartMate-II® aussi bien *in vitro* qu'*in vivo*. Après réversion instantanée de la sténose aortique dans le modèle lapin, une correction rapide du déficit plasmatique en VWF-HPM était observée après la levée de l'obstacle, partielle dès cinq minutes et complète trente minutes après normalisation des forces de cisaillement trans-aortiques (Figure 1).

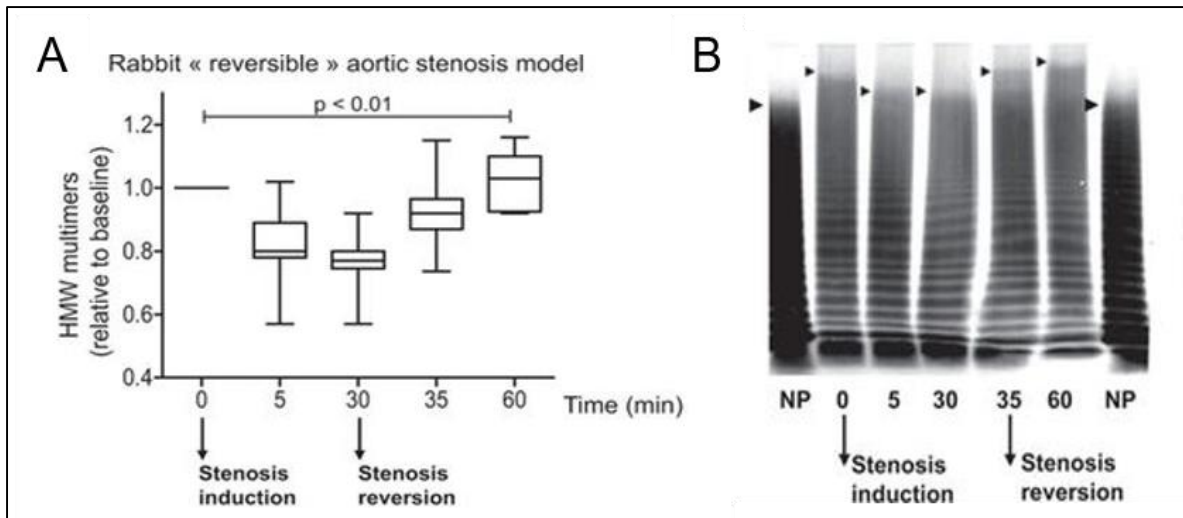


Figure 1 : Modèle animal de sténose aiguë et réversible de l'aorte ascendante. A) Cinétique du déficit plasmatique en VWF-HPM dans les 30 min suivant l'induction puis la réversion de la sténose (quantification densitométrique > 15 mers après électrophorèse sur SDS-agarose), B) profil multimérique représentatif.

De même chez l'homme, en cas de traitement efficace du RAO par TAVI, nous avons observé une normalisation en quelques minutes du déficit plasmatique en VWF-HPM (Figure 2A) alors que ce déficit persistait en fin de procédure en cas de correction uniquement partielle de la sténose aortique par valvuloplastie au ballon (Figure 2B). Cette normalisation rapide du profil multimérique du VWF suggérait que l'arrêt de la protéolyse du VWF ne pouvait être le seul mécanisme impliqué. L'augmentation concomitante des taux plasmatique du propeptide du VWF a en effet permis d'identifier un mécanisme de relargage endothélial du VWF dans les minutes suivant une correction complète du RAO par TAVI.

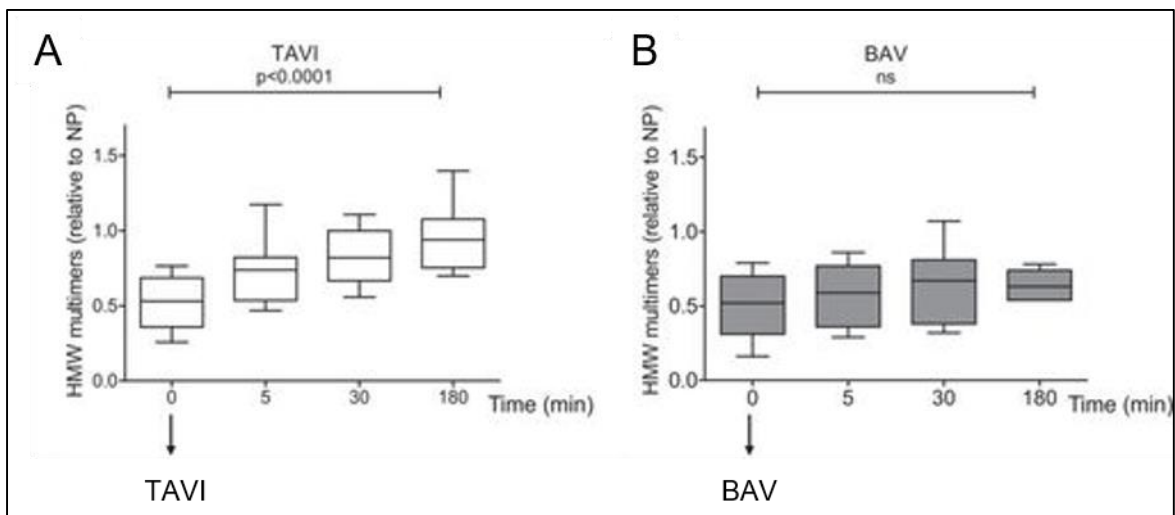


Figure 2 : Cinétique péri-procédurale de réversion du déficit plasmatique en VWF-HPM (quantification densitométrique > 15 mers relative à un pool plasmatique contrôle après électrophorèse sur SDS-agarose) : A) après correction totale du RAO par TAVI, B) après correction partielle du RAO par valvuloplastie cardiaque (BAV).

Une fuite para-valvulaire (FPV) peut survenir chez 10 à 20% des patients bénéficiant d'un TAVI si l'apposition de la bioprothèse sur l'anneau aortique est incomplète générant une(des) zone(s) de fuite(s) résiduelle(s) permettant la régurgitation du sang à forces de cisaillement élevées à travers ce/ces orifice(s)⁹. De façon notable, nous avons observé qu'un déficit plasmatique en VWF-HPM persistait en cas de TAVI compliqué d'une FPV. En effet dans la cohorte TAVI, seuls les quatre patients dont le déficit plasmatique en VWF-HPM n'était pas normalisé en fin de procédure présentaient une FPV significative en échographie cardiaque.

Dans cette étude pilote exploratoire, le TO-ADP avait une cinétique superposable à celle des VWF-HPM avec une correction partielle de son allongement dans le groupe « valvuloplastie » et complète dans le groupe « TAVI » (Figure 3A) excepté chez les quatre patients présentant une FPV en fin de procédure (Figure 3B).

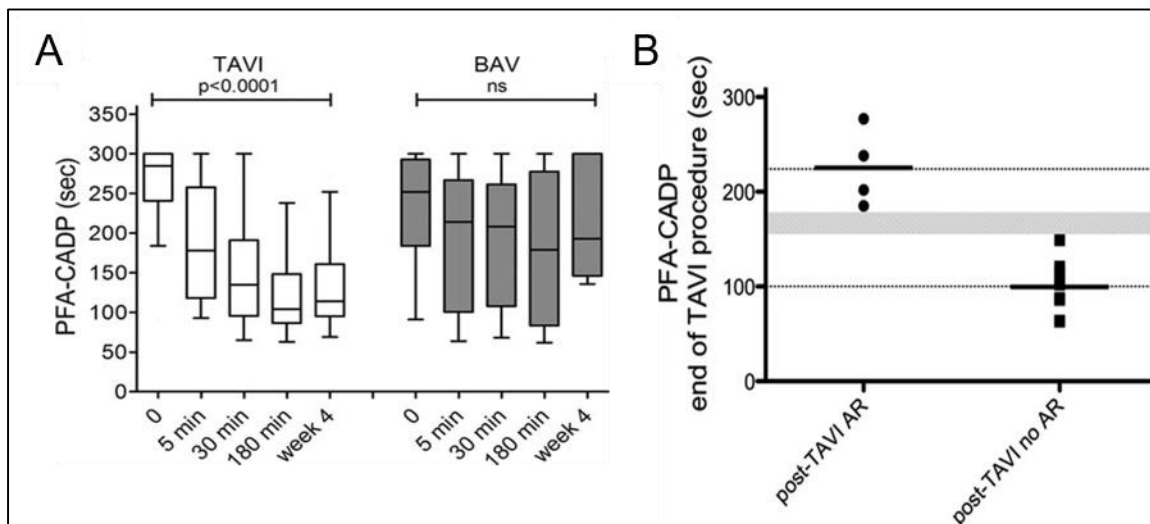


Figure 3 : A) Cinétique péri-procédurale du TO-ADP (en sec) après correction totale (procédure TAVI) ou partielle (procédure BAV) du RAo par voie transcathéter B) TO-CADP (en sec) en fin de procédure TAVI selon la présence ou non d'une fuite para-valvulaire (AR : aortic regurgitation) par échographie trans-oesophagienne.

Conclusion et perspectives

Ce travail a permis de confirmer chez l'homme les variations extrêmement dynamiques de multimérisation du VWF plasmatique en réponse à des variations aiguës d'intensité des forces de cisaillement intracardiaques. Il a ainsi fait émerger un nouveau concept selon lequel le VWF plasmatique constitue un biomarqueur d'anomalies de flux sanguin dans les cardiopathies à forces de cisaillement élevées (Publication : Von Willebrand Factor As A Biological Sensor Of Blood Flow To Monitor Percutaneous Aortic Valve Interventions. Circ Res.2015).

2) Syndrome de Willebrand acquis sous assistance circulatoire mécanique: physiopathologie, nouvelles approches diagnostiques et thérapeutiques.

L'obtention d'une extension d'indication à demeure (« destination therapy ») de l'ACM-FC pour les patients insuffisants cardiaques inéligibles à une transplantation cardiaque¹⁰ a mis en perspective de façon plus aigüe la problématique du syndrome de Willebrand acquis secondaire à des forces de cisaillement intracardiaque élevées. L'hypothèse d'un syndrome de Willebrand acquis sous ACM-FC s'est rapidement imposée sur la base d'arguments cliniques et biologiques. A l'exception des hémorragies du site opératoire survenant dans les jours suivant l'implantation chirurgicale de l'ACM-FC, la majorité des saignements concerne les muqueuses ORL et gastro-intestinale orientant vers un trouble de l'hémostase primaire. La fréquence des complications hémorragiques sous ACM-FC est trop élevée pour être attribuée aux seuls traitements anticoagulants ou antiagrégants plaquettaires également administrés chez ces patients. La fréquence des hémorragies digestives sous ACM-FC est supérieure à celle des hémorragies de toutes causes chez les patients porteurs d'une valve cardiaque mécanique et bénéficiant d'un traitement combiné par antiagrégants plaquettaires et anti-vitamines K. Par ailleurs, un surdosage en anti-vitamines K n'est pas prédictif de la sévérité des complications hémorragiques sous ACM-FC¹¹. Ceci suggère l'existence d'un mécanisme additionnel et intrinsèque aux ACM-FC dans la genèse de ces complications hémorragiques. Il a rapidement été mis en évidence par plusieurs travaux dont un mené en collaboration avec l'EA 2693¹² qu'une dégradation du VWF circulant survenait systématiquement sous ACM-FC aussi bien avec les pompes rotatives que centrifuges¹³ alors que ce phénomène n'était pas observé avec la génération antérieure d'ACM à flux pulsatile (ACM-FP). Le(s) mécanisme(s) sous-jacents à cette dégradation du VWF sous ACM-FC restait cependant mal caractérisé(s) au début de mon travail de thèse même si l'implication d'un excès de protéolyse du VWF par l'ADAMTS13 au sein de la pompe d'ACM-FC était suspectée au vu des forces de cisaillement élevées générées par ces dispositifs.

1- Physiopathologie de la dégradation du VWF sous ACM-FC

La prise en charge des saignements sous ACM-FC constitue souvent une impasse thérapeutique. Il existe une indication d'anticoagulation sous ACM-FC en prévention primaire d'évènements thromboemboliques qui complexifie la prise en charge des complications hémorragiques. Il n'existe pas de traitement hémostatique dont l'efficacité et la sécurité soient validées par des études cliniques en cas d'hémorragie sous ACM-FC. Le sevrage de l'ACM-FC permet un traitement étiologique du syndrome de Willebrand acquis mais cette option ne concerne en pratique qu'une minorité de patients en raison d'une contre-indication fréquente à la transplantation cardiaque dans l'indication « destination therapy ». La compréhension de la physiopathologie de la maladie de Willebrand acquise sous ACM-FC est donc essentielle

pour développer de nouvelles approches diagnostiques et thérapeutiques permettant d'identifier les patients à haut risque hémorragique et mieux les prendre en charge.

Résultats

Dans la première partie de ce travail, nous avons développé un modèle d'ACM-FC *in vitro* (Figure 4) afin de confirmer expérimentalement le rôle causal de l'ADAMTS13 dans la dégradation du VWF. Grâce à ce modèle, nous avons pu caractériser le caractère aigu et forces de cisaillement dépendant de la dégradation du VWF sous ACM-FC. Nous avons également pu confirmer que cette dégradation du VWF était de caractère enzymatique et non mécanique comme évoqué par d'autres équipes¹⁴ en raison de son inhibition totale en présence d'EDTA *in vitro*. Nous avons pu démontrer secondairement le rôle causal de l'ADAMTS13 dans le cadre d'un travail collaboratif avec l'équipe du Pr Vanhoorelbeke à Courtrai (Laboratory for Thrombosis Research, Kulak, KU Leuven Camus) avec une inhibition totale de la dégradation des VWF-HPM dans notre modèle d'ACM-FC *in vitro* avec un anticorps monoclonal ciblant le domaine métallo-protéase de l'ADAMTS13, au sein duquel se trouve le site catalytique de cette enzyme.

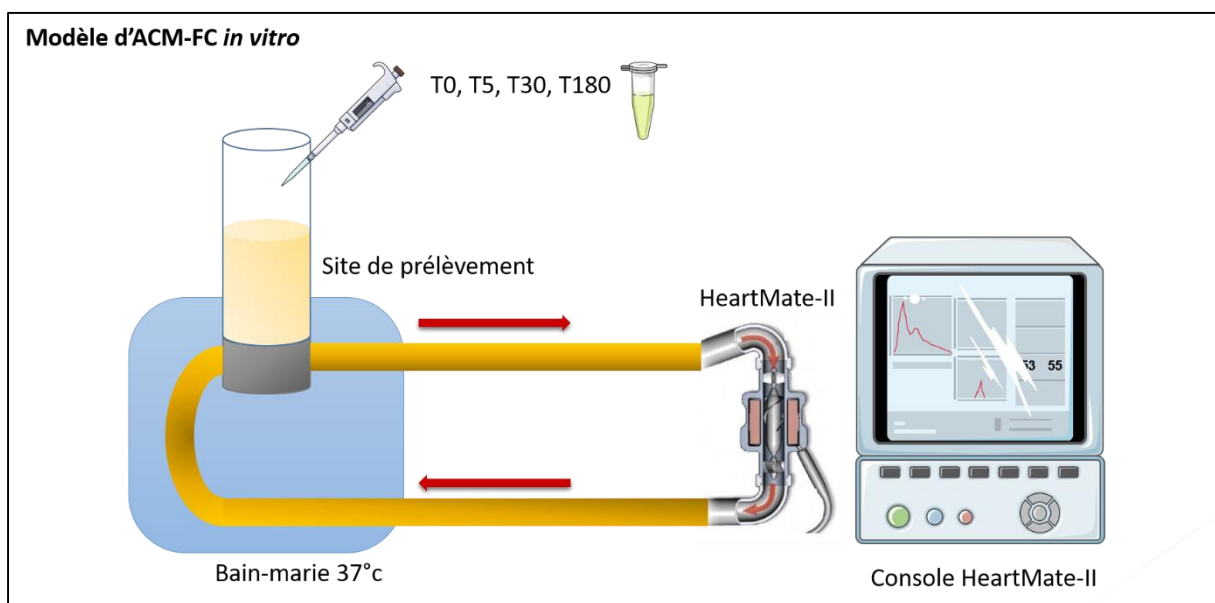


Figure 4 : Modèle d'ACM-FC basé sur l'emploi d'une pompe d'assistance mono-ventriculaire (HeartMate-II)

2- Quelle(s) approche(s) moléculaire(s) pour inhiber la dégradation du VWF sous ACM-FC ?

Les bases moléculaires de la protéolyse du VWF par l'ADAMTS13 sont bien établies. L'ADAMTS13 a pour substrat unique le VWF, qu'elle protéolyse au niveau d'une liaison peptidique unique localisée dans le domaine A2 entre les résidus Tyrosine 1605 et Méthionine 1606. Cette protéolyse nécessite une interaction préalable entre le VWF et l'ADAMTS13, impliquant côté VWF des exo-sites localisés au niveau des domaines A2 et D4 ^{15,16}. Le

développement de molécules ciblant un des exo-sites impliqués dans la liaison VWF-ADAMTS13 semble une approche pertinente car cette interaction est nécessaire pour permettre la protéolyse du VWF. De plus, cette approche est théoriquement compatible avec le maintien d'une protéolyse résiduelle du VWF minimisant ainsi le risque de purpura thrombotique thrombocytopénique (PTT) pharmaco-induit contrairement à une approche reposant sur une inhibition directe du site catalytique de l'ADAMTS13.

Nous avons testé deux classes de molécules dans cette optique : i) une librairie d'anticorps monoclonaux murins anti-VWF ou anti-ADAMTS13 issus de lignées d'hybridomes, ii) des fragments recombinants de VWF ou d'ADAMTS13 produits par transfection stables de cellules eucaryotes BHK. Nous avons d'abord sélectionnés comme molécules d'intérêt celles inhibant partiellement *in vitro* la liaison d'une ADAMTS13 recombinante humaine à du VWF purifié d'origine plasmatique. Cette approche a identifié deux molécules candidates, le fragment recombinant VWF A2-Fc et l'anticorps monoclonal murin 508 (LTX-508), dont nous avons ensuite évalué la capacité à inhiber la protéolyse du VWF par l'ADAMTS13 en conditions de flux. En conditions de flux, seul l'anticorps LTX-508 s'est révélé inhiber la protéolyse du VWF par l'ADAMTS13. Nous avons ensuite caractérisé le mode d'action et le potentiel thérapeutique de cet anticorps monoclonal. L'étude de la liaison du LTX-508 à différents fragments de VWF d'origine recombinante ou obtenus par digestion enzymatique a permis de localiser son épitope dans la partie distale du domaine D4 du VWF. Grâce à un panel de peptides synthétiques biotinylés de séquences chevauchantes, nous avons ensuite réduit l'épitope du LTX-508 à une courte séquence polypeptidique de 12 acides aminés au sein du domaine D4, semblant jouer un rôle critique dans la liaison du VWF natif, sous sa conformation globulaire, à la partie distale de l'ADAMTS13. Nous avons ensuite établi que l'anticorps LTX-508 présentait une affinité moyenne et interagissait de façon dose-dépendante avec le VWF immobilisé. Via un test d'inhibition en microplaque de la liaison VWF-ADAMTS13, nous avons estimé que la concentration inhibitrice 50 (IC50) du LTX-508 était de 0.9 µg.mL⁻¹, soit une concentration compatible avec une utilisation *in vivo*.

Nous avons utilisé un modèle *in vitro* en sang total pour évaluer l'efficacité du LTX-508 à prévenir la dégradation du VWF en présence de forces de cisaillement élevées induites par une ACM-FC. Dans ce modèle, l'anticorps LTX-508 inhibe de façon dose-dépendante la dégradation des VWF-HPM induite par une ACM-FC de type HeartMate-II®. De façon notable, il persiste une protéolyse résiduelle du VWF en présence de fortes concentrations de LTX-508 comparé à l'inhibition complète observée avec l'EDTA (Figure 5).

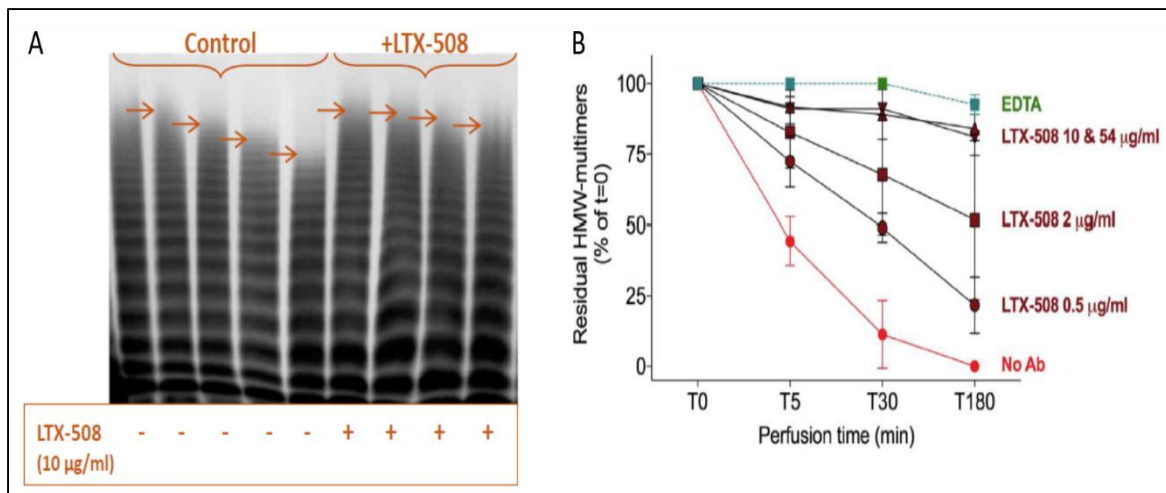


Figure 5 : Cinétique de dégradation du VWF dans le modèle d'ACM-FC HeartMate-II in vitro : A) profil multimétrique représentatif illustrant l'inhibition partielle de la dégradation du VWF par l'anticorps anti-VWF D4 (LTX-508) en présence de forces de cisaillement élevées (vitesse = 9000 rpm), B) Caractère dose-dépendant et saturable de l'inhibition de la dégradation du VWF par l'anticorps anti-VWF D4 (LTX-508) comparé à l'inhibition totale en présence d'EDTA (10mM)

Conclusions

Ce travail a permis de valider le concept selon lequel une prévention pharmacologique de la dégradation du VWF sous ACM-FC est possible via un anticorps monoclonal dirigé contre le domaine D4 du VWF, inhibant l'interaction VWF-ADAMTS13. Cette approche présente comme avantage de préserver un niveau résiduel de protéolyse plasmatique du VWF minimisant ainsi le risque de PTT pharmaco-induit. Ce travail a fait l'objet d'une publication (*Antibody-based prevention of von Willebrand factor degradation mediated by circulatory assist devices. Thromb Haemost. 2014*) et d'un brevet (Inserm transfert BIO13050).

3- Nouvelles approches diagnostiques

Seules les techniques électrophorétiques ont une sensibilité satisfaisante pour le diagnostic des syndromes de Willebrand acquis d'origine cardio-vasculaire. Elles permettent en effet de mettre en évidence : 1) de façon semi-quantitative l'excès de protéolyse du VWF par l'ADAMTS13 caractéristique de ces situations par l'analyse des bandes satellites jouxtant les dimères et tétramères de VWF¹⁷; 2) et le déficit plasmatique en VWF-HPM résultant de leur protéolyse par l'ADAMTS13. Cependant, ces techniques électrophorétiques ne sont pas adaptées à un contexte d'urgence diagnostique ou thérapeutique car elles sont chronophages et requièrent une expertise technique importante ce qui limite leur disponibilité à de rares laboratoires. L'objectif de ce travail était de développer une méthode analytique ELISA permettant de quantifier sur plasma pauvre en plaquettes la protéolyse du VWF par l'ADAMTS13 de façon plus simple et rapide que la technique électrophorétique de référence.

Pour cela, nous avons développé un test ELISA « maison » reposant sur l'utilisation: 1) à l'étape de capture d'un anticorps monoclonal murin anti-VWF/domaine A2 clivé (mAb27642, R&D Systems / Biotechne) reconnaissant un épitope de 10 acides aminés (D1596-Y1605) adjacent au site de protéolyse dans le domaine A2 uniquement accessible après clivage par l'ADAMTS13¹⁸; 2) d'un anticorps polyclonal de lapin anti-VWF humain conjugué à la peroxydase; 3) d'un standard maison de fragments de protéolyse du VWF obtenu après co-incubation pendant 16 heures d'un concentré de VWF plasmatique d'origine humaine avec de l'ADAMTS13. Nous avons établi qu'au terme de cette durée d'incubation l'intensité du déficit en VWF-HPM induit *in vitro* était similaire à celui observé chez les patients atteints d'un RAO sévère.

Les performances diagnostiques de cet ELISA pilote ont été évaluées dans 4 modèles : i) un modèle d'ACM-FC *in vitro* de type HeartMate-II® décrit auparavant, ii) une cohorte de patients avec une maladie de Willebrand (MW) constitutionnelle (n=89) ayant fait l'objet d'une caractérisation phénotypique et génotypique exhaustive par le CRMW, iii) une cohorte de patients insuffisants cardiaques avec initiation d'un ACM-FC HeartMate-II® (n=9), iv) une cohorte de patients RAO traités par TAVI (n=11).

Résultats

Dans le modèle d'ACM-FC *in vitro*, nous avons observé une association significative entre l'intensité de la protéolyse du VWF plasmatique mesurée par ELISA et la vitesse d'assistance. La protéolyse des VWF-HPM mesurée par cet ELISA en présence de forces de cisaillement élevées était totalement inhibée en présence d'EDTA et partiellement inhibée en présence de l'anticorps LTX-508 dirigé contre le domaine D4 du VWF. Dans une cohorte de MW constitutionnelle, la protéolyse du VWF était comme attendu significativement plus élevée chez les patients atteints d'une MW de type 2A(IIA) ou 2B comparé à des sujets sains contrôles. Dans une cohorte de MW acquise, la protéolyse du VWF était significativement augmentée 3 heures après initiation d'une ACM-FC et l'excès de protéolyse du VWF présent chez les patients atteints d'un RAO sévère était corrigé après correction de la valvulopathie par TAVI.

Conclusion et perspectives

Le développement et la validation de ce test ELISA permettant une quantification de l'excès de protéolyse du VWF survenant dans certaines formes constitutionnelles de MW ou en présences de forces de cisaillement intracardiaques élevées induites par un RAO ou une ACM-FC, a fait l'objet d'une publication (Publication *A novel ELISA-based diagnosis of acquired VWD with increased VWF proteolysis. Thromb Haemost. 2016*).

Suite à l'identification du concept assimilant le VWF à un biomarqueur d'anomalies de flux intracardiaques et aux résultats obtenus avec ce test pilote, notre équipe a souhaité aller plus loin dans le développement d'un test de quantification de la protéolyse du VWF plasmatique, reposant sur le même principe mais employant un anticorps de capture différent de façon à pouvoir être breveté en vue d'une utilisation non seulement dans la MW constitutionnelle mais également pour un monitoring biologique de la qualité de l'implantation valvulaire par la procédure de cardiologie interventionnelle TAVI.

Valorisation

Cette thèse a été valorisée par trois publications dans des revues internationales à comité de lecture et un dépôt de brevet.

Manuscrits:

1. Von Willebrand Factor As A Biological Sensor Of Blood Flow To Monitor Percutaneous Aortic Valve Interventions. Van Belle E*, **Rauch A***, Vincentelli A, Jeanpierre E, Legendre P, Juthier F, Hurt C, Banfi C, Rousse N, Godier A, Caron C, Elkalioubie A, Corseaux D, Dupont A, Zawadzki C, Delhaye C, Mouquet F, Schurtz G, Deplanque D, Chinetti G, Staels B, Goudemand J, Jude B, Lenting PJ, Susen S. *Circ Res.*2015; 116(7):1193-201 (IF: 11,551). ***coauteurs**
2. Antibody-based prevention of von Willebrand factor degradation mediated by circulatory assist devices. **Rauch A**, Legendre P, Christophe OD, Goudemand J, van Belle E, Vincentelli A, Denis CV, Susen S, Lenting PJ. *Thromb Haemost.* 2014; 112(5):1014-23. (IF: 4,984)
3. A novel ELISA-based diagnosis of acquired VWD with increased VWF proteolysis. **Rauch A**, Caron C, Vincent F, Jeanpierre E, Ternisien C, Boisseau P, Zawadzki C, Fressinaud E, Borel-Derlon A, Hernoire S, Paris C, Lavenu-Bombled C, Veyradier A, Ung A, Vincentelli A, van Belle E, Lenting PJ, Goudemand J, Susen S.. *Thromb Haemost.* 2016; 115(5):950-9. (IF : 5,627)

Brevet:

1. Antibodies for the prevention and treatment of bleeding episodes associated with acquired Von Willebrand Syndrome. Lenting PJ, Denis C, Susen, S, **Rauch A**, Van Belle E, Vincentelli A. (Inserm Transfert BIO13050 – LENTING /AS)

Travaux post doctoraux

Une grande partie de mes travaux post doctoraux se sont inscrits dans la continuité de ma thèse d'université qui avait démontré : i) la pertinence du concept assimilant le VWF à un biomarqueur d'anomalies de flux sanguin intracardiaque, ii) l'intérêt d'un anticorps monoclonal dirigé contre le domaine D4 du VWF pour prévenir la dégradation enzymatique du VWF sous ACM-FC. Suite à ces travaux et aux résultats de l'étude WITAWI (présentés ci-dessous), l'équipe 2 de l'UMR 1011 a obtenu un financement de Recherche Hospitalo-Universitaire en santé pour le projet WillAssistHeart (ANR-17-RHUS-0011). Ce projet coordonné par le Pr Susen a deux objectifs principaux : 1) développer un test "point of care" de quantification de la protéolyse du VWF à partir d'un anticorps anti-VWF A2 clivé développé spécifiquement à cet effet afin d'identifier en salle de cathétérisme les patients chez qui la procédure TAVI est compliquée d'une FPV et de contrôler l'efficacité ou non des mesures correctrices de la FPV par le cardiologue interventionnel; 2) identifier les patients sous d'ACM-FC à haut risque de saignements et développer pour ces patients de nouvelles approches thérapeutiques. Dans le contexte pandémique, notre équipe a également été très impliquée dans des travaux de recherche clinique et fondamentale soulignant l'importance des phénomènes d'endothéliopathie et d'immuno-thrombose dans la physiopathologie des formes sévères de COVID-19.

1. Le VWF comme biomarqueur d'anomalies de flux : du concept à son application en cardiologie interventionnelle

1.1. Le VWF comme biomarqueur péri-procédural du TAVI

La présence d'une fuite para valvulaire (FPV) post-TAVI a une mauvaise incidence pronostique. Elle reste actuellement une complication relativement fréquente (10-20%) malgré la mesure préimplantatoire par scanner aortique des dimensions de l'anneau aortique et les améliorations technologiques pour faciliter l'implantation prothétique⁹. Un contrôle de l'étanchéité de la valve par échographie trans-oesophagienne (ETO) demeure donc nécessaire pendant le TAVI ce qui impose le recours à une anesthésie générale. Cependant, l'ETO réalisée en salle de cathétérisme ne permet pas toujours une évaluation fiable de la FPV soulignant l'intérêt de disposer d'une méthode alternative qui permettrait d'envisager un TAVI mini-invasif sous anesthésie locale.

Un travail préliminaire de notre équipe avait identifié le caractère potentiellement discriminant d'une évaluation directe (par électrophorèse) ou indirecte (par la mesure du TO-ADP) de la multimérisation du VWF plasmatique pour évaluer la qualité de l'implantation valvulaire

pendant la procédure TAVI (Publication : Von Willebrand Factor As A Biological Sensor Of Blood Flow To Monitor Percutaneous Aortic Valve Interventions. Circ Res.2015). Cette observation a conduit à la mise en place de la cohorte prospective WITAVI (NCT02628509) qui avait pour objectif de confirmer l'utilité du VWF et du TO-ADP pour le diagnostic des FPV compliquant le traitement du RAO par TAVI.

Résultats

L'étude WITAVI a inclus une première cohorte mono-centrique de 183 patients (cohorte primaire, CHU de Lille) bénéficiant d'un TAVI et d'une ETO pour le diagnostic de FPV significative définies par un grade \geq modéré. Les patients chez qui le TAVI se compliquait d'une FPV persistante avaient un déficit en VWF-HPM non corrigé par la procédure TAVI. Chez les patients sans FPV ou pour lesquels la FPV était corrigée par une post-dilatation de la valve implantée, les VWF-HPM recouvraient leur niveau normal en fin de procédure TAVI (Figure 6). De façon notable, la cinétique du TO-ADP était superposable à celle des VWF-HPM selon la présence ou non d'une FPV et sa correction ou non par la post-dilatation de la valve.

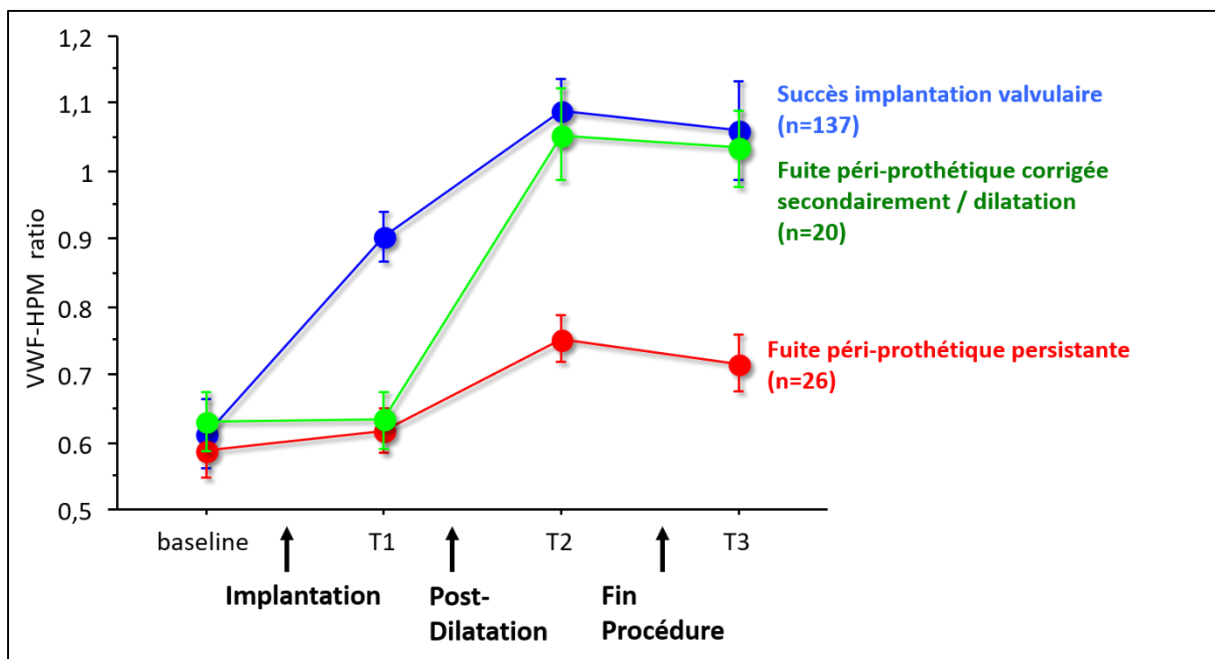


Figure 6 : Cinétique péri-procédurale de réversion du déficit plasmatique en VWF-HPM (quantification densitométrique > 15 mers relative à un pool plasmatique contrôle après électrophorèse sur SDS-agarose) lors du traitement du RAO par voie transcathéter (TAVI) en cas de succès immédiat de l'implantation valvulaire (absence de FPV, $n=137$), de la présence d'une FPV corrigée secondairement par une dilatation transcathéter de la valve ($n=20$), de la persistance d'une FPV en fin de procédure.

Une analyse par courbe ROC a identifié qu'un ratio seuil de VWF-HPM à 0,8 permettait de différencier les patients avec ou sans FPV en ETO avec une sensibilité, une spécificité et une valeur prédictive négative de respectivement 92%, 94%, et 98%. Concernant le TO-ADP,

l'analyse par courbe ROC a identifié une valeur seuil optimale de 180 sec pour le diagnostic de FPV avec une sensibilité, une spécificité et une valeur prédictive négative de respectivement de 92%, 92% et 98%. Cette association entre un ratio VWF-HPM < 0.8 ou un TO-ADP>180 sec et la présence d'une FPV en fin de procédure restait significative après ajustement sur l'âge, le sexe, la prise ou non de clopidogrel et la présence ou non d'une insuffisance mitrale.

Une deuxième cohorte multicentrique (CHU Toulouse et CHU Strasbourg) utilisée comme cohorte de validation a permis de confirmer une valeur seuil optimale de TO-ADP à 180 sec pour le diagnostic de FPV. De plus la mesure post-procédurale d'un TO-ADP>180 sec avait également une forte valeur pronostique, supérieure à la présence ou non d'une FPV en ETO, avec un risque de mortalité augmenté d'un facteur 3,5.

Conclusions et perspectives

L'étude WITAWI a démontré l'apport diagnostique et pronostique de l'analyse péri-procédurale de la multimérisation du VWF pour le diagnostic des FPV post-TAVI soit directement par électrophorèse, soit indirectement par un test sanguin de diagnostic rapide sensible aux anomalies de multimérisation du VWF. Les cardiologues de notre unité évaluent si ce concept est également transposable à la prise en charge de l'insuffisance mitrale par réparation mitrale percutanée (procédure MitraClip). Au-delà de son intérêt comme marqueur péri-procédural de la qualité de l'implantation valvulaire dans le TAVI, l'analyse directe (par électrophorèse) ou indirecte (par le TO-ADP) de la multimérisation du VWF pourrait avoir également un intérêt pour dépister une dégénérescence de la bio-prothèse aortique. Le suivi au long cours des patients inclus dans la cohorte WITAVI permettra de préciser ce point.

1.2. Vers un TAVI mini-invasif grâce à un monitoring *point of care* du VWF

L'examen de référence pour l'analyse de la multimérisation du VWF repose sur une technique électrophorétique chronophage incompatible avec un monitoring péri-procédural du VWF dans le TAVI. Le TO-ADP est un paramètre biologique très sensible à la présence d'anomalies constitutionnelles ou acquises de multimérisation du VWF, et qui présente comme avantages d'être reproductible et rapidement réalisable, ce qui permet d'envisager son utilisation en salle de cathétérisme cardiaque comme test de biologie délocalisée pour évaluer la qualité de l'implantation prothétique dans la procédure TAVI. Un essai national multicentrique (étude WITAVI-Real, NCT03728049) est en cours afin d'évaluer en vie réelle l'impact du suivi du VWF par la mesure du TO-ADP dans la procédure TAVI. Cet essai coordonné par le Dr Vincent (cardiologue) a obtenu une subvention du PHRC-N 2017. En parallèle, l'un des objectifs du RHU WillAssistHeart est de développer un test *point of care* en vue d'une mesure péri-procédurale de la protéolyse du VWF pendant la procédure TAVI sans être tributaire du

laboratoire d'hématologie. Afin d'être brevetable, ce test sera basé sur l'emploi d'un autre anticorps anti VWF-A2 clivé que l'anticorps commercial (mAb27642) utilisé lors de mon travail de thèse pour la mise au point d'un test pilote de quantification de la protéolyse du VWF par méthode ELISA. Nous avons en effet pu démontrer que l'anticorps mAb27642 ne se lie qu'aux formes les moins multimérisées de VWF clivé (dimères, tétramères). Ce résultat indique que la quantification de la protéolyse du VWF peut encore être optimisée en utilisant un autre anticorps reconnaissant spécifiquement le VWF clivé indépendamment de sa longueur multimérique. Le développement et la validation d'un nouveau test de quantification de la protéolyse du VWF en vue d'une application dans le TAVI fait l'objet d'une collaboration avec l'UMR-1176 (ex U770) et l'entreprise Stago dans le cadre du RHU WillAssistHeart. Après criblage d'une librairie synthétique de nanobodies humanisés anti-VWF, l'UMR-1176 a identifié 2 nanobodies candidats : l'un spécifique du VWF clivé, l'autre du VWF non clivé. Les performances de ces nanobodies anti-VWF sont actuellement évaluées par notre équipe sur une plasmathèque de MW constitutionnelle ou acquise afin d'identifier le meilleur candidat pour la mise au point par la société Stago d'un test ELISA pilote puis d'un dispositif *point of care* de mesure de la protéolyse du VWF. L'objectif final sera d'évaluer dans un essai clinique l'intérêt de ce dispositif *point of care* dans le TAVI pour détecter en temps réel une FPV et évaluer l'efficacité de sa correction.

Manuscrits :

1. CT-ADP Point-of-Care Assay Predicts 30-Day Paravalvular Aortic Regurgitation and Bleeding Events following Transcatheter Aortic Valve Replacement. Kibler M, Marchandot B, Messas N, Caspar T, Vincent F, Von Hunolstein JJ, Grunebaum L, Reydel A, **Rauch A**, Crimizade U, Kindo M, Hoang Minh T, Trinh A, Petit-Eisenmann H, De Poli F, Leddet P, Jesel L, Ohlmann P, Susen S, Van Belle E, Morel O. *Thromb Haemost.* 2018;118(5):893-905. (IF: 4.7)
2. Von Willebrand Factor and Management of Heart Valve Disease: JACC Review Topic of the Week. Van Belle E, Vincent F, **Rauch A**, Casari C, Jeanpierre E, Loobuyck V, Rosa M, Delhay C, Spillemaeker H, Paris C, Debry N, Verdier B, Vincentelli A, Dupont A, Lenting PJ, Susen S. *J Am Coll Cardiol.* 2019;73(9):1078-1088. (IF: 20.5)
3. Von Willebrand Factor for Aortic Valve Intervention: From Bench to Real-Time Bedside Assessment. Vincent F, **Rauch A**, Loobuyck V, Moussa M, Juthier F, Debry N, Jeanpierre E, Lenting PJ, Susen S, Van Belle E. *Circ Res.* 2018;122(11):1499-1500. (IF: 15.8)
4. Real-Time Monitoring of von Willebrand Factor in the Catheterization Laboratory: The Seatbelt of Mini-Invasive Transcatheter Aortic Valve Replacement? Vincent F, **Rauch A**, Spillemaeker H, Vincentelli A, Paris C, Rosa M, Dupont A, Delhay C, Verdier B, Robin E, Lenting PJ, Susen S, Van Belle E. *JACC Cardiovasc Interv.* 2018;11(17):1775-1778. (IF: 9.5)
5. Von Willebrand Factor Multimers during Transcatheter Aortic Valve Replacement. Van Belle E*, **Rauch A***, Vincent F, Robin E, Kibler M, Labreuche J, Jeanpierre E, Levade M, Hurt C, Rousse N, Dally JB, Debry N, Dallongeville J, Vincentelli A, Delhay C, Auffray JL, Juthier F, Schurtz G, Lemesle G, Caspar T, Morel O, Dumonteil N, Duhamel A, Paris C, Dupont-Prado A, Legendre P, Mouquet F, Marchant B, Hermoire S, Corseaux D, Moussa K, Manchuelle A, Bauchart JJ, Loobuyck V, Caron C, Zawadzki C, Leroy F, Bodart JC, Staels B, Goudemand J, Lenting PJ, Susen S. *N Engl J Med.* 2016; 375(4):335-44. (IF: 72.4)

2. Hémostase et assistances circulatoires mécaniques : nouvelles approches diagnostiques et thérapeutiques

Le deuxième axe de travail de mon post doctorat a porté sur les ACM- avec comme objectifs : i) d'améliorer l'identification des patients à haut risque de saignement, ii) d'identifier de nouvelles approches thérapeutiques, pharmacologiques ou non, permettant de limiter l'impact de ces dispositifs sur l'hémostase.

1.1. Identification des patients à haut risque de saignement sous ECMO

Il existe un faisceau d'arguments suggérant qu'un déficit plasmatique congénital ou acquis en VWF-HPM induit une dérégulation de l'angiogénèse traduisant par la formation d'angiodysplasies digestives ou nasales (« first hit ») pouvant être responsables d'hémorragies à répétition¹⁹. La problématique des hémorragies digestives et nasales est plus aiguë sous ACM-FC que dans les formes concernées de MW constitutionnelle car une anticoagulation est requise pour la prévention d'évènements thrombo-emboliques sous ACM-FC (« second-hit ») alors que la prescription d'anti-thrombotiques est classiquement contre-indiquée dans la MW. Cette association entre angiodysplasies et déficit plasmatique en VWF-HPM pourrait résulter soit d'un rôle anti-angiogénique des VWF-HPM, soit d'un rôle pro-angiogénique du VWF clivé. L'étude WITECMO-H (NCT03070912) dont je suis l'investigateur principal a ainsi pour objectif d'évaluer si la quantification de la protéolyse du VWF et/ou la mesure de la densité capillaire par vidéo-microscopie sublinguale à 48 heures de l'implantation d'une ECMO améliorent la valeur prédictive d'un score hémorragique spécifiquement développé et validé dans cette indication. La quantification de la protéolyse du VWF sera effectuée avec la version ELISA du test développé en partenariat avec l'U1176 et l'entreprise Stago reposant sur l'utilisation d'un anticorps reconnaissant spécifiquement les multimères de VWF sous une forme clivée et indépendamment de leur taille. La mesure de densité capillaire par vidéo-microscopie sublinguale a été choisie pour évaluer la présence ou non d'anomalies de la microcirculation car il s'agit d'un examen non-invasif facilement réalisable sous ECMO contrairement à une naso-fibroscopie ou une endoscopie digestive.

1.2. Prévention du syndrome de Willebrand acquis sous ACM-FC

1.2.1. Approches pharmacologiques

Approche substitutive par concentrés de VWF

Une première approche pharmacologique dite substitutive consiste à administrer par voie intraveineuse un concentré de VWF soit en curatif en cas de saignement, soit en prophylaxie primaire. Cette administration exogène de VWF-HPM est susceptible d'améliorer l'hémostase non seulement en restaurant une adhésion et une agrégation plaquettaire normale mais

également par une action anti-angiogénique. Elle est parfois proposée hors AMM en vie réelle lors de saignements incontrôlés notamment sous ECMO. Cette approche substitutive n'est cependant pas dénuée de risque thrombotique au vu des comorbidités cardio-vasculaires des patients sous ACM-FC et du risque thrombotique en lien avec une administration trop intensive de concentrés de VWF susceptible d'entraîner une augmentation très importante du taux de facteur VIII. Aussi, seule l'utilisation d'un concentré de VWF pauvre en facteur VIII (Wilfactin®) a été retenue par notre équipe dans le cadre de l'essai national multicentrique randomisé en ouvert PHAM (NCT02488525, subvention du PHRC-N, investigateur principal : Pr Susen) qui avait pour objectif d'évaluer l'efficacité et la sécurité de cet approche pour les patients bénéficiant d'une assistance mono-ventriculaire gauche à flux continu (HeartMate-II® ou HeartWare®) dans les trois mois suivants l'implantation de l'ACM-FC où l'incidence des complications hémorragiques est la plus élevée. Bien que cet essai ait dû être interrompu prématurément en raison d'un défaut d'inclusions, nous disposons de données pharmacocinétiques indiquant que cette approche substitutive ne permet pas de restaurer de façon complète et prolongée le déficit plasmatique en VWF-HPM sous ACM-FC. Une fois l'analyse des données cliniques complétée, ce travail sera soumis pour publication.

Inhibition de la protéolyse du VWF par un anticorps monoclonal humanisé

Protéolyse du VWF sous ACM-FC : un mécanisme 2A- ou 2B-like ?

L'intensité des forces de cisaillement produites par le flux sanguin régule non seulement la protéolyse du VWF par l'ADAMTS13 mais également la liaison du VWF à la glycoprotéine Iba (GPIba) plaquettaire. L'élongation du VWF par les forces de cisaillement favorise l'exposition du domaine A1, où se trouve le site de liaison à la GPIba plaquettaire³. Le VWF lié aux plaquettes est plus susceptible au clivage par l'ADAMTS13 ce qui explique l'excès de protéolyse du VWF également présent dans la MW congénitale de type 2B. Par analogie à la MW congénitale de type 2B où une mutation gain de fonction augmente l'affinité du domaine A1 du VWF pour la GPIba, certains auteurs ont émis l'hypothèse que l'ACM-FC pourrait également induire un gain d'interaction du VWF pour la GPIba plaquettaire.

Le rapport initial d'expertise du projet RHU Will-Assist Heart avait ainsi logiquement souligné l'importance d'évaluer si la dégradation du VWF sous ACM-FC était secondaire soit à un gain d'interaction VWF-GPIba mimant une MW de type 2B, soit à un excès de protéolyse du VWF non lié aux plaquettes mimant une MW de type 2A. Cette question est centrale car elle conditionne : i) le choix de l'approche candidate pour développer une molécule inhibant la protéolyse du VWF sous ACM-FC; ii) le choix du VWF clivé comme outil biologique d'évaluation de la qualité de l'implantation valvulaire lors du traitement du RAo par TAVI. Nous avons adapté notre modèle initial d'ACM-FC *in vitro* afin de développer un nouveau circuit

basé sur l'utilisation d'une pompe d'ECMO afin d'étudier la dynamique d'interaction entre VWF et plaquettes en conditions de flux.

Résultats

Dans ce nouveau modèle, nous avons confirmé une inhibition quasi-totale de la protéolyse du VWF en présence de l'anticorps LTX-508 alors que cette inhibition n'est que partielle avec un anticorps anti-VWF A1 inhibant l'interaction VWF-GPIIb α plaquettaire. Lors de la perfusion de plasma pauvre en plaquettes dans le modèle d'ECMO, la cinétique de dégradation du VWF est identique à celle observée avec la perfusion de plasma ayant un contenu normal en plaquettes et demeure quasi-totalement inhibée en présence du LTX-508. Nous avons également observé la présence d'un shedding des récepteurs d'enveloppe plaquettaire GPIIb α et GPVI dépendant de l'intensité des forces de cisaillement appliquées dans ce modèle d'ECMO *in vitro*. L'inhibition de l'interaction VWF-GPIIb α par un anticorps anti-VWF A1 ne modifie pas la cinétique du shedding de GPIIb α . La cinétique de shedding de GPIIb α n'est pas modifiée en présence dans le circuit d'une concentration élevée de concentré de VWF recombinant, similaire à celle observée chez les patients sous ECMO, bien que ce type de concentré contienne des VWF-THPM avec un nombre plus élevé de sites d'interaction pour les plaquettes. Nous avons également observé avec un nanobody de l'U1176 reconnaissant spécifiquement le domaine A1 du VWF dans sa conformation active de haute affinité pour le récepteur GPIIb α , qu'il n'y avait pas de modification de l'affinité du VWF pour les plaquettes en présence de forces de cisaillement élevées dans une condition où la protéolyse des VWF-HPM par l'ADAMTS13 est totalement inhibée par une concentration élevée d'EDTA.

Conclusion

Ces résultats encore non publiés démontrent que la dégradation du VWF sous ACM-FC est indépendante de l'interaction VWF-GPIIb α confirmant ainsi l'intérêt d'une inhibition sélective de la protéolyse du VWF par l'ADAMTS13 plutôt qu'une approche basée sur l'inhibition de l'interaction VWF-GPIIb α plaquettaire. Il existe actuellement au moins 2 projets concurrents de développement d'un anticorps monoclonal humanisé inhibant la protéolyse du VWF par l'ADAMTS13 sous ACM-FC : i) celui du Laboratory for Thrombosis Research (Kulak, KU Leuven, Courtrai, Belgique) reposant sur un anticorps anti-ADAMTS13 dirigé contre le domaine métallo-protéase contenant le site catalytique de l'enzyme ; ii) celui de notre équipe reposant sur un anticorps anti-VWF dirigé contre le domaine D4 du VWF contenant un exosite critique pour la liaison de la portion C-terminale de l'ADAMTS13 au VWF. Notre approche présente comme avantage de préserver un niveau résiduel de protéolyse du VWF par l'ADAMTS13, minimisant ainsi le risque de PTT pharmaco-induit.

Humanisation de l'anticorps monoclonal murin anti-VWF D4 (LTX-508)

Ce travail correspond au Work package 2 du RHU WillAssistHeart qui a pour objectif de développer à partir de l'anticorps murin LTX-508 un anticorps thérapeutique monoclonal humanisé en vue d'une indication dans la prévention des complications hémorragiques sous ECMO. Ce travail fait l'objet d'une nouvelle collaboration avec l'U1176. Après séquençage de l'anticorps parental à partir de la lignée d'hybridome, l'U1176 a utilisé une approche d'humanisation *in silico* pour obtenir des variants humanisés recombinants du LTX-508. Après sélection des variants conservant une liaison au VWF similaire à l'anticorps parental de référence, l'U1176 a évalué la capacité de ces variants à inhiber la protéolyse du VWF par l'ADAMTS13 dans un modèle de vortex *in vitro*. Cette évaluation préliminaire a permis d'identifier trois variants candidats qui sont actuellement produits en plus grande quantité afin d'être ensuite évalué dans notre modèle d'ACM-FC *in vitro*. Si ces tests sont concluants, les leads pourront être sélectionnés pour i) une étape d'ingénierie du fragment Fc de façon à générer un anticorps d'isotype IgG1 ou IgG4, ii) évaluation de leurs propriétés pharmacocinétiques dans un modèle de souris humanisée pour le récepteur FcRn. L'anticorps candidat final sera ensuite évalué dans deux modèles animaux: i) un modèle murin de maladie de Willebrand de type 2A en cours de développement par l'U1176 (souris avec une expression hétérozygote de VWF/p.R1597W à l'origine d'une susceptibilité accrue du VWF plasmatique à la protéolyse par l'ADAMTS13 et humanisée pour la portion extracellulaire du récepteur plaquettaire Gplb α) ; ii) un modèle porcin d'ACM-FC développé par notre équipe.

1.2.2. Approche non pharmacologique : préservation de la pulsatilité artérielle

Les ACM-FC induisent des forces de cisaillement supra-physiologiques induisant un déficit acquis en VWF-HPM résultant d'un excès de protéolyse par l'ADAMTS13 mais également une diminution de la pulsatilité artérielle. Sous ACM-FC, le degré de diminution de la pulsatilité artérielle est variable en fonction de la persistance ou non d'une pulsatilité cardiaque native et une faible pulsatilité résiduelle est un facteur de risque de saignement²⁰. Lors du traitement du RAo par voie transcathéter, nous avons observé deux profils différents d'évolution des taux plasmatique du propeptide du VWF (VWFpp) : i) soit une élévation aiguë concomitante à la normalisation du profil multimérique du VWF en cas de traitement efficace du RAo par TAVI, ii) soit un taux stable de VWFpp en cas de traitement partiel du RAo par valvuloplastie associé à la persistance d'un déficit plasmatique en VWF-HPM. Le VWFpp étant contenu dans les corps de Weibel-Palade intra-endothéliaux, cette observation suggérait que le TAVI induisait un relargage endothélial aigu de VWF contrairement à la valvuloplastie. Bien que le mécanisme sous-jacent à ce relargage endothélial de VWF n'ait pas été formellement caractérisé, nous avons émis l'hypothèse d'un rôle causal de la pulsatilité artérielle sur des

arguments indirects : i) le RAO est associé à une diminution de la pulsatilité artérielle et sa correction à une normalisation de celle-ci; ii) l'endothélium vasculaire a la propriété de réagir *in vitro* à des stimuli physiques (forces de cisaillement engendrées par un flux laminaire ou « stretch aiguë hypertensif ») via un relargage endothélial de VWF à partir des corps de Weibel-Palade^{21,22}. Nous avons donc développé un modèle animal afin d'évaluer si le niveau de pulsatilité résiduelle sous ACM-FC pouvait atténuer les anomalies de multimérisation de VWF par l'intermédiaire d'une stimulation du relargage endothélial du VWF dans un environnement à forces de cisaillement élevées. L'élaboration de ce modèle animal a fait l'objet du travail de Master 2 de Flavien Vincent. Afin d'isoler le rôle de la pulsatilité artérielle, nous avons développé un modèle animal porcin d'ACM-FC à forces de cisaillement élevées permettant de moduler le niveau de pulsatilité artérielle résiduelle en fonction du positionnement transcathéter de la pompe dans le ventricule gauche (perte de la pulsatilité cardiaque secondaire à une éjection ventriculaire continue indépendamment du cycle diastole/systole) ou dans l'aorte ascendante (modèle à pulsatilité cardiaque conservée).

Résultats

Nous avons tout d'abord caractérisé *in vitro* l'effet intrinsèque des 2 pompes d'ACM-FC destinées à être utilisées dans le modèle animal sur la dégradation du VWF en l'absence d'endothélium. Dans un premier modèle animal d'ACM-FC à forces de cisaillement élevées sur cœur sain, nous avons évalué la cinétique d'apparition des anomalies de multimérisation du VWF dans trois conditions de pulsatilité artérielle résiduelle (basse, intermédiaire ou normale) en fonction du positionnement de chaque pompe dans le ventricule gauche ou dans l'aorte. Que ce soit par électrophorèse ou analyse de la liaison du VWF au collagène, une perte significative des VWF-HPM a été observée dans les trois conditions étudiées. Cependant, la cinétique de perte des VWF-HPM était plus prononcée en l'absence de pulsatilité qu'en présence d'une pulsatilité de niveau intermédiaire ou normale. Afin de s'affranchir d'une variabilité inter-animale, nous avons développé un second modèle animal d'ACM à forces de cisaillement élevées sur cœur sain avec une pulsatilité variable en cross-over. Dans ce nouveau modèle, nous avons confirmé que la préservation d'une pulsatilité artérielle résiduelle était associée à une réduction des anomalies de multimérisation du VWF sous ACM-FC à forces de cisaillement constantes. Nous avons également mis en évidence une augmentation aiguë des taux de VWF, facteur VIII et d'angiopoiétine-2 après exposition de l'endothélium à une pulsatilité élevée. Ces trois protéines étant stockées dans les corps de Weibel-Palade endothéliaux, cette observation suggère qu'un relargage endothélial de VWF intervient rapidement en réponse à la normalisation de la pulsatilité dans un environnement de forces de cisaillement élevées. Pour illustrer ce concept, nous avons également décrit le cas d'un patient ayant bénéficié d'une séquence inédite d'ACM (ACM-FC et ACM-FP)

caractérisée par des niveaux variables de pulsatilité artérielle. Chez ce patient, nous avons observé une rapide dégradation des VWF-HPM sous ACM-FC puis une normalisation rapide des anomalies de multimérisation du VWF après implantation d'une ACM-FP.

Conclusion et perspectives

En conclusion, cette étude ouvre une piste non pharmacologique pour la prévention des saignements sous ACM-FC reposant sur la préservation d'une pulsatilité artérielle élevée pour réduire les anomalies de multimérisation du VWF dans le compartiment plasmatique (Figure 7).

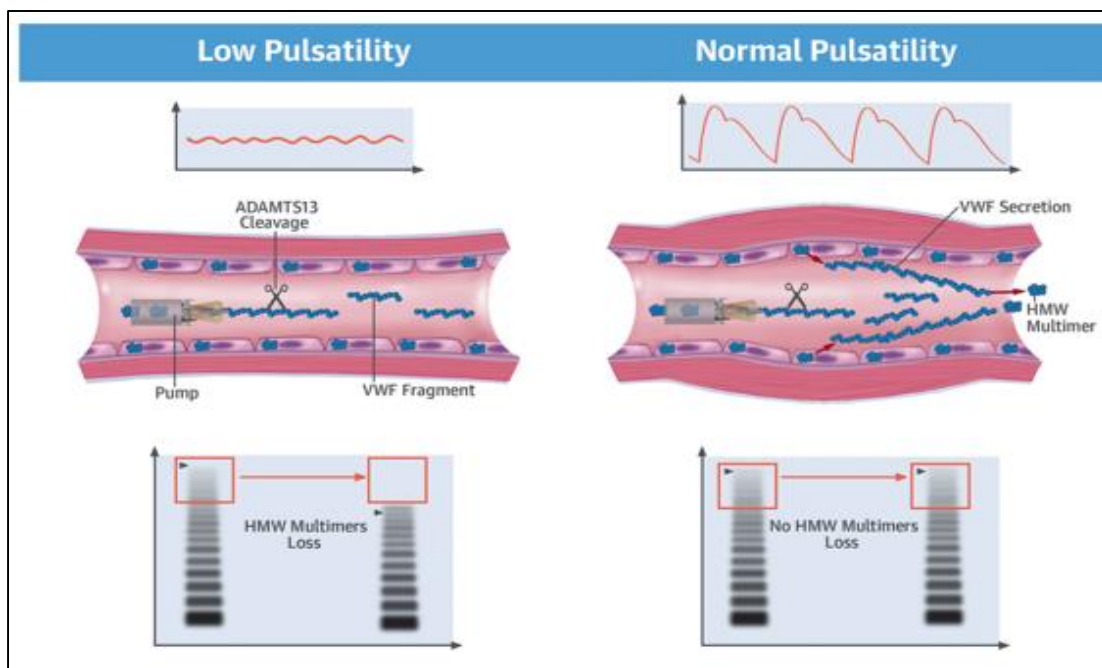


Figure 7 : modulation du déficit plasmatique en VWF-HPM en fonction du niveau résiduel de pulsatilité artérielle dans un environnement à forces de cisaillement élevées sous ACM-FC. En présence d'une faible pulsatilité sous ACM-FC, l'excès de protéolyse du VWF par l'ADAMTS13 induit une élimination rapide des VWF-HPM du plasma. En présence d'une pulsatilité résiduelle élevée sous ACM-FC, la stimulation de la libération endothéliale de VWF compense au moins partiellement le déficit en VWF-HPM résultant de l'excès de protéolyse par l'ADAMTS13

Deux limitations empêchent à ce stade de transposer ces résultats aux patients sous ACM-FC : i) alors que ces résultats ont été obtenus dans un modèle animal à endothélium sain, on ne peut exclure que la dysfonction endothéliale associée à l'insuffisance cardiaque sévère des patients bénéficiant d'une ACM-FC limite le relargage ou la production endothéliale de VWF et donc le bénéfice supposé d'une plus grande pulsatilité résiduelle ; ii) il reste nécessaire de confirmer si ce phénomène observé sur quelques heures se maintient sur une plus grande échelle de temps avant de considérer une application potentielle en clinique.

Ce travail a une nouvelle fois souligné l'intérêt du VWF comme marqueur rhéologique afin d'optimiser l'ingénierie de nouveaux prototypes d'assistances circulatoires. Nous avons ainsi participé à l'évaluation préclinique *in vitro* et *in vivo* du cœur artificiel pulsatile CARMAT montrant que la structure et l'activité du VWF sont préservées avec ce dispositif. En 2018, notre équipe a également obtenu en association avec le partenaire industriel CORWAVE un financement PSPC (« programme de soutien aux pôles de compétitivité») de BpiFrance pour le projet CALYPSO dont l'objectif est de développer un dispositif d'assistance circulatoire pulsatile disposant d'une meilleure hémocompatibilité pour les patients en insuffisance cardiaque terminale inéligibles à la greffe. Le projet PSPC Calypso inclut également un travail de recherche fondamentale qui a pour objectif principal d'évaluer l'impact des conditions de flux sur la synthèse et la sécrétion de VWF par l'endothélium vasculaire dans le cadre d'une collaboration scientifique avec le laboratoire d'Hydrodynamique de l'Ecole polytechnique dirigé par le Pr Barakat. Ce projet a également pour objectif secondaire d'identifier de nouveaux marqueurs endothéliaux et voies de signalisation sensibles aux conditions de flux via une approche transcriptomique. Nous utiliserons un modèle d'artère humaine perfusée²³ permettant d'évaluer l'impact endothélial de différentes conditions de flux selon le niveau de forces de cisaillement et de pulsatilité.

Manuscrits :

1. Acquired von Willebrand Syndrome in Patients With Ventricular Assist Device. **Rauch A**, Susen S, Zieger B. *Front Med (Lausanne)*. 2019;6:7. (IF: 3.9)
2. Arterial Pulsatility and Circulating von Willebrand Factor in Patients on Mechanical Circulatory Support. Vincent F*, **Rauch A***, Loobuyck V, Robin E, Nix C, Vincentelli A, Smadja DM, Leprince P, Amour J, Lemesle G, Spillemaeker H, Debry N, Latremouille C, Jansen P, Capel A, Moussa M, Rousse N, Schurtz G, Delhay C, Paris C, Jeanpierre E, Dupont A, Corseaux D, Rosa M, Sottejeau Y, Barth S, Mourran C, Gomane V, Coisne A, Richardson M, Caron C, Preda C, Ung A, Carpentier A, Hubert T, Denis C, Staels B, Lenting PJ, Van Belle E, Susen S. *J Am Coll Cardiol*. 2018;71(19):2106-2118. (IF: 18.6) *coauteurs
3. The Carmat Bioprosthetic Total Artificial Heart Is Associated With Early Hemostatic Recovery and no Acquired von Willebrand Syndrome in Calves. Smadja DM, Susen S, **Rauch A**, Cholley B, Latremouille C, Duvéau D, Zilberstein L, Méléard D, Boughenou MF, Belle EV, Gaussem P, Capel A, Jansen P, Carpentier A. *J Cardiothorac Vasc Anesth*. 2017;31(5):1595-1602. (IF: 1.5)
4. Circulatory support devices: Fundamental aspects & clinical management of bleeding and thrombosis. Susen S, **Rauch A**, Van Belle E, Vincentelli A, Lenting PJ. *J Thromb Haemost* 2015; 13(10):1757-67. (IF: 5.5)

3. Rôle du cross-talk hémostase-inflammation dans la COVID-19

La pandémie COVID-19 a joué un rôle structurant dans notre équipe puisqu'elle nous a permis d'initier une série de travaux associant approches cliniques et fondamentales sur une thématique *Hémostase et inflammation*.

Dans la majorité des cas, la COVID-19 est une infection bénigne limitée aux voies aériennes supérieures. Toutefois, 15 à 20 % des patients infectés développent une pneumopathie qui peut évoluer vers un syndrome de détresse respiratoire aigu (SDRA), parfois associé à une défaillance multi-viscérale. Le récepteur de l'enzyme de conversion de l'angiotensine 2 (ACE2) constitue la porte d'entrée du SARS-CoV-2 pour infecter ses cellules cibles. Ce récepteur est très fortement exprimé non seulement par les cellules épithéliales pulmonaires mais également par les cellules endothéliales vasculaires suggérant un possible tropisme endothélial du SARS-CoV-2. Plusieurs équipes dont la nôtre ont rapidement fait état d'une incidence anormalement élevée d'événements thrombotiques veineux ou artériels chez les patients hospitalisés pour une forme sévère de COVID-19. Dans la cohorte lilloise, l'incidence des thromboses pulmonaires dans les formes réanimatoires de COVID-19 était de l'ordre de 20 à 30% chez les patients de la première vague épidémique versus 7.5% chez les patients avec un SDRA d'origine grippale et 6% chez les patients avec un SDRA toute cause confondue (Susen S et al, Circulation 2020, étude détaillée dans la section « recherche clinique »). Des études anatomo-pathologiques ont ensuite soulignées que ce risque thrombotique concernait également la microcirculation avec une fréquence plus élevée de micro-thrombi dans les capillaires alvéolaires pulmonaires de patients décédés du COVID-19 que chez ceux décédés d'une pneumopathie grippale H1N1. Ces autopsies ont également mis en évidence que les formes sévères de COVID-19 s'accompagnaient de lésions endothéliales diffuses au niveau pulmonaire mais également dans d'autres organes^{24,25}. Ces données préliminaires suggéraient un excès d'activation de la coagulation en lien avec l'intensité de la réponse inflammatoire réactionnelle à la COVID-19 et la présence de lésions endothéliales.

3.1. Cytotoxicité endothéliale induite par le plasma dans les formes sévères de COVID-19

En l'absence de preuve d'un effet cytopathogène du SARS-CoV-2 sur les cellules endothéliales, nous avons émis l'hypothèse que l'intensité du processus thrombo-inflammatoire réactionnel à la COVID-19 pouvait jouer un rôle critique dans l'induction de lésions endothéliales au niveau du lit vasculaire pulmonaire. A partir d'un modèle de culture de cellules endothéliales pulmonaires humaines (HPMVEC), nous avons évalué si le plasma de patients COVID-19 prélevés à différents stades de la maladie pouvait induire l'apparition

de lésions endothéliales *in vitro*. La cytotoxicité des plasmas COVID-19 vis-à-vis des cellules HPMVEC a été évaluée par la mesure de l'activité mitochondriale résiduelle (WST-1 test) après une heure de co-incubation. Nous avons observé une perte significative de la viabilité cellulaire des HPMVEC au contact de plasmas de patients hospitalisés pour COVID-19 comparé aux résultats obtenus avec des plasmas de sujets sains. Au sein du groupe COVID-19, la cytotoxicité endothéliale était plus élevée avec les plasmas de patients atteints d'une forme réanimatoire de COVID-19 comparé à ceux atteints d'une forme non-réanimatoire. Nous avons également observé une réduction du niveau de cytotoxicité endothéliale chez les patients convalescents d'une forme réanimatoire de COVID-19 comparé au niveau de cytotoxicité observé à l'admission. Nous avons également observé une association entre la sévérité de la cytotoxicité endothéliale induite par le plasma *in vitro* et les taux plasmatiques de marqueurs de lésions d'organe, de marqueurs de lésion endothéliale ou de marqueurs reflétant l'intensité de la réponse immunitaire réactionnelle *in vivo*. Nous avons alors émis l'hypothèse que le cross-talk endothéliopathie-dérégulation immunitaire présente dans les formes sévères de COVID-19 pouvait non seulement contribuer aux événements macro-thrombotiques veineux ou artériels mais également à l'apparition d'une micro-angiopathie aggravant la défaillance respiratoire et susceptible de contribuer à d'autres défaillances d'organes.

3.2. Etude du cross-talk endothéliopathie- dérégulation immunitaire dans les formes sévères de COVID-19

Ceci a conduit à une deuxième étude ayant pour objectif d'évaluer dans une cohorte de patients admis en réanimation pour une forme sévère de COVID-19 le rôle du cross-talk entre endothéliopathie et dérégulation immunitaire dans la progression de la défaillance respiratoire et la survenue d'autres défaillances d'organes. Pour cela, nous avons dosé à l'admission en réanimation les taux plasmatiques de marqueurs: i) de lésion endothéliale (VWF, TFPI, PAI-1, syndécan-1, thrombomoduline soluble) ii) de l'intensité de la réponse inflammatoire réactionnelle (cytokines, fractions activées du complément, nucléosomes solubles). Nous avons observé que le degré d'endothéliopathie à l'admission était significativement associé à l'intensité de la dérégulation immunitaire présente à l'admission et à la survenue d'une dysfonction hépatique et d'une défaillance multi-viscérale en cours d'hospitalisation. Bien qu'ils ne permettent pas d'établir de lien de causalité, ces résultats renforcent l'hypothèse d'un cross-talk entre dérégulation immunitaire et endothéliopathie dans la physiopathologie des défaillances d'organes dans les formes sévères de COVID-19.

L'originalité de cette étude provenait également de l'inclusion de patients ayant requis une assistance respiratoire par ECMO veino-veineuse. Nous avons pu analyser chez 8 patients

explantés vivants la composition des caillots recueillis prospectivement au niveau de la tête de pompe, de l'oxygénateur ou des tubulures d'ECMO. Nous avons limité cette analyse histologique aux patients avec une durée limitée de support par ECMO afin de minimiser l'effet confondant de complications non-spécifiques de la réanimation. Cette analyse histologique a mis en évidence une quantité plus importante d'histones citrullinées, un marqueur spécifique de NETs (neutrophil extracellular traps) dans les caillots provenant de patients COVID-19 comparés à ceux prélevés chez des patients ECMO contrôles. Ce résultat suggère l'implication de la NETose dans l'hypercoagulabilité caractéristique des formes sévères de COVID-19.

Conclusion et perspectives

Les formes sévères de COVID-19, contrairement à d'autres infections respiratoires virales apparentées, s'accompagnent de lésions endothéliales diffuses en lien avec l'intensité du processus inflammatoire réactionnel. Ce cross-talk contribue à l'état d'hypercoagulabilité macro- et micro-vasculaire caractéristique de cette infection. Bien que les mécanismes impliqués dans la cytotoxicité endothéliale induite par le plasma restent à identifier, ces résultats suggèrent l'intérêt de traitements ciblant la composante thromboinflammatoire chez les patients à risque de développer une forme sévère de COVID-19.

Manuscrits:

1. Vascular Endothelial Damage in the Pathogenesis of Organ Injury in Severe COVID-19. Dupont A*, **Rauch A***, Staessens S, Moussa M, Rosa M, Corseaux D, Jeanpierre E, Goutay J, Caplan M, Varlet P, Lefevre G, Lassalle F, Bauters A, Faure K, Lambert M, Duhamel A, Labreuche J, Garrigue D, De Meyer SF, Staels B, Vincent F, Rousse N, Kipnis E, Lenting P, Poissy J, Susen S; Lille Covid Research Network (LICORNE). *Arterioscler Thromb Vasc Biol.* 2021 Feb 25:ATVBAHA120315595. In press (*IF: 6.6*) *coauteurs
2. Endotheliopathy Is Induced by Plasma From Critically ill Patients and Associated With Organ Failure in Severe COVID-19. **Rauch A***, Dupont A*, Goutay J, Caplan M, Staessens S, Moussa M, Jeanpierre E, Corseaux D, Lefevre G, Lassalle F, Faure K, Lambert M, Duhamel A, Labreuche J, Garrigue D, De Meyer SF, Staels B, Van Belle E, Vincent F, Kipnis E, Lenting PJ, Poissy J, Susen S; Lille COVID Research Network (LICORNE); Members of the LICORNE Scientific Committee. *Circulation.* 2020;142(19):1881-1884. (*IF: 23.6*) *coauteurs

Recherche clinique

1. Thématique *Maladies hémorragiques constitutionnelles* (filiale MHEMO)

La prise en charge des patients atteints de maladie de Willebrand (MW) ou d'hémophilie s'effectue en France dans les Centres de Ressources et de Compétences constitutifs de la Filière de Santé Maladies Hémorragiques constitutionnelles (MHEMO). Au sein de la filiale MHEMO, le service d'hémostase clinique du CHU de Lille est labellisé Centre de Ressources et de Compétences pour l'hémophilie et Centre national de Référence pour la Maladie de Willebrand (CRMW). En parallèle de mon activité de recherche au sein de l'U1011, j'ai donc participé au sein de la filiale MHEMO en tant qu'investigateur à des essais clinique à promotion industrielle ainsi qu'à des projets académiques portés par le CRMW concernant des patients atteints d'hémophilie ou de MW. Seuls deux projets académiques en lien avec le CRMW sont détaillés dans ce manuscrit : il s'agit de l'étude PHAM mentionnée plus haut et d'une étude détaillée ci-dessous qui visait à préciser l'apport de la vidéocapsule endoscopique dans le bilan étiologique d'une hémorragie digestive dans un contexte de MW.

Certaines formes de MW sont caractérisées par une incidence élevée d'hémorragies digestives sur angiodysplasies. Il s'agit principalement de la MW de type 3 (dans lesquelles le déficit en VWF concerne à la fois le compartiment endothélial, plasmatique et plaquettaire) et des formes constitutionnelles ou acquises de MW associées à un déficit plasmatique en VWF-HPM. L'identification des angiodysplasies digestives est souvent difficile par endoscopie conventionnelle car ces lésions sont volontiers multiples et localisées au niveau de l'intestin grêle. La vidéocapsule endoscopique constitue ainsi l'examen endoscopique de référence pour le diagnostic d'angiodysplasies digestives. Ceci a motivé la réalisation d'une étude afin d'évaluer dans la MW constitutionnelle l'intérêt diagnostique et pronostique de la vidéocapsule endoscopique en complément de l'endoscopie conventionnelle lors de l'exploration d'une hémorragie digestive.

Résultat

Cette étude multicentrique rétrospective impliquant 18 centres de la filiale MHEMO a inclus un total de 50 patients avec présenté au moins un épisode d'hémorragie digestive sur la période 2015-2018. Elle confirme que les angiodysplasies digestives constituent la cause principale d'hémorragies digestives dans la MW. La localisation de la source des saignements gastro-intestinaux était significativement améliorée lors de l'exploration par endoscopie utilisant la vidéocapsule, et ce même chez les patients sans antécédent d'angiodysplasie. Les patients atteints d'angiodysplasie présentaient plus de récurrences hémorragiques gastro-intestinales. Une survie sans récurrence plus faible était observée chez les patients atteints

d'angiodysplasie, et en particulier lorsque les lésions étaient localisées à l'intestin grêle, et ce, même après l'électrocoagulation endoscopique au plasma argon.

Conclusion

La vidéocapsule endoscopique doit être utilisée plus systématiquement chez les patients atteints de MW avec des saignements gastro-intestinaux inexpliqués ou récurrents à la recherche d'une angiodysplasie à haut risque de rechute et/ou éligible à une électrocoagulation endoscopique. Ces données observationnelles renforcent l'hypothèse d'une dérégulation de l'angiogénèse dans la MW, plus particulièrement dans les types de MW associés à un déficit endothélial et/ou plasmatique en VWF-HPM (type 2A, 2B et 3).

Manuscripts:

1. Final Results of PUPs B-LONG Study: Evaluating Safety and Efficacy of rFIXFc in Previously Untreated Patients With Hemophilia B. Nolan B, Klukowska A, Shapiro A, **Rauch A**, Recht M, Ragni M, Curtin J, Gunawardena S, Poloskey S, Jayawardene D, Winding B, Fischer K, Liesner R. *Blood Adv.* 2021 (in press).
2. Gastrointestinal bleeding from angiodysplasia in von Willebrand disease: Improved diagnosis and outcome prediction using videocapsule on top of conventional endoscopy. **Rauch A**, Paris C, Repesse Y, Branche J, D'Oiron R, Harroche A, Ternisien C, Castet SM, Lebreton A, Pan-Petes B, Volot F, Claeysens S, Chamouni P, Gay V, Berger C, Desprez D, Falaise C, Biron Andreani C, Marichez C, Pradines B, Zawadzki C, Itzhar Baikian N, Borel-Derlon A, Goudemand J, Gerard R, Susen S; French Reference Center on von Willebrand Disease. *J Thromb Haemost.* 2021;19(2):380-386. (IF: 4,157)
3. Relevance of platelet desialylation and thrombocytopenia in type 2B von Willebrand disease: preclinical and clinical evidence. Dupont A, Soukaseum C, Cheptou M, Adam F, Nipoti T, Lourenco-Rodrigues MD, Legendre P, Proulle V, **Rauch A**, Kawecki C, Bryckaert M, Rosa JP, Paris C, Ternisien C, Boisseau P, Goudemand J, Borgel D, Lasne D, Maurice P, Lenting PJ, Denis CV, Susen S, Kauskot A. *Haematologica.* 2019;104(12):2493-2500. (IF: 7.1)
4. Natural history and clinical characteristics of inhibitors in previously treated haemophilia A patients: a case series. Iorio A, Barbara AM, Makris M, Fischer K, Castaman G, Catarino C, Gilman E, Kavakli K, Lambert T, Lassila R, Lissitchkov T, Mauser-Bunschoten E, Mingot-Castellano ME, Ozdemir N, Pabinger I, Parra R, Pasi J, Peerlinck K, **Rauch A**, Roussel-Robert V, Serban M, Tagliaferri A, Windyga J, Zanon E. *Haemophilia.* 2017;23(2):255-263. (IF: 2.7)

2. Thématique COVID-19

Le laboratoire d'hémostase du CHU de Lille s'est fortement impliqué dans des travaux de recherche clinique portant sur cette thématique en collaboration avec les services d'urgence et d'anesthésie-réanimation. Les premières études chinoises rapportaient un risque de décès en réanimation plus élevé chez les patients présentant une élévation des D-dimères à l'admission ou des signes d'orage cytokinique traduisant une réponse immunitaire excessive suggérant l'existence d'une coagulopathie spécifique à la COVID-19. Nous avons ensuite été alertés par nos collègues urgentistes et réanimateurs confrontés à des cas d'embolies pulmonaires chez des patients atteints d'une forme sévère de COVID-19. Notre équipe a alors émis l'hypothèse d'une incidence augmentée de thromboses pulmonaires, y compris *in situ*, dans les formes hyper-inflammatoires de COVID-19.

Résultats

J'ai participé à l'étude pilote conduit par les Pr Susen et Poissy qui a confirmé une incidence significativement plus élevée d'embolie pulmonaire diagnostiquée par angioscanner thoracique chez les patients COVID-19 atteints de SDRA comparé à une cohorte historique de patients hospitalisés en réanimation en 2019 soit pour un SDRA de toute cause soit pour un SDRA d'origine grippale. Nous avons également évalué à titre exploratoire dans cette première étude si les taux de VWF mesurés à l'admission était associé au risque de développer une embolie pulmonaire en cours d'hospitalisation. L'endothélium pulmonaire étant la principale source de VWF circulant et l'hypoxie étant un facteur établi de sur-activation de la transcription du VWF par les cellules endothéliales²⁶, nous avons émis hypothèse d'une libération très importante de VWF à partir des corps de Weibel-Palade endothéliaux dans les formes sévères de COVID-19. Nous avons en effet confirmé dans cette cohorte que les taux de VWF, FVIII et D-dimères à l'admission étaient significativement associés à la survenue d'une embolie pulmonaire dans les formes réanimatoires de COVID-19. Au vu des données de la littérature supportant un rôle du VWF dans la physiopathologie de la maladie thrombo-embolique veineuse^{27,28}, nous avons alors initié une deuxième étude qui avait pour objectif d'évaluer si les marqueurs standards de la coagulation (dont le VWF) mesurés à l'admission chez des patients hospitalisés pour COVID-19 étaient prédictifs d'une aggravation respiratoire ou d'un évènement thromboembolique indépendamment de la présence de facteurs de risque de développer une forme sévère de COVID-19 (âge, sexe ou présence d'un syndrome métabolique). Cette étude portant sur un total de 303 patients couvrant tout le spectre de gravité de l'infection a mis en évidence : i) que le taux de VWF plasmatique mesuré à l'admission était associé au degré d'oxygène-réquerance; ii) qu'un ratio FVIII/VWF:Ag bas à l'admission était significativement associé à la survenue d'une aggravation respiratoire dans

les 30 jours suivant l'hospitalisation indépendamment de l'âge, du sexe ou de la présence d'un syndrome métabolique.

Conclusion

Ces travaux de recherche clinique ont confirmé l'importance du cross-talk hémostase-inflammation dans la survenue de complications macro-thrombotiques dans les formes sévères de COVID-19. Ils nous ont également incités à développer les approches plus fondamentales détaillées plus haut afin d'évaluer si ce cross-talk hémostase-inflammation pouvait être impliqué dans la physiopathologie de la défaillance respiratoire et d'autres défaillances d'organe via la survenue de thromboses micro-vasculaires.

Manuscripts:

1. Coagulation biomarkers are independent predictors of increased oxygen requirements in COVID-19. **Rauch A**, Labreuche J, Lassalle F, Goutay J, Caplan M, Charbonnier L, Rohn A, Jeanpierre E, Dupont A, Duhamel A, Faure K, Lambert M, Kipnis E, Garrigue D, Lenting PJ, Poissy J, Susen S. *J Thromb Haemost.* 2020;18(11):2942-2953. (IF: 4.1)
2. Coagulation markers are independent predictors of increased oxygen requirements and thrombosis in COVID-19: Response from Original Authors Susen, et al. Susen S, **Rauch A**, Lenting PJ. *J Thromb Haemost.* 2020;18(12):3385-3386. (IF: 4.1)
3. Pulmonary Embolism in Patients With COVID-19: Awareness of an Increased Prevalence. Poissy J, Goutay J, Caplan M, Parmentier E, Duburcq T, Lassalle F, Jeanpierre E, **Rauch A**, Labreuche J, Susen S; Lille ICU Haemostasis COVID-19 Group. *Circulation.* 2020;142(2):184-186. (IF: 23.6)

Activités d'encadrement

Mes activités d'encadrement au sein de l'équipe 2 de l'UMR1011, codirigée par les Pr Susen et Van Belle, se sont inscrites dans le cadre des projets déjà détaillés précédemment. Depuis ma soutenance de Thèse d'université en 2014, j'ai ainsi encadré quatre étudiants en Master 2 et un étudiant en Thèse d'université.

Projets et étudiants encadrés

Master 2 :

Flavien Vincent (Interne Cardiologie) Encadrement 50%, codirection avec le Pr Van Belle Financement : Année recherche Master 2 BCPP, Option Vaisseaux Hémostase, Université Paris Diderot Rôle de la pulsatilité artérielle dans la régulation du VWF dans un modèle animal d'assistance mono-ventriculaire continue	2014-2015
Wanlin Han (Université de Shanghai) Encadrement 50%, codirection avec le Pr Susen EDBSL, Université Lille Hémocompatibilité in-vitro du prototype d'assistance circulatoire mécanique pulsatile CorWave®	2015-2016
Valentin Loobuyck (Interne Chirurgie Cardiaque) Encadrement 50%, codirection avec le Pr Vincentelli EDBSL, Université Lille Evaluation des variations de multimérisation du VWF dans un modèle ovin d'assistance circulatoire mécanique à pulsatilité variable	2016-2017
Maximilien Desvages (Interne Biologie médicale) Encadrement 50%, codirection avec le Pr Susen Master 2 BiVATH, Option Vaisseaux Hémostase, Université Paris Diderot Impact des assistances circulatoires mécaniques à flux continu sur l'axe facteur Willebrand – Glycoprotéine Ib plaquettaire	2017-2018

Thèse d'université :

Flavien Vincent (CCA Cardiologie) Encadrement 50%, codirection avec le Pr Van Belle EDBSL, Université Lille.	2015-2018
---	-----------

Facteur Willebrand et modifications hémodynamiques associées à l'utilisation de dispositifs cardiovasculaires : mécanisme et applications cliniques

Soutenue le 11/12/2018

Perspectives de recherche

Objectifs principaux

Mes perspectives de recherche actuelles au sein de l'U1011 restent centrées sur la thématique *Hémostase et anomalies de flux* au sein d'un groupe conduit par le Pr Sophie Susen et comprenant en plus des étudiants en M2 et en thèse, Mickaël Rosa (MCU), Delphine Corseaux (MCU), Annabelle Dupont (PU-PH). S'agissant d'une thématique large, mes projets continueront de cibler plus particulièrement le retentissement de l'assistance circulatoire mécanique sur le VWF, les plaquettes et la dérégulation de l'angiogénèse. Dans la lancée des travaux effectués sur la thématique *Hémostase et inflammation* pendant la pandémie COVID-19, je souhaite également développer une nouvelle approche centrée sur l'analyse du cross-talk hémostase-inflammation pour évaluer l'hémocompatibilité des dispositifs d'assistance et l'impact des traitements anticoagulants prescrits dans cette indication (Axe 1).

Je continuerai également à m'impliquer dans les travaux de recherche académique et fondamentale portant sur la maladie de Willebrand portés par le CRMW notamment sur la thématique *angiodysplasies digestives*. L'objectif sera d'avancer dans la compréhension des mécanismes impliqués dans la dérégulation de l'angiogénèse afin d'identifier de nouvelles approches diagnostiques et thérapeutiques en collaboration avec Cécile Denis, Peter Lenting et Caterina Casari, membres de l'U1176, avec qui nous collaborons déjà dans le cadre du projet RHU WillAssistHeart et avec qui nous partageons un intérêt commun pour cette thématique (Axe 2).

Je souhaite également développer mes activités de recherche sur la thématique hémophilie en cohérence avec mon activité clinique et l'importance de la file active de patients hémophiles du site lillois au sein de la filière MHEMO. Le contexte est favorable car le traitement de l'hémophile connaît un changement complet de paradigme avec l'introduction de nombreuses approches thérapeutiques dont la thérapie génique. Ces travaux auront pour objectif de préciser l'index thérapeutique des nouvelles thérapies anti-hémophiliques qui sera très certainement évolutif en fonction de l'âge et des comorbidités des patients via des travaux transversaux mêlant approches épidémiologiques et fondamentales au sein de l'U1011 (Axe 3).

Ma mobilité s'effectuera dans le service d'Epidémiologie clinique du Pr Frits Rosendaal dont l'expertise dans l'exploitation de grandes bases de données appliquées aux maladies hémorragiques constitutionnelles et à la maladie thromboembolique veineuse est reconnue internationalement. Ce choix de mobilité vise à acquérir le complément de formation et établir

les collaborations indispensables au positionnement de notre équipe sur des travaux d'envergure dans le domaine de l'épidémiologie des pathologies hémorragiques constitutionnelles ou acquises. La connexion à venir des bases France Coag et CRMW, attachées respectivement au Centre de Référence pour l'Hémophilie et au Centre de Référence pour la Maladie de Willebrand, sera en effet favorable à des projets d'études épidémiologiques d'ampleur sur ces thématiques.

Projet de mobilité

La MW est une maladie rare caractérisée par une grande hétérogénéité génotypique et phénotypique. Ceci rend les études épidémiologiques difficiles et confère de l'imprécision aux résultats obtenus quand ceux-ci n'intègrent pas la connaissance du type précis de MW. Or, si les conséquences de la maladie sur le risque de saignements itératifs spontanés ou lors de procédures invasives sont en général décrites dans la littérature, il existe très peu de données robustes intégrant les conséquences du type de MW sur les grands cadres pathologiques liés au vieillissement comme les pathologies néoplasiques ou cardiovasculaires. On ne dispose ainsi pas de données permettant d'évaluer l'impact du type de MW ou de la sévérité du déficit en VWF sur le risque d'évènements cardiovasculaires ischémiques et la mortalité associée. Ceci rend complexe la prescription d'anti-thrombotiques dans la MW alors même que celle-ci bénéficie d'un haut niveau de recommandation dans la population générale. L'objectif principal de l'étude WILL-FREE sera de comparer l'incidence d'hospitalisations de causes cardiovasculaires majeures selon la présence ou non d'une MW. Le rapport bénéfice-risque de la prescription d'anti-thrombotiques sera également évalué en fonction du type et de la sévérité de la MW. Cette étude portera sur plus de 4000 patients inclus dans la cohorte du CRMW pour qui nous disposons d'une caractérisation complète, phénotypique et moléculaire, de leur MW. L'analyse croisée de la base du CRMW et des données du parcours de soins (CépiDC, PMSI, SNIIRAM) collectées par le Health Data Hub permettra d'obtenir des informations uniques et pertinentes afin de mieux évaluer la prise en charge et le parcours de soin des patients atteints de MW.

Axe 1 : Thématique *Hémostase et Inflammation* (U1011)

En parallèle des travaux centrés sur le VWF dans le cadre du RHU WillAssistHeart, notre équipe a élargie l'étude de l'impact des anomalies de flux générées par les valvulopathies cardiaques ou les dispositifs d'ACM-FC sur d'autres acteurs de l'hémostase dont les éléments figurés du sang (plaquettes, monocytes) et l'endothélium vasculaire. La pandémie COVID-19 également a joué un rôle structurant puisqu'elle a conduit à initier dans notre équipe une série de travaux sur une thématique *Hémostase et inflammation*. Je souhaite continuer à développer

cette thématique hors COVID au sein de l'U1011 avec des travaux centrés sur l'assistance circulatoire mécanique.

Rôle des forces de cisaillement dans la clairance plaquettaire sous ECMO

Lors de mon post-doctorat, nous nous sommes intéressés à l'impact des anomalies de flux sanguin sur l'interaction VWF-GPIIb/IIIa plaquettaire. Le premier volet de ce projet avait confirmé que la dégradation du VWF sous ACM-FC était indépendante de l'interaction VWF-GPIIb/IIIa. Sur le versant plaquettaire, nos récents travaux confirment également *in vitro* et *in vivo* la présence d'un shedding du récepteur GPIIb/IIIa plaquettaire dont l'importance dépend de l'intensité des forces de cisaillement. Il a été récemment mis en évidence que les plaquettes après shedding de leur récepteur GPIIb/IIIa sont éliminés plus rapidement de la circulation sanguine²⁹. A l'aide d'un modèle de souris NOD-SCID, nous confirmons que les plaquettes humaines exposées à des forces de cisaillement élevées dans un modèle miniaturisé d'ECMO de façon à induire le shedding de GPIIb/IIIa puis transfusées à des souris immunodéprimés sont éliminés plus rapidement de la circulation sanguine que des plaquettes contrôles. Ces résultats feront l'objet d'une publication dans une revue à comité de lecture très prochainement.

Etude du cross-talk hémostase-inflammation sous ECMO via l'histologie du caillot

Nous avons décrit dans une série de patients COVID-19 avec un SDRA ayant requis une ECMO veino-veineuse une proportion plus importante leucocytes et de neutrophils extracellulaires au sein des thrombi d'ECMO comparés à des patients non-COVID-19 (Publication *Vascular Endothelial Damage in the Pathogenesis of Organ Injury in Severe COVID-19. Arterioscler Thromb Vasc Biol. 2021*). Ce résultat préliminaire suggère que l'analyse histologique de ces thrombi reflète l'importance du processus d'immunothrombose résultant du cross-talk entre hémostase et inflammation sous ECMO. Les résultats du travail de thèse de Senna Staessens montrent également que la composition des thrombi recueillis à l'explantation d'une ECMO varie selon l'oxygénateur utilisé au sein du dispositif d'ECMO utilisé (concept d'hémocompatibilité). Notre hypothèse est que la composition histologique des thrombi pourrait également varier selon l'intensité de la réponse inflammatoire sous ECMO ou la nature du traitement anticoagulant administré. Dans le cadre de l'étude multicentrique WITECMO-H effectuée en collaboration avec le service de Chirurgie thoracique et cardiaque de l'Hôpital Marie Lannelongue, nous allons donc constituer une large banque de thrombi collectés prospectivement au niveau des tubulures, tête de pompe ou de membrane de l'oxygénateur au retrait d'ECMO. Nous avons également mis en évidence une proportion importante à la fois de VWF, de leucocytes et de NETs au sein des thrombi d'ECMO de patients COVID-19. Une étude récemment publiée indique également que le VWF pourrait jouer un rôle critique dans le recrutement de leucocytes activés et de NETs au sein du

thrombus³⁰. A titre exploratoire, nous souhaitons donc également évaluer l'impact de la multimérisation du VWF sur le recrutement des leucocytes activés et des NETs au sein du thrombus par microscopie confocale dans un modèle murin de thrombose mésentérique. Cette question est potentiellement d'importance dans différents modèles pathologiques humains comme l'ACM-FC et le PTT.

Impact hépatique et incidence pronostique de l'interaction NAFLD/ COVID-19

L'étude COVER a pour objectif d'évaluer l'impact de l'interaction entre stéatose hépatique non alcoolique (NAFLD) et COVID-19. Nous avons récemment décrit l'existence d'une dysfonction hépatique chez une proportion importante de patients hospitalisés pour une forme réanimatoire de COVID-19 qui était significativement associée à l'intensité de la réponse immunitaire au SARS-CoV2 (Publication *Vascular Endothelial Damage in the Pathogenesis of Organ Injury in Severe COVID-19. Arterioscler Thromb Vasc Biol. 2021*). L'obésité est à la fois un facteur de risque majeur de développer une forme sévère de COVID-19 et une NAFLD. Dans la NAFLD, la modification des populations immunitaires, en particulier des lymphocytes T, est associée à une progression de la NAFLD aussi bien dans des modèles précliniques que chez les patients. Notre hypothèse est que l'interaction entre NAFLD et COVID-19 pourrait potentialiser l'effet délétère de l'activation immunitaire sur l'endothélium vasculaire hépatique et/ou les cellules hépatiques et ainsi aggraver l'évolution de la COVID-19. L'étude COVER qui porte sur une large cohorte de patients admis aux urgences du CHU de Lille pour COVID-19 couvrant tout le spectre de gravité de l'infection (patients ambulatoires, hospitalisés ou réanimatoires) aura pour objectifs d'évaluer : 1) si une NAFLD préexistante a une incidence sur le pronostic de la COVID-19, 2) d'analyser le degré de dysfonction hépatique à l'admission et son profil évolutif selon la présence ou non d'une NAFLD chez les patients COVID-19, 3) d'analyser dans un modèle de culture cellulaire la cytotoxicité induite par le plasma de patients COVID-19 selon la présence de marqueurs de dysfonctionnement hépatique et leur profil évolutif chez ces patients. Ce travail fera l'objet d'une collaboration avec l'équipe 3 de l'U1011 spécialisée dans l'immunoinflammation des récepteurs nucléaires et l'immunométabolisme.

Axe-2 : Thématique *VWF-angiogénèse-angiodyplasies digestives*

Rôle du pool plasmatique de VWF-HPM dans l'angiogénèse

Bien que l'on dispose de données cliniques et fondamentales en faveur d'un rôle du VWF dans l'angiogénèse, les mécanismes sous-jacents à la dérégulation de ce processus dans la MW restent indéterminés. Faute de modèle animal disponible, il n'était pas possible jusqu'ici d'étudier le rôle des VWF-HPM présents dans le compartiment plasmatique et/ou de leurs fragments de protéolyse dans ce processus. Alors que l'on dispose aujourd'hui dans le

traitement de la MW de plusieurs concentrés de VWF dont l'un se différencie par un contenu plus important en VWF-HPM, il est important de déterminer si le maintien d'un pool plasmatique de VWF-HPM joue un rôle important dans l'angiogénèse physiologique et par quel(s) mécanisme(s). Le modèle murin humanisé de maladie de Willebrand de type 2A développé par le Dr Casari (U1176) et le développement d'un anticorps humanisé dérivé du LTX-508 dans le cadre du RHU WillAssistHeart ouvrent comme perspective de pouvoir préciser le rôle des VWF-HPM dans l'angiogénèse via plusieurs approches complémentaires (culture de progéniteurs endothéliaux, analyse de la densité capillaire, modèle de cicatrisation de plaie cutanée).

Etude des anomalies de la micro-vascularisation dans la MW constitutionnelle et acquise

VIDEOBLEED est une étude mono-centrique qui a pour objectif principal d'évaluer si la densité capillaire mesurée par vidéo-microscopie est variable en fonction du type et de la sévérité de la MW. L'hypothèse sous-jacente à cette étude est qu'il pourrait exister des anomalies de la microcirculation secondaire à une dérégulation de l'angiogénèse dans certaines formes de MW notamment celles associées à un déficit endothélial et/ou plasmatique en VWF-HPM. A titre exploratoire, nous évaluerons également si la densité capillaire mesurée par vidéo-microscopie est prédictive de la sévérité du phénotype hémorragique notamment au niveau des muqueuses ORL et digestives. L'analyse de la densité capillaire sublinguale sera effectuée par vidéo-microscopie en consultation. Les autorisations réglementaires (CPP, CNIL) à la constitution de cette cohorte ont été obtenues. L'étude VIDEOBLEED apportera ainsi des informations complémentaires à celle de l'étude WITECMO-H qui comporte également une analyse par vidéo-microscopie de la densité capillaire afin d'évaluer si ce paramètre améliore la prédiction du risque hémorragique chez les patients présentant un déficit acquis en VWF-HPM sous ECMO.

Axe-3 : Thématique *Hémophilie et innovations thérapeutiques*

Définir les modalités de suivi des nouvelles thérapies anti-hémophiliques améliorant l'hémostase selon des mécanismes parfois non physiologiques et de prise en charge des facteurs de risque et pathologies cardio-vasculaires va devenir un axe de recherche important dans l'hémophilie dans un contexte de vieillissement de cette population. L'étude EMICARE a ainsi pour objectif d'évaluer l'intérêt du suivi des taux plasmatiques d'emicizumab par chromatographie liquide couplée à la spectrométrie de masse en tandem (UPLC-MS/MS) dans la prédiction du risque hémorragique chez ces patients. Les autorisations réglementaires (CPP, CNIL) à la constitution de cette cohorte ont été obtenues. En complément de cette étude de recherche clinique, deux autres projets conjuguant approches cliniques et fondamentales, porterons également sur cette thématique.

Etude de la prévalence et du retentissement des microhémorragies cérébrales dans l'hémophilie

En imagerie par résonance magnétique (IRM), les microhémorragies cérébrales (MHC) apparaissent comme des petites lésions arrondies et en hyposignal correspondant à des dépôts d'hémosidérine. La prévalence des MHC dans la population générale est d'environ 15%. Elles sont plus fréquemment observées chez les patients hypertendus et leur présence est associée à une augmentation du risque d'hémorragie intracrânienne ou de déclin cognitif. Ce projet aura pour objectifs principaux d'évaluer: 1) la prévalence des MHC par IRM 7 Tesla chez les adultes atteints d'hémophilie sévère en comparaison à des sujets contrôles appariés sur l'âge et la présence ou non d'une hypertension artérielle; 2) le retentissement de ces MHC sur : i) le risque d'hémorragie intracrânienne non traumatique à l'aide d'un modèle murin de MHC induite par injection stéréotaxique de microbilles selon la présence (souris FVIII-KO, INSERM U1176, Dr Denis) ou non (souris WT) d'une hémophilie sévère ; ii) sur le plan cognitif via un suivi prospectif des données de santé recueillies par le Health Data Hub pour ces patients.

Impact de l'emicizumab sur l'arthropathie hémophilique via la modulation de polarisation des monocytes/macrophages

L'emicizumab est un anticorps monoclonal humanisé FVIII-mimétique qui a obtenu une extension d'AMM en 2020 dans le traitement des hémophiles A sévères sans inhibiteur. Nous disposons de données préliminaires montrant que l'emicizumab comme d'autres anticorps thérapeutiques de même isotype (IgG4) peut se lier via son domaine Fc au récepteur Fc γ RI exprimé à la surface des monocytes/macrophages. Cette interaction est susceptible d'activer des voies de signalisation modifiant la polarisation des monocytes/macrophages vers un phénotype pro- (M1) ou anti-inflammatoire (M2). Les objectifs de ce projet sont d'évaluer l'impact de l'emicizumab sur la polarisation des monocytes/macrophages et ses conséquences sur l'inflammation articulaire. L'étude de l'impact de l'emicizumab sur la polarisation des monocytes/macrophages reposera : i) *in vitro* sur l'analyse du transcriptome de monocytes/macrophages en culture exposés à des doses croissantes d'emicizumab et des cytokines sécrétées dans le surnageant de culture; ii) *in vivo* sur la comparaison de l'immunophénotypage des monocytes circulants chez des hémophiles A sévères traités ou non par emicizumab.

Références

1. Siedlecki CA, Lestini BJ, Kottke-Marchant KK, Eppell SJ, Wilson DL, Marchant RE. Shear-dependent changes in the three-dimensional structure of human von Willebrand factor. *Blood*. 1996;88(8):2939-50.
2. Zhang X, Halvorsen K, Zhang CZ, Wong WP, Springer TA: Mechanoenzymatic cleavage of the ultralarge vascular protein von Willebrand factor. *Science* 2009, 324(5932):1330-4.
3. Springer TA. von Willebrand factor, Jedi knight of the bloodstream. *Blood*. 2014;124(9):1412-25.
4. Vincentelli A, Susen S, Le Tourneau T, Six I, Fabre O, Juthier F, Bauters A, Decoene C, Goudemand J, Prat A, Jude B. Acquired von Willebrand syndrome in aortic stenosis. *N Engl J Med*. 2003;349(4):343-9.
5. Le Tourneau T, Susen S, Caron C, Millaire A, Maréchaux S, Polge AS, Vincentelli A, Mouquet F, Ennezat PV, Lamblin N, de Groote P, Van Belle E, Deklunder G, Goudemand J, Bauters A, Jude B. Functional impairment of von Willebrand factor in hypertrophic cardiomyopathy: relation to rest and exercise obstruction. *Circulation*. 2008;118(15):1550-7.
6. Cribier A, Eltchaninoff H, Bash A, Borenstein N, Tron C, Bauer F, Derumeaux G, Anselme F, Laborde F, Leon MB: Percutaneous transcatheter implantation of an aortic valve prosthesis for calcific aortic stenosis: first human case description. *Circulation* 2002, 106(24):3006- 3008.
7. Leon MB, Smith CR, Mack M, Miller DC, Moses JW, Svensson LG, Tuzcu EM, Webb JG, Fontana GP, Makkar RR, Brown DL, Block PC, Guyton RA, Pichard AD, Bavaria JE, Herrmann HC, Douglas PS, Petersen JL, Akin JJ, Anderson WN, Wang D, Pocock S; PARTNER Trial Investigators. Transcatheter aortic-valve implantation for aortic stenosis in patients who cannot undergo surgery. *N Engl J Med*. 2010;363(17):1597-607.
8. Fressinaud E, Veyradier A, Truchaud F, Martin I, Boyer-Neumann C, Trossaert M, Meyer D. Screening for von Willebrand disease with a new analyzer using high shear stress: a study of 60 cases. *Blood*. 1998;91(4):1325-31.
9. Van Belle E, Juthier F, Susen S, Vincentelli A, Jung B, Dallongeville J, Eltchaninoff H, Laskar M, Leprince P, Lievre M, Banfi C, Auffray JL, Delhay C, Donzeau-Gouge P, Chevreur K, Fajadet J, Leguerrier A, Prat A, Gilard M, Teiger E; FRANCE 2 Investigators. Postprocedural aortic regurgitation in balloon-expandable and self-expandable transcatheter aortic valve replacement procedures: analysis of predictors and impact on long-term mortality: insights from the FRANCE2 Registry. *Circulation*. 2014;129(13):1415-27.
10. Slaughter MS, Rogers JG, Milano CA, Russell SD, Conte JV, Feldman D, Sun B, Tatroles AJ, Delgado RM 3rd, Long JW, Wozniak TC, Ghumman W, Farrar DJ, Frazier OH; HeartMate II Investigators. Advanced heart failure treated with continuous-flow left ventricular assist device. *N Engl J Med*. 2009;361(23):2241-51.
11. Bunte MC, Blackstone EH, Thuita L, Fowler J, Joseph L, Ozaki A, Starling RC, Smedira NG, Mountis MM: Major bleeding during HeartMate II support. *J Am Coll Cardiol* 2013, 62(23):2188-2196.
12. Uriel N, Pak SW, Jorde UP, Jude B, Susen S, Vincentelli A, Ennezat PV, Cappleman S, Naka Y, Mancini D. Acquired von Willebrand syndrome after continuous-flow mechanical device support contributes to a high prevalence of bleeding during long-term support and at the time of transplantation. *J Am Coll Cardiol*. 2010 Oct 5;56(15):1207-13.
13. Meyer AL, Malehsa D, Budde U, Bara C, Haverich A, Strueber M: Acquired von Willebrand syndrome in patients with a centrifugal or axial continuous flow left ventricular assist device. *JACC Heart Fail* 2014, 2(2):141-145.
14. Dassanayaka S, Slaughter MS, Bartoli CR. Mechanistic pathway(s) of acquired von willebrand syndrome with a continuous-flow ventricular assist device: in vitro findings. *ASAIO J*. 2013;59(2):123-9.
15. Crawley JT, de Groot R, Xiang Y, Luken BM, Lane DA: Unraveling the scissile bond: how ADAMTS13 recognizes and cleaves von Willebrand factor. *Blood* 2011, 118(12):3212-3221.
16. Zanardelli S, Chion AC, Groot E, Lenting PJ, McKinnon TA, Laffan MA, Tseng M, Lane DA: A novel binding site for ADAMTS13 constitutively exposed on the surface of globular VWF. *Blood* 2009, 114(13):2819-2828.

17. Furlan M, Robles R, Affolter D, Meyer D, Baillod P, Lammle B: Triplet structure of von Willebrand factor reflects proteolytic degradation of high molecular weight multimers. *Proc Natl Acad Sci U S A* 1993, 90(16):7503-7507.
18. Kato S, Matsumoto M, Matsuyama T, Isonishi A, Hiura H, Fujimura Y. Novel monoclonal antibody-based enzyme immunoassay for determining plasma levels of ADAMTS13 activity. *Transfusion*. 2006 Aug;46(8):1444-52.
19. Randi AM, Smith KE, Castaman G. von Willebrand factor regulation of blood vessel formation. *Blood*. 2018 ;132(2):132-140.
20. Wever-Pinzon O, Selzman CH, Drakos SG, Saidi A, Stoddard GJ, Gilbert EM, Labedi M, Reid BB, Davis ES, Kfoury AG, Li DY, Stehlik J, Bader F. Pulsatility and the risk of nonsurgical bleeding in patients supported with the continuous-flow left ventricular assist device HeartMate II. *Circ Heart Fail*. 2013;6(3):517-26.
21. Xiong Y, Hu Z, Han X, Jiang B, Zhang R, Zhang X, Lu Y, Geng C, Li W, He Y, Huo Y, Shibuya M, Luo J. Hypertensive stretch regulates endothelial exocytosis of Weibel-Palade bodies through VEGF receptor 2 signaling pathways. *Cell Res*. 2013 ;23(6):820-34.
22. Galbusera M, Zoja C, Donadelli R, Paris S, Morigi M, Benigni A, Figliuzzi M, Remuzzi G, Remuzzi A. Fluid shear stress modulates von Willebrand factor release from human vascular endothelium. *Blood*. 1997;90(4):1558-64.
23. Antoine EE, Cornat FP, Barakat AI. The stentable in vitro artery: an instrumented platform for endovascular device development and optimization. *J R Soc Interface*. 2016;13(125):20160834.
24. Varga Z, Flammer AJ, Steiger P, Haberecker M, Andermatt R, Zinkernagel AS, Mehra MR, Schuepbach RA, Ruschitzka F, Moch H. Endothelial cell infection and endotheliitis in COVID-19. *Lancet*. 2020;395:1417–1418. doi: 10.1016/S0140-6736(20)30937-5
25. Ackermann M, Verleden SE, Kuehnel M, Haverich A, Welte T, Laenger F, Vanstapel A, Werlein C, Stark H, Tzankov A, et al. Pulmonary vascular endothelialitis, thrombosis, and angiogenesis in Covid-19. *N Engl J Med*. 2020;383:120–128.
26. Mojiri A, Nakhaii-Nejad M, Phan WL, Kulak S, Radziwon-Balicka A, Jurasz P, Michelakis E, Jahroudi N. Hypoxia results in upregulation and de novo activation of von Willebrand factor expression in lung endothelial cells. *Arterioscler Thromb Vasc Biol*. 2013;33(6):1329-38.
27. Brill A, Fuchs TA, Chauhan AK, Yang JJ, De Meyer SF, Köllnberger M, Wakefield TW, Lämmle B, Massberg S, Wagner DD. von Willebrand factor-mediated platelet adhesion is critical for deep vein thrombosis in mouse models. *Blood*. 2011; 117:1400–1407.
28. Michels A, Dwyer CN, Mewburn J, Nesbitt K, Kawecki C, Lenting P, Swystun LL, Lillicrap D. von Willebrand Factor Is a Critical Mediator of Deep Vein Thrombosis in a Mouse Model of Diet-Induced Obesity. *Arterioscler Thromb Vasc Biol*. 2020;40(12):2860-2874.
29. Zirka G, Robert P, Tilburg J, Tishkova V, Maracle CX, Legendre P, van Vlijmen BJM, Alessi MC, Lenting PJ, Morange PE, Thomas GM. Impaired adhesion of neutrophils expressing Slc44a2/HNA-3b to VWF protects against NETosis under venous shear rate. *Blood*. 2021 Feb 8: blood.2020008345.
30. Chen W, Liang X, Syed AK, Jessup P, Church WR, Ware J, Josephson CD, Li R. Inhibiting GPIIb/IIIa Shedding Preserves Post-Transfusion Recovery and Hemostatic Function of Platelets After Prolonged Storage. *Arterioscler Thromb Vasc Biol*. 2016;36(9):1821-8.

Liste des publications

Indices bibliométriques

- 39 publications
- 26 articles originaux dont 8 en (co)premier auteur avec IF>4
- Score Sigaps : 506 points
- 700 citations, h-index : 12 (sampra)

Publications scientifiques originales

1. The homozygous variant p.Gln1311* in exon 28 of VWF is associated with the development of alloantibodies in 3 unrelated patients with type 3 VWD. Lassalle F, Zawadzki C, Harroche A, Biron-Andréani C, Falaise C, Boisseau P, Duployez N, Jeanpierre E, **Rauch A**, Paris C, Susen S, Goudemand J. Haemophilia. 2021. In press (IF: 2.9)
2. Vascular Endothelial Damage in the Pathogenesis of Organ Injury in Severe COVID-19. Dupont A*, **Rauch A***, Staessens S, Moussa M, Rosa M, Corseaux D, Jeanpierre E, Goutay J, Caplan M, Varlet P, Lefevre G, Lassalle F, Bauters A, Faure K, Lambert M, Duhamel A, Labreuche J, Garrigue D, De Meyer SF, Staels B, Vincent F, Rousse N, Kipnis E, Lenting P, Poissy J, Susen S; Lille Covid Research Network (LICORNE). Arterioscler Thromb Vasc Biol. 2021 Feb 25:ATVBAHA120315595. In press (IF: 6.6) *coauteurs
3. Gastrointestinal bleeding from angiodysplasia in von Willebrand disease: Improved diagnosis and outcome prediction using videocapsule on top of conventional endoscopy. **Rauch A**, Paris C, Repesse Y, Branche J, D'Oiron R, Harroche A, Ternisien C, Castet SM, Lebreton A, Pan-Petes B, Volot F, Claeysens S, Chamouni P, Gay V, Berger C, Desprez D, Falaise C, Biron Andreani C, Marichez C, Pradines B, Zawadzki C, Itzhar Baikian N, Borel-Derlon A, Goudemand J, Gerard R, Susen S; French Reference Center on von Willebrand Disease. J Thromb Haemost. 2021;19(2):380-386. (IF: 4.1)
4. Pharmacological Blockade of Glycoprotein VI Promotes Thrombus Disaggregation in the Absence of Thrombin. Ahmed MU, Kaneva V, Loyau S, Nechipurenko D, Receveur N, Le Bris M, Janus-Bell E, Didelot M, **Rauch A**, Susen S, Chakfé N, Lanza F, Gardiner EE, Andrews RK, Panteleev M, Gachet C, Jandrot-Perrus M, Mangin PH. Arterioscler Thromb Vasc Biol. 2020;40(9):2127-2142. (IF: 6.6)
5. Clinico-Biological Features and Clonal Hematopoiesis in Patients with Severe COVID-19. Duployez N, Demonchy J, Berthon C, Goutay J, Caplan M, Moreau AS, Bignon A, Marceau-Renaut A, Garrigue D, Raczkiwicz I, Geffroy S, Bucci M, Alidjinou K, Demaret J, Labalette M, Brousseau T, Dupont A, **Rauch A**, Poissy J, Susen S, Preudhomme C, Quesnel B. Cancers (Basel). 2020;12(7):1992. (IF: 6.1)
6. Coagulation biomarkers are independent predictors of increased oxygen requirements in COVID-19. **Rauch A**, Labreuche J, Lassalle F, Goutay J, Caplan M, Charbonnier L, Rohn A, Jeanpierre E, Dupont A, Duhamel A, Faure K, Lambert M, Kipnis E, Garrigue D, Lenting PJ, Poissy J, Susen S. J Thromb Haemost. 2020;18(11):2942-2953. (IF: 4.1)
7. Hemostatic profile of infants with spontaneous prematurity: can we predict intraventricular hemorrhage development? Hochart A, Nuytten A, Pierache A, Bauters A, **Rauch A**, Wibaut B, Susen S, Goudemand J. Ital J Pediatr. 2019;45(1):113. (IF: 2.1)
8. FranceCoag: a 22-year prospective follow-up of the national French cohort of patients with inherited bleeding disorders. Doncarli A, Demiguel V, Guseva Canu I, Goulet V, Bayart S, Calvez T, Castet S, Dalibard V, Demay Y, Frotscher B, Goudemand J, Lambert T, Milien V, Oudot C, Sannié T, Chambost H; FranceCoag Network. Eur J Epidemiol. 2019;34(5):521-532. (IF: 7.1)
9. Relevance of platelet desialylation and thrombocytopenia in type 2B von Willebrand disease: preclinical and clinical evidence. Dupont A, Soukaseum C, Cheptou M, Adam F, Nipoti T, Lourenco-Rodrigues MD, Legendre P, Proulle V, **Rauch A**, Kawecki C, Bryckaert M, Rosa JP, Paris C, Ternisien C, Boisseau P, Goudemand J, Borgel D, Lasne D, Maurice P, Lenting PJ, Denis CV, Susen S, Kauskot A. Haematologica. 2019;104(12):2493-2500. (IF: 7.1)
10. CT-ADP Point-of-Care Assay Predicts 30-Day Paravalvular Aortic Regurgitation and Bleeding Events following Transcatheter Aortic Valve Replacement. Kibler M, Marchandot B, Messas N, Caspar T, Vincent F, Von Hunolstein JJ, Grunebaum L, Reydel A, **Rauch A**, Crimizade U, Kindo M, Hoang Minh T, Trinh A, Petit-Eisenmann H, De Poli F, Leddet P, Jesel L, Ohlmann P, Susen S, Van Belle E, Morel O. Thromb Haemost. 2018;118(5):893-905. (IF: 4.7)

11. Determinants of adherence and consequences of the transition from adolescence to adulthood among young people with severe haemophilia (TRANSEMO): study protocol for a multicentric French national observational cross-sectional study. Resseguier N, Rosso-Delsemme N, Beltran Anzola A, Baumstarck K, Milien V, Ardillon L, Bayart S, Berger C, Bertrand MA, Biron-Andreani C, Borel-Derlon A, Castet S, Chamouni P, Claeysens Donadel S, De Raucourt E, Desprez D, Falaise C, Frotscher B, Gay V, Goudemand J, Gruel Y, Guillet B, Harroche A, Hassoun A, Huguenin Y, Lambert T, Lebreton A, Lienhart A, Martin M, Meunier S, Monpoux F, Mourey G, Negrier C, Nguyen P, Nyombe P, Oudot C, Pan-Petes B, Polack B, Rafowicz A, **Rauch A**, Rivaud D, Schneider P, Spiegel A, Stoven C, Tardy B, Trossaert M, Valentin JB, Vanderbecken S, Volot F, Voyer-Ebrard A, Wibaut B, Leroy T, Sannie T, Chambost H, Auquier P. *BMJ Open*. 2018;8(7):e022409. (IF: 2.3)
12. Arterial Pulsatility and Circulating von Willebrand Factor in Patients on Mechanical Circulatory Support. Vincent F*, **Rauch A***, Loobuyck V, Robin E, Nix C, Vincentelli A, Smadja DM, Leprince P, Amour J, Lemesle G, Spillemaeker H, Debry N, Latremouille C, Jansen P, Capel A, Moussa M, Rousse N, Schurtz G, Delhay C, Paris C, Jeanpierre E, Dupont A, Corseaux D, Rosa M, Sottejeau Y, Barth S, Mourran C, Gomane V, Coisne A, Richardson M, Caron C, Preda C, Ung A, Carpentier A, Hubert T, Denis C, Staels B, Lenting PJ, Van Belle E, Susen S. *J Am Coll Cardiol*. 2018;71(19):2106-2118. (IF: 18.6) *coauteurs
13. Subacute right heart failure revealing three simultaneous causes of post-embolic pulmonary hypertension in metastatic dissemination of breast cancer. Vincent F, Lamblin N, Classe M, Schurtz G, **Rauch A**, Fertin M, De Groote P. *ESC Heart Fail*. 2017;4(1):75-77. (IF: 3.4)
14. Leptin induces osteoblast differentiation of human valvular interstitial cells via the Akt and ERK pathways. Rosa M, Paris C, Sottejeau Y, Corseaux D, Robin E, Tagzirt M, Juthier F, Jashari R, **Rauch A**, Vincentelli A, Staels B, Van Belle E, Susen S, Dupont A. *Acta Diabetol*. 2017;54(6):551-560. (IF: 3.1)
15. Natural history and clinical characteristics of inhibitors in previously treated haemophilia A patients: a case series. Iorio A, Barbara AM, Makris M, Fischer K, Castaman G, Catarino C, Gilman E, Kavakli K, Lambert T, Lassila R, Lissitchkov T, Mauser-Bunschoten E, Mingot-Castellano ME, Ozdemir N, Pabinger I, Parra R, Pasi J, Peerlinck K, **Rauch A**, Rousel- Robert V, Serban M, Tagliaferri A, Windyga J, Zanon E. *Haemophilia*. 2017;23(2):255-263. (IF: 2.7)
16. The Carmat Bioprosthetic Total Artificial Heart Is Associated With Early Hemostatic Recovery and no Acquired von Willebrand Syndrome in Calves. Smadja DM, Susen S, **Rauch A**, Cholley B, Latremouille C, Duveau D, Zilberstein L, Méléard D, Boughenou MF, Belle EV, Gaussem P, Capel A, Jansen P, Carpentier A. *J Cardiothorac Vasc Anesth*. 2017;31(5):1595-1602. (IF: 1.5)
17. Von Willebrand Factor Multimers during Transcatheter Aortic Valve Replacement. Van Belle E*, **Rauch A***, Vincent F, Robin E, Kibler M, Labreuche J, Jeanpierre E, Levade M, Hurt C, Rousse N, Dally JB, Debry N, Dallongeville J, Vincentelli A, Delhay C, Auffray JL, Juthier F, Schurtz G, Lemesle G, Caspar T, Morel O, Dumonteil N, Duhamel A, Paris C, Dupont-Prado A, Legendre P, Mouquet F, Marchant B, Hermoire S, Corseaux D, Moussa K, Manchuelle A, Bauchart JJ, Loobuyck V, Caron C, Zawadzki C, Leroy F, Bodart JC, Staels B, Goudemand J, Lenting PJ, Susen S. *N Engl J Med*. 2016; 375(4):335-44. (IF: 72.4) *coauteurs
18. Microparticle phenotypes are associated with driver mutations and distinct thrombotic risks in essential thrombocythemia. Charpentier A, Lebreton A, **Rauch A**, Bauters A, Trillot N, Nibourel O, Tintillier V, Wemeau M, Demory JL, Preudhomme C, Jude B, Lecompte T, Cambier N, Susen S. *Haematologica*. 2016;101(9):e365-8. doi: 10.3324/haematol.2016.144279. (IF: 7.7)
19. Postpartum haemorrhage related early increase in D-dimers is inhibited by tranexamic acid: haemostasis parameters of a randomized controlled open labelled trial. Ducloy-Bouthors AS, Duhamel A, Kipnis E, Tournoys A, Prado-Dupont A, Elkalioubie A, Jeanpierre E, Debize G, Peynaud-Debayle E, DeProst D, Huissoud C, **Rauch A**, Susen S. *Br J Anaesth*. 2016;116(5):641-8. (IF: 6.2)
20. Compliance with evidence-based clinical management guidelines in bleeding trauma patients. Godier A, Bacus M, Kipnis E, Tavernier B, Guidat A, **Rauch A**, Drumez E, Susen S, Garrigue-Huet D. *Br J Anaesth*. 2016;117(5):592-600. (IF: 6.2)
21. PROS1 genotype phenotype relationships in a large cohort of adults with suspicion of inherited quantitative protein S deficiency. Alhenc-Gelas M, Plu-Bureau G, Horellou MH, **Rauch A**, Suchon P; GEHT genetic thrombophilia group. *Thromb Haemost*. 2016;115(3):570-9. (IF: 5.6)
22. A novel ELISA-based diagnosis of acquired VWD with increased VWF proteolysis. **Rauch A**, Caron C, Vincent F, Jeanpierre E, Ternisien C, Boisseau P, Zawadzki C, Fressinaud E, Borel-Derlon A, Hermoire S, Paris C, Lavenu-Bombled C, Veyradier A, Ung A, Vincentelli A, van Belle E, Lenting PJ, Goudemand J, Susen S. *Thromb Haemost*. 2016; 115(5):950-9. (IF: 5.6)

23. Abacavir has no prothrombotic effect on platelets in vitro. Diallo YL, Ollivier V, Joly V, Faille D, Catalano G, Jandrot-Perrus M, **Rauch A**, Yeni P, Ajzenberg N. *J Antimicrob Chemother.* 2016;71(12):3506-3509. (IF: 5)
24. Von Willebrand Factor As A Biological Sensor Of Blood Flow To Monitor Percutaneous Aortic Valve Interventions. Van Belle E*, **Rauch A***, Vincentelli A, Jeanpierre E, Legendre P, Juthier F, Hurt C, Banfi C, Rousse N, Godier A, Caron C, Elkalioubie A, Corseaux D, Dupont A, Zawadzki C, Delhaye C, Mouquet F, Schurtz G, Deplanque D, Chinetti G, Staels B, Goudemand J, Jude B, Lenting PJ, Susen S. *Circ Res.*2015; 116(7):1193-201 (IF: 11.5) *coauteurs
25. M1 and M2 macrophage proteolytic and angiogenic profile analysis in atherosclerotic patients reveals a distinctive profile in type 2 diabetes. Roma-Lavisse C, Tagzirt M, Zawadzki C, Lorenzi R, Vincentelli A, Haulon S, Juthier F, **Rauch A**, Corseaux D, Staels B, Jude B, Van Belle E, Susen S, Chinetti-Gbaguidi G, Dupont A. *Diab Vasc Dis Res.* 2015;12(4):279-89. (IF: 3)
26. Antibody-based prevention of von Willebrand factor degradation mediated by circulatory assist devices. **Rauch A**, Legendre P, Christophe OD, Goudemand J, van Belle E, Vincentelli A, Denis CV, Susen S, Lenting PJ. *Thromb Haemost.* 2014; 112(5):1014-23. (IF: 4.9)

Lettres à l'éditeur

1. Coagulation markers are independent predictors of increased oxygen requirements and thrombosis in COVID-19: Response from Original Authors Susen, et al. Susen S, **Rauch A**, Lenting PJ. *J Thromb Haemost.* 2020;18(12):3385-3386. (IF: 4.1)
2. Endotheliopathy Is Induced by Plasma From Critically ill Patients and Associated With Organ Failure in Severe COVID-19. **Rauch A***, Dupont A*, Goutay J, Caplan M, Staessens S, Moussa M, Jeanpierre E, Corseaux D, Lefevre G, Lassalle F, Faure K, Lambert M, Duhamel A, Labreuche J, Garrigue D, De Meyer SF, Staels B, Van Belle E, Vincent F, Kipnis E, Lenting PJ, Poissy J, Susen S; Lille COVID Research Network (LICORNE); Members of the LICORNE Scientific Committee. *Circulation.* 2020;142(19):1881-1884. (IF: 23.6) *coauteurs
3. Pulmonary Embolism in Patients With COVID-19: Awareness of an Increased Prevalence. Poissy J, Goutay J, Caplan M, Parmentier E, Duburcq T, Lassalle F, Jeanpierre E, **Rauch A**, Labreuche J, Susen S; Lille ICU Haemostasis COVID-19 Group. *Circulation.* 2020;142(2):184-186. (IF: 23.6)

Revues et publications didactiques

1. Management of bleeding and invasive procedures in haemophilia A patients with inhibitor treated with emicizumab (Hemlibra®): Proposals from the French network on inherited bleeding disorders (MHMO), the French Reference Centre on Haemophilia, in collaboration with the French Working Group on Perioperative Haemostasis (GIHP). Susen S, Gruel Y, Godier A, Harroche A, Chambost H, Lasne D, **Rauch A**, Roullet S, Fontana P, Goudemand J, de Maistre E, Chamouard V, Wibaut B, Albaladejo P, Négrier C. *Haemophilia.* 2019;25(5):731-737. (IF: 2.9)
2. Acquired von Willebrand Syndrome in Patients With Ventricular Assist Device. **Rauch A**, Susen S, Zieger B. *Front Med (Lausanne).* 2019;6:7. (IF: 3.9)
3. Von Willebrand Factor and Management of Heart Valve Disease: JACC Review Topic of the Week. Van Belle E, Vincent F, **Rauch A**, Casari C, Jeanpierre E, Loobuyck V, Rosa M, Delhaye C, Spillemaeker H, Paris C, Debry N, Verdier B, Vincentelli A, Dupont A, Lenting PJ, Susen S. *J Am Coll Cardiol.* 2019;73(9):1078-1088. (IF: 20.5)
4. Von Willebrand Factor for Aortic Valve Intervention: From Bench to Real-Time Bedside Assessment. Vincent F, **Rauch A**, Loobuyck V, Moussa M, Juthier F, Debry N, Jeanpierre E, Lenting PJ, Susen S, Van Belle E. *Circ Res.* 2018;122(11):1499-1500. (IF: 15.8)
5. Real-Time Monitoring of von Willebrand Factor in the Catheterization Laboratory: The Seatbelt of Mini-Invasive Transcatheter Aortic Valve Replacement? Vincent F, **Rauch A**, Spillemaeker H, Vincentelli A, Paris C, Rosa M, Dupont A, Delhaye C, Verdier B, Robin E, Lenting PJ, Susen S, Van Belle E. *JACC Cardiovasc Interv.* 2018;11(17):1775-1778. (IF: 9.5)
6. Circulatory support devices: Fundamental aspects & clinical management of bleeding and thrombosis. Susen S, **Rauch A**, Van Belle E, Vincentelli A, Lenting PJ. *J Thromb Haemost* 2015; 13(10):1757-67. (IF: 5.5)
7. Meta-Analysis of Abdominal Aortic Aneurysm in Patients With Coronary Artery Disease. Elkalioubie A, Haulon S, Duhamel A, Rosa M, **Rauch A**, Staels B, Susen S, Van Belle E, Dupont A. *Am J Cardiol.* 2015;116(9):1451-6. (IF: 3.1)

Tirés à part des principales publications

1. Vascular Endothelial Damage in the Pathogenesis of Organ Injury in Severe COVID-19. Dupont A*, **Rauch A***, Staessens S, Moussa M, Rosa M, Corseaux D, Jeanpierre E, Goutay J, Caplan M, Varlet P, Lefevre G, Lassalle F, Bauters A, Faure K, Lambert M, Duhamel A, Labreuche J, Garrigue D, De Meyer SF, Staels B, Vincent F, Rousse N, Kipnis E, Lenting P, Poissy J, Susen S; Lille Covid Research Network (LICORNE). *Arterioscler Thromb Vasc Biol.* 2021 Feb 25:ATVBAHA120315595. In press (*IF: 6.6*) *coauteurs
2. Gastrointestinal bleeding from angiodysplasia in von Willebrand disease: Improved diagnosis and outcome prediction using videocapsule on top of conventional endoscopy. **Rauch A**, Paris C, Repesse Y, Branche J, D'Oiron R, Harroche A, Ternisien C, Castet SM, Lebreton A, Pan-Petes B, Volot F, Claeysens S, Chamouni P, Gay V, Berger C, Desprez D, Falaise C, Biron Andreani C, Marichez C, Pradines B, Zawadzki C, Itzhar Baikian N, Borel-Derlon A, Goudemand J, Gerard R, Susen S; French Reference Center on von Willebrand Disease. *J Thromb Haemost.* 2021;19(2):380-386. (*IF: 4.1*)
3. Endotheliopathy Is Induced by Plasma From Critically ill Patients and Associated With Organ Failure in Severe COVID-19. **Rauch A***, Dupont A*, Goutay J, Caplan M, Staessens S, Moussa M, Jeanpierre E, Corseaux D, Lefevre G, Lassalle F, Faure K, Lambert M, Duhamel A, Labreuche J, Garrigue D, De Meyer SF, Staels B, Van Belle E, Vincent F, Kipnis E, Lenting PJ, Poissy J, Susen S; Lille COVID Research Network (LICORNE); Members of the LICORNE Scientific Committee. *Circulation.* 2020;142(19):1881-1884. (*IF: 23.6*) *coauteurs
4. Coagulation biomarkers are independent predictors of increased oxygen requirements in COVID-19. **Rauch A**, Labreuche J, Lassalle F, Goutay J, Caplan M, Charbonnier L, Rohn A, Jeanpierre E, Dupont A, Duhamel A, Faure K, Lambert M, Kipnis E, Garrigue D, Lenting PJ, Poissy J, Susen S. *J Thromb Haemost.* 2020;18(11):2942-2953. (*IF: 4.1*)
5. Arterial Pulsatility and Circulating von Willebrand Factor in Patients on Mechanical Circulatory Support. Vincent F*, **Rauch A***, Loobuyck V, Robin E, Nix C, Vincentelli A, Smadja DM, Leprince P, Amour J, Lemesle G, Spillemaeker H, Debry N, Latremouille C, Jansen P, Capel A, Moussa M, Rousse N, Schurtz G, Delhay C, Paris C, Jeanpierre E, Dupont A, Corseaux D, Rosa M, Sottejeau Y, Barth S, Mourran C, Gomane V, Coisne A, Richardson M, Caron C, Preda C, Ung A, Carpentier A, Hubert T, Denis C, Staels B, Lenting PJ, Van Belle E, Susen S. *J Am Coll Cardiol.* 2018;71(19):2106-2118. (*IF: 18.6*) *coauteurs
6. Von Willebrand Factor Multimers during Transcatheter Aortic Valve Replacement. Van Belle E*, **Rauch A***, Vincent F, Robin E, Kibler M, Labreuche J, Jeanpierre E, Levade M, Hurt C, Rousse N, Dally JB, Debry N, Dallongeville J, Vincentelli A, Delhay C, Auffray JL, Juthier F, Schurtz G, Lemesle G, Caspar T, Morel O, Dumonteil N, Duhamel A, Paris C, Dupont-Prado A, Legendre P, Mouquet F, Marchant B, Hermoire S, Corseaux D, Moussa K, Manchuelle A, Bauchart JJ, Loobuyck V, Caron C, Zawadzki C, Leroy F, Bodart JC, Staels B, Goudemand J, Lenting PJ, Susen S. *N Engl J Med.* 2016; 375(4):335-44. (*IF: 72.4*) *coauteurs
7. A novel ELISA-based diagnosis of acquired VWD with increased VWF proteolysis. **Rauch A**, Caron C, Vincent F, Jeanpierre E, Ternisien C, Boisseau P, Zawadzki C, Fressinaud E, Borel-Derlon A, Hermoire S, Paris C, Lavenu-Bombled C, Veyradier A, Ung A, Vincentelli A, van Belle E, Lenting PJ, Goudemand J, Susen S. *Thromb Haemost.* 2016; 115(5):950-9. (*IF: 5.6*)
8. Von Willebrand Factor As A Biological Sensor Of Blood Flow To Monitor Percutaneous Aortic Valve Interventions. Van Belle E*, **Rauch A***, Vincentelli A, Jeanpierre E, Legendre P, Juthier F, Hurt C, Banfi C, Rousse N, Godier A, Caron C, Elkalioubie A, Corseaux D, Dupont A, Zawadzki C, Delhay C, Mouquet F, Schurtz G, Deplanque D, Chinetti G, Staels B, Goudemand J, Jude B, Lenting PJ, Susen S. *Circ Res.* 2015; 116(7):1193-201 (*IF: 11.5*) *coauteurs
9. Antibody-based prevention of von Willebrand factor degradation mediated by circulatory assist devices. **Rauch A**, Legendre P, Christophe OD, Goudemand J, van Belle E, Vincentelli A, Denis CV, Susen S, Lenting PJ. *Thromb Haemost.* 2014; 112(5):1014-23. (*IF: 4.9*)

ORIGINAL RESEARCH

Vascular Endothelial Damage in the Pathogenesis of Organ Injury in Severe COVID-19

Annabelle Dupont*, Antoine Rauch¹, Senna Staessens¹, Mouhamed Moussa, Mickael Rosa, Delphine Corseaux, Emmanuelle Jeanpierre, Julien Goutay, Morgan Caplan¹, Pauline Varlet, Guillaume Lefevre, Fanny Lassalle¹, Anne Bauters, Karine Faure, Marc Lambert, Alain Duhamel, Julien Labreuche¹, Delphine Garrigue, Simon F. De Meyer, Bart Staels¹, Flavien Vincent¹, Natacha Rousse, Eric Kipnis¹, Peter Lenting, Julien Poissy¹, Sophie Susen¹; the Lille Covid Research Network (LICORNE)

OBJECTIVE: Whether endotheliopathy only mirrors coronavirus disease 2019 (COVID-19) severity or plays an intrinsic role in microvascular thrombosis and organ failure remains unanswered. We assessed whether markers of endothelial damage and immune dysregulation were associated with organ failure, thrombus formation, and death.

APPROACH AND RESULTS: Markers of endothelial damage (VWF:Ag [von Willebrand factor antigen], PAI-1 [plasminogen activator inhibitor-1], syndecan-1, TFPI [tissue factor pathway inhibitor], and soluble thrombomodulin), complement activation (C5a and C5b-9), cytokines (IL [interleukin]-6, TNF [tumor necrosis factor]- α , and IL-2R), and neutrophil extracellular traps (cell-free DNA, nucleosomes, and myeloperoxidase-DNA) were measured at intensive care unit admission in 82 patients with COVID-19. We also analyzed the histological composition of thrombi collected in critically ill living patients successfully weaned from extracorporeal membrane oxygenation. Beside respiratory failure, VWF:Ag, PAI-1, TFPI, and syndecan-1 were independently associated with liver injury and multiorgan failure development, underlining the direct role of endotheliopathy in organ failure. Nucleosomes were also associated with liver injury, multiorgan failure, and death which occurred in 38%, 60%, and 27% of patients, respectively. Moreover, dysregulated immune response including cytokines, complement, and neutrophil extracellular traps was associated with markers of endothelial damage, respiratory failure, and liver injury. COVID-19 thrombi retrieved from extracorporeal membrane oxygenation circuitry contained accumulation of neutrophils, VWF, and significantly higher amount of neutrophil extracellular traps when compared with non-COVID-19 thrombi.

CONCLUSIONS: We provide new associative data supporting that endotheliopathy and dysregulated immune responses are involved in respiratory and liver failure through microvascular damage in patients with severe COVID-19.

Key Words: coronavirus ■ cytokines ■ death ■ endothelium ■ thrombosis

Severe acute respiratory syndrome coronavirus 2 (SARS-CoV-2) that causes coronavirus disease 2019 (COVID-19), preferentially infects respiratory epithelial cells, but can also result in extrapulmonary manifestations, such as myocardial, hepatocellular, or acute kidney injury.^{1,2} COVID-19 is also associated with a prothrombotic phenotype, elevated laboratory markers of coagulopathy, and an increased risk of thrombosis first

identified through manifestations of large vessels thrombosis.³⁻⁸ There is also growing evidence suggesting that microvascular thrombosis is likely a major pathophysiologic event in COVID-19.^{9,10}

The ACE2 (angiotensin-converting enzyme 2) receptor, essential for SARS-CoV-2 uptake by host cells, is highly expressed on endothelial cells. Postmortem lung histological analyses have reported the presence

Correspondence to: Sophie Susen, MD, PhD, Heart and Lung Institute, Hemostasis Department, Bd du Pr Leclercq, CHU Lille, 59037 Lille Cedex, France. Email sophiesusen@aol.com

*A. Dupont and A. Rauch contributed equally.

The Data Supplement is available with this article at <https://www.ahajournals.org/doi/suppl/10.1161/ATVBAHA.120.315595>.

For Sources of Funding and Disclosures, see page XXX.

© 2021 American Heart Association, Inc.

Arterioscler Thromb Vasc Biol is available at www.ahajournals.org/journal/atvb

Nonstandard Abbreviations and Acronyms

ACE2	angiotensin-converting enzyme 2
ARDS	acute respiratory distress syndrome
BMI	body mass index
COVID-19	coronavirus disease 2019
CRP	C-reactive protein
ICU	intensive care unit
NET	neutrophil extracellular trap
PAD4	peptidyl arginine deiminase type 4
PAI-1	plasminogen activator inhibitor-1
SARS-CoV-2	severe acute respiratory syndrome coronavirus 2
SOFA	sequential organ failure assessment
TFPI	tissue factor pathway inhibitor
TNF	tumor necrosis factor
VV-ECMO	veno-venous extracorporeal membrane oxygenation
VWF:Ag	von Willebrand factor antigen

Highlights

- In patients with severe COVID-19 (coronavirus disease 2019), the degree of endotheliopathy at intensive care unit admission is associated with different organ dysfunctions even after adjustment for other risk factors, age, sex, and body mass index further underlining the direct involvement of endotheliopathy in organ failure.
- There is a relationship between endothelial damage and the extent of immune inflammatory responses in patients with severe COVID-19 highlighting that inflammatory-driven processes are likely primary drivers of endothelial damage leading to microvascular thrombosis and organ failure in COVID-19.
- Histopathologic comparison of COVID-19 thrombi collected from extracorporeal membrane oxygenation with non-COVID-19 specimens shows a specific involvement of neutrophil extracellular traps in COVID-19 thrombogenesis.
- VWF released from damaged endothelial cells interacts with neutrophil extracellular traps released from neutrophils and could play a major role as a scaffold for thrombus formation in COVID-19 pathophysiology.

of vascular inflammation and severe endothelial injury as a direct consequence of SARS-CoV-2 intracellular infection.^{11,12} Although direct viral tissue damage is a plausible mechanism of endothelial injury, a dysregulated immune response could also be involved.² Using cultured human pulmonary microvascular endothelial cells, we demonstrated that plasma collected from critically ill patients with COVID-19 triggers endothelial damage in vitro.¹³ Interestingly, this plasma-induced endothelial cytotoxicity was associated in patients with a more pronounced hypoxemia and higher circulating levels of biomarkers of endothelial damage and a dysregulated immune response. This in vitro response could be a marker of in vivo microvascular damage. Once injured, endothelial cells can activate coagulation leading to widespread microvascular thrombi and promote multiorgan failure.

To date, reports assessing the presence of endothelial damage and microvascular thrombosis in patients with COVID-19 focused on respiratory failure or death as main outcomes.^{14–18}

To address the question whether endothelial damage and microvascular thrombosis could occur in other organs, we assessed whether the degree of endotheliopathy at intensive care unit (ICU) admission is an early indicator of organ failure (hepatic, renal, hemodynamic, or multiorgan failure) in addition to respiratory failure by investigating a large panel of endothelial damage markers (VWF [von Willebrand factor], PAI-1 [plasminogen activator inhibitor-1], TFPI [tissue factor pathway inhibitor], and sThrombomodulin [soluble thrombomodulin]) and endothelial glycocalyx disruption (syndecan-1). As a dysregulated immune response in COVID-19 has also

been proposed to mediate organ dysfunction through several pathways inducing endothelial damage and microvascular thrombosis, we evaluated if endotheliopathy and organ failure are associated with a dysregulated immune response.^{19,20} Finally, we investigated the composition of thrombi collected in living critically ill patients with COVID-19.

MATERIALS AND METHODS

The data that support the findings of this study are available from the corresponding author upon reasonable request.

Patients

Consecutive patients admitted for COVID-19 were recruited from the ICU of Lille University Hospital between March 21 and April 16, 2020. Inclusion criteria were individuals aged 18 years or older with a positive SARS-CoV-2 real-time polymerase chain reaction. Patients received enoxaparin or unfractionated heparin according to their renal status and the need for invasive procedures. In overweight and obese patients, the dosing regimen was adapted according to the European Society of Cardiology proposals.²¹ From April 6th onwards, patients received thromboprophylaxis according to the GFHT/GIHP proposals.²² This study was approved by the French institutional authority for personal data protection (Commission Nationale de l'Informatique et des Libertés, registration number DEC20-086), and ethics committee (ID-CRB-2020-A00763-36), and informed consent was obtained from all participants. The protocol was registered as a clinical trial (URL: <https://www.clinicaltrials.gov>; Unique identifier: NCT04327180).

Outcomes

The outcomes were the occurrence of any organ injury, respiratory failure, and development of renal, hemodynamic, liver injury, or multiorgan injury within 14 days of ICU admission or all-cause 28-day mortality. Secondary respiratory failure was defined by the need for mechanical ventilation. Kidney, liver, and shock components of the sequential organ failure assessment (SOFA) score were used to assess the presence of renal, liver, or hemodynamic injuries. Renal failure was defined as presence or any aggravation of renal SOFA and Kidney Disease: Improving Global Outcomes score from ICU admission; liver injury as presence or any aggravation of hepatic SOFA score from ICU admission or alanine aminotransferase or aspartate transaminase values more than thrice the upper limit of normal; hemodynamic dysfunction as a need for epinephrine or norepinephrine support at a dose $>0.1 \mu\text{g}/\text{kg}$ per minute. SOFA scores were evaluated at ICU admission and on ICU days 4, 7, and 14. If the patient was discharged from ICU before day 14, the last SOFA score recorded during ICU stay was used. Multiorgan injury was defined by the presence of more than one dysfunction.

Follow-up period was limited to 14 days to minimize the contribution of long-term ICU complications unspecific to COVID-19 as confounding event in outcome assessment.

Laboratory Testing

Blood was collected at ICU admission for each patient on 0.109 mol/L trisodium citrate tube (BD Vacutainer, BD Diagnostics, Sparks, MD). All analyses were performed on platelet-poor plasma obtained after a double centrifugation at 2500g for 15 minutes at room temperature.

ELISA assays were performed to measure sThrombomodulin, syndecan-1, and nucleosomes using Human Thrombomodulin/BDC-3 Quantikine ELISA kit (R&D Systems, Minneapolis, MN), Human sCD138 ELISA kit (Diaclone, Besançon, France), and Cell Death Detection ELISAPLUS kit (Roche Diagnostics, Bâle, Suisse), respectively. TFPI was measured with Asserachrom total TFPI (Diagnostica Stago, Asnières sur Seine, France) and PAI-1 with Asserachrom PAI-1 (Diagnostica Stago). C5a and C5b-9 were measured using standard ELISA kits (Quidel, San Diego, CA). Prothrombin time and fibrinogen were measured on an STA R Max analyzer (Diagnostica Stago) using STA Neoplastin (Diagnostica Stago) and LiquidFib (Diagnostica Stago). D-dimers levels were measured in $\mu\text{g}/\text{mL}$ fibrinogen equivalent units using an immunoturbidimetric latex-particle assay (Liatest DDI-Plus, Diagnostica Stago) on the STA R Max analyzer (Diagnostica Stago). VWF:Ag was measured using an immunoturbidimetric assay (LIAPHEN VWF:Ag, HYPHEN BioMed, Andresy, France), both on a CS 2400 analyzer (Sysmex, Kobe, Japan). ADAMTS13 activity was measured with the Technozym ADAMTS13 activity ELISA kit (Technoclone, Vienna, Austria).

Cell-free DNA was measured by spectrofluorimetry at 520 nm after excitation at 480 nm with Quant-iT PicoGreen dsDNA assay (Thermo Fischer Scientific, Waltham, MA) on a SAFAS spectrophotometer (Monaco, France). For MPO-DNA complexes quantification, we used the Cell Death Detection Elisa kit (Roche, Basel, Switzerland). All samples were analyzed in duplicate.

IL (Interleukin)-6, TNF (tumor necrosis factor)- α , and soluble IL-2R (IL-2 receptor) concentrations were assessed using

the Ella Automated Immunoassay System (ProteinSimple, San Jose, CA).

Other laboratory blood dosages including a complete blood count, CRP (C-reactive protein), liver transaminases, bilirubin, and creatinine by standard methods as part of patient's care in the Biology and Pathology Center of Lille University Hospital.

Thrombi Analysis

Histological analysis was performed on thrombi collected immediately after veno-venous extracorporeal membrane oxygenation (VV-ECMO) removal from 8 patients with COVID-19 and 3 patients without COVID-19 with successful weaning of ECMO. Thrombi were washed in saline, incubated in 4% paraformaldehyde for 24 hours at room temperature, and analyzed as previously described.^{23,24}

Statistical Analysis

Quantitative variables were expressed as means (\pm SD) or medians (interquartile range) and categorical variables as frequencies (percentage). We assessed the association of the endothelial markers and nucleosomes with the occurrence of organ injury (censored at 14 days) and death during ICU stay using Student test and ANCOVA for adjusted analysis on age, sex, and body mass index (BMI). A log transformation of original markers data was performed if required. For each outcome, P values were adjusted for multiple comparisons using the false discovery rate procedure. We computed the adjusted effect sizes of the 6 markers using the Cohen d formula for ANCOVA with the 95% CI. For other analyses, Spearman rank coefficient correlation was used to test the association between quantitative variables, and Mann-Whitney U test or Kruskal-Wallis test (followed by Dunn pairwise post hoc comparisons) for comparison of quantitative variables according to subgroups. Statistical analyses were performed using the SAS software package version 9.4 (SAS Institute, Cary, NC).

RESULTS

Patients Characteristics

A total of 82 patients with COVID-19 were admitted in ICU (Table 1). At admission, median $\text{PaO}_2/\text{FiO}_2$ was 146 mmHg, and median SOFA score was 5.9 (2–9). All patients had increased oxygen requirements with 48 patients (59%) requiring mechanical ventilation, 19 (23%) high-flow oxygen therapy, and 15 (18%) low-flow oxygen therapy. Respiratory failure requiring mechanical ventilation was observed in 12 more patients in the 14 days after ICU admission. Eleven patients (13%) presented with hemodynamic failure while hepatic or renal dysfunction unrelated to preexisting liver or renal disease were observed in 15 (18%) and 34 (41%) patients, respectively. Worsening of the hemodynamic, hepatic, or renal status was observed in 12 (15%), 16 (20%), and 6 (7%) patients, respectively. Hepatic dysfunction and hemodynamic failure occurred at a significantly later stage than renal or respiratory failure ($P<0.001$). Ten patients required a VV-ECMO

Table 1. Baseline Patients' Characteristics According to Occurrence of Organ Injury or Death in ICU

	All (n=82)	No organ failure* (n=11)	Respiratory failure (n=60)	Renal injury (n=40)	Liver injury (n=31)	Hemodynamic failure (n=23)	Multiorgan injury (n=49)	Death (n=22)
Demographics								
Age, y	60 (14)	59 (10)	59 (15)	61 (14)	56 (14)	64 (15)	60 (15)	68 (15)
Sex (male)	64 (78)	7 (70)	48 (80)	31 (77)	25 (80)	20 (87)	40 (81)	18 (82)
Body mass index, kg/m ²	31.2 (7)	31.4 (7)	32.2 (7)	32 (8)	31.4 (7)	30.8 (6)	31.8 (7)	31.1 (7)
Comorbidities								
Diabetes	22 (27)	4 (40)	15 (25)	12 (30)	5 (15)	4 (17)	11 (22)	8 (36)
Hypertension	44 (54)	70 (70)	30 (50)	20 (50)	16 (48)	12 (52)	26 (53)	16 (73)
Chronic pulmonary disease	21 (26)	1 (10)	15 (25)	14 (35)	8 (26)	5 (22)	16 (32)	7 (32)
Chronic heart failure	6 (8)	2 (20)	5 (8)	5 (12)	1 (3)	3 (13)	5 (10)	1 (4)
Coronary/peripheral arterial disease	8 (10)	0	6 (10)	6 (15)	3 (9)	3 (13)	6 (12)	4 (18)
Stroke	4 (5)	1 (10)	1 (2)	2 (5)	0	0	1 (2)	1 (4)
Chronic liver disease	2 (2)	0	0	2 (5)	0	1 (4)	0	0
Chronic kidney disease	7 (8)	1 (10)	3 (5)	5 (12)	3 (9)	2 (8)	4 (8)	1 (4)
Time to illness onset, d	10.4 (5.5)	10.3 (4)	11.3 (5.5)	10 (6.3)	11 (4.6)	10.7 (5.5)	11.1 (5.8)	10.6 (6.3)
Organ dysfunctions								
Total SOFA score†	5.9 (4)	1.9 (1.3)	7 (4)	7 (4.4)	7.4 (4)	7.3 (4.6)	7.1 (4.2)	7 (4.1)
Pao ₂ /FiO ₂ ratio, mmHg	146 (88)	161 (76)	126 (68)	152 (103)	118 (71)	131 (74)	124 (67)	120 (74)
Need for invasive ventilation†	48 (59)	0	48 (80)	20 (50)	11 (35)	10 (43)	32 (65)	14 (63)
Renal SOFA score†	0 [0–1]	1 [0–2]	0 [0–1]	0 [0–1]	0 [0–1]	0 [0–2]	0 [0–1]	0 [0–2]
KDIGO score†	1 [0–2]	0 [0–0.25]	1 [0–3]	2 [0–3]	1 [0–2]	1.5 [0–3]	1 [0–3]	1 [0–2.5]
Hepatic SOFA score†	0 [0–0]	0 [0–0]	0 [0–0]	0 [0–0]	0 [0–1]	0 [0–0]	0 [0–0]	0 [0–0]
Hepatic SOFA score ≥1†	10 (12)	1 (10)	8 (13)	5 (12)	8 (26)	4 (17)	7 (14)	2 (9)
ALT or AST > thrice ULN†	8 (10)	0	8 (13)	4 (10)	7 (22)	4 (17)	8 (16)	3 (14)
Hepatic SOFA score ≥1 or ALT/AST > thrice ULN†	14 (17)	0	12 (20)	7 (17)	15 (48)	6 (26)	11 (22)	4 (18)
Need for epinephrine or nor-epinephrine support at a dose > 0.1 µg/kg per minute†	11 (48)	0	10 (16)	6 (15)	5 (16)	11 (48)	11 (48)	5 (23)
Median time to organ dysfunction or death, d			0 (0–4)	0 (0–7)	4 (0–14)	4 (0–14)	0 (0–7)	6 (1–38)
Laboratory markers								
CRP, mg/L	169 (124)	87 (55)	201 (128)	190 (121)	199 (113)	219 (153)	208 (128)	183 (112)
PT ratio	1.28 (0.6)	1.28 (0.44)	1.22 (0.2)	1.38 (0.8)	1.20 (0.15)	1.43 (1.08)	1.33 (0.77)	1.53 (1.12)
D-dimer, µg/mL	2.4 [1.1–4.7]	1 [0.8–6.1]	3 [1.6–4.7]	2.7 [1.3–4.6]	3 [1.4–5.7]	3.3 [2.1–6.6]	2.9 [1.5–4.6]	3.1 [1.8–4.7]
Platelets, G/L	271 (114)	261 (82)	287 (122)	258 (108)	289 (132)	276 (121)	278 (126)	276 (133)
Neutrophils, G/L	9 (5.3)	5.8 (2.4)	10.2 (5.5)	11.7 (6.3)	11.2 (6.2)	10.6 (4.9)	11.1 (5.7)	10.2 (4.5)
ALT, IU/L	54 (41)	40 (10)	58 (45)	47 (33)	77 (52)	57 (44)	59 (47)	52 (39)
AST, IU/L	73 (58)	39 (13)	81 (64)	74 (53)	107 (68)	89 (73)	89 (69)	87 (74)
Bilirubin, mg/L	6.8 (4.3)	6 (2.9)	6.9 (4.5)	6.7 (4.2)	9.2 (5.5)	8.2 (5.8)	7.2 (4.8)	7.1 (5.1)
Creatinine, mg/dL	90 [70–140]	130 [90–230]	90 [70–130]	90 [70–140]	90 [70–120]	90 [80–190]	90 [70–120]	95 [77–200]

Values are number (%) otherwise stated: mean (SD) or median [interquartile range]. Secondary respiratory failure was defined by the need for mechanical ventilation. Kidney, liver, and shock components of the SOFA score were used to assess the presence of renal, liver, or hemodynamic dysfunctions. Renal failure was defined as presence or any aggravation of renal SOFA and/or KDIGO score from ICU admission. Liver injury was defined as presence or any aggravation of hepatic SOFA score from ICU admission or ALT or AST values more than thrice the upper limit of normal in accordance with the modified version of the US National Cancer Institute's (NCI's) Common Terminology Criteria for Adverse Events (CTCAE) (2017). Hemodynamic dysfunction was defined as a need for epinephrine or norepinephrine support at a dose > 0.1 µg/kg/min. SOFA scores were evaluated for all ICU patients at ICU admission and on ICU days 4, 7, and 14. If the patient was discharged from ICU before day 14, the last SOFA score recorded during ICU stay was used. Multiorgan dysfunction was defined by the presence of more than one dysfunction. ALT indicates alanine transaminase; AST, aspartate transaminase; CRP, C-reactive protein; FiO₂, fraction of inspired oxygen; ICU, intensive care unit; KDIGO, kidney disease: improving global outcomes; Pao₂, arterial oxygen partial pressure; PT, prothrombin time; and SOFA, sequential organ failure assessment.

*Indication for ICU admission (n=1 unless otherwise stated): pneumonia (n=9); 8 of the 9 patients required high-flow oxygen therapy during ICU stay but none required mechanical ventilation, myocardial infarction, and ischemic stroke.

†Baseline values.

support after ICU admission (Table I in the [Data Supplement](#) for description). Eleven patients were receiving heparin (unfractionated heparin, n=8; low molecular weight heparin, n=3).

Endotheliopathy and Dysregulated Immune Response Are Associated With Altered Baseline Markers of Respiratory and Liver Function

Baseline levels of VWF:Ag ($P<0.0001$), syndecan-1 ($P<0.0001$), TFPI ($P=0.03$), and PAI-1 ($P=0.03$) were significantly higher in patients requiring high-flow oxygen therapy or mechanical ventilation at admission than in patients with lower oxygen requirements (Figure I in the [Data Supplement](#)).

Bilirubin, aspartate transaminase, and alanine aminotransferase correlated with most of the endothelial damage biomarkers (VWF:Ag, syndecan-1, TFPI, and PAI-1; Table 2). We also observed a correlation between either P_{aO_2}/F_{iO_2} ratio, alanine aminotransferase, or bilirubin and markers of complement activation (C5a) and neutrophil extracellular trap (NET)osis. Bilirubin was also correlated with IL-6. Aspartate transaminase was correlated with C5a, cytokines, and markers of NETosis (cell-free DNA and nucleosomes). Among cytokines, NETs and complement activation markers, nucleosomes were the immune parameter which was the most consistently and significantly associated with impaired liver and respiratory functions. No correlation was observed between endothelial markers, cytokines, complement, or NETosis markers with creatinine levels.

Furthermore, a severe imbalance between VWF and ADAMTS13 concentrations (ADAMTS13/VWF:Ag ratio =0.17 [0.12-0.26]) was present at admission suggesting an impairment in hemostasis promoting microvascular thrombosis.

Overall, when assessing the pattern of organ injury at ICU admission, the association between immune

response and biomarkers of organ dysfunction was mostly apparent for the lungs and the liver.

Occurrence of Respiratory Failure, Liver Injury, Multiorgan Injury, and Death Are Associated With Endotheliopathy and Nucleosomes Levels

As shown in Figure 1 and Table II in the [Data Supplement](#), 2 endothelial damage markers (syndecan-1 and PAI-1) were significantly associated with respiratory failure at admission or occurring during follow-up. After adjustment for age, sex, and BMI, these associations remained significant with the strongest effect size for syndecan-1. Overall, this association of endothelial damage at admission with the occurrence of respiratory failure independently of age, sex, and BMI suggests its direct involvement in COVID-19 pneumonia pathogenesis.

We further assessed whether the degree of endothelial damage was also associated with the occurrence of specific organ dysfunctions. Occurrence of liver injury was strongly associated with baseline levels of VWF:Ag, syndecan-1, TFPI, PAI-1, and nucleosomes. After adjustment for age, sex, and BMI, these associations remained significant with the highest effect sizes for TFPI, syndecan-1, and nucleosomes.

As thrombomodulin levels are dependent on renal function in patients without endothelial damage,²⁵ we evaluated the association of renal failure and sThrombomodulin/creatinine ratio. Only high TFPI and sThrombomodulin/creatinine ratio baseline levels were significantly associated with the occurrence of renal failure. This association remained significant after adjustment. No association was observed between the other endothelial damage markers at admission and the occurrence of hemodynamic failure.

Syndecan-1, TFPI, and nucleosomes levels at ICU admission were significantly associated with the occurrence of multiorgan injury. After adjustment for age,

Table 2. Correlations Between Baseline Values of All Biomarkers and Respiratory and Liver Function Criteria

		VWF:Ag	Syndecan-1	TFPI	PAI-1	sTM	C5a	C5b-9	TNF- α	IL-6	IL-2R	Neutrophils	Cell-free DNA	MPO-DNA	Nucleosomes
P_{aO_2}/F_{iO_2}	R*	-0.28†	-0.43†	-0.33†	-0.13	-0.10	-0.25†	-0.032	0.006	-0.14	-0.14	-0.36†	-0.20	0.039	-0.31†
	P value	0.01†	<0.0001†	0.005†	0.26	0.38	0.02†	0.77	0.96	0.21	0.21	0.004†	0.08	0.73	0.008†
ALT	R*	0.35†	0.34†	0.28†	0.09	0.046	0.19†	0.25†	-0.02	-0.009	0.03	0.26†	0.17	0.088	0.25†
	P value	0.001†	0.002†	0.02†	0.4	0.69	0.09†	0.02†	0.83	0.93	0.76	0.04†	0.15	0.44	0.03†
AST	R*	0.41†	0.38†	0.37†	0.35†	0.28†	0.24†	0.04	0.31†	0.21†	0.31†	0.27†	0.38†	-0.014	0.27†
	P value	0.0001†	0.0004†	0.001†	0.001†	0.014†	0.03†	0.7	0.005†	0.05†	0.004†	0.03†	0.001†	0.9	0.02†
Bilirubin	R*	0.24†	0.24†	0.27†	0.26†	0.09	0.37†	0.40†	0.12	0.30†	0.14	0.32†	0.44†	0.31†	0.32†
	P value	0.03†	0.03†	0.02†	0.017†	0.44	0.001†	0.0002†	0.26	0.006†	0.21	0.009†	0.0001†	0.006†	0.005†

ALT indicates alanine aminotransferase; AST, aspartate aminotransferase; F_{iO_2} , fractional inspired oxygen; IL, interleukin; PAI-1, plasminogen activator inhibitor-1; P_{aO_2} , arterial oxygen partial pressure; sTM, soluble thrombomodulin; TFPI, tissue factor pathway inhibitor; TNF, tumor necrosis factor; and VWF:Ag, von Willebrand factor antigen.

*Squared Spearman rank coefficient correlation.

†

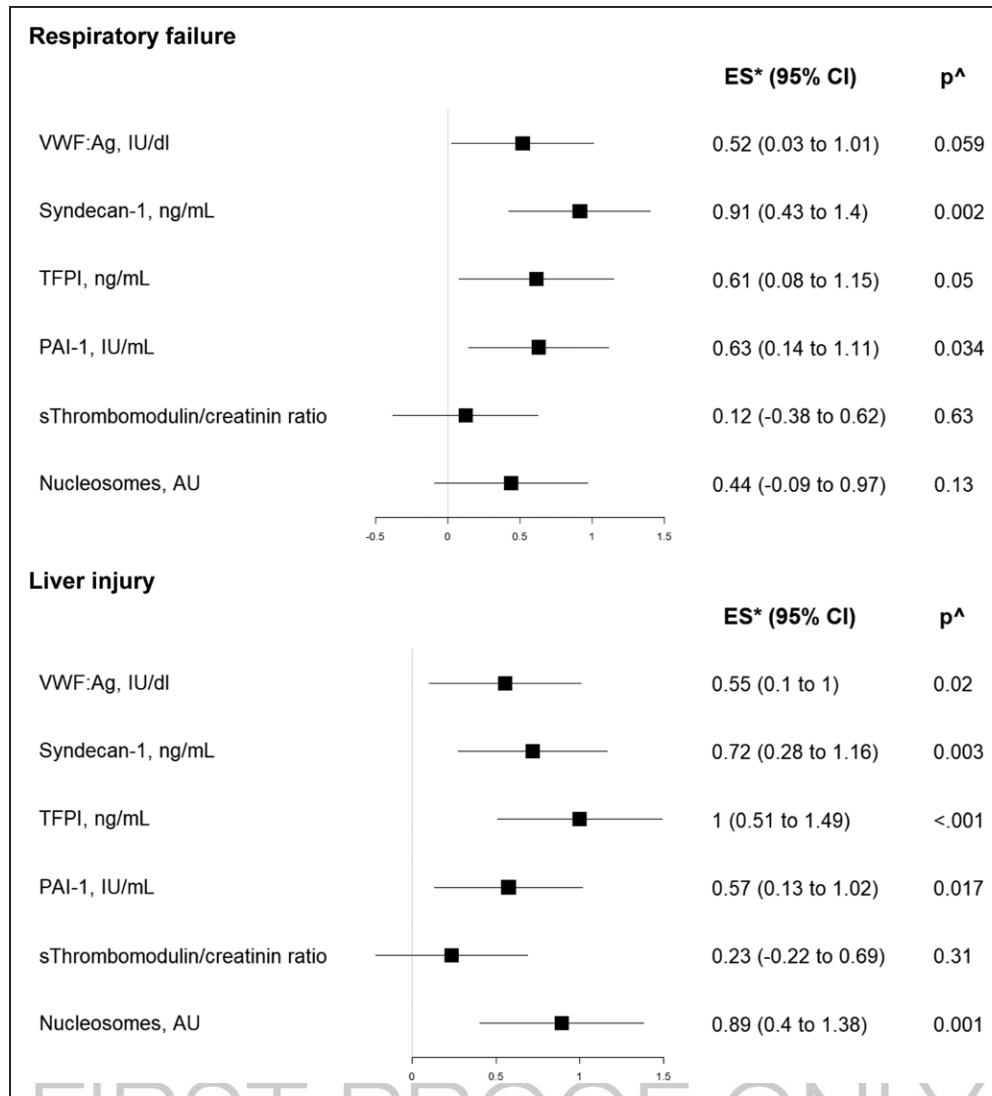


Figure 1. Association of biomarkers related to endothelial damage and nucleosomes measured at admission in intensive care unit (ICU) with occurrence of organ failures within 14 d of ICU admission or all-cause 28-d mortality.

Forest plots of adjusted effect sizes; (A): respiratory failure; (B): liver injury; (C): renal failure; (D): hemodynamic failure; (E): multiorgan failure; and (F): death. Associations were tested using ANCOVA after log transformation of original data. *Effect size (Cohen d for ANCOVA) adjusted on prespecified covariates (age, sex, and body mass index [BMI]). [^] False discovery rate adjusted *P* value; correction for multiple comparisons was performed using the Benjamini-Hochberg procedure. ES indicates effect size; PAI-1, plasminogen activator inhibitor-1; s, soluble; TFPI, tissue factor pathway inhibitor; and VWF:Ag, von Willebrand factor antigen.

sex, and BMI, these associations remained significant for all parameters (Table II in the [Data Supplement](#) for unadjusted and age, sex, and BMI adjusted relations). It was also noticed that VWF:Ag, syndecan-1, TFPI, and PAI-1 were increased according to the number of organ-injuries (Figure II in the [Data Supplement](#)). PAI-1 and nucleosomes levels at ICU admission were significantly associated with all-cause-of-death, and this association remained significant for nucleosomes after adjustment.

Interestingly, the 10 patients who required a VV-ECMO support for acute respiratory distress syndrome (ARDS) presented at ICU admission higher levels of endothelial damage markers (VWF, syndecan-1, and

TFPI) and of IL-6 and a tendency for higher nucleosome levels ($P=0.09$; Figure 2).

Overall, we demonstrated a strong association between endothelial damage markers and nucleosomes, a marker of NETs, at ICU admission and the occurrence of liver injury and multiorgan failure in critically ill patients with COVID-19.

Endotheliopathy Is Associated With a Dysregulated Immune Response

We further investigated whether cytokine levels, complement activation, and NETosis were associated with the intensity of endotheliopathy (Figure 3). The relation

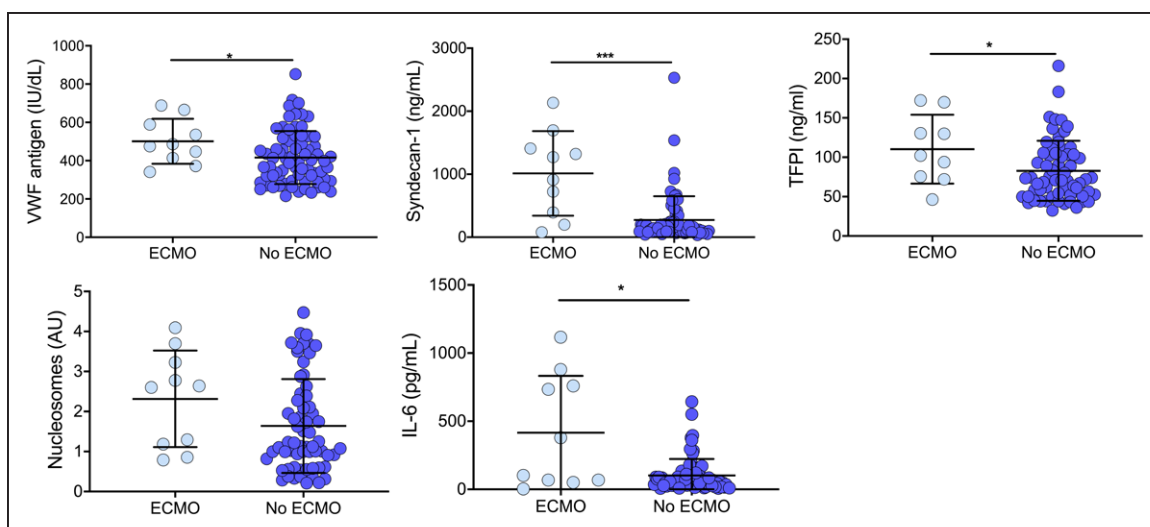


Figure 2. Comparison of main plasma levels of parameters related to endothelial dysfunction and dysregulated immune response at intensive care unit (ICU) admission according to veno-venous extracorporeal membrane oxygenation (VV-ECMO) requirement.

Data points indicate individual measurements whereas horizontal bars show mean (SD). AU indicates arbitrary units; ICU, intensive care unit; TFPI, tissue factor pathway inhibitor; and VWF:Ag, von Willebrand factor antigen. * $P < 0.05$, *** $P < 0.001$ (Mann-Whitney U test).

between baseline values of endotheliopathy biomarkers and dysregulated immune response is presented in Table III in the [Data Supplement](#). All cytokines correlated with VWF:Ag levels. IL-2R and TNF- α also correlated with syndecan-1, PAI-1, and sThrombomodulin/creatinine levels. All NETs markers correlated with VWF:Ag while cell-free DNA and nucleosomes both correlated with syndecan-1 and TFPI levels. Cell-free DNA was also correlated with PAI-1 levels. When assessing complement activation, only VWF:Ag correlated with C5b-9 levels. We also observed a correlation between most of the immune markers and D-dimer levels (IL-2R: $r = 0.29$, $P = 0.008$; IL-6: $r = 0.26$, $P = 0.02$; cell-free DNA: $r = 0.27$, $P = 0.02$; nucleosomes: $r = 0.25$, $P = 0.03$; and C5b-9: $r = 0.35$, $P = 0.001$), a coagulopathy marker consistently associated with worse outcomes across COVID-19 studies.

Overall, a dysregulated immune response, including NETosis, was associated with endothelial damage markers highlighting an interaction between inflammatory-driven processes and endothelial damage leading to organ failure in critically ill patients with COVID-19.

Immune Response and Endotheliopathy Promote Immunothrombosis

In inflammatory disorders, microvascular thrombosis as a consequence of endothelial damage is involved in organ failure. We aimed to investigate the main drivers of thrombogenicity in COVID-19 through the combined analysis of circulating blood biomarkers reflecting endothelial damage and by investigating the composition of in vivo generated thrombi collected in alive patients.

We investigated whether the composition of thrombi collected in critically ill living patients with COVID-19

reflected the involvement of both circulating markers of endothelial damage, measured by VWF staining and immune dysregulation, measured by neutrophils and NETs staining.

We performed a histological analysis of thrombi collected from VV-ECMO tubings from 8 patients with COVID-19 and 3 patients without COVID-19 presenting with ARDS (for main characteristics of patients included in this histological analysis, see Table I in the [Data Supplement](#)). As expected, Martius Scarlet Blue and hematoxylin and eosin stainings revealed a strong presence of fibrin and VWF. No prominent differences in red blood cells, fibrin, platelet, or VWF content between COVID-19 and the control thrombi were observed (Figure 4). In contrast, a striking accumulation of nucleated cellular infiltration was found in thrombi from patients with COVID-19 compared with control. Neutrophil elastase staining revealed that leukocyte infiltrates in COVID-19 thrombi consisted predominantly of neutrophils, with few macrophages detected. Quantitative analysis revealed a significant higher area of citrullinated histones H3 staining in thrombi from patients with COVID-19 compared with patients without COVID-19.

In plasma, neutrophil count correlated with markers of NETosis (cell-free DNA: $r = 0.51$, $P < 0.0001$ and nucleosomes: $r = 0.45$, $P = 0.0005$), endothelial damage (VWF: $r = 0.46$, $P = 0.0001$; TFPI: $r = 0.55$, $P < 0.0001$; syndecan-1: $r = 0.43$, $P = 0.0003$; and PAI-1: $r = 0.26$, $P = 0.04$), and cytokine (IL-2R: $r = 0.29$, $P = 0.02$). Patients with COVID-19 displayed higher levels of CRP and fibrinogen than the 3 patients without COVID-19 (295 versus 50 mg/L, $P = 0.01$; 8.62 versus 6.1 g/L, $P = 0.05$, respectively). Compared with control thrombi, COVID-19 thrombi contained significant amounts of

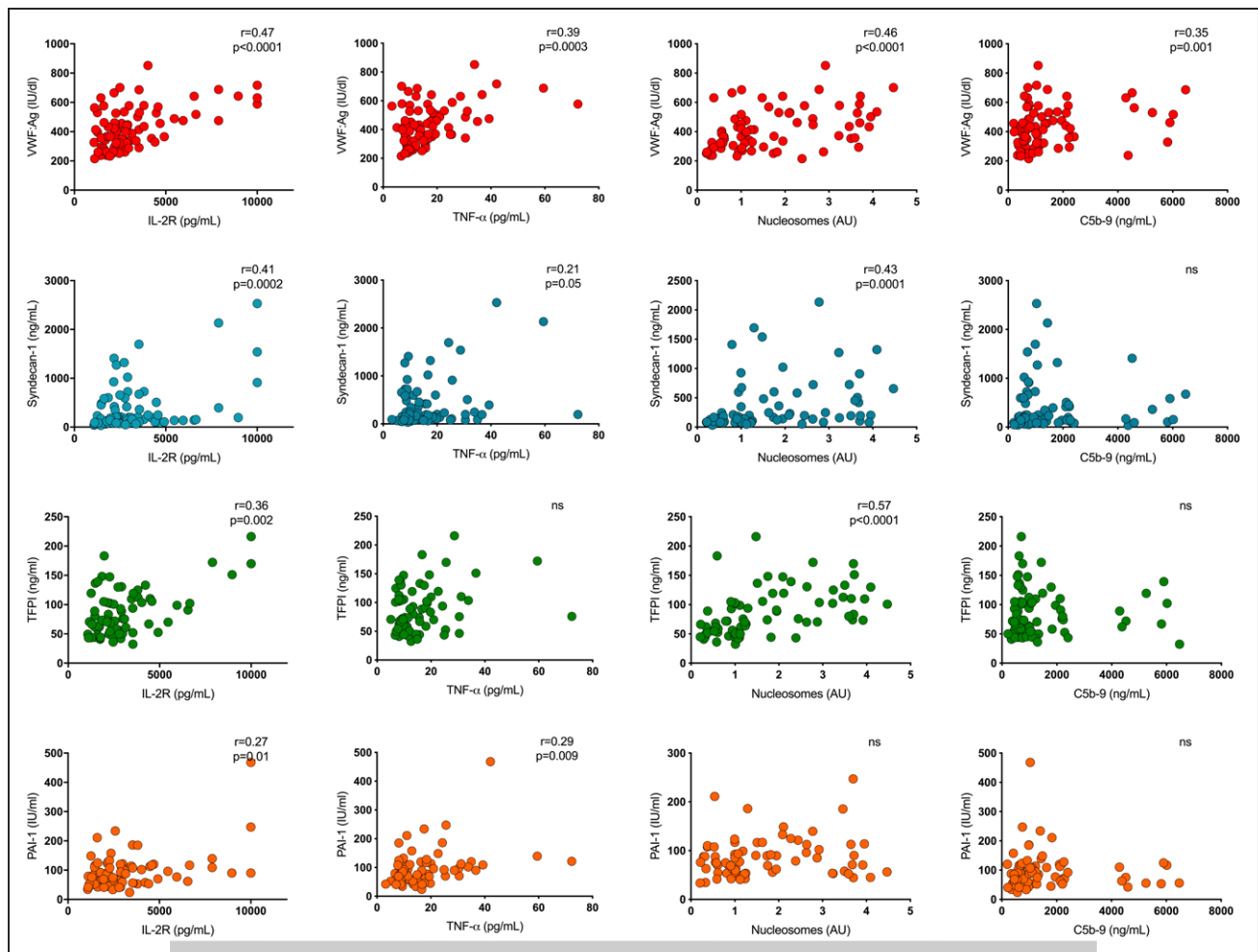


Figure 3. Association of von Willebrand factor antigen (VWF:Ag), syndecan-1, TFPI (tissue factor pathway inhibitor), and PAI-1 (plasminogen activator inhibitor-1) levels with plasmatic levels of cytokines, neutrophil extracellular trap (NET)osis, and complement markers.

Correlations were evaluated with Spearman rank-correlation statistical tool. AU indicates arbitrary units; C5b-9, complement membrane attack complex; IL-2R, soluble interleukin-2 receptor; TFPI, tissue factor pathway inhibitor; and TNF- α , tumor necrosis factor α .

intracellular and extracellular citrullinated histones H3, suggestive of NETosis.

Overall, we provide evidence for immunothrombosis through endothelial damage and dysregulated immune responses, in particular NETs formation, in the pathogenesis of severe COVID-19. VWF released from damaged endothelial cells interacts with NETs released from neutrophils to provide a scaffold for platelet adhesion and thrombus formation.²⁶

DISCUSSION

Using endotheliopathy circulating biomarkers, we demonstrate that endothelial damage is associated with respiratory failure, liver injury, multiorgan failure, and death in COVID-19. These complications occurred in 73%, 38%, 60%, and 27% of patients included in the study, respectively, in accordance with previous studies in ICU patients with COVID-19.^{2,27} We also observed a relationship

between endothelial damage and the extent of immune inflammatory responses highlighting that inflammatory-driven processes are likely primary drivers of endothelial damage leading to microvascular thrombosis and organ failure in COVID-19. These findings are consistent with our previous finding on the direct in vitro acute cytotoxic effect on vascular endothelial cells of plasma collected from critically ill COVID-19.¹³ Finally, we provide evidence for a major role of neutrophils, NETosis, and VWF as a scaffold for thrombus formation and new associative data to support the concept that endothelial damage and dysregulated immune responses are involved in thrombus formation and organ failure.

The pathophysiology of multiorgan dysfunction in patients with COVID-19 is still poorly understood. Patients with COVID-19 seem to have a specific respiratory failure pattern characterized by an initial good compliance despite severe hypoxemia.²⁷ This discrepancy could be linked to ventilation-perfusion mismatch and

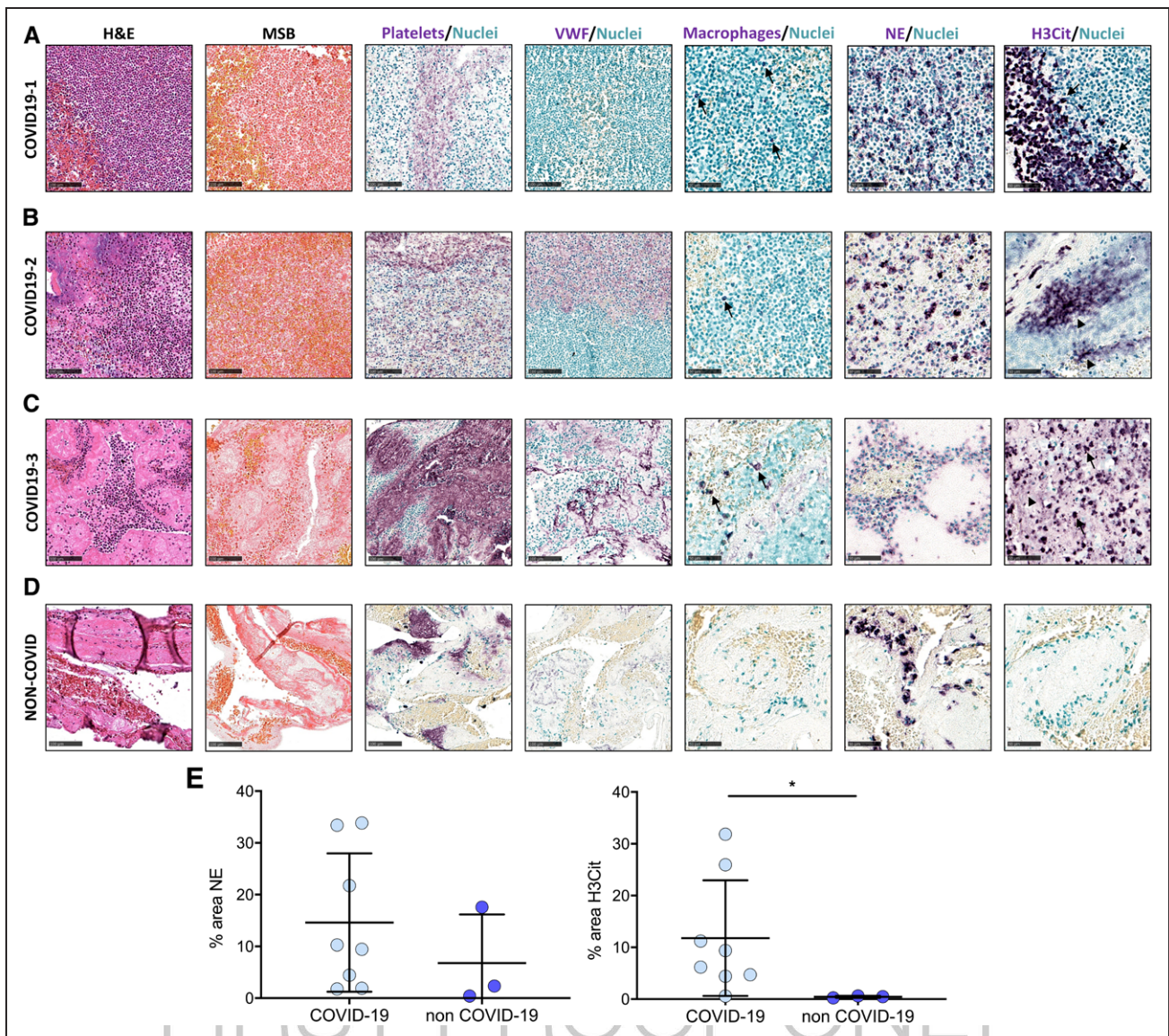


Figure 4. Histological analysis of clots retrieved from extracorporeal membrane oxygenation (ECMO) circuits after veno-venous ECMO removal in recovered patients.

Representative ECMO thrombi from 8 living patients with coronavirus disease 2019 (COVID-19) of ECMO support and from 3 patients without COVID-19 with acute respiratory distress syndrome. Consecutive thrombus sections were stained with hematoxylin and eosin (H&E) to have a general overview, Martius Scarlet Blue (MSB) to identify fibrin (red) and RBCs (yellow) and immunohistochemical agents (purple) for platelets, VWF (von Willebrand factor), macrophages, neutrophil elastase (NE), and citrullinated histones H3 (H3Cit). Nuclei are indicated in light green in the immunohistochemical stainings. **A–C**, H&E, MSB, and the nuclear counterstain on immunostainings reveal a massive amount of cellular infiltration in COVID-19 thrombi compared with **(D)** control. **A–C**, No substantial differences in fibrin, platelet, and VWF content is observed compared with **(D)** control. **A–C**, NE staining indicates that the large proportion of leukocytes in patients with COVID-19 are neutrophils whereas only a few macrophages (arrows) are found. **A–C**, COVID-19 thrombi contain both intracellular (arrows) and extracellular H3Cit (arrowheads), suggestive of neutrophil extracellular trap (NET)osis. Scale bar=100 μ m for H&E, MSB, platelet, and VWF staining. Scale bar=50 μ m for macrophages, NE, and H3Cit staining. **E**, Quantitative analysis of NE and H3Cit staining area in ECMO thrombi from 8 COVID-19 and 3 controls patients. * $P<0.05$ (Mann-Whitney U test).

the loss of hypoxic pulmonary vasoconstriction because of endothelial damage with subsequent activation of coagulation and widespread microvascular thrombi formation in the lungs and other organs. In the lung, the progressive injury increases vascular permeability then causes the alveolar changes, ground-glass appearance in the parenchymal lung injury, and clearly ARDS.^{28,29} Supporting this concept, we observed that endothelial

damage markers are significantly associated with the development of respiratory failure in ICU upon admission to ICU.³⁰ Endothelial glycocalyx damage was evidenced by increased plasma levels of syndecan-1 and TFPI. As TFPI is mainly associated with endothelial cells through binding to heparan sulfate proteoglycans, a main component of the glycocalyx at the surface of endothelial cells, this result further strengthens the hypothesis

that glycocalyx disruption is a key-feature of critically ill patients with COVID-19.³¹ Endothelial damage was also evidenced by unusually high VWF concentrations indicative of an acute release of endothelial Weibel-Palade bodies content in patients with COVID-19, as previously reported for angiopoietin also stored in the same organelles.¹⁴ However, it should be mentioned that the presence of endothelial injury is not specific of COVID-19 since the prognostic value of endothelial biomarker levels was already reported in patients with septic shock or acute lung injury.³² Prior reports have also extensively linked aberrant NETs formation to pulmonary diseases, particularly ARDS. Neutrophils from patients with pneumonia-associated ARDS appear primed to form NETs, and both the extent of priming and the level of NETs in blood correlate with disease severity and mortality.^{33,34} It is, therefore, likely that NETs, as a source of extracellular histones, contribute to ARDS and sepsis.^{35,36}

There are increasing reports addressing the pathophysiology of ARDS related to COVID-19 using seasonal influenza patients as controls. To date, most of the data were derived from autopsy studies performing comparisons with historical controls such as patients who died from seasonal influenza. Ackermann et al¹² showed distinctive vascular features between patients who died from COVID-19 and influenza with lung autopsy of COVID-19 specimens showing more severe endothelial injury with disrupted endothelial cell membranes and alveolar-capillary microthrombi. Likewise, Nicolai et al^{37,38} reported a significantly higher percentage of vessels with features of immunothrombosis in the lung vasculature in patients with COVID-19 than in patients without COVID-19 pneumonia ones. While being pivotal in the understanding of the pathophysiology of respiratory failure in COVID-19, the major limitation of such studies is inherent to their postmortem nature with potential confoundings related to long-term ICU complications unspecific to COVID-19. Our study was designed to overcome such limitation using a dual approach including the dosing of an extensive set of biomarkers related to endothelial damage and NETosis at ICU admission and a thrombus analysis performed on thrombi retrieved from alive patients with COVID-19 at ECMO weaning. Our study gives further evidence supporting a critical role for endotheliopathy and immunothrombosis in COVID-19 ARDS pathophysiology since we observed that these biomarkers upon admission were significantly associated with the development not only of respiratory failure but also hepatic and multiorgan failure in ICU.

Beyond respiratory failure, kidney, and liver injuries were frequently observed in our COVID-19 cohort as previously reported.^{18,39–41} The direct relation between biomarkers of endothelial damage, NETosis with different organ dysfunctions has not been established so far during COVID-19 apart from autopsy findings.^{11,12} It is noteworthy to report that the extent of endotheliopathy

and microvascular damage at ICU admission in patients with COVID-19 is associated not only with respiratory failure but also with the occurrence of multiorgan failure. Indeed, high baseline levels of most endothelial biomarkers were associated with the development of liver injury while this association was not found for hemodynamic failure and only observed with TFPI levels for renal failure suggesting that different mechanisms are contributing to liver and renal injuries in patients with COVID-19. Moreover, liver injury occurred at a later stage than renal dysfunction. Thrombomodulin is increased in patients with renal dysfunction, a situation frequently encountered in critically ill patients with COVID-19.^{25,41} As such, we only found a weak association between the sThrombomodulin over creatinine ratio and the development of renal injury. A renal tropism of SARS-CoV-2 with a direct cytopathic effect on podocytes and renal tubular epithelial cells could explain our results,⁴² although ultrastructure evidence of direct viral replication in the kidney is lacking.

Liver injury occurs in 14% to 53% of patients with COVID-19 according to the definition criteria used across studies and patient's illness severity.^{43,44} Raised transaminase levels are also frequently reported despite the fact that ACE2 is poorly expressed on hepatocytes and that SARS-CoV-2 RNAs were not detected in hepatocytes from patients with COVID-19.^{45,46} In contrast, given that ACE2 is highly expressed in the endothelial layer of small hepatic blood vessels, hepatic dysfunction could be related to endotheliopathy rather than to a cytopathic viral effect. The significant association between the degree of endotheliopathy and the development of liver injury is in line with this hypothesis. Liver injury at admission was most frequently observed in patients with elevated cytokines, complement activation, and NETosis suggesting that inflammatory-driven processes could promote hepatocyte or liver sinusoidal cell damage in patients with COVID-19. Patients with COVID-19 with nonalcoholic steatohepatitis have a higher likelihood of developing a severe illness, irrespective of obesity.⁴⁷ Interestingly, altered hepatic immune function has been also recently reported to mediate the progression of fatty liver to nonalcoholic steatohepatitis through pronounced changes in blood immune cell populations.⁴⁸ Whether nonalcoholic steatohepatitis presence exacerbates the SARS-CoV-2-induced inflammatory process thereby contributing mechanistically to severe COVID-19 deserves further research.

We also clearly demonstrated that thrombi are infiltrated with neutrophils and contain markers suggestive of NETs, confirming the role of neutrophils and NETs in the immunothrombotic complications that characterize COVID-19 pathology.^{37,38,49,50} We also provide new evidence for a major role of VWF, a binding partner of NETs, as a scaffold for thrombus formation in critically ill patients with COVID-19.⁵¹

Albeit being observational, our results strengthen the concept that mechanical vessel obstruction by aggregated NETs is a major pathogenic determinant of severe COVID-19 leading to vascular damage, thrombosis, and organ dysfunction. In vitro, it has been shown that sera from patients with COVID-19 trigger NETs release from control neutrophils.⁵² There is also some evidence that SARS-CoV-2 infection promotes an immunologic response unseen with seasonal influenza. This difference is well illustrated in our ECMO cohort with patients with COVID-19 displaying significantly higher levels of CRP and fibrinogen than the 3 patients without COVID ARDS. This is in line with the recently published case series also reporting a significantly higher content of NETs in the coronary thrombi of COVID-19 patients with ST-segment-elevation myocardial infarction compared with historical non-COVID-19 ST-segment-elevation myocardial infarction.⁵³ Whether this increased NETosis is due to complement activation or to specific interactions between monocytes and neutrophils or to other mechanisms is currently under investigation. Our results clearly suggest a specific role of neutrophils and NETs in the thrombotic process of circulating blood. A marked imbalance between VWF and ADAMTS13 was present at admission indicative of a reduced capacity of ADAMTS13 to process ultralarge VWF multimers, a finding associated with microvascular thrombosis and organ failure in sepsis.⁵⁴ Given that the prothrombotic role of VWF fibers included in NETs is dependent on their multimeric size, potent inhibitors of ADAMTS13 activity such as thrombospondin-1 and α -defensins released locally by activated platelets and neutrophils, respectively, could potentiate thrombus growth by VWF fibers.^{55–57}

Targeting dysregulated immune responses, including neutrophils and NETosis or endotheliopathy, might be a valuable and feasible therapeutic approach to prevent thrombosis and improve clinical outcomes of COVID-19. Drugs that target NETs include molecules that block neutrophils function such as glucocorticoids that prevent NETosis such as neutrophil elastase and PAD4 (peptidyl arginine deiminase type 4) inhibitors and that dismantle NETs with DNases I.^{58,59} Improving NETs clearance through exogenous DNase treatment with recombinant human DNase I is currently under investigation for safety and efficacy in nine clinical trials in COVID-19. Targeting the VWF-ADAMTS13 axis is also an attractive hypothesis. *N*-acetylcysteine that dissolves ultralarge VWF multimers under different conditions in both animal models and humans is also currently under investigation.⁶⁰

The main strengths of our study are (1) our outcomes were not restricted to respiratory failure or death and other organ dysfunctions were investigated and (2) we assessed the occurrence of organ injury in the first 14 days only after ICU admission and the composition of extrapulmonary thrombi collected at the acute phase of the disease. Thus, our results are less likely to be affected

by confounding related to long-term complications unspecific to COVID-19, (3) we combined a large panel of markers and adjusted our results to the main COVID-19 comorbidities to disentangle the role of SARS-CoV-2 on top of comorbidities. Assessing whether the biomarkers associated with multiorgan dysfunction in our study are specific to SARS-CoV-2 or could be translated to other viruses such as SARS, MERS, or influenza is a major limitation.

In conclusion, our results suggest that organ injury due to endothelial and microvascular damage is associated to immunopathology and may occur in parallel to SARS-CoV-2 intracellular infection.

ARTICLE INFORMATION

Received November 3, 2020; accepted February 2, 2021.

Affiliations

University of Lille, Inserm, CHU Lille, Institut Pasteur de Lille, U1011-EGID, France (A. Dupont, A.R., S. Staessens, M.M., M.P., D.C., E.J., F.L., B.S., F.V., S. Susen). CHU Lille, Intensive Care Department, Pôle de Réanimation, France (J.G., M.C.). University of Lille, Inserm, CHU Lille, U1286-INSITU - Institute for Translational Research in Inflammation, France (P.V., G.L.). CHU Lille, Institut d'Hématologie-Transfusion, France (A.B.). University of Lille, Inserm, CHU Lille, Institut Pasteur de Lille, UMR1019-CIL, France (K.F.). University of Lille, Inserm, CHU Lille, INSERM U 1167, Institut Pasteur, France (M.L.). University of Lille, CHU Lille, ULR 2694 - METRICS: Évaluation des technologies de santé et des pratiques médicales, France (A. Duhamel, J.L.). CHU Lille, Surgical Critical Care, Department of Anesthesiology and Critical Care, France (D.G.). Laboratory for Thrombosis Research, KU Leuven Campus Kulak Kortrijk, Belgium (S.F.D.M.). CHU Lille, Service de Chirurgie Cardiaque, France (N.R.). University of Lille, CNRS, Inserm, CHU Lille, Institut Pasteur de Lille, U1019 - UMR 9017 - CIL - Center for Infection and Immunity of Lille, France (E.K.). Inserm, UMR_1176, Université Paris-Saclay, France (P.L.). University of Lille, Inserm U1285, CHU Lille, CNRS, UMR 8576 - UGSF - Unité de Glycobiologie Structurale et Fonctionnelle, France (J.P.).

Acknowledgments

We thank all physicians and medical staff involved in patient care. Special thanks are addressed to Eric Boulleaux, Laureline Bourgeois, Vincent Dalibard, Aurélie Jospin, Catherine Marichez, Bénédicte Pradines, Sandrine Vanderziepe, all the biologists and technicians of the Hemostasis Department for their support during the coronavirus disease 2019 (COVID-19) pandemic.

Sources of Funding

This study was supported by the French government through the Programme Investissement d'Avenir (I-SITE ULNE/ANR-16-IDEX-0004 ULNE) and with the Hospital-University Research in Health program (Recherche Hospitalo-Universitaire, WILL-ASSIST HEART ANR-17-RHUS-0011) managed by the Agence Nationale de la Recherche and by KU Leuven through IOF C3/DOA and BOF ISP funding.

Disclosures

None.

Supplemental Materials

Online Tables I–III
Online Figure I and II

REFERENCES

- Zhou F, Yu T, Du R, Fan G, Liu Y, Liu Z, Xiang J, Wang Y, Song B, Gu X, et al. Clinical course and risk factors for mortality of adult inpatients with COVID-19 in Wuhan, China: a retrospective cohort study. *Lancet*. 2020;395:1054–1062. doi: 10.1016/S0140-6736(20)30566-3
- Gupta A, Madhavan MV, Sehgal K, Nair N, Mahajan S, Sehrawat TS, Bikdeli B, Ahluwalia N, Ausiello JC, Wan EY, et al. Extrapulmonary manifestations of

- COVID-19. *Nat Med*. 2020;26:1017–1032. doi: 10.1038/s41591-020-0968-3
3. Connors JM, Levy JH. COVID-19 and its implications for thrombosis and anticoagulation. *Blood*. 2020;135:2033–2040. doi: 10.1182/blood.2020006000
 4. Helms J, Tacquard C, Severac F, Leonard-Lorant I, Ohana M, Delabranche X, Merdji H, Clere-Jehl R, Schenck M, Fagot Gandet F, et al; CRICS TRIGGERSEP Group (Clinical Research in Intensive Care and Sepsis Trial Group for Global Evaluation and Research in Sepsis). High risk of thrombosis in patients with severe SARS-CoV-2 infection: a multicenter prospective cohort study. *Intensive Care Med*. 2020;46:1089–1098. doi: 10.1007/s00134-020-06062-x
 5. Klok FA, Kruip MJHA, van der Meer NJM, Arbous MS, Gommers DAMPJ, Kant KM, Kaptein FHJ, van Paassen J, Stals MAM, Huisman MV, et al. Incidence of thrombotic complications in critically ill ICU patients with COVID-19. *Thromb Res*. 2020;191:145–147. doi: 10.1016/j.thromres.2020.04.013
 6. Poissy J, Goutay J, Caplan M, Parmentier E, Duburcq T, Lassalle F, Jeanpierre E, Rauch A, Labreuche J, Susen S; Lille ICU Haemostasis COVID-19 Group. Pulmonary embolism in patients with COVID-19: awareness of an increased prevalence. *Circulation*. 2020;142:184–186. doi: 10.1161/CIRCULATIONAHA.120.047430
 7. Middeldorp S, Coppens M, van Haaps TF, Foppen M, Vlaar AP, Müller MCA, Bouman CCS, Beenen LFM, Kootte RS, Heijmans J, et al. Incidence of venous thromboembolism in hospitalized patients with COVID-19. *J Thromb Haemost*. 2020;18:1995–2002. doi: 10.1111/jth.14888
 8. Zhang L, Feng X, Zhang D, Jiang C, Mei H, Wang J, Zhang C, Li H, Xia X, Kong S, et al. Deep vein thrombosis in hospitalized patients with COVID-19 in Wuhan, China: prevalence, risk factors, and outcome. *Circulation*. 2020;142:114–128. doi: 10.1161/CIRCULATIONAHA.120.046702
 9. Pons S, Fodil S, Azoulay E, Zafrani L. The vascular endothelium: the cornerstone of organ dysfunction in severe SARS-CoV-2 infection. *Crit Care*. 2020;24:353. doi: 10.1186/s13054-020-03062-7
 10. Rovas A, Osiaevi I, Buscher K, Sackarnd J, Tepasse PR, Fobker M, Kühn J, Braune S, Göbel U, Thölking G, et al. Microvascular dysfunction in COVID-19: the MYSTIC study [published online October 14, 2020]. *Angiogenesis*. 2020:1–13. doi: 10.1007/s10456-020-09753-7
 11. Varga Z, Flammer AJ, Steiger P, Haberecker M, Andermatt R, Zinkernagel AS, Mehra MR, Schuepbach RA, Ruschitzka F, Moch H. Endothelial cell infection and endotheliitis in COVID-19. *Lancet*. 2020;395:1417–1418. doi: 10.1016/S0140-6736(20)30937-5
 12. Ackermann M, Verleden SE, Kuehnel M, Haverich A, Welte T, Laenger F, Vanstapel A, Werlein C, Stark H, Tzankov A, et al. Pulmonary vascular endotheliitis, thrombosis, and angiogenesis in Covid-19. *N Engl J Med*. 2020;383:120–128. doi: 10.1056/NEJMoa2015432
 13. Rauch A, Dupont A, Goutay J, Caplan M, Staessens S, Moussa M, Jeanpierre E, Corseaux D, Lefevre G, Lassalle F, et al; Lille COVID Research Network (LICORNE); Members of the LICORNE Scientific Committee. Endotheliopathy is induced by plasma from critically ill patients and associated with organ failure in severe COVID-19. *Circulation*. 2020;142:1881–1884. doi: 10.1161/CIRCULATIONAHA.120.050907
 14. Smadja DM, Guerin CL, Chocron R, Yatim N, Boussier J, Gendron N, Khider L, Hadjadj J, Goudot G, Debuc B, et al. Angiotensin-2 as a marker of endothelial activation is a good predictor factor for intensive care unit admission of COVID-19 patients. *Angiogenesis*. 2020;23:611–620. doi: 10.1007/s10456-020-09730-0
 15. Goshua G, Pine AB, Meizlish ML, Chang CH, Zhang H, Bahel P, Baluha A, Bar N, Bona RD, Burns AJ, et al. Endotheliopathy in COVID-19-associated coagulopathy: evidence from a single-centre, cross-sectional study. *Lancet Haematol*. 2020;7:e575–e582. doi: 10.1016/S2352-3026(20)30216-7
 16. Masi P, Hékimian G, Lejeune M, Chommeloux J, Desnos C, Pineton De Chambrun M, Martin-Toutain I, Nieszowska A, Lebreton G, Bréchet N, et al. Systemic inflammatory response syndrome is a major contributor to COVID-19-associated coagulopathy: insights from a prospective, single-center cohort study. *Circulation*. 2020;142:611–614. doi: 10.1161/CIRCULATIONAHA.120.048925
 17. Liu PP, Blet A, Smyth D, Li H. The science underlying COVID-19: implications for the cardiovascular system. *Circulation*. 2020;142:68–78. doi: 10.1161/CIRCULATIONAHA.120.047549
 18. Yeh CH, de Wit K, Levy JH, Weitz JI, Vaezzadeh N, Liaw PC, Fox-Robichaud A, Soliman K, Kim PY. Hypercoagulability and coronavirus disease 2019-associated hypoxic respiratory failure: mechanisms and emerging management paradigms. *J Trauma Acute Care Surg*. 2020;89:e177–e181. doi: 10.1097/TA.0000000000002938
 19. Libby P, Lüscher T. COVID-19 is, in the end, an endothelial disease. *Eur Heart J*. 2020;41:3038–3044. doi: 10.1093/eurheartj/ehaa623
 20. Perico L, Benigni A, Casiraghi F, Ng LFP, Renia L, Remuzzi G. Immunity, endothelial injury and complement-induced coagulopathy in COVID-19. *Nat Rev Nephrol*. 2021;17:46–64. doi: 10.1038/s41581-020-00357-4
 21. Rocca B, Fox KAA, Ajjan RA, Andreotti F, Baigent C, Collet JP, Grove EL, Halvorsen S, Huber K, Morais J, et al. Antithrombotic therapy and body mass: an expert position paper of the ESC Working Group on Thrombosis. *Eur Heart J*. 2018;39:1672–1686f. doi: 10.1093/eurheartj/ehy066
 22. Susen S, Tacquard CA, Godon A, Mansour A, Garrigue D, Nguyen P, Godier A, Testa S, Levy JH, Albaladejo P, et al; GIHP and GFHT. Prevention of thrombotic risk in hospitalized patients with COVID-19 and hemostasis monitoring. *Crit Care*. 2020;24:364. doi: 10.1186/s13054-020-03000-7
 23. Staessens S, Denorme F, Francois O, Desender L, Dewaele T, Vanacker P, Deckmyn H, Vanhoorelbeke K, Andersson T, De Meyer SF. Structural analysis of ischemic stroke thrombi: histological indications for therapy resistance. *Haematologica*. 2020;105:498–507. doi: 10.3324/haematol.2019.219881
 24. Laridan E, Denorme F, Desender L, François O, Andersson T, Deckmyn H, Vanhoorelbeke K, De Meyer SF. Neutrophil extracellular traps in ischemic stroke thrombi. *Ann Neurol*. 2017;82:223–232. doi: 10.1002/ana.24993
 25. Hergesell O, Andrassy K, Geberth S, Nawroth P, Gabath S. Plasma thrombomodulin levels are dependent on renal function. *Thromb Res*. 1993;72:455–458. doi: 10.1016/0049-3848(93)90246-k
 26. Kolaczowska E, Jenne CN, Surewaard BG, Thanabalasuriar A, Lee WY, Sanz MJ, Mowen K, Opendakker G, Kubes P. Molecular mechanisms of NET formation and degradation revealed by intravital imaging in the liver vasculature. *Nat Commun*. 2015;6:6673. doi: 10.1038/ncomms7673
 27. Grasselli G, Zangrillo A, Zanella A, Antonelli M, Cabrini L, Castelli A, Cereda D, Coluccello A, Foti G, Fumagalli R, et al; COVID-19 Lombardy ICU Network. Baseline characteristics and outcomes of 1591 patients infected with SARS-CoV-2 admitted to ICUs of the Lombardy Region, Italy. *JAMA*. 2020;323:1574–1581. doi: 10.1001/jama.2020.5394
 28. Marini JJ, Gattinoni L. Management of COVID-19 respiratory distress. *JAMA*. 2020;323:2329–2330. doi: 10.1001/jama.2020.6825
 29. Leisman DE, Deutschman CS, Legrand M. Facing COVID-19 in the ICU: vascular dysfunction, thrombosis, and dysregulated inflammation. *Intensive Care Med*. 2020;46:1105–1108. doi: 10.1007/s00134-020-06059-6
 30. Rauch A, Labreuche J, Lassalle F, Goutay J, Caplan M, Charbonnier L, Rohn A, Jeanpierre E, Dupont A, Duhamel A, et al. Coagulation biomarkers are independent predictors of increased oxygen requirements in COVID-19. *J Thromb Haemost*. 2020;18:2942–2953. doi: 10.1111/jth.15067
 31. Kato H. Regulation of functions of vascular wall cells by tissue factor pathway inhibitor: basic and clinical aspects. *Arterioscler Thromb Vasc Biol*. 2002;22:539–548. doi: 10.1161/01.atv.0000013904.40673.cc
 32. Hyseni A, Kemperman H, de Lange DW, Kesecioglu J, de Groot PG, Roest M. Active von Willebrand factor predicts 28-day mortality in patients with systemic inflammatory response syndrome. *Blood*. 2014;123:2153–2156. doi: 10.1182/blood-2013-08-508093
 33. Adrover JM, Aroca-Crevillén A, Crainciuc G, Ostos F, Rojas-Vega Y, Rubio-Ponce A, Cilloniz C, Bonzón-Kulichenko E, Calvo E, Rico D, et al. Programmed 'disarming' of the neutrophil proteome reduces the magnitude of inflammation. *Nat Immunol*. 2020;21:135–144. doi: 10.1038/s41590-019-0571-2
 34. Bendib I, de Chaisemartin L, Mekontso Dessap A, Chollet-Martin S, de Prost N. Understanding the role of neutrophil extracellular traps in patients with severe pneumonia and ARDS. *Chest*. 2019;156:1278–1280. doi: 10.1016/j.chest.2019.08.2179
 35. Chaput C, Zychlinsky A. Sepsis: the dark side of histones. *Nat Med*. 2009;15:1245–1246. doi: 10.1038/nm1109-1245
 36. Lefrançois E, Looney MR. Neutralizing extracellular histones in acute respiratory distress syndrome: a new role for an endogenous pathway. *Am J Respir Crit Care Med*. 2017;196:122–124. doi: 10.1164/rccm.201701-0095ED
 37. Nicolai L, Leunig A, Brambs S, Kaiser R, Weinberger T, Weigand M, Muenchhoff M, Hellmuth JC, Ledderose S, Schulz H, et al. Immunothrombotic dysregulation in COVID-19 pneumonia is associated with respiratory failure and coagulopathy. *Circulation*. 2020;142:1176–1189. doi: 10.1161/CIRCULATIONAHA.120.048488
 38. Nicolai L, Leunig A, Brambs S, Kaiser R, Joppich M, Hoffknecht ML, Gold C, Engel A, Polewka V, Muenchhoff M, et al. Vascular neutrophilic inflammation and immunothrombosis distinguish severe COVID-19 from influenza pneumonia [published online November 20, 2020]. *J Thromb Haemost*. doi: 10.1111/jth.15179
 39. Guan WJ, Ni ZY, Hu Y, Liang WH, Ou CQ, He JX, Liu L, Shan H, Lei CL, Hui DSC, et al; China Medical Treatment Expert Group for Covid-19.

- Clinical characteristics of coronavirus disease 2019 in China. *N Engl J Med*. 2020;382:1708–1720. doi: 10.1056/NEJMoa2002032
40. Zhang C, Shi L, Wang FS. Liver injury in COVID-19: management and challenges. *Lancet Gastroenterol Hepatol*. 2020;5:428–430. doi: 10.1016/S2468-1253(20)30057-1
 41. Battle D, Soler MJ, Sparks MA, Hiremath S, South AM, Welling PA, Swaminathan S; COVID-19 and ACE2 in Cardiovascular, Lung, and Kidney Working Group. Acute kidney injury in COVID-19: emerging evidence of a distinct pathophysiology. *J Am Soc Nephrol*. 2020;31:1380–1383. doi: 10.1681/ASN.2020040419
 42. Su H, Yang M, Wan C, Yi LX, Tang F, Zhu HY, Yi F, Yang HC, Fogo AB, Nie X, et al. Renal histopathological analysis of 26 postmortem findings of patients with COVID-19 in China. *Kidney Int*. 2020;98:219–227. doi: 10.1016/j.kint.2020.04.003
 43. Chen F, Chen W, Chen J, Xu D, Xie W, Wang X, Xie Y. Clinical features and risk factors of COVID-19-associated liver injury and function: a retrospective analysis of 830 cases. *Ann Hepatol*. 2020;21:100267. doi: 10.1016/j.aohep.2020.09.011
 44. Kullar R, Patel AP, Saab S. Hepatic injury in patients with COVID-19. *J Clin Gastroenterol*. 2020;54:841–849. doi: 10.1097/MCG.0000000000001432
 45. Yang JK, Lin SS, Ji XJ, Guo LM. Binding of SARS coronavirus to its receptor damages islets and causes acute diabetes. *Acta Diabetol*. 2010;47:193–199. doi: 10.1007/s00592-009-0109-4
 46. Wang XX, Shao C, Huang XJ, Sun L, Meng LJ, Liu H, Zhang SJ, Li HJ, Lv FD. Histopathological features of multiorgan percutaneous tissue core biopsy in patients with COVID-19 [published online August 26, 2020]. *J Clin Pathol*. doi: 10.1136/jclinpath-2020-206623
 47. Targher G, Mantovani A, Byrne CD, Wang XB, Yan HD, Sun QF, Pan KH, Zheng KI, Chen YP, Eslam M, et al. Risk of severe illness from COVID-19 in patients with metabolic dysfunction-associated fatty liver disease and increased fibrosis scores. *Gut*. 2020;69:1545–1547. doi: 10.1136/gutjnl-2020-321611
 48. Haas JT, Vonghia L, Mogilenko DA, Verrijken A, Molendi-Coste O, Fleury S, Deprince A, Nikitin A, Woitrain E, Ducrocq-Geoffroy L, et al. Transcriptional network analysis implicates altered hepatic immune function in NASH development and resolution. *Nat Metab*. 2019;1:604–614. doi: 10.1038/s42255-019-0076-1
 49. Skendros P, Mitsios A, Chrysanthopoulou A, Mastellos DC, Metallidis S, Rafailidis P, Ntinopoulou M, Sertaridou E, Tsironidou V, Tsigalou C, et al. Complement and tissue factor-enriched neutrophil extracellular traps are key drivers in COVID-19 immunothrombosis. *J Clin Invest*. 2020;130:6151–6157. doi: 10.1172/JCI141374
 50. Middleton EA, He XY, Denorme F, Campbell RA, Ng D, Salvatore SP, Mostyka M, Baxter-Stoltzfus A, Borczuk AC, Loda M, et al. Neutrophil extracellular traps contribute to immunothrombosis in COVID-19 acute respiratory distress syndrome. *Blood*. 2020;136:1169–1179. doi: 10.1182/blood.202007008
 51. Grässle S, Huck V, Pappelbaum KI, Gorzelanny C, Aponte-Santamaría C, Baldauf C, Gräter F, Schneppenheim R, Obser T, Schneider SW. von Willebrand factor directly interacts with DNA from neutrophil extracellular traps. *Arterioscler Thromb Vasc Biol*. 2014;34:1382–1389. doi: 10.1161/ATVBAHA.113.303016
 52. Veras FP, Pontelli MC, Silva CM, Toller-Kawahisa JE, de Lima M, Nascimento DC, Schneider AH, Caetité D, Tavares LA, Paiva IM, et al. SARS-CoV-2-triggered neutrophil extracellular traps mediate COVID-19 pathology. *J Exp Med*. 2020;217:e20201129. doi: 10.1084/jem.20201129
 53. Blasco A, Coronado MJ, Hernández-Terciado F, Martín P, Royuela A, Ramil E, García D, Goicolea J, Del Trigo M, Ortega J, et al. Assessment of neutrophil extracellular traps in coronary thrombus of a case series of patients with COVID-19 and myocardial infarction [published online December 29, 2020]. *JAMA Cardiol*. doi: 10.1001/jamacardio.2020.7308
 54. Fukushima H, Nishio K, Asai H, Watanabe T, Seki T, Matsui H, Sugimoto M, Matsumoto M, Fujimura Y, Okuchi K. Ratio of von Willebrand factor propeptide to ADAMTS13 is associated with severity of sepsis. *Shock*. 2013;39:409–414. doi: 10.1097/SHK.0b013e3182908ea7
 55. Sorvillo N, Mizurini DM, Coxon C, Martinod K, Tilwawala R, Cherpokova D, Salinger AJ, Seward RJ, Staudinger C, Weerapana E, et al. Plasma peptidylarginine deiminase IV promotes VWF-platelet string formation and accelerates thrombosis after vessel injury. *Circ Res*. 2019;125:507–519. doi: 10.1161/CIRCRESAHA.118.314571
 56. Bonnefoy A, Daenens K, Feys HB, De Vos R, Vandervoort P, Vermynen J, Lawler J, Hoylaerts MF. Thrombospondin-1 controls vascular platelet recruitment and thrombus adherence in mice by protecting (sub)endothelial VWF from cleavage by ADAMTS13. *Blood*. 2006;107:955–964. doi: 10.1182/blood-2004-12-4856
 57. Pillai VG, Bao J, Zander CB, McDaniel JK, Chetty PS, Seeholzer SH, Bdeir K, Cines DB, Zheng XL. Human neutrophil peptides inhibit cleavage of von Willebrand factor by ADAMTS13: a potential link of inflammation to TTP. *Blood*. 2016;128:110–119. doi: 10.1182/blood-2015-12-688747
 58. Jin Y, Ji W, Yang H, Chen S, Zhang W, Duan G. Endothelial activation and dysfunction in COVID-19: from basic mechanisms to potential therapeutic approaches. *Signal Transduct Target Ther*. 2020;5:293. doi: 10.1038/s41392-020-00454-7
 59. Thierry AR, Roch B. Neutrophil extracellular traps and by-products play a key role in COVID-19: pathogenesis, risk factors, and therapy. *J Clin Med*. 2020;9:2942. doi: 10.3390/jcm9092942
 60. Martínez de Lizarrondo S, Gakuba C, Herbig BA, Repessé Y, Ali C, Denis CV, Lenting PJ, Touzé E, Diamond SL, Vivien D, et al. Potent thrombolytic effect of N-acetylcysteine on arterial thrombi. *Circulation*. 2017;136:646–660.

BRIEF REPORT



Gastrointestinal bleeding from angiodysplasia in von Willebrand disease: Improved diagnosis and outcome prediction using videocapsule on top of conventional endoscopy

Antoine Rauch¹ | Camille Paris¹ | Yohann Repesse² | Julien Branche³ | Roseline D'Oiron⁴ | Annie Harroche⁵ | Catherine Ternisien⁶ | Sabine-Marie Castet⁷ | Aurélien Lebreton⁸ | Brigitte Pan-Petes⁹ | Fabienne Volot¹⁰ | Segolene Claeysens¹¹ | Pierre Chamouni¹² | Valérie Gay¹³ | Claire Berger¹⁴ | Dominique Desprez¹⁵ | Céline Falaise¹⁶ | Christine Biron Andreani¹⁷ | Catherine Marichez¹ | Benedicte Pradines¹ | Christophe Zawadzki¹ | Nathalie Itzhar Baikian¹⁸ | Annie Borel-Derlon² | Jenny Goudemand¹ | Romain Gerard³ | Sophie Susen¹ | for the French Reference Center on von Willebrand Disease

¹Department of Hematology and Transfusion, CHU Lille, Institut d'Hématologie Transfusion, Lille, France

²Laboratoire d'hématologie, CHU de Caen, Caen, France

³Department of Gastroenterology, CHU Lille, Lille, France

⁴Center for Hemophilia and Rare Congenital Bleeding Disorders, University Hospital Paris-Sud, AP-HP, Bicêtre Hospital, Le Kremlin-Bicêtre, France

⁵Hôpital Necker Enfants Malades APHP, Paris, France

⁶Laboratoire d'Hématologie, CHU Nantes, Nantes, France

⁷CHU Bordeaux Pellegrin, Bordeaux, France

⁸CHU Clermont Ferrand, Clermont Ferrand, France

⁹Unité Hémostase clinique, Service Hématologie CHU Brest, Brest, France

¹⁰CHU Dijon, Dijon, France

¹¹CHU Toulouse, Toulouse, France

¹²CHU Rouen, Rouen, France

Abstract

Background: Despite a high prevalence of angiodysplasia, no specific guidelines are available for the modalities of endoscopic exploration of gastrointestinal (GI) bleeding in von Willebrand disease (VWD). Whether VWD patients could benefit from video capsule endoscopy (VCE) looking for angiodysplasia eligible to endoscopic treatment or at high risk of bleeding is unknown.

Objectives: To assess the diagnostic efficacy for angiodysplasia and the prognostic value of VCE on top of conventional endoscopy in VWD patients with GI bleeding.

Patients/Methods: A survey was sent to the 30 centers of the French-network on inherited bleeding disorders to identify VWD patients referred for endoscopic exploration of GI bleeding from January 2015 to December 2017. Data obtained included patient characteristics, VWD phenotype/genotype, GI bleeding pattern, results of endoscopic investigations, and medical management applied including endoscopic therapy. We assessed by Kaplan-Meier analysis the recurrence-free survival after the first GI bleeding event according to endoscopic categorization and, in patients with angiodysplasia, to the presence of small-bowel localizations on VCE exploration.

Manuscript handled by: David Lillicrap.

Final decision: David Lillicrap, 21-Oct-2020.

© 2020 International Society on Thrombosis and Haemostasis

¹³CH Métropole Savoie - Site de Chambéry, Chambéry, France

¹⁴CHU Saint-Etienne, St Etienne, France

¹⁵CHU Strasbourg, Strasbourg, France

¹⁶Centre régional de traitement des hémophiles, Hôpital de La Timone, AP-HM, Marseille, France

¹⁷Laboratoire d'Hématologie, CHU Montpellier, Montpellier, France

¹⁸Laboratoire d'Hématologie, GH St-Louis Lariboisière F.Widal - Hôpital Lariboisière APHP, Paris, France

Correspondence

Sophie Susen, CHU Lille, Hematology Transfusion, Lille, France; INSERM, U1011, Univ. Lille, U1011 EGID, Institut Pasteur de Lille, Lille, France.
Email: sophiesusen@aol.com

Results: GI bleeding source localization was significantly improved when including VCE exploration ($P < .01$), even in patients without history of angiodysplasia ($P < .05$). Patients with angiodysplasia had more GI bleeding recurrences ($P < .01$). A lower recurrence-free survival was observed in patients with angiodysplasia (log-rank test, $P = .02$), and especially when lesions were located in the small bowel (log-rank test, $P < .01$), even after endoscopic treatment with argon plasma coagulation (log-rank test, $P < .01$).

Conclusion: VCE should be more systematically used in VWD patients with unexplained or recurrent GI bleeding looking for angiodysplasia eligible to endoscopic treatment or at high risk of relapse.

KEYWORDS

angiodysplasia, argon plasma coagulation, gastrointestinal bleeding, video capsule endoscopy, von Willebrand disease

1 | INTRODUCTION

Gastrointestinal (GI) bleeding is the most frequent cause of hospitalization in von Willebrand disease (VWD).^{1,2} VWD patients often present with recurrent overt or occult GI bleeding from an unidentified source on conventional endoscopy.³ This clinical picture is assumed to be related to an increased incidence of GI angiodysplasia in VWD.⁴ The mechanism could involve a dysregulated angiogenesis related to the lack of von Willebrand factor (VWF) high molecular weight multimers⁵⁻⁷ because GI bleeding from angiodysplasia is more frequent in VWD types 2A, 2B, and 3^{8,9} and in acquired von Willebrand syndrome.^{10,11} The management of angiodysplasia has been revolutionized with the advent of video capsule endoscopy (VCE), which is now the gold standard investigation to detect small-bowel angiodysplasia when no GI bleeding source is identified after conventional endoscopy and to screen for lesions eligible to argon plasma coagulation (APC), the most effective endoscopic therapy.^{12,13} Despite a high prevalence of angiodysplasia in VWD, no specific guidelines are available for the modalities of GI tract exploration in patients with GI bleeding. Current endoscopic exploration in these patients relies on a nonstandardized strategy and its efficiency to predict outcome remains poorly reported.

2 | AIMS

To investigate in current practice the diagnostic efficacy for angiodysplasia detection and the prognostic value of implementing VCE on top of conventional endoscopy in VWD patients with GI bleeding.

3 | METHODS

A survey was sent to the 30 centers involved in the French network on inherited bleeding disorders (MHEMO) to identify VWD patients referred for endoscopic exploration of at least one GI bleed from

Essentials

- VCE improves the diagnostic yield for angiodysplasia in VWD.
- Patients with obscure or recurrent GI-bleeding should benefit from VCE.

January 2015 to December 2017 and describe the practices. The follow-up period was limited to 3 years because of rapid changes in devices allowing endoscopic treatment.¹⁴ Only VWD patients fulfilling the inclusion criteria of the French reference center for VWD¹⁵ were included. VWD diagnosis was confirmed centrally in all patients including genotyping. GI bleeding episode was defined as any overt or occult GI bleeding (unexplained iron deficiency anemia causing a drop of hemoglobin level by > 2 g/dL from baseline). We analyzed patient characteristics, VWD type/subtype, GI bleeding pattern, nature (gastroscopy, colonoscopy, or VCE), and results of the endoscopic exploration and management that was applied: endoscopic therapy by APC, on-demand/prophylactic VWF replacement therapy, use of antiangiogenic drugs. If angiodysplasia without another bleeding source was identified, GI bleeding was categorized as "angiodysplasia." GI bleeding was categorized as "no angiodysplasia" if another lesion was identified and as "obscure GI bleeding" if no bleeding source was identified. Patients with angiodysplasia were categorized as "new additional angiodysplasia" or "de novo angiodysplasia" whether there was preexisting angiodysplasia at start of follow-up. Recurrence was defined as evidence of overt or occult GI bleeding (drop of hemoglobin level by > 2 g/dL from baseline). The study was approved by the institutional data protection authority of all participating centers (CNIL registration number DEC19-252).

Continuous variables were expressed as mean (\pm standard error of the mean or standard deviation) or median (with interquartile range) and categorical data as n (%). Univariate analysis involved

Mann-Whitney test for continuous variables and chi-squared or Fisher tests for binary variables. We assessed by Kaplan-Meier analysis the recurrence-free survival after the first GI bleeding event according to endoscopic categorization and in patients with angiodysplasia the rate of GI bleeding recurrence according to the presence of small-bowel localizations on VCE exploration. Statistical analysis was performed with SPSS® software. Differences with P values $< .05$ were considered significant.

4 | RESULTS AND DISCUSSION

Seventy-seven percent of the MHEMO centers answered the survey allowing further analysis of each case. All centers had access to the full set of endoscopic exploration including VCE. Patient characteristics and results are summarized in Table 1. A total of 127 GI bleeding episodes were reported in 50 patients (mean = 0.84 GI bleeding episode per patient-year). At inclusion, 20% had preexisting angiodysplasia, 16% were receiving VWF prophylaxis (with GI bleeding as primary indication in half of them), 8% were treated with antiangiogenic drugs (octreotide, $n = 2$; atorvastatin, $n = 2$), and 8% with antithrombotic drugs.

During follow-up, angiodysplasia were identified endoscopically in 46% of patients confirming angiodysplasia as the leading cause of GI bleeding in VWD.² Patients with angiodysplasia were older than patients with obscure GI bleeding ($P = .002$) and their most frequent presentation was melena. A total of five children, VWD type 2A ($n = 2$) or type 3 ($n = 3$), were explored for GI bleeding. The bleeding source was not identified in three children, whereas a diagnosis of gastric angiodysplasia and anal fissure was established in the others. GI bleeding and angiodysplasia were more frequently observed in VWD patients with type 2A, 2B, or 3 compared with patients without high molecular weight multimers defect (respectively, $n = 40/815$ vs $n = 10/1082$, $P < .0001$; and $n = 17/815$ vs $6/108$, $P = .005$).

GI bleeding management in VWD patients with angiodysplasia is challenging because of the severity and the recurrence of bleeding episodes.^{16,17} Off-label use of antiangiogenic drugs is sometimes considered in patients with refractory GI bleeding.^{18,19} In our cohort, 73% of patients with angiodysplasia or obscure GI bleeding were treated prophylactically with either VWF-containing concentrates ($n = 15$), antiangiogenic drugs (octreotide, $n = 4$; atorvastatin, $n = 3$), or both (VWF prophylaxis and octreotide, $n = 3$) during follow-up. VWF prophylaxis was more frequently introduced or intensified for GI bleeding in patients with angiodysplasia or obscure GI bleeding compared with patients with no angiodysplasia (43%, 72%, and 6%; $P = .01$ and $P < .001$, respectively).

The sequential endoscopic investigations during follow-up are summarized in Figure 1. All patients were explored at least once with conventional endoscopy. Overall, angiodysplasia were identified in 26% of patients after conventional endoscopy: new additional angiodysplasia was identified in 50% of patients with preexisting angiodysplasia and de novo angiodysplasia in 20% of patients without preexisting angiodysplasia, a proportion in line with a recent study also reporting

the frequency of angiodysplasia on conventional endoscopy.² Besides angiodysplasia, other lesions were identified in 32% of patients after conventional endoscopy (Table 1). In the remaining 42% of patients, the bleeding source was not identified after conventional endoscopy. This high proportion of VWD patients still having a negative exploration after conventional endoscopy highlights the need for a more systematic and multimodal approach to identify angiodysplasia.^{12,13} Among these 21 patients without bleeding source identification after conventional endoscopy, 15 underwent at least one VCE exploration and angiodysplasia were identified in 10/15 (66%) of them. In patients with angiodysplasia lesions already identified after conventional endoscopy, synchronous small-bowel lesions were identified in 3/8 (38%) of patients who underwent at least one VCE exploration. No difference in VCE referral was observed whether patients had preexisting bleeding angiodysplasia or not (6/10 and 19/40 patients, respectively, $P = .48$). A trend for more GI bleeding events was observed in patients referred for VCE compared with patients without VCE referral (3 ± 2.1 , $n = 25$ vs 2 ± 1.5 , $n = 11$; $P = .11$).

No adverse events associated with VCE exploration were reported. Although all the patients eligible to VCE exploration were not investigated, de novo angiodysplasia was identified in 40% of patients without preexisting angiodysplasia and new additional angiodysplasia in 70% of patients with preexisting angiodysplasia when combining VCE to conventional endoscopy (Table 1). Overall, the endoscopic localization of the bleeding source was significantly improved when using VCE exploration ($P < .01$). This result remained significant even after excluding the 10 patients with preexisting angiodysplasia ($P < .05$). In our cohort, VCE allowed to further identify angiodysplasia in two-thirds of patients with negative conventional endoscopy. Of the 11 patients with obscure GI bleeding at the end of the follow-up who should have been further explored, six were not investigated despite VCE availability. This suggests a need for dedicated guidelines for endoscopic exploration in VWD patients with GI bleeding strengthening the role for VCE on top of conventional endoscopy.

No death related to GI bleeding occurred during follow-up. A high rate of recurrence was observed (median per patient = 1 [0-2]; range: 0-7). At least one recurrence was observed in 58% of patients and 32% of them had at least two recurrences. The frequency of recurrences was higher in patients with angiodysplasia compared with patients with another bleeding lesion (log rank test, $P = .02$; Figure 2A).

At least one complete revision of the GI tract, including VCE exploration, was performed in 18 patients with angiodysplasia during their follow-up. More GI bleeding recurrences were observed in patients with small-bowel angiodysplasia on VCE than in patients without such localization (median = 2.5 [2-4.5], $n = 12$ vs 0 [0-1], $n = 6$; $P < .01$), whereas there was no significant difference in age and duration of follow-up between both groups. Accordingly, a lower survival rate before first GI bleeding recurrence was observed in patients with small-bowel angiodysplasia (log-rank test, $P < .01$), with most of them having their first recurrence within 12 months (Figure 2B).

Eighteen patients with angiodysplasia (78%) were treated at least once with APC for a total of 22 procedures. GI bleeding relapsed in 55% of these patients and following 50% of procedures. VCE status

TABLE 1 Clinical characteristics according to endoscopic categorization

Variables	All (n = 50)	Angiodysplasia (n = 23)	No Angiodysplasia (n = 16)	Obscure GI Bleeding (n = 11)	P value
Age (median) [IQR]	61 [40-68]	65 [49-70]	47 [38-69]	46 [13-62]	0.06 ^a , 0.002 ^b
Male/female	26/24	13/10	8/8	5/6	ns ^{a,b}
VWD, n (relative % ^h)					
Type 1 ¹	1 (0.2%)	1 (0.2%)	0	0	-
Type 2 ²					
2A	13 (3.5%)	9 (2.4%)	2	2	
2B	16 (4.2%)	5 (1.3%)	7	4	
2M	8 (1.8%)	4 (0.9%)	3	1	
2N	1 (0.7%)	1 (0.7%)	0	0	
Type 3 ³	11 (16%)	3 (4.5%)	4	4	
VWF:Ag IU/dL (median, IQR)	25 [10-40]	29 [15-50]	22 [3-35]	16 [0-40]	ns ^{a,b}
VWF:RCo IU/dL (median, IQR)	10 [5-16]	8 [5-14]	12 [1-20]	10 [0-20]	ns ^{a,b}
FVIII:C IU/dL (median, IQR)	32 [20-49]	33 [24-58]	34 [13-50]	31 [2-53]	ns ^{a,b}
Use of antithrombotic drugs, n	4	3 ^f	1 ^g	0	ns ^{a,b}
GI bleeding					
GI bleeding events, n (median, IQR) per patient	2 [1-3]	3 [1-4]	1 [1-2]	2 [1-2]	0.01 ^a , 0.04 ^b
Patients with ≥ 1 GI bleeding recurrence, n (%)	29 (58%)	17 (74%) ^j	5 (31%)	7 (63%)	<0.001 ^a , 0.04 ^b
Endoscopic procedures					
Gastroscopy, n (median, IQR) per patient	1 [1-2]	2 [1-3]	0.5 [0-1]	1 [1-2]	<0.001 ^a , ns ^b
Coloscopy, n (median, IQR) per patient	1 [1-2]	1 [1-2]	1 [0.25-1]	1 [1-2]	ns ^{a,b}
Completion of VCE during follow-up, n (%)	25 (50%)	18 (78%)	2 (12.5%)	5 (45%)	
Lesions identified after conventional endoscopy					
Angiodysplasia	13/50				
New additional lesions ^c	5/10	-	-	-	-
De novo angiodysplasia ^d	8/40				
Other lesions ^e	16/50				
No diagnosis	21/50				
Lesions identified in patients negative after conventional endoscopy					
Angiodysplasia		10/15			
New additional lesions ^c	-	2/3	-	-	-
De novo angiodysplasia ^d		8/12			
Medical management					
VWF prophylaxis					
At baseline, n (%)	8 (16%)	4 (17%)	1 (6%)	3 (27%)	
Introduction or intensification during follow-up, n (%)	19 (38%)	10 (43%)	1 (6%)	8 (72%)	
Antiangiogenic drugs					
At baseline, n (%)	4 (8%)	3 (13%)	0	1	

(Continues)

TABLE 1 (Continues)

Variables	All (n = 50)	Angiodysplasia (n = 23)	No Angiodysplasia (n = 16)	Obscure GI Bleeding (n = 11)	P value
At the end of follow-up, n (%)	9 (18%)	8 (34%) ⁱ	0	1	
Argon plasma coagulation, n (%)	-	18 (78%)	-	-	

ns, nonsignificant.

VWD genotyping (n = 1 unless otherwise stated):

Type 1¹: p.Arg1205Leu.

Type 2²: 2A: p.Tyr1146Cys, p.Glu1554_Gln1556del (n = 2), p.Leu1580Pro, p.Leu1582Pro, p.Arg1583Trp/p.Tyr1584Cys, p.Arg1597Trp (n = 3), p.Thr1608Pro, p.Val1665_Cys1669del, delExon17-19; 2B: p.Met1304dup (n = 4), p.Arg1306Gln, p.Arg1306Trp, p.Arg1308Pro (n = 2), p.Arg1308Cys, p.Val1316Met, p.Arg1341Gln (n = 5), p.Ile1380Lys; Type 2M: p.Arg1315Cys (n = 3), p.Arg1374Cys, p.Ser1378Phe, p.Tyr1735Asn, p.Leu1383Pro; Type 2N: p.Arg854Gln

Type 3³: p.Arg273Trp/p.Gln1311*, p.Pro812Argfs*31homozygous, p.Arg34*/p.Arg960*, c.55 + 1G>T/p.Pro812Argfs*31, p.Pro1266Gln/p.Val1279Ile, p.Gln1311*/c.8254-10T > C, p.Gln1311* homozygous, delExon1-52 homozygous, p.Cys1130* homozygous, p.Glu2742*/c.8190_8253 + 1dup64, p.Arg447Trp/p.Cys2248Tyr/p.Leu2786Pro.

¹P value for "no angiodysplasia" vs "angiodysplasia."

²P value for "obscure GI bleeding" vs "angiodysplasia."

³Patients diagnosed with angiodysplasia with preexisting angiodysplasia at start of follow-up.

⁴Patients diagnosed with angiodysplasia without preexisting angiodysplasia at start of follow-up.

⁵Other lesions (n = 1 unless otherwise stated): peptic ulcer (n = 5), hemorrhoidal bleeding (n = 5), colorectal adenoma (n = 3), colorectal adenocarcinoma, diverticular bleeding, anal fissure.

⁶Aspirin for coronaropathy in a 67-y-old male with VWD type 2A diagnosed with small-bowel angiodysplasia: no aspirin withdrawal, 3 relapses; Dual aspirin + clopidogrel therapy in a 68-y-old female with VWD type 2M diagnosed with small-bowel angiodysplasia: 1 relapse after clopidogrel withdrawal; apixaban uptake for atrial flutter in a 80-y-old female with VWD 2N diagnosed with small-bowel angiodysplasia: after 2 recurrences under apixaban, a radiofrequency catheter ablation was performed to remove apixaban. No further relapse occurred after apixaban withdrawal.

⁷Fluindione uptake for atrial fibrillation in an 80-y-old male with VWD type 2M diagnosed with gastric ulcer and diverticular polyposis: no fluindione withdrawal, 4 relapses.

⁸Relative percentage of VWD patients with GI bleeding or angiodysplasia relative to the total number of VWD patients followed in the centers who completed the survey.

⁹One patient stopped atorvastatin uptake before the end of follow-up owing to a lack of efficacy and the presence of muscular side effects.

¹⁰11/17 patients without preexisting angiodysplasia and 6/7 patients with preexisting angiodysplasia experienced repeated bleeding.

was available for 13 patients treated with APC (through conventional endoscopy [n = 11] or double-balloon enteroscopy [n = 2]). The median time to rebleeding after APC of gastric, duodenal, or colonic angiodysplasia was 6.5 months in patients having a concomitant small-bowel lesion ineligible to APC (n = 7), whereas only one of the six patients without such localization relapsed after 21 months (log-rank test, $P < .01$). Three patients with angiodysplasia relapsed while on antithrombotics suggesting that recurrence may also be medication related.

In our cohort, there was a large heterogeneity in the duration and intensity of the VWF prophylaxis regimen. However, an increased use of VWF prophylaxis and/or antiangiogenic drugs was observed during follow-up in patients with small-bowel angiodysplasia compared with other angiodysplasia patients without such localization (10/12, 83% and 2/6, 33%, respectively; $P = .03$). Antiangiogenic treatment was initiated in six patients, with five of them having small-bowel angiodysplasia ineligible to APC. These data suggest that the presence of small-bowel lesions inaccessible to endoscopic treatment is associated with a worse outcome^{4,20} and should be included in the decision to introduce or intensify VWF prophylaxis or to use antiangiogenics. Identifying a lesion on endoscopy does not prove this lesion is the cause of GI bleeding unless active or signs of recent bleeding are also identified. The detection of nonbleeding

angiodysplasia is likely to be higher when repeating endoscopic investigations including VCE. In non-VWD patients, the prevalence of incidental colonic angiodysplasia is rare, and these lesions are characterized by a benign course with almost no recurrence at 3 years.²¹ By contrast, in our cohort, patients with angiodysplasia had more GI bleeding recurrence and an increased need for VWF replacement therapy or antiangiogenic drugs. Moreover, the endoscopic treatment of lesions accessible to APC was efficient in one-half of the patients to prevent further GI bleeding. These data provide indirect evidence of the clinical relevance of these lesions in VWD patients.

Altogether our results provide evidence that using VCE on top of conventional endoscopy in VWD patients with GI bleeding improves the diagnostic yield for angiodysplasia and outcome prediction. Our results support a more intensive exploration of the GI tract in VWD patients with unexplained or recurrent GI bleeding with a systematic use of VCE allowing to identify new lesions eligible for local endoscopic treatment or helping to adapt medical treatment.

Because relapse may not only indicate failure of endoscopic treatment but also the presence of untreated lesions, such endoscopic strategy aiming to optimize the identification and treatment of angiodysplasia could limit the GI bleeding recurrences and improve outcomes in VWD patients.

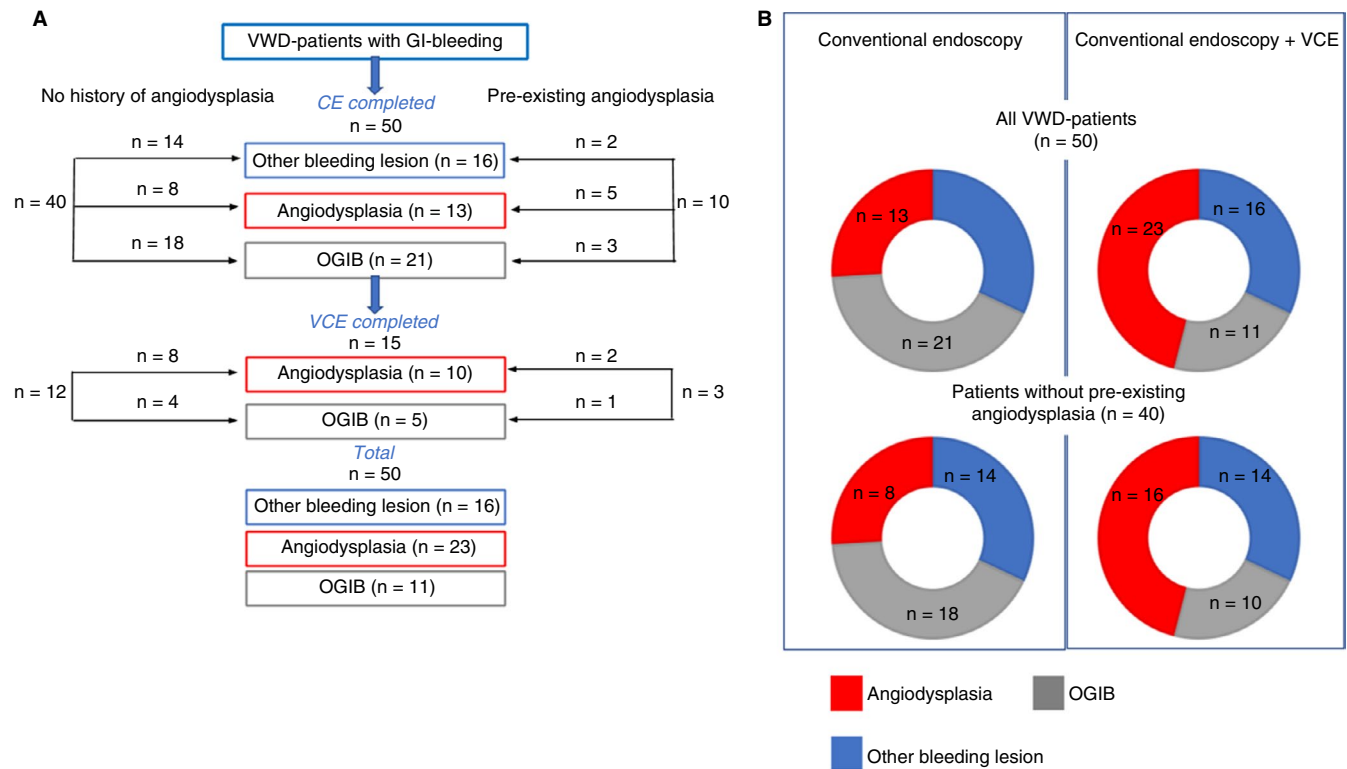


FIGURE 1 Diagnosis yield of video capsule on top of conventional endoscopy in VWD patients with GI bleeding. A, Flow diagram of sequential endoscopic explorations detailing for both patients with and without preexisting angiodysplasia at the start of follow-up the proportion of patients who completed VCE and the results of endoscopic exploration (angiodysplasia, other bleeding lesion, or obscure GI bleeding). B, Diagnostic yield of CE + VCE endoscopic strategy compared with CE alone for angiodysplasia: in all VWD patients (n = 50, chi-squared test, $**P < .01$) and in VWD patients without preexisting angiodysplasia at start of follow-up (n = 40, chi-squared test, $*P < .05$). CE, conventional endoscopy; GI, gastrointestinal; OGIB, obscure GI bleeding; VCE, video capsule endoscopy [Colour figure can be viewed at wileyonlinelibrary.com]

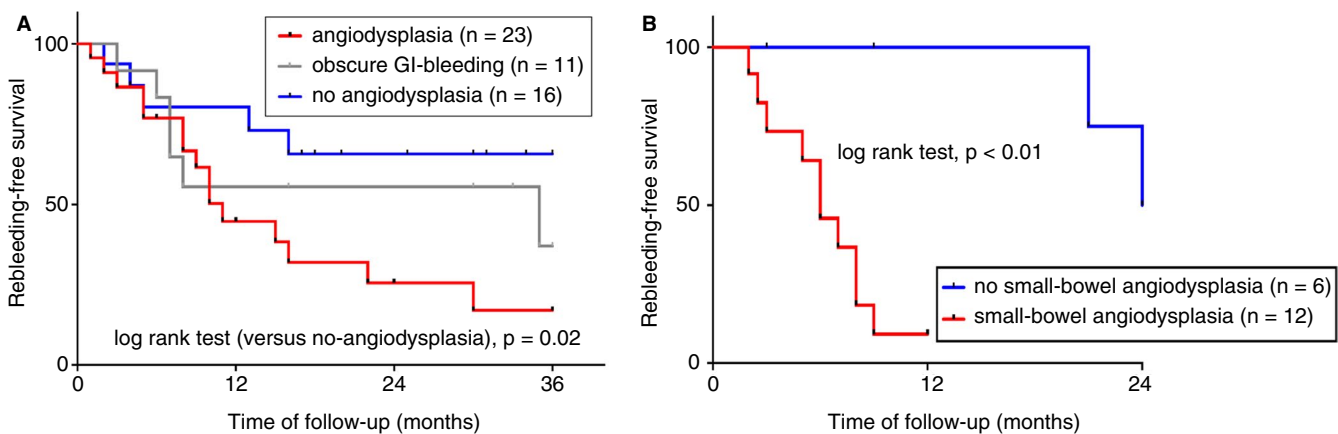


FIGURE 2 Risk stratification of GI bleeding recurrence in VWD patients with GI bleeding. A, Comparison of the recurrence-free survival after the first GI bleeding event according to final endoscopic categorization as “angiodysplasia,” “obscure GI bleeding,” or “no angiodysplasia.” The recurrence rate was significantly higher in patients with angiodysplasia compared with patients with another bleeding lesion ($P = .02$, log-rank test). B, Comparison of the recurrence-free survival after the first GI bleeding event in patients with (n = 12: VWD type 1 [n = 1], 2A [n = 5], 2B [n = 3], 2M [n = 1], 2N [n = 1], and 3 [n = 1]) or without small-bowel angiodysplasia (n = 6: VWD type 2A [n = 2], 2B [n = 1], and 2M [n = 3]) on VCE.[†] The recurrence rate was significantly higher in the presence of small-bowel angiodysplasia ($P = .005$, log rank test). [†]Analysis restricted to the 18 angiodysplasia patients who underwent at least one complete revision of their gastrointestinal tract (including VCE exploration) during their follow-up. Of the 13 patients with a positive VCE, 12 had a small-bowel localization, and one patient a gastric lesion [Colour figure can be viewed at wileyonlinelibrary.com]

Two large academic centers (representing 21% of the cohort) accounted for 12 of the 25 patients referred for VCE. It could be related to an increased awareness of angiodysplasia burden in VWD

leading to a closer collaboration between hematologists and gastroenterologists in largest centers. This intercenter heterogeneity reflects real-life data and underlines the need for specific guidelines

dedicated to the modalities of endoscopic exploration in VWD patients with GI bleeding.

5 | CONCLUSION

VWD patients with GI bleeding could benefit from a better standardized management with a more systematic use of VCE looking for angiodysplasia eligible to endoscopic treatment or at high risk of relapse. VCE could be useful to improve the diagnostic yield of angiodysplasia and to tailor the intensity and duration of VWF prophylaxis and the schedule of the endoscopic follow-up considering also VWD severity. Whether such a management taking into account the multifocal localization of GI angiodysplasia could translate into improved outcomes in VWD deserves further studies. A multidisciplinary approach including close collaboration between hematologists and gastroenterologists and access to full set of endoscopic procedures should be the standard of care in VWD patients with GI bleeding.

CONFLICT OF INTEREST

The authors declared no conflict of interest.

AUTHOR CONTRIBUTIONS

Antoine Rauch designed the study, conducted the data analysis, and wrote the manuscript. Camille Paris, Yohann Repesse, Julien Branche, Roseline D'Oiron, Annie Harroche, Catherine Ternisien, Sabine-Marie Castet, Aurélien Lebreton, Brigitte Pan-Petes, Fabienne Volot, Segolene Claeysens, Pierre Chamouni, Valérie Gay, Claire Berger, Dominique Desprez, Céline Falaise, Christine Biron Andreani, Catherine Marichez, Benedicte Pradines, Christophe Zawadzki, Nathalie Itzhar Baikian, Annie Borel-Derlon, Jenny Goudemand, and Romain Gerard conducted the data collection and critically reviewed the manuscript. Sophie Susen designed the study, conducted data analysis, and critically reviewed the manuscript.

ORCID

Antoine Rauch  <https://orcid.org/0000-0002-1182-4131>

Aurélien Lebreton  <https://orcid.org/0000-0002-1650-0427>

Sophie Susen  <https://orcid.org/0000-0001-5953-163X>

REFERENCES

- Holm E, Carlsson KS, Lövdahl S, Lail AE, Abshire TC, Berntorp E. Bleeding-related hospitalization in patients with von Willebrand disease and the impact of prophylaxis: results from national registers in Sweden compared with normal controls and participants in the von Willebrand Disease Prophylaxis Network. *Haemophilia*. 2018;24:628-633.
- Tsagianni A, Comer DM, Yabes JG, Ragni MV. Von Willebrand disease and gastrointestinal bleeding: a national inpatient sample study. *Thromb Res*. 2019;178:119-123.
- Franchini M, Mannucci PM. Von Willebrand disease-associated angiodysplasia: a few answers, still many questions. *Br J Haematol*. 2013;161:177-182.
- Jackson CS, Gerson LB. Management of gastrointestinal angiodysplastic lesions (GIADs): a systematic review and meta-analysis. *Am J Gastroenterol*. 2014;109:474-483.
- Starke RD, Ferraro F, Paschalaki KE, et al. Endothelial von Willebrand factor regulates angiogenesis. *Blood*. 2011;117:1071-1080.
- Starke RD, Paschalaki KE, Dyer CE, et al. Cellular and molecular basis of von Willebrand disease: studies on blood outgrowth endothelial cells. *Blood*. 2013;121:2773-2784.
- Randi AM, Smith KE, Castaman G. von Willebrand factor regulation of blood vessel formation. *Blood*. 2018;132:132-140.
- Fressinaud E, Meyer D. International survey of patients with von Willebrand disease and angiodysplasia. *Thromb Haemost*. 1993;70:546.
- Castaman G, Federici AB, Tosetto A, et al. Different bleeding risk in type 2A and 2M von Willebrand disease: a 2-year prospective study in 107 patients. *J Thromb Haemost*. 2012;10:632-638.
- Vincentelli A, Susen S, Le Tourneau T, et al. Acquired von Willebrand syndrome in aortic stenosis. *N Engl J Med*. 2003;349:343-349.
- Blackshear JL, Stark ME, Agnew RC, et al. Remission of recurrent gastrointestinal bleeding after septal reduction therapy in patients with hypertrophic obstructive cardiomyopathy-associated acquired von Willebrand syndrome. *J Thromb Haemost*. 2015;13:191-196.
- Raju GS, Gerson L, Das A, Lewis B; American Gastroenterological Association. American Gastroenterological Association (AGA) Institute medical position statement on obscure gastrointestinal bleeding. *Gastroenterology*. 2007;133:1694-1696.
- Gerson LB, Fidler JL, Cave DR, Leighton JA. ACG clinical guideline: diagnosis and management of small bowel bleeding. *Am J Gastroenterol*. 2015;110:1265-1287.
- Dioscoridi L, Forti E, Pugliese F, Cintolo M, Italia A, Mutignani M. Thulium laser coagulation: a new effective endotherapy to treat gastrointestinal angiodysplasia. *Gastrointest Endosc*. 2019;90:319-320.
- Veyradier A, Boisseau P, Fressinaud E, et al. A laboratory phenotype/genotype correlation of 1167 French patients from 670 families with von Willebrand disease: a new epidemiologic picture. *Medicine (Baltimore)*. 2016;95:e3038.
- Makris M, Federici AB, Mannucci PM, et al. The natural history of occult or angiodysplastic gastrointestinal bleeding in von Willebrand disease. *Haemophilia*. 2015;21:338-342.
- Abshire T, Cox-Gill J, Kempton CL, et al. Prophylaxis escalation in severe von Willebrand disease: a prospective study from the von Willebrand Disease Prophylaxis Network. *J Thromb Haemost*. 2015;13:1585-1589.
- Sohal M, Laffan M. Von Willebrand disease and angiodysplasia responding to atorvastatin. *Br J Haematol*. 2008;142:308-309.
- Bowers M, McNulty O, Mayne E. Octreotide in the treatment of gastrointestinal bleeding caused by angiodysplasia in two patients with von Willebrand's disease. *Br J Haematol*. 2000;108:524-527.
- Sakai E, Endo H, Taguri M, et al. Frequency and risk factors for rebleeding events in patients with small bowel angioectasia. *BMC Gastroenterol*. 2014;14:200.
- Foutch PG, Rex DK, Lieberman DA. Prevalence and natural history of colonic angiodysplasia among healthy asymptomatic people. *Am J Gastroenterol*. 1995;90:564-567.

How to cite this article: Rauch A, Paris C, Repesse Y, et al; for the French Reference Center on von Willebrand Disease. Gastrointestinal bleeding from angiodysplasia in von Willebrand disease: Improved diagnosis and outcome prediction using videocapsule on top of conventional endoscopy. *J Thromb Haemost*. 2021;19:380-386. <https://doi.org/10.1111/jth.15155>

RESEARCH LETTER

Endotheliopathy Is Induced by Plasma From Critically Ill Patients and Associated With Organ Failure in Severe COVID-19

Long histological analyses revealed the presence of vascular inflammation and severe endothelial injury as a direct consequence of intracellular severe acute respiratory syndrome coronavirus 2 (SARS-CoV-2) infection and ensuing host inflammatory response in coronavirus disease 2019 (COVID-19).¹ Endothelial cells promote coagulation following injury, leading to widespread formation of microthrombi, provoking microcirculatory failure or large-vessel thrombosis.² Growing evidence suggests that microvascular thrombosis is a major pathophysiological event in COVID-19 pathogenesis. Damaged endothelial cells could be closely implicated in the prothrombotic state commonly reported in severe patients in the intensive care unit (ICU). How SARS-CoV-2 exerts its cytopathic effects is still a matter of debate, and ultrastructural evidence of direct viral replication in endothelial cells remains to be demonstrated. Although direct viral tissue damage is a plausible mechanism of injury,³ endothelial damage and thromboinflammation associated with dysregulated immune responses, inducing microvascular thrombosis, represent an attractive alternative hypothesis.² Using cultured human pulmonary microvascular endothelial cells (HPMVEC), we assessed whether plasma collected from patients with COVID-19 at different disease stages could trigger endothelial damage in vitro. The cytotoxicity of plasma samples on HPMVEC was evaluated by assessing mitochondrial activity (WST-1 test) 1 hour after incubation of cells with plasma as previously described.⁴ We further investigated the association of plasma-induced cytotoxicity with levels of circulating biomarkers related to organ dysfunction (Pao₂ [partial pressure of oxygen in arterial blood]/Fio₂ [fraction of inspired oxygen], widely used as an indicator of oxygenation requirements, lactate dehydrogenase, creatinine, and aspartate transaminase), endothelial damage (von Willebrand factor antigen; ADAMTS13; plasminogen activator inhibitor-1; syndecan-1), tissue injury (cell-free DNA, a damage-associated molecular patterns marker), and levels of circulating cytokines related to the activation of innate (interleukin [IL]-6 and tumor necrosis factor- α) and adaptive immune cell responses (soluble IL-2 receptor). Inclusion criteria were individuals aged 18 years or older with a positive SARS-CoV-2 real-time reverse-transcriptase polymerase chain reaction on nasal or tracheal samples admitted to the Lille University Hospital. Patients on treatment with direct oral anticoagulant or vitamin K antagonists were switched to therapeutic heparin therapy on admission. Patients not in the ICU received once daily thromboprophylaxis with enoxaparin according to their body weight. Patients in the ICU received enoxaparin or unfractionated heparin according to their renal status, their body weight, and the need for invasive procedures. This study was approved by the French institutional authority for personal data protection (Commission Nationale de l'Informatique et des Libertés No. DEC20-086) and the ethics committee (IRB 2020-A00763-36), and informed consent was obtained from all participants.

HPMVEC viability was assessed after coincubation with plasma sampled on admission from 28 consecutive patients (non-ICU, n=16; ICU, n=12) hospitalized for

Antoine Rauch, MD, PhD*

Annabelle Dupont, PharmD, PhD*

:

Sophie Susen^{ID}, MD, PhD
For the Lille COVID Research Network (LICORNE)[†]

*Drs Rauch and Dupont contributed equally.

[†]A list of all members of the LICORNE scientific committee is given in the Appendix.

The full author list is available on page 1883.

Key Words: cell death ■ endothelial cell ■ endotheliopathy ■ liver injury ■ renal failure ■ respiratory failure ■ SARS-CoV-2

© 2020 American Heart Association, Inc.

<https://www.ahajournals.org/journal/circ>

COVID-19 at the Lille University Hospital between March 30, 2020, and April 8, 2020, in convalescent patients with COVID-19 ($n=6$ from the 12 patients in the ICU) sampled after ICU discharge (mean \pm SD, 21 \pm 7 days) and in control healthy donors ($n=8$). Compared with healthy donor plasma, plasma from patients with COVID-19 significantly decreased HPMVEC viability, with plasma from

patients in the ICU inducing the greatest cytotoxicity (Figure [A]). It is interesting that HPMVEC viability was partially restored to control when plasma from convalescent patients after ICU discharge was tested and compared with plasma of the same patients at the time of ICU admission. Moreover, markers of organ dysfunction were correlated with plasma-induced cytotoxicity (Figure [B]).

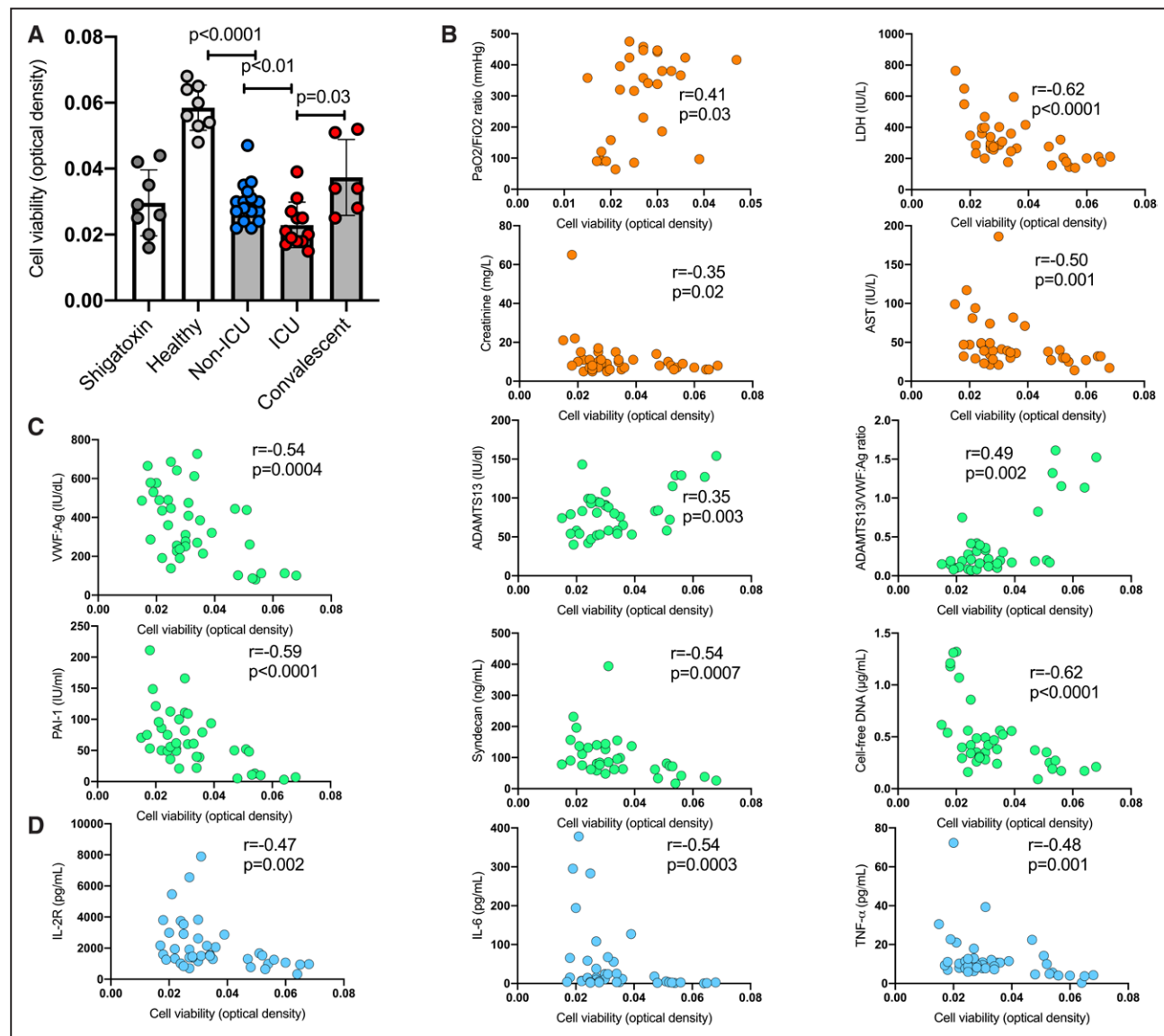


Figure. Endothelial cell cytotoxicity induced by plasma sampled from critically ill and convalescent patients with coronavirus disease 2019 (COVID-19).

The cytotoxicity of platelet-poor plasma samples (obtained after a double centrifugation of citrate tubes at 2500 g for 15 minutes at room temperature) from patients with COVID-19 and controls on HPMVEC was evaluated with a colorimetric assay using 4-[3-(4-iodophenyl)-2-(4-nitrophenyl)-2H-5-tetrazolo]-1,3-benzene disulfonate (WST-1), which in viable cells is cleaved by mitochondrial dehydrogenases. After incubation, the cells were washed with phosphate buffered saline and incubated with WST-1 (Roche, Basel, Switzerland) at a dilution of 1:10 (10 μ L) for 2 h at 37°C. Absorbance was measured using a multiwell plate reader (Synergy HTX multi-mode plate reader, BioTek Instruments, Highland Park, VT) at 450 nm with a reference wavelength of 620 nm. As a positive control for endothelial cell injury, Shigatoxin 145 (Sigma-Aldrich, Saint Quentin Fallavier, France) was spiked in plasma from healthy adults (10 μ g/mL final concentration) and incubated at 37°C for 15 minutes, before addition to HPMVECs. Experiments were performed in triplicate for each patient sample. **A**, HPMVEC viability after exposure to plasma sampled in healthy subjects ($n=8$), in non-ICU ($n=16$), and in ICU ($n=12$) on admission and in 6 convalescent patients with COVID-19 sampled after ICU discharge (mean \pm SD, 21 \pm 7 days). Data points represent individual sample measurements, whereas horizontal bars show the mean (\pm SD). Comparisons between groups were done using the Mann-Whitney U test, except for comparison between ICU and convalescent patients, where we used Wilcoxon signed-rank test on matched pairs ($n=6$). Correlations between HPMVEC viability and **(B)** markers of organ dysfunction: the PaO₂/F_iO₂ ratio, widely used as an indicator of oxygenation requirements, LDH, creatinine and AST; **(C)** parameters related to endothelial dysfunction and tissue injury: VWF:Ag, ADAMTS13, ADAMTS13:VWF ratio, PAI-1, syndecan-1, and cell-free DNA; and **(D)** plasma cytokine concentrations: IL-2R, IL-6, and TNF- α . Correlations were evaluated with the Spearman rank-correlation statistical test. No adjustment for multiple comparisons was done, and the result should be interpreted as hypothesis-generating. AST indicates aspartate transaminase; HPMVEC, human pulmonary microvascular endothelial cells; ICU, intensive care unit; IL, interleukin; IL-2R, soluble IL-2 receptor; LDH, lactate dehydrogenase; PAI-1, plasminogen activator inhibitor-1; TNF- α , tumor necrosis factor- α ; and VWF:Ag, von Willebrand factor antigen.

HPMVEC viability also correlated with most plasma markers related to endothelial damage or tissue injury (Figure [C]). Soluble IL-2 receptor and tumor necrosis factor- α levels negatively correlated with HPMVEC viability (Figure [D]). Overall, the degree of vascular endothelial cell injury induced by plasma sampled from patients with COVID-19 correlated to both clinical illness severity at admission and the levels of biomarkers related to endothelial injury, tissue injury, and proinflammatory cytokines.

Our data shed new light on the pathophysiology of COVID-19 by demonstrating the direct and rapid cytotoxic effect of plasma collected from critically ill patients on vascular endothelial cells. This rapid effect (1 hour after plasma exposure) excludes a direct cytopathic effect of SARS-CoV-2 infection, as the progression of viral infection and visible cytopathogenic effects are in general only apparent 12 to 24 hours after infection.⁵ A higher cytotoxic effect of plasma on endothelial cells was associated with a more pronounced hypoxemia and organ dysfunction as reflected by the correlation with Pao_2/FiO_2 , lactate dehydrogenase, creatinine, and aspartate transaminase. This cytotoxic effect also correlated with circulating markers of endothelial damage, indicating that this *in vitro* functional assay reflects microvascular endothelial damage *in vivo*. Different pathways could be involved in endothelial cell injury during the course of COVID-19, ie, complement activation, cellular hypoxia, platelets, and direct cytotoxicity of cytokines such as IL-6, IL-1 β , and tumor necrosis factor- α . We observed a relationship between this cytotoxic effect and the level of proinflammatory cytokines, suggesting that cytotoxicity could be related to overproduction of proinflammatory cytokines. However, this article does not provide the supportive evidence of convalescent plasma for treating severe patients with COVID-19.

In conclusion, we provide for the first time the results of a functional assay demonstrating a direct effect of dysregulation of immune response on endothelial damage in COVID-19. Endotheliopathy is an essential part of the pathological response on severe COVID-19, leading to respiratory failure, multiorgan dysfunction, and thrombosis. Endothelial and microvascular damage are associated with immunopathology and may occur in parallel with intracellular SARS-CoV-2 infection.

ARTICLE INFORMATION

Data sharing: The data that support the findings of this study are available from the corresponding author upon request.

Registration: URL: <https://www.clinicaltrials.gov>; Unique identifier: NCT-04327180.

Authors

Antoine Rauch, MD, PhD; Annabelle Dupont, PharmD, PhD; Julien Goutay, MD; Morgan Caplan , MD; Senna Staessens, MSc; Mouhamed Moussa, MD; Emmanuelle Jeanpierre, PharmD; Delphine Corseaux, PhD; Guillaume Lefevre, MD, PhD; Fanny Lassalle , PharmD; Karine Faure, MD, PhD; Marc Lambert, MD, PhD; Alain Duhamel, MD, PhD; Julien Labreuche, BST; Delphine Garrigue, MD; Simon F. De Meyer, PhD; Bart Staels , PhD; Eric Van Belle , MD, PhD; Flavien Vincent , MD, PhD; Eric Kipnis , MD, PhD; Peter J. Lenting , PhD; Julien Poissy , MD, PhD; Sophie Susen , MD, PhD; For the Lille COVID Research Network (LICORNE)

Correspondence

Sophie Susen, MD, PhD, Heart and Lung Institute, Hemostasis Department, Bd du Pr Leclercq, CHU Lille, 59037 Lille cedex, France. Email sophiesusen@aol.com

Affiliations

Univ. Lille, Inserm, CHU Lille, Institut Pasteur de Lille, U1011-EGID, F-59000 Lille, France (A.R., A. Dupont, M.M., E.J., D.C., F.L., B.S., E.V.B., F.V., S. Susen), Surgical Critical Care, Department of Anesthesiology and Critical Care (M.M.), Department of Infectious Diseases (K.F.), Department of Internal Medicine, Institut national de la santé et de la recherche médicale U 1167 (M.L.), Department Cardiology (E.V.B., F.V.), Centre national de la recherche scientifique, Surgical Critical Care, Department of Anesthesiology and Critical Care, U1019 - Unité mixte de recherche 9017 - Center for Infection and Immunity of Lille (E.K.), Institut Pasteur de Lille, UMR1011-EGID (S. Staessens, D.C., B.S.), Institut d'Immunologie, U1286 - INFINITE - Institute for Translational Research in Inflammation (G.L.), ULR 2694 - METRICS: Évaluation des technologies de santé et des pratiques médicales (A. Duhamel, J.L.), Institut national de la santé et de la recherche médicale U1285, Pôle de réanimation, Centre national de la recherche scientifique, Unité mixte de recherche 8576 - Unité de Glycobiologie Structurale et Fonctionnelle (J.P.), Univ. Lille, CHU Lille, France. Intensive Care Department, Pôle de Réanimation (J.G., M.C.), Surgical Critical Care, Department of Anesthesiology and Critical Care (D.G.), Centre Hospitalier Universitaire Lille, France. Laboratory for Thrombosis Research, Katholieke Universiteit Leuven Campus Kulak Kortrijk, Belgium (S. Staessens, S.F.D.M.). Institut national de la santé et de la recherche médicale, UMR_1176, Université Paris-Saclay, 94276 Le Kremlin-Bicêtre, France (P.L.).

Acknowledgments

The authors thank all physicians and medical staff involved in patient care. Special thanks are addressed to Eric Bouleaux, Laureline Bourgeois, Aurélie Jospin, Catherine Marichez, Vincent Dalibard, Bénédicte Pradines, Sandrine Vanderzeipe, and all the biologists and technicians of the Hemostasis Department for their support during the COVID-19 pandemic. A.R. and A. Dupont collected clinical data, analyzed the data, and wrote the article. J.G., M.C., S. Staessens, M.D.M., E.J., D.C., G.L., F.L., K.F., M.L., D.G., S.D.M., and J.P. collected data. J.G., M.C., S. Staessens, E.J., and S.D.M. analyzed the data. J.L. and A. Duhamel performed the statistical analysis. B.S., E.V., F.V., J.P., E.K., and P.L. provided critical input in the interpretation of data and critically reviewed the article. S. Susen designed the study, analyzed the data, wrote, and critically reviewed the article. All authors provided editorial review and assisted in writing the article.

Sources of Funding

This study was supported by the French government through the Program Investissement d'Avenir (I-SITE ULNE/ANR-16-IDEX-0004 ULNE).

Disclosures

None.

APPENDIX

Members of the LICORNE Scientific Committee:

Dominique Deplanque (Clinical Investigation Center, CHU Lille, France)
Karine Faure (Department of Infectious Diseases, CHU Lille, France)
Guillaume Lefevre (Department of Immunology, CHU Lille, France)
Enagnon Kazali Alidjinou (Department of Virology, CHU Lille, France)
Régis Bordet (Department of Medical Pharmacology, CHU Lille, France)
Marie-Charlotte Chopin (Department of Infectious Diseases, CHU Lille, France)
Ilka Engelmann (Department of Virology, CHU Lille, France)
Delphine Garrigue (Department of Emergency, CHU Lille, France)
Anne Goffard (Department of Virology, CHU Lille, France)
Eric Kipnis (Department of Anesthesia and Critical Care, CHU Lille, France)
Myriam Labalette (Department of Immunology, CHU Lille, France)
Marc Lambert (Department of Internal Medicine, CHU Lille, France)
David Launay (Department of Internal Medicine, CHU Lille, France)
Daniel Mathieu (Department of Intensive Care, CHU Lille, France)
Claude-Alain Maurage (Department of Anatomopathology, CHU Lille, France)
Julien Poissy (Department of Intensive Care, CHU Lille, France)
Boualem Sendid (Department of Parasitology, CHU Lille, France)
Sophie Susen (Department of Hematology, CHU Lille, France)

REFERENCES

1. Ackermann M, Verleden SE, Kuehnel M, Haverich A, Welte T, Laenger F, Vanstapel A, Werlein C, Stark H, Tzankov A, et al. Pulmonary vascular endothelialitis, thrombosis, and angiogenesis in Covid-19. *N Engl J Med*. 2020;383:120–128. doi: 10.1056/NEJMoa2015432
2. Gupta A, Madhavan MV, Sehgal K, Nair N, Mahajan S, Sehrawat TS, Bikdeli B, Ahluwalia N, Ausiello JC, Wan EY, et al. Extrapulmonary manifestations of COVID-19. *Nat Med*. 2020;26:1017–1032. doi: 10.1038/s41591-020-0968-3
3. Puelles VG, Lütgehetmann M, Lindenmeyer MT, Sperhake JP, Wong MN, Allweiss L, Chilla S, Heinemann A, Wanner N, Liu S, et al. Multiorgan and renal tropism of SARS-CoV-2. *N Engl J Med*. 2020;383:590–592. doi: 10.1056/NEJMc2011400
4. Gavriilaki E, Yuan X, Ye Z, Ambinder AJ, Shanbhag SP, Streiff MB, Kickler TS, Moliterno AR, Sperati CJ, Brodsky RA. Modified Ham test for atypical hemolytic uremic syndrome. *Blood*. 2015;125:3637–3646. doi: 10.1182/blood-2015-02-629683
5. Bojkova D, Klann K, Koch B, Widera M, Krause D, Ciesek S, Cinatl J, Münch C. Proteomics of SARS-CoV-2-infected host cells reveals therapy targets. *Nature*. 2020;583:469–472. doi: 10.1038/s41586-020-2332-7

Coagulation biomarkers are independent predictors of increased oxygen requirements in COVID-19

Antoine Rauch¹  | Julien Labreuche² | Fanny Lassalle¹  | Julien Goutay³ | Morgan Caplan³ | Leslie Charbonnier⁴ | Aurelien Rohn⁴ | Emmanuelle Jeanpierre¹ | Annabelle Dupont¹ | Alain Duhamel² | Karine Faure⁵ | Marc Lambert⁶ | Eric Kipnis⁷ | Delphine Garrigue⁴ | Peter J. Lenting⁸  | Julien Poissy⁹ | Sophie Susen¹  

¹Department of Hematology and Transfusion, Pôle de Biologie Pathologie Génétique, Institut Pasteur de Lille, UMR1011-EGID, Univ. Lille, Inserm, CHU Lille, Lille, France

²ULR 2694 - METRICS: Évaluation des technologies de santé et des pratiques médicales, Univ. Lille, CHU Lille, Lille, France

³Intensive Care Department, Pôle de Réanimation, Centre Hospitalier Universitaire Lille, Lille, France

⁴Emergency Department, Pôle de l'Urgence, Centre Hospitalier Universitaire Lille, Lille, France

⁵Department of Infectious Diseases, Institut Pasteur de Lille, UMR1019-CIIL, Univ. Lille, Inserm, CHU Lille, Lille, France

⁶Department of Internal Medicine, INSERM U 1167, Institut Pasteur, Univ. Lille, Inserm, CHU Lille, Lille, France

⁷Surgical Critical Care, Department of Anesthesiology and Critical Care, Institut Pasteur de Lille, U1019 - UMR 9017 - CIIL - Center for Infection and Immunity of Lille, Univ. Lille, CNRS, Inserm, CHU Lille, Lille, France

⁸UMR_1176, Inserm, Université Paris-Saclay, Le Kremlin-Bicêtre, France

⁹Pôle de Réanimation, CNRS, UMR 8576 - UGSF - Unité de Glycobiologie Structurale et Fonctionnelle, Univ. Lille, Inserm U1285, CHU Lille, Lille, France

Correspondence

Sophie Susen, Institut Cœur-Poumon (Heart and Lung Institute), Hemostasis Department, Bd du Pr Leclercq, CHU Lille, 59037 Lille Cedex, France.
Email: sophiesusen@aol.com

Abstract

Background: Hypercoagulability seems to contribute to SARS-CoV-2 pneumonia pathogenesis. However, age and metabolic syndrome are potential confounders when assessing the value of coagulation biomarkers' prediction of COVID-19 outcomes. We assessed whether coagulation biomarkers, including factor VIII (FVIII) and von Willebrand factor (VWF) levels, measured at time of admission, were predictive of COVID-19 adverse outcomes irrespective of age and major comorbidities associated with metabolic syndrome.

Methods: Blood was sampled at admission in 243 adult COVID-19 patients for analysis of coagulation biomarkers including FVIII and VWF on platelet-poor plasma. The association between baseline C-reactive protein (CRP), activated partial thromboplastin time ratio, prothrombin time ratio, D-dimers, fibrinogen, FVIII, VWF antigen (VWF:Ag), and FVIII/VWF:Ag ratio levels and adverse outcomes (increased oxygen requirements, thrombosis, and death at day 30) was assessed by regression analysis after adjustment on age, sex, body mass index (BMI), diabetes, and hypertension.

Results: In univariable regression analysis increased CRP (subdistribution hazard ratio [SHR], 1.68; 95% confidence interval [CI], 1.26-2.23), increased fibrinogen (SHR, 1.32; 95% CI, 1.04-1.68), and decreased FVIII/VWF:Ag ratio (SHR, 0.70; 95% CI, 0.52-0.96) levels at admission were significantly associated with the risk of increased oxygen requirement during follow-up. Leucocytes (SHR, 1.36; 95% CI, 1.04-1.76), platelets (SHR, 1.71; 95% CI, 1.11-2.62), D-dimers (SHR, 2.48; 95% CI, 1.66-3.78), and FVIII (SHR, 1.78; 95% CI, 1.17-2.68) were associated with early onset of thrombosis after admission. After adjustment for age, sex, BMI, hypertension, and diabetes, these associations were not modified.

Conclusion: Coagulation biomarkers are early and independent predictors of increased oxygen requirement in COVID-19 patients.

Julien Poissy, Pôle de Réanimation, Hôpital Roger Salengro, Rue Emile Laine, CHU Lille, 59037 Lille Cedex, France.
Email: julien.poissy@chru-lille.fr

Funding information

This study was supported by the French government through the Programme Investissement d'Avenir (I-SITE ULNE/ ANR-16-IDEX-0004 ULNE) managed by the Agence Nationale de la Recherche.

KEY WORDS

body mass index, factor VIII, oxygen, SARS-CoV2, von Willebrand factor

1 | INTRODUCTION

Coronavirus disease 2019 (COVID-19) is frequently associated with laboratory markers of hypercoagulability.¹ These coagulation changes, mainly characterized by increased D-dimers and fibrinogen levels, are generally observed in critically ill patients, especially those with hypoxemia reflecting inflammation.² This increase in D-dimers at admission, without signs of disseminated intravascular coagulation, has been reported to be associated with the risk of death.^{3,4}

Evidence for an increased risk of thrombosis in COVID-19 has been first identified through clinical manifestations of large vessel thrombosis. Venous thromboembolic events (VTE) and pulmonary embolism (PE) are reported in 20% to 30% of intensive care unit (ICU) patients⁵⁻⁸ and other thrombotic complications, such as arterial thrombosis or thrombosis of central lines and in extracorporeal circuits, have also been described.⁶ All post mortem analyses have confirmed the high frequency of pulmonary vascular thrombosis in ventilated and non-ventilated patients receiving thromboprophylaxis or not.^{9,10} Post mortem histological data also show local direct vascular injury characterized by severe endothelial injury with intracellular SARS-CoV-2, widespread vascular thrombosis with microangiopathy and occlusion of alveolar capillaries, and angiogenesis.^{11,12} Altogether, these findings suggest that COVID-19-induced hypercoagulability and inflammation result in both microangiopathy involved in multiple organ failure and macroangiopathy involved in large vessel thrombosis.¹³

An increased risk for more severe forms of COVID-19 with ICU admission and death is associated with age, sex, body weight, hypertension, and diabetes.¹⁴⁻¹⁶ All these factors increase the risk for thrombotic disease in part through the generation of hypercoagulation. Von Willebrand factor (VWF) and factor VIII (FVIII) are also elevated in patients with COVID-19.^{6,7,17,18} FVIII and VWF are associated with inflammation and thrombotic risk but are also related to endothelial damage. Lung endothelium is a dominant source of circulating VWF, the levels of which might be differentially altered compared to FVIII, which is mainly synthesized in the liver.¹⁹ Investigations as to whether VWF and FVIII levels are related to outcome in COVID-19 disease have not been reported yet. Whether the laboratory markers of hypercoagulability, including FVIII and VWF, and the risk of thrombosis in COVID-19 are mainly explained by comorbidities or whether they independently

Essentials

- Von Willebrand factor (VWF) levels are associated with severity and oxygen need in COVID-19 at admission.
- Low factor VIII (FVIII)/VWF ratio at admission is predictive of increased oxygen requirements.
- Coagulation biomarkers predict outcome independently of major comorbidities in COVID-19.
- FVIII is predictive of early thrombotic events irrespective of body mass index in COVID-19.

reflect SARS-CoV-2-induced vascular damage has not yet been elucidated.

The objective of the study was to assess whether hypercoagulability markers in COVID-19 patients, including FVIII and VWF levels, measured at admission to the emergency department were predictive of increased oxygen requirement and to evaluate the influence of major comorbidities, including age, sex, body weight, diabetes, and hypertension, on this relation. We also aimed to evaluate if these hypercoagulability markers were predictive of thrombotic events.

2 | PATIENTS AND METHODS

2.1 | Patients

Consecutive adult patients admitted for COVID-19 infection were recruited from the emergency department (ED) of the Lille University Hospital between 20 March and 17 April 2020. Inclusion criteria were: individuals aged 18 years or older with either a positive COVID-19 nasal or tracheal real-time reverse transcriptase polymerase chain reaction (RT-PCR) or with radiological signs of interstitial pneumonia on chest x-rays or computed tomography (CT) scan and a high probability score according to the score for COVID-19 of Liao et al.²⁰ Following admission, all hospitalized patients received thromboprophylaxis as standard of care unless contra-indicated. Patients admitted while treated with direct oral anticoagulant (DOAC) or vitamin K antagonists (VKA) were switched to curative heparin therapy. Ward patients received thromboprophylaxis with enoxaparin 4000 or 6000 IU once daily according to their body weight. ICU patients received enoxaparin or unfractionated heparin according to their

renal status and the need for invasive procedures. In overweight and obese patients, the dosing regimen was adapted according to the European Society of Cardiology proposals.²¹ From 1 April onward, patients received thromboprophylaxis according to the GFHT/GIHP (French study group on thrombosis and haemostasis/French working group on perioperative haemostasis) proposals.²² Limitation, withholding, or withdrawal of life-sustaining treatment in the ICU was based on French guidelines in compliance with French law.²³ Deaths in this context were recorded to analyze the real contribution to death of SARS-CoV-2 infection.

2.2 | Data collection

Epidemiological data, demographic information, past medical history and treatments, clinical data, and outcomes were prospectively collected from the hospital electronic medical records from emergency department admission to hospital discharge. Comorbidities including hypertension and diabetes were defined according to the presence of an antihypertensive or antidiabetic drug at baseline or according to the medical records. Body mass index (BMI) was measured upon admission. The clinical status of patients who were directly discharged home from the emergency department was assessed at day 30 by phone interview. The study was approved by the Institutional Review Board (N°CPP 20-LILL-02, NCT04341792) in strict compliance with the French reference methodology MR-004 and informed consent was obtained from all participants.

2.3 | Laboratory testing

For each subject, a 3 mL blood sample was collected at admission on a 0.109 mol/L trisodium citrate tube (BD Vacutainer®, BD Diagnostics). All hemostasis tests were performed on platelet poor plasma obtained after double centrifugation of citrate tubes at 2000 g for 15 minutes at room temperature. Assays included prothrombin time (PT), activated partial thromboplastin time (aPTT), fibrinogen, D-dimer, FVIII, and VWF antigen (VWF:Ag) levels. The PT, aPTT, and fibrinogen assays were measured on a STA R Max® analyzer (Diagnostica Stago SAS) using STA Neoplastin R®, Triniclot® aPTT HS, T Coag®, and STA Liquid Fib® (Diagnostica Stago SAS). D-dimer levels were measured in µg/mL fibrinogen equivalent units (FEU) using an immunoturbidimetric latex-particle assay Liatest DDI-Plus® on the STA R Max analyser (Diagnostica Stago SAS). The reading area is equal to the measuring area and range from 0.27 µg/mL (FEU) to 20 µg/mL (FEU). FVIII activity was measured by a one-stage clotting aPTT-based assay using Triniclot® aPTT HS, T Coag®, and factor VIII-deficient plasma, on a Sysmex CS 2400 analyzer (Siemens Healthineers AG). VWF:Ag was measured using an immunoturbidimetric assay, LIAPHEN vWF:Ag (HYPHEN BioMed). Other lab tests including a complete blood count, C-reactive protein (CRP), high sensitivity cardiac troponin, lactate dehydrogenase (LDH) levels, and ABO blood group were prospectively assessed by standard methods

as part of patients' care in the Biology and Pathology Center (CHU Lille).

2.4 | Study outcomes

The primary outcome of the study was the increase in oxygen requirement defined as a need for re-admission after discharge for a limitation of activities and/or a change in oxygen requirements (no oxygen, supplemental oxygen, non-invasive ventilation or high-flow oxygen, invasive mechanical ventilation, or extracorporeal membrane oxygenation) and/or death related to acute respiratory distress syndrome without limitation, withholding, or withdrawal of life-sustaining treatment at day 30. This composite criterion includes any worsening of the respiratory status in patients and comprises different severity of illness without focusing on the most critically ill patients. The secondary outcomes were occurrence of any thromboembolic event (symptomatic PE, deep vein thrombosis [DVT], catheter-related thrombosis, myocardial infarction [MI], or stroke) at day 30 and all-cause mortality at day 30. The association between outcomes and the baseline values of leucocytes, lymphocytes, monocytes, platelets, CRP, aPTT ratio, PT ratio, D-dimers, fibrinogen, FVIII, VWF:Ag, and FVIII/VWF:Ag ratio were evaluated.

2.5 | Statistical analysis

Quantitative variables were expressed as means (standard deviation) in the case of normal distribution or medians (interquartile range [IQR]) otherwise. Normality of distributions was assessed using histograms and the Shapiro-Wilk test. Categorical variables were expressed as numbers (percentage). Cumulative incidence of respiratory worsening and thrombotic events within 30 days of admission were estimated using the Kalbfleisch and Prentice method²⁴ (by taking into account death related to limitation, withholding, or withdrawal of life-sustaining treatment as competing event for respiratory worsening, and any death as competing event for thrombotic events). Cumulative incidence of all-cause mortality was estimated using Kaplan-Meier method.

Main biological markers (PaO₂/FiO₂ ratio, CRP, fibrinogen, D-dimers, FVIII, VWF:Ag, FVIII/VWF:Ag) were compared according to admission type and oxygen requirements at admission by using one-way analysis of variance (or Kruskal Wallis test according to normality of distribution); in case of significant difference, post hoc pairwise comparisons were done using linear contrast (or using Dunn's test).

We assessed the association of biological markers measured at admission to the ED with the occurrence of increase in oxygen requirements, thrombotic events, and all-cause mortality within 30 days of admission using univariable and multivariable regression models. For biological markers with a skewed distribution, the log-transformed values were used in regression models. For respiratory worsening and thrombotic events, we used Fine and Gray

models before and after pre-specified adjustment for age, sex, BMI, diabetes, and hypertension by treating death (related to limitation, withholding, or withdrawal of life-sustaining treatment for increased oxygen requirement and all-cause death for thrombotic events) as a competing event. For all-cause mortality, we used Cox's proportional hazard models before and after adjustment for age, sex, BMI, diabetes and hypertension. We assessed the proportional hazard (PH) assumptions by examining the Schoenfeld residuals; in cases of PH departure, the association was modeled using time-dependent coefficients. We assessed the log-linearity assumptions by using restricted cubic spline functions;²⁵ in cases of departure, the association was modeled using the quartiles of biomarker distributions. Strength of the associations were evaluated by deriving from regression models, the subhazard ratios (Fine and Gray models) or hazard ratios (Cox model) per one standard deviation increase in biological data as effect sizes (for blood group, effect sizes were calculated for O versus other blood groups).

Multivariate regression analyses were performed after handling missing data on biological markers and covariates using multiple imputation procedure. Imputation procedure was performed using regression-switching approach²⁶(chained equations with $m = 10$ obtained) under the missing at random assumption using all baseline characteristics (see Table 1), with a predictive mean matching method for quantitative variables and logistic regression model (binary, ordinal, or multinomial) for categorical variables. Estimates obtained in the different imputed data sets were combined using Rubin's rules.²⁷

Finally, the association of occurrence of thrombosis events with oxygen requirements and all-cause mortality was investigated using Cox's proportional hazard regression models by treating the occurrence of thrombosis events as a time-dependent covariate; hazard ratio associated with the time period with thrombosis events was derived as effect size.

Statistical testing was performed at the two-tailed α level of 0.05. No correction for multiple testing was done regarding the exploratory nature of the present study and results should be interpreted with caution and as hypothesis generating. Data were analyzed using the SAS software package, release 9.4 (SAS Institute).

3 | RESULTS

3.1 | Clinical and biological characteristics on emergency department admission

Of the 303 patients with high probability or confirmed COVID-19 admitted to the ED at our hospital from 20 March to 17 April 2020, 243 patients (155 men and 88 women) were included in the study with a median age of 63.9 years. Patients transferred to our hospital from another hospital were not included in the study (Figure S1 in supporting information). The proportion of patients with hypertension, diabetes, and overweight-to-obese (BMI > 25) was 48.6%,

23.0%, and 76.2% respectively. Other underlying comorbidities are detailed in Table 1. Thirty-two patients were receiving antithrombotic treatment at baseline (DOAC, $n = 19$; VKA, $n = 8$; enoxaparin, $n = 5$).

Upon arrival in the ED, 30.9% of patients were directly admitted to the ICU and 65% were first admitted to the ED. Twenty-three (9.4%) patients were directly discharged home from the ED after medical assessment for standardized ambulatory clinical follow-up. All other patients were hospitalized in the medical ward dedicated to COVID-19.

Median time from illness onset to admission was 8 (IQR, 5-11) days. At admission, 169 (69.5%) patients required oxygen support and all had radiological signs of interstitial pneumonia on chest X-rays or CT scan. Baseline median respiratory rate and $\text{PaO}_2/\text{FiO}_2$ were 24 (IQR, 20-28) per min and 357 (IQR, 252-448) mm Hg, respectively. In accordance with local guidelines to prevent overwhelming the virology lab, RT-PCR testing was limited to COVID-19 patients requiring hospitalization. RT-PCR was positive for COVID-19 in 220 (90.5%) patients at baseline.

The values of the main biological markers at baseline are presented in Table 1. The $\text{PaO}_2/\text{FiO}_2$ ratio was significantly different according to the admission type with the lowest values for patients directly admitted to the ICU (outpatients, ward, and ICU, respectively 505 [461-523], 381 [324-458], 197 [130-302], $P < .001$). Also depending on admission type (outpatient, ward, or ICU), CRP, D-dimers, fibrinogen, and VWF levels were highest for patients directly admitted to the ICU (Figure 1). As RT-PCR testing was in most cases limited to COVID-19 patients requiring hospitalization, respiratory illness at admission was less severe in the RT-PCR negative patient group despite the presence of radiological signs of pneumonia. Among the 23 patients without RT-PCR testing, only 2 were admitted to the medical ward dedicated to COVID-19 whereas the 21 others were outpatients. As shown in Figure 1A, outpatients had a higher $\text{PaO}_2/\text{FiO}_2$ and a lower respiratory rate (20.6 ± 5 versus 24.4 ± 6 , $P = .003$) upon admission in ED and none of them needed oxygen supply during follow-up.

As shown in Figure 2, CRP, fibrinogen, D-dimers, and VWF:Ag levels were increased depending on oxygen requirements at admission, with the lowest levels for patients with no oxygen and the highest for patients requiring high-flow oxygen or invasive ventilation. FVIII levels were not affected by oxygen requirements.

3.2 | Increase in oxygen requirement and biomarkers

At the time of analysis (20 May 2020), all patients either died ($n = 32$) or reached the 30-day follow-up after admission. Respiratory worsening was observed in 71 patients (30-day incidence, 29.2%; 95% CI, 23.6%-35.0%) during follow-up: 2 patients were re-admitted for dyspnea, 59 required an escalation in oxygen supply (low flow oxygen, $n = 13$; non-invasive ventilation or high flow oxygen devices, $n = 9$; invasive mechanical ventilation, $n = 37$) and 10 died

TABLE 1 Patient clinical and biological characteristics at admission to the emergency department in the overall study population

Characteristics	N	Values
Age, years (mean ± SD)	243	63.9 ± 16.2
Male sex	243	155 (63.8)
Body mass index, kg/m ² (mean ± SD)	200	28.0 ± 6.1
Chronic medical illness		
Diabetes	243	56 (23.0)
Hypertension	243	118 (48.6)
Chronic pulmonary disease	243	38 (15.6)
Cardiopathy	243	36 (14.8)
Myocardial infarction	243	22 (9.1)
Stroke	243	22 (9.1)
Hepatopathy	243	5 (2.1)
Chronic renal failure	243	17 (7.0)
Active cancer	243	23 (9.5)
Immunocompromised	242	11 (4.5)
Number of medical illness		
None		79 (32.5)
One		65 (26.8)
More than one medical illness		99 (40.7)
Illness characteristics		
Time from illness onset to admission, days	243	8 (5-11)
Admission type		
Emergency department		158 (65.0)
Ward		10 (4.1)
ICU		75 (30.9)
Severity of respiratory illness at admission		
Respiratory rate/min (mean SD)	236	24.0 ± 5.9
PaO ₂ /FiO ₂ ratio (mmHg)	236	357 (252-448)
Oxygen requirement at admission		
No oxygen	243	74 (30.5)
Supplemental oxygen		102 (42)
Non-invasive ventilation or high flow oxygenation		20 (8.2)
Invasive mechanical ventilation		47 (19.3)
Biological data		
ABO blood group		
A	192	85 (44.3)
AB		11 (5.7)
B		19 (9.9)
O		77 (40.1)
Leucocytes/mm ³ (mean ± SD)	229	181
Neutrophils/mm ³	7674 ± 3749	5000 (3700-7000)

(Continues)

TABLE 1 (Continued)

Characteristics	N	Values
Lymphocytes/mm ³ (mean ± SD)	182	1060 ± 611
Monocytes/mm ³	182	400 (300-700)
Platelets, G/L (mean ± SD)	238	228 ± 113
Creatinine, mg/L	227	8 (7-11)
Lactate dehydrogenase, IU/L	199	377 (286-479)
Troponin, ng/L	204	15.0 (7.5-25.5)
CRP, mg/L	227	69 (31-126)
aPTTr	211	1.13 (1.03-1.23)
PTTr	211	1.10 (1.04-1.16)
D-dimers, µg/mL	227	1.00 (0.70-1.80)
Fibrinogen, g/L (mean ± SD)	227	6.1 ± 1.6
FVIII, IU/dL (mean ± SD)	210	241 ± 96
VWF:Ag, IU/dL (mean ± SD)	212	361 ± 128
FVIII/VWF:Ag ratio (mean ± SD)	210	0.72 ± 0.27

Note: Values are number (%) or median (interquartile range) unless otherwise as indicated.

Abbreviations: aPTTr, activated partial thromboplastin time ratio; FVIII, factor VIII; ICU, intensive care unit; PTTr, prothrombin time ratio; SD, standard deviation; VWF, von Willebrand factor.

from acute respiratory distress syndrome (ARDS) without context of limitation, withholding, or withdrawal of life-sustaining treatment. In patients presenting an increase in oxygen requirement there was a significant decrease of PaO₂/FiO₂ ratio the day of increase in oxygen requirement compared to baseline values (172 [122-233] versus 313 [185-396], *P* < .01; Figure S2 in supporting information) Most of the increased oxygen requirement events (87.3%, *n* = 62) occurred in the first 10 days following admission (Figure S3A in supporting information). Among the 71 patients with aggravation according to the increase of oxygen requirements, we observed no significant difference in the timing of aggravation according to the severity of oxygen requirements (3 [1-4] days for escalation of non-invasive oxygen supply versus 3 [1-5] days for the need of invasive ventilation); however, death from ARDS occurred at a significantly later stage (12 [5-19] days, *P* = .001).

In univariable Fine and Gray regression analysis considering the 16 deaths in the context of limitation of life-sustaining treatment as competing events, increased CRP (subdistribution hazard ratio [SHR], 1.68; 95% confidence interval [CI], 1.26-2.23), increased fibrinogen (SHR, 1.32; 95% CI, 1.04-1.68), and decreased FVIII/VWF:Ag ratio (SHR, 0.70; 95% CI, 0.52-0.96) levels at admission were significantly associated with the risk of respiratory degradation during follow-up (Table 2). After adjustment for age, sex, BMI, hypertension, and diabetes, these associations were not modified (Table 2). In multivariate analysis, the association between decreased lymphocytes and risk of increased oxygen requirement reached the significance level, with an adjusted SHR of 0.71 (95% CI, 0.50-0.99). In conclusion, CRP, fibrinogen, the FVIII/VWF ratio, and reduced lymphocyte count were

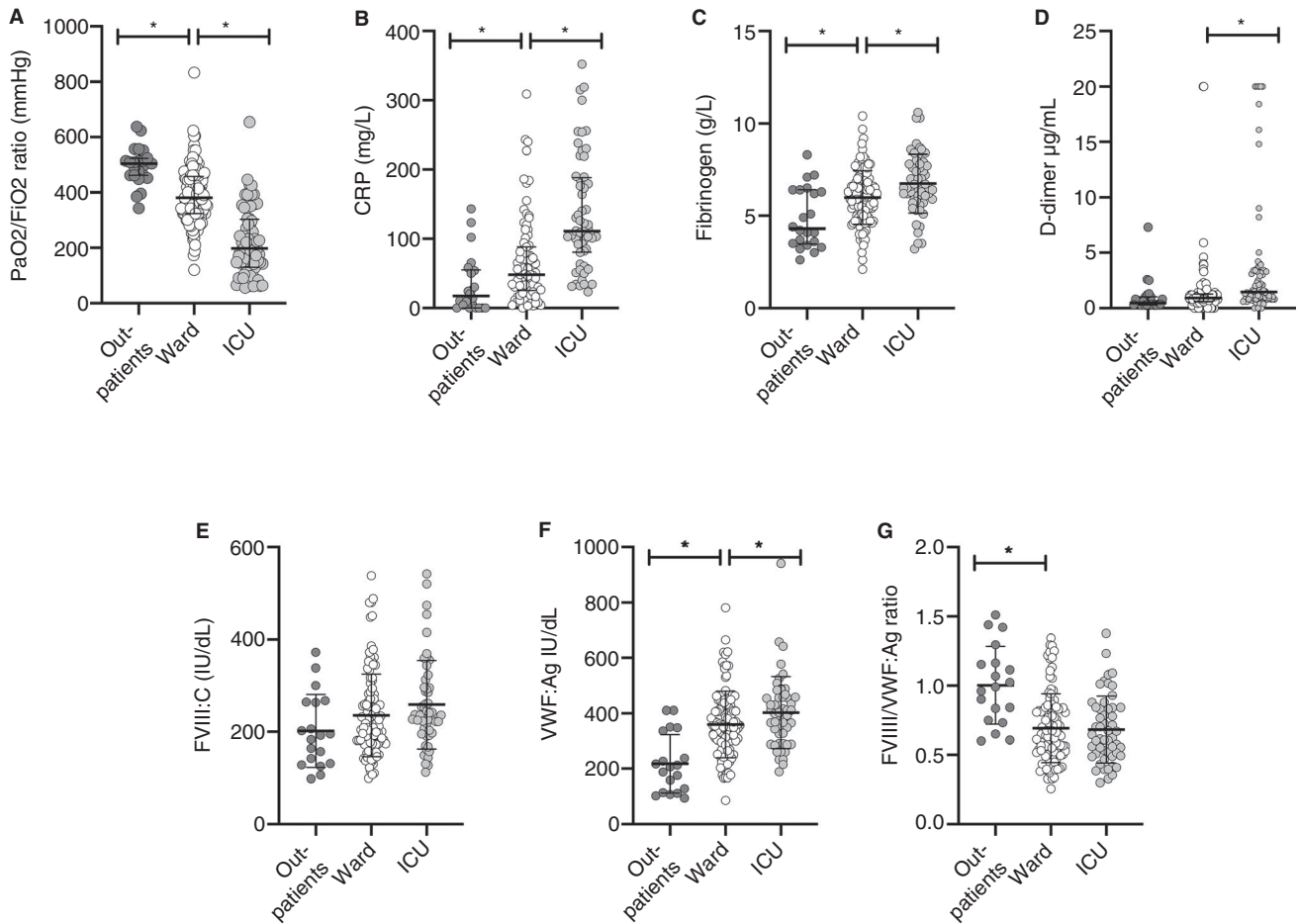


FIGURE 1 Baseline values of main biomarkers according to admission type. Scatter plots of (A) PaO₂/FiO₂ ratio, (B) C-reactive protein, (C) fibrinogen, (D) D-dimers, (E) factor VIII (FVIII), (F) von Willebrand factor antigen (VWF:Ag), and (G) FVIII/VWF:Ag ratio. Bars indicate median and interquartile range or means ± standard deviation as appropriate. ICU = intensive care unit. *P < .05.

all independently associated with the increased need for oxygen support.

3.3 | Thrombotic events and biomarkers

The cumulative incidence of 30-day any thrombotic event was 12.8% (95% CI, 8.9%-17.3%); there were 22 patients presenting PE (1 troncular, 3 lobar, 12 segmental, and 6 subsegmental), 4 DVT, 1 MI, 2 ischemic stroke, and 2 catheter-related thrombosis of the jugular vein. The 31 thrombotic events occurred with a median time from hospital admission to thrombotic events of 8 (IQR, 1-11) days (Figure S3B). As shown in Table 3, the proportional subhazard assumptions for several biomarkers were not satisfied with a positive association with occurrence of thrombotic event during the first 5 days for leucocytes (SHR, 1.36; 95% CI, 1.04-1.76), platelets (SHR, 1.71; 95% CI, 1.11-2.62), D-dimers (SHR, 2.48; 95% CI, 1.66-3.78), FVIII (SHR, 1.78; 95% CI, 1.17-2.68). Intriguingly a negative association with occurrence of thrombotic event after 5 days was observed for FVIII (SHR, 0.46; 95% CI 0.26-0.82) and VIII/VWF:Ag ratio (SHR, 0.47; 95% CI, 0.25-0.87). However, patients presenting a thrombotic event after 5 days had lower FVIII

levels at baseline compared to patients presenting a thrombotic event before day 5 or no thrombotic event (190 ± 45, 314 ± 143, and 232 ± 82, respectively; P < .01). After 4 days, FVIII increased in patients presenting a thrombotic event after 5 days and remained stable in patients presenting early thrombosis and the difference between both groups was no longer significant (Figure S4 in supporting information). Time interval between symptom onset and thrombosis was longer in the group with early thrombotic event after admission when compared to late thrombotic event after admission, although not significant (11 [8-12] days versus 9.5 [7-11]).

Thromboembolic complications were significantly associated with a higher risk of increase in oxygen requirements (% per patients-days exposed versus non-exposed to thrombosis events: 1.9% versus 0.4%), with a hazard ratio (HR) 2.66 (95% CI, 1.26-5.60). Most events occurred in ICU.

We also observed a positive association between thromboembolic events during the entire follow-up period (without deviation to proportional subhazard assumptions) for neutrophils (SHR, 1.40; 95% CI, 1.06-1.84), and lactate dehydrogenase (LDH; SHR 1.79; 95% CI, 1.36-2.36). After adjustment for pre-specified confounders, these associations were not modified (Table 3).

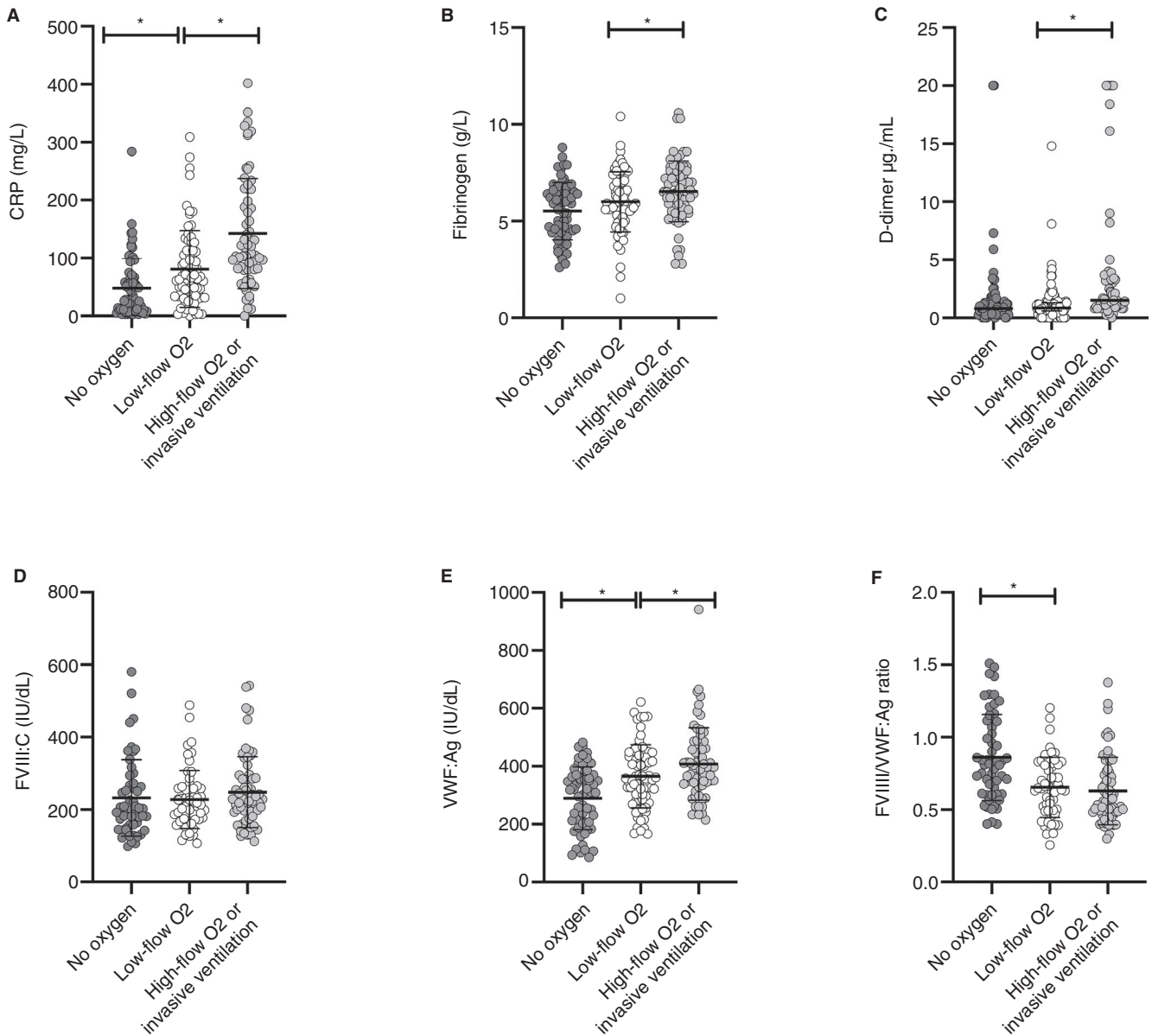


FIGURE 2 Baseline values of main biomarkers according to oxygen requirements at admission to the emergency department. Scatter plots of (A) C-reactive protein, (B) fibrinogen, (C) D-dimers, (D) factor VIII (FVIII), (E) von Willebrand factor antigen (VWF:Ag) and (F) FVIII/VWF:Ag ratio. Bars indicate median and interquartile range or means \pm standard deviation as appropriate. * $P < .05$

3.4 | All-cause mortality and biomarkers

The 30-day mortality was 13.2% (95% CI, 9.2%-17.8%; Figure S3C) with half of patients in a context of limitation, withholding, or withdrawal of life-sustaining treatment, mainly limitation of invasive mechanical ventilation in case of worsening respiratory status. Thromboembolic complications were not significantly associated with all-cause mortality (% per patients-days exposed versus non-exposed to thrombosis events: 0.8% versus 0.4%) with an HR of 2.07 (95% CI, 0.79-5.43). However, the numbers of both thrombotic events and deaths were too low to achieve a significant difference. The results are presented in Table S4 in supporting information.

4 | DISCUSSION

In this study, we provide evidence that coagulation biomarkers, including FVIII and VWF, at admission to the ED are associated with the severity of COVID-19 and predict a higher risk of increase in oxygen requirements irrespective of age, sex, BMI, diabetes, and hypertension. Our results support the hypothesis that SARS-CoV-2-associated thromboinflammatory hypercoagulability could directly contribute to the underlying pulmonary pathogenesis.

The objective of this study was to assess whether COVID-19 hypercoagulability and especially markers associated with inflammation and endothelial damage such as FVIII and VWF were associated

TABLE 2 Associations of biological data with 30-day increase of oxygenation requirements

Biological data	30-day aggravation		Unadjusted		Adjusted ^a	
	No (n = 172)	Yes (=71)	SHR (95% CI)	P	SHR (95% CI)	P
O blood group, n (%)	56 (42.1)	21 (35.6)	0.78 (0.46-1.32) ^b	.35	0.80 (0.46-1.39) ^b	.44
Leucocytes/mm ³	7676 ± 3796	7667 ± 3663		.31 ^f		.26 ^f
0-5 days ^d			1.12 (0.89-1.40)	.16	1.13 (0.89-1.43)	.32
6-30 days ^d			0.65 (0.31-1.33)	.24	0.66 (0.32-1.34)	.24
Neutrophils/mm ³	4700 (3600-6500)	5350 (4400-7500)	1.29 (0.96-1.74) ^c	.090	1.19 (0.88-1.61) ^c	.24
Lymphocytes/mm ³	1109 ± 646	927 ± 485	0.74 (0.54-1.01)	.061	0.71 (0.50-0.99)	.041
Monocytes/mm ³	500 (300-700)	400 (300-700)	0.97 (0.75-1.25) ^c	.81	0.91 (0.72-1.16) ^c	.44
Platelets, G/L	236 ± 120	214 ± 98		.073 ^f		.28 ^f
0-5 days ^d			0.94 (0.73-1.21)	.62	0.95 (0.72-1.24)	.69
6-30 days ^d			0.66 (0.45-0.94)	.023	0.66 (0.43-1.01)	.057
Creatinine, mg/L	8 (7-11)	10 (7-12)	1.20 (0.95-1.51) ^c	.12	1.10 (0.83-1.47) ^c	.48
Lactate dehydrogenase, IU/L	359 (280-476)	426 (312-508)	1.22 (0.96-1.54) ^c	.090	1.11 (0.87-1.43) ^c	.38
Troponin ^e ng/L	14 (7-26)	16 (9-24)		.25 ^f		.50 ^f
<8	41 (28.1)	10 (17.2)	1.00 (ref.)	-	1.00 (ref.)	-
8-14	33 (22.6)	17 (29.3)	1.90 (0.88-4.04)	.098	1.16 (0.61-2.18)	.65
15-25	34 (23.3)	18 (31.0)	1.99 (0.93-4.23)	.075	1.19 (0.60-2.31)	.62
>25	38 (26.0)	13 (22.5)	1.36 (0.61-3.04)	.46	0.71 (0.33-1.53)	.38
C-reactive protein, mg/L	60 (25-111)	101 (56-143)	1.68 (1.26-2.23) ^c	<.001	1.66 (1.25-2.19) ^c	<.001
aPTT	1.13 (1.00-1.26)	1.13 (1.06-1.23)	1.02 (0.85-1.23) ^c	.82	1.02 (0.84-1.24) ^c	.85
PTr	1.09 (1.04-1.16)	1.10 (1.05-1.18)	1.15 (0.98-1.35) ^c	.081	1.10 (0.89-1.38) ^c	.34
D-dimers, µg/mL	1.00 (0.70-1.80)	1.00 (0.80-1.90)	1.04 (0.77-1.40) ^c	.80	1.01 (0.74-1.38) ^c	.95
Fibrinogen, g/L	5.9 ± 1.7	6.4 ± 1.5	1.32 (1.04-1.68)	.021	1.34 (1.04-1.74)	.022
Factor VIII, IU/dL	244 ± 104	233 ± 79	0.93 (0.73-1.17)	.51	0.89 (0.71-1.13)	.34
VWF:Ag ^e , IU/dL	351 ± 141	381 ± 98		.30 ^f		.39 ^f
<270	44 (28.6)	9 (15.5)	1.00 (ref.)	-	1.00 (ref.)	-
270-354	35 (22.7)	17 (29.3)	2.09 (0.94-4.60)	.068	1.71 (0.77-3.78)	.18
355-430	38 (24.7)	16 (27.6)	1.86 (0.83-4.14)	.13	1.86 (0.87-3.93)	.11
>430	37 (24.0)	16 (27.6)	1.94 (0.86-4.35)	.11	1.80 (0.82-3.97)	.14
FVIII/VWF:Ag ratio	0.74 ± 0.27	0.64 ± 0.24	0.70 (0.52-0.96)	.025	0.71 (0.51-0.98)	.036

Note: Values are median (interquartile range) or means ± standard deviation. SubHazard ratios (SHRs) were calculated using Fine and Gray models taking into account the mortality in the context of withholding or withdrawal of life-sustaining treatment (n = 16) as competing events and were expressed per one standard deviation unless otherwise as indicated.

Abbreviations: aPTT, activated partial thromboplastin time ratio; CI, confidence interval; CRP, C-reactive protein; FVIII, factor VIII activity; PTr, prothrombin time ratio; SD, standard deviation; SHR, subhazard ratio; VWF: Ag, von Willebrand factor antigen.

^aAdjusted for age, sex, body mass index, hypertension, and diabetes calculated after handling missing values (in biological and confounding factors) by multiple imputation.

^bSHR calculated for O versus others blood groups.

^cSHR calculated per one standard deviation in log-transformed values.

^dModeled with time-dependent coefficients to accommodate deviation in proportional subhazard assumption.

^eModeled as categorical variables based on quartiles to accommodate deviation in log linear relationship.

^fP-value for overall effect calculated using a likelihood ratio test.

with disease severity. To better understand this role of coagulation in SARS-CoV-2 pneumonia pathogenesis we aimed to adjust the predictive value of coagulation biomarkers to confounding factors such as major comorbidities. Moreover, we aimed to evaluate the

severity according to oxygen requirements rather than only admission to ICU or death given that these outcomes associated with COVID-19 are heavily influenced by the presence of other underlying comorbidities.

In our cohort, biomarkers that have already been associated with a poor outcome such as lymphopenia, elevated CRP, and fibrinogen were predictive of respiratory worsening.²⁸⁻³⁰ Reflecting the inclusion of all consecutive primary admissions irrespective of the initial severity, the initial admitting respiratory rate and PaO₂/FiO₂ were, although not completely normal,

within a reasonable spectrum. However, we identified a gradual increase in VWF levels according to oxygen requirements at admission with only 10 patients presenting with normal VWF levels, all of them discharged from the ED with outpatient follow-up. Unusually high circulating VWF levels have been reported in patients with severe COVID-19 infection.^{6,17}

TABLE 3 Associations of biological data with 30-day thrombotic events

Biological data	30-day thrombotic events		Unadjusted		Adjusted ^a	
	No (n = 212)	Yes (=31)	SHR (95% CI)	P	SHR (95% CI)	P
O blood group, n (%)	67 (41.6)	10 (32.3)	0.69 (0.32-1.45) ^b	.32	0.76 (0.35-1.61) ^b	.47
Leucocytes/mm ³	7542 ± 3784	8512 ± 3461		.070 ^e		.14 ^e
0-5 days ^d			1.36 (1.04-1.76)	.022	1.50 (1.11-2.03)	.008
6-30 days ^d			1.02 (0.72-1.45)	.89	1.11 (0.74-1.65)	.60
Neutrophils/mm ³	4900 (3600-6500)	6550 (5200-8200)	1.40 (1.06-1.84) ^c	.018	1.42 (1.03-1.95) ^c	.031
Lymphocytes/mm ³	1070 ± 633	974 ± 368	0.85 (0.60-1.20)	.36	0.92 (0.60-1.40)	.69
Monocytes/mm ³	400 (300-700)	400 (200-800)		.086 ^e		.35 ^e
0-5 days ^d			1.47 (0.79-2.73) ^c	.22	1.28 (0.53-3.07) ^c	.57
6-30 days ^d			0.72 (0.51-1.02) ^c	.064	0.75 (0.50-1.11) ^c	.15
Platelets, G/L	226 ± 112	246 ± 120		.020 ^e		.053 ^e
0-5 days ^d			1.71 (1.11-2.62)	.014	1.71 (1.10-2.66)	.016
6-30 days ^d			0.78 (0.52-1.18)	.23	0.78 (0.51-1.18)	.24
Creatinine, mg/L	8.5 (7-11.5)	8.0 (6-11)	0.84 (0.58-1.21) ^c	.35	0.92 (0.62-1.34) ^c	.64
Lactate dehydrogenase, IU/L	360 (280-456)	495 (383-599)	1.79 (1.36-2.36) ^c	<.001	1.87 (1.36-2.58) ^c	<.001
Troponin, ng/L	15.0 (7.5-26.0)	11.5 (7.5-23.0)	1.08 (0.69-1.70) ^c	.73	1.35 (0.84-2.15) ^c	.21
C-reactive protein, mg/L	69 (31-123)	79 (28-157)	1.08 (0.71-1.62) ^c	.73	1.20 (0.77-1.86) ^c	.40
aPTTr	1.10 (1.03-1.23)	1.17 (1.03-1.26)	1.25 (0.89-1.73) ^c	.19	1.10 (0.71-1.72) ^c	.66
PTr	1.09 (1.04-1.15)	1.15 (1.08-1.20)	1.13 (0.94-1.35) ^c	.17	1.10 (0.83-1.46) ^c	.51
D-dimers, µg/mL	1.00 (0.70-1.60)	1.60 (1.10-4.20)		<.001 ^e		<.001 ^e
0-5 days ^d			2.48 (1.66-3.70) ^c	<.001	2.90 (1.86-4.50) ^c	<.001
6-30 days ^d			1.01 (0.31-3.30) ^c	.99	1.21 (0.33-4.40) ^c	.77
Fibrinogen, g/L	6.1 ± 1.6	5.9 ± 1.8	0.90 (0.60-1.32)	.31	0.96 (0.65-1.41)	.84
Factor VIII, IU/dL	239 ± 91	251 ± 123		<.001 ^e		.007 ^e
0-5 d ^d			1.78 (1.17-2.68)	.006	1.72 (1.15-2.55)	.007
6-30 days ^d			0.46 (0.26-0.82)	.008	0.50 (0.27-0.91)	.022
VWF:Ag, IU/dL	358 ± 131	381 ± 107	1.18 (0.90-1.55)	.22	1.23 (0.92-1.63)	.16
FVIII/VWF:Ag ratio	0.72 ± 0.27	0.67 ± 0.29		.035 ^e		.063 ^e
0-5 days ^d			1.23 (0.69-2.16)	.48	1.09 (0.61-1.92)	.77
6-30 days ^d			0.47 (0.25-0.87)	.015	0.47 (0.26-0.85)	.012

Note: Values are median (interquartile range) or means ± standard deviation. Subhazard ratios (SHRs) were calculated using Fine and Gray models taking into account the mortality (n = 27) as competing events and were expressed per one standard deviation unless otherwise as indicated.

Abbreviations: aPTTr, activated partial thromboplastin time ratio; CI, confidence interval; CRP, C-reactive protein; FVIII, factor VIII activity; PTr, prothrombin time ratio; SD, standard deviation; SHR, subhazard ratio; VWF:Ag, von Willebrand factor antigen.

^aAdjusted for age, sex, body mass index, hypertension, and diabetes calculated after handling missing values (in biological and confounding factors) by multiple imputation.

^bSHR calculated for O versus others blood groups.

^cSHR calculated per one standard deviation in log-transformed values.

^dModeled with time-dependent coefficients to accommodate deviation in proportional subhazard assumption.

^eP-value for overall effect calculated using a likelihood ratio test.

The vascular endothelium is emerging as a key target-organ of SARS-Cov-2. SARS-Cov-2 infects target cells in the lung, heart, intestine, and kidney using the angiotensin converting enzyme 2 (ACE2) receptor, which is also widely expressed on endothelial cells. Recent autopsy findings suggest that SARS-Cov-2 infection induces widespread endothelial dysfunction and inflammation that could shift the endothelial balance toward a procoagulant state.¹¹ VWF endothelial expression is characterized by a vascular-bed heterogeneity^{31,32} with lung endothelial cells being the first source of circulating VWF.²² VWF expression and release from endothelial cell Weibel-Palade bodies is also stimulated by hypoxia.^{33,34} Hypoxia-induced VWF upregulation is associated with the presence of thrombi in heart and lung vascular beds and promotes recruitment of leukocytes.³⁵

In our cohort including COVID-19 patients with varying degrees of illness, a decrease in FVIII/VWF ratio values on admission was associated with a higher risk of worsening respiratory status, as evidenced by an increase in oxygen requirements. This suggests that both inflammation and a SARS-CoV-2-induced endotheliopathy could contribute to lung damage pathogenesis. The different levels of FVIII and VWF as evaluated by their ratio could reflect a major synthesis and release of VWF in the lung due to inflammation, hypoxia, and direct SARS-CoV-2 destruction of endothelial cells, while the levels of FVIII are less increased because the liver is only exposed to pro-inflammatory cytokines.

Age, male sex, increased BMI, and metabolic syndrome are significantly associated with an increased risk of severe forms and death from COVID-19 infection.³⁶ Importantly, the prediction of an increase in oxygen requirement remained significant after adjusting for these metabolic comorbidities, confirming the direct involvement of procoagulant changes in COVID-19 pneumonia pathogenesis.

Thrombosis was associated with biomarkers reflecting inflammation including increased leucocyte, neutrophil, and platelet counts. We also observed an association with higher LDH, D-dimers, and FVIII levels. In a recent meta-analysis, an association between elevated LDH levels measured at earliest time point in hospitalization and worse outcomes was reported in patients with COVID-19³⁷ as observed in patients with Middle East respiratory syndrome (MERS).³⁸ Several mechanisms may account for LDH increase in COVID-19 including thrombotic microangiopathy, upregulation of the glycolytic pathway in a context of severe hypoxia, and direct cell damage because this intracellular enzyme is found in pneumocytes, the main target cell of SARS-CoV-2.

D-dimers at admission or increasing D-dimers over time have been associated with an increased risk of respiratory degradation, thrombosis, and death from COVID-19 infection.^{2,14,39} Reports to date have not accounted for age or other major comorbidities that contribute to D-dimer elevation as potential confounders in risk prediction. Of note, in our cohort the predictive value of D-dimers on the occurrence of thrombosis remained significant after adjustment on major metabolic comorbidities associated with COVID-19 and also risk factors for thrombosis such as BMI and age. Similarly,

high FVIII levels at admission were also associated with an increased risk of early-onset thrombosis (eg, in the 5 days following admission) independently of major comorbidities. Among coagulation factors, high levels of FVIII and VWF were the strongest identified risk factors and recently a causal role of these two proteins in thrombotic events has been suggested.^{40,41} As we observed a secondary increase of FVIII in patients with late-onset thrombosis we suspect that this factor can only predict events in a short time frame, and so should be closely and frequently monitored. VWF levels upon admission were not predictive of thrombotic events during follow-up. This could suggest that the important increase in VWF observed in almost all patients related to endothelial injury in the lung, as reflected by the relation with the oxygen requirements at admission, is not a marker of patients at higher risk for thrombosis.

Altogether, these biological features make the link between SARS-CoV2 infection and the severity of hypoxemia. Indeed activation of coagulation cascade leading to widespread thrombosis in the lung and endothelial damages are thought to be involved in the disruption of pulmonary vasoregulation especially the vasoconstriction secondary to alveolar hypoxia.⁴²

The main strengths of our study are: (a) our study was prospective with a systematic follow-up in all patients at day 30; (b) in order to prevent referral bias, this study was performed in COVID-19 patients with radiological signs of pneumonia but with varying severity of illness; (c) adjustment for established risk factors for disease progression and death and accounting for limitation of life-sustaining treatment as competing events for adverse outcomes are two other major strengths of the present study; (d) potential limitation, withholding, or withdrawal of life-sustaining treatment in frail elderly patients is a potential confounder that should be taken into account as a competing event when assessing the association between biomarkers and the risk of adverse outcomes in COVID-19 patients.⁴³ In our study we considered death with limitation, withholding, or withdrawal of life-sustaining treatment as a competing event for the evaluation of respiratory worsening meaning that death with respiratory failure was not considered as worsening when occurring in the context of limited, withheld, or withdrawn life-sustaining treatment. However, this study has three main limitations. First, this was a single-center study, second the thrombotic complications were not diagnosed through systematic screening with doppler ultrasound or CT pulmonary angiogram. The prevalence of VTE and PE was therefore probably underestimated because the access doppler ultrasound and CT pulmonary angiogram was limited in COVID-19 patients hospitalized in ICU for practical reasons. Furthermore, as seasonal influenza outbreak was over in Europe at the start of the COVID-19 pandemic, we could not include patients with interstitial pneumonia related to viruses other than SARS-Cov2 as controls. It remains to be assessed whether the biomarkers associated with worse outcomes in our study are specific to COVID-19 pneumonia or could be translated to pneumonia related to other viruses such as SARS, MERS, or influenza.

5 | CONCLUSION

We provide evidence that levels of coagulation biomarkers including FVIII and VWF at time of admission to the ED are associated with the severity of COVID-19 and predict risk of increased oxygen requirements irrespective of age, sex, BMI, diabetes, and hypertension.

ACKNOWLEDGMENTS

The authors wish to thank Laureline Bourgeois, Aurélie Jospin, Catherine Marichez, Vincent Dalibard, Bénédicte Pradines, Sandrine Vanderziepe, all the biologists and technicians of the Hemostasis Department, and the Lille COVID Research Network (LICORNE) for their support during the COVID-19 pandemic.

CONFLICTS OF INTEREST

No disclosures relevant to the manuscript.

AUTHOR CONTRIBUTIONS

AR and SS designed the study, analyzed the data, and wrote the manuscript. FL, JG, MC, LC, AR, EJ, AD, KF, and ML collected clinical data. JL and AD performed the statistical analysis. EK, DG, PL, and JP provided critical input and analysis. All authors provided editorial review and assisted in writing the manuscript.

DATA AVAILABILITY STATEMENT

For original data, please contact sophiesusen@aol.com.

ORCID

Antoine Rauch  <https://orcid.org/0000-0002-1182-4131>

Fanny Lassalle  <https://orcid.org/0000-0003-0494-823X>

Peter J. Lenting  <https://orcid.org/0000-0002-7937-3429>

Sophie Susen  <https://orcid.org/0000-0001-5953-163X>

TWITTER

Sophie Susen  @sophie_susen

REFERENCES

- Connors JM, Levy JH. COVID-19 and its implications for thrombosis and anticoagulation. *Blood*. 2020;135(23):2033-2040.
- Tang N, Li D, Wang X, Sun Z. Abnormal coagulation parameters are associated with poor prognosis in patients with novel coronavirus pneumonia. *J Thromb Haemost*. 2020;18(4):844-847.
- Zhou F, Yu T, Du R, et al. Clinical course and risk factors for mortality of adult inpatients with COVID-19 in Wuhan, China: a retrospective cohort study. *Lancet*. 2020;395(10229):1054-1062.
- Wu C, Chen X, Cai Y, et al. Risk factors associated with acute respiratory distress syndrome and death in patients with coronavirus disease 2019 pneumonia in Wuhan, China. *JAMA Intern Med*. 2020;180(7):934.
- Klok FA, Kruip MJHA, van der Meer NJM, et al. Incidence of thrombotic complications in critically ill ICU patients with COVID-19. *Thromb Res*. 2020;191:145-147.
- Helms J, Tacquard C, Severac F, et al. High risk of thrombosis in patients with severe SARS-CoV-2 infection: a multicenter prospective cohort study. *Intensive Care Med*. 2020;46(6):1089-1098.
- Poissy J, Goutay J, Caplan M, et al. Pulmonary embolism in COVID-19 patients: awareness of an increased prevalence. *Circulation*. 2020;142(2):184-186.
- Middelcorp S, Coppens M, van Haaps TF, et al. Incidence of venous thromboembolism in hospitalized patients with COVID-19. *J Thromb Haemost*. 2020;18(8):1995-2002.
- Wichmann D, Sperhake J-P, Lütgehetmann M, et al. Autopsy findings and venous thromboembolism in patients with COVID-19. *Ann Intern Med*. 2020;173(4):268-277.
- Lax SF, Skok K, Zechner P, et al. Pulmonary arterial thrombosis in COVID-19 with fatal outcome: results from a prospective, single-center, clinicopathologic case series. *Ann Intern Med*. 2020;173(5):350-361.
- Varga Z, Flammer AJ, Steiger P, et al. Endothelial cell infection and endotheliitis in COVID-19. *Lancet*. 2020;395(10234):1417-1418.
- Ackermann M, Verleden SE, Kuehnel M, et al. Pulmonary vascular endothelialitis, thrombosis, and angiogenesis in Covid-19. *N Engl J Med*. 2020;383(2):120-128.
- Iba T, Levy JH, Levi M, Connors JM, Thachil J. Coagulopathy of coronavirus disease 2019. *Crit Care Med*. 2020;48(9):1358-1364.
- Huang C, Wang Y, Li X, et al. Clinical features of patients infected with 2019 novel coronavirus in Wuhan, China. *Lancet*. 2020;395(10223):497-506.
- Grasselli G, Zangrillo A, Zanella A, et al. Baseline characteristics and outcomes of 1591 patients infected With SARS-CoV-2 admitted to ICUs of the Lombardy Region, Italy. *JAMA*. 2020;323(16):1574.
- Richardson S, Hirsch JS, Narasimhan M, et al. Presenting characteristics, comorbidities, and outcomes among 5700 patients hospitalized with COVID-19 in the New York City Area. *JAMA*. 2020;323(20):2052-2059.
- Panigada M, Bottino N, Tagliabue P, et al. Hypercoagulability of COVID-19 patients in intensive care unit. A report of thromboelastography findings and other parameters of hemostasis. *J Thromb Haemost*. 2020;18(7):1738-1742.
- Escher R, Breakey N, Lämmle B. Severe COVID-19 infection associated with endothelial activation. *Thromb Res*. 2020;190:62.
- Pan J, Dinh TT, Rajaraman A, et al. Patterns of expression of factor VIII and von Willebrand factor by endothelial cell subsets in vivo. *Blood*. 2016;128(1):104-109.
- Liao X, Wang B, Kang Y. Novel coronavirus infection during the 2019-2020 epidemic: preparing intensive care units-the experience in Sichuan Province, China. *Intensive Care Med*. 2020;46(2):357-360.
- Rocca B, Fox KAA, Ajjan RA, et al. Antithrombotic therapy and body mass: an expert position paper of the ESC Working Group on Thrombosis. *Eur Heart J*. 2018;39(19):1672-1686f.
- Susen S, Tacquard CA, Godon A, et al. Prevention of thrombotic risk in hospitalized patients with COVID-19 and hemostasis monitoring. *Crit Care*. 2020;24(1):364
- Société de réanimation de langue. Limitation et arrêt des traitements en réanimation adulte. Actualisation des recommandations de la Société de réanimation de langue française. *Réanimation*. 2010;19(8):679-698.
- Prentice RL, Kalbfleisch JD, Peterson AV, et al. The analysis of failure times in the presence of competing risks. *Biometrics*. 1978;34(4):541-554.
- Harrell FE, Lee KL, Mark DB. Multivariable prognostic models: issues in developing models, evaluating assumptions and adequacy, and measuring and reducing errors. *Stat Med*. 1996;15(4):361-387.
- van Buuren S, Groothuis-Oudshoorn K. Multivariate imputation by chained equations in R. *J Stat Soft*. 2011;45(3).
- Rubin GJ, Donald B. *Multiple Imputation for Nonresponse in Surveys*. Chichester, New York, Brisbane, Toronto, Singapore: John Wiley & Sons; 1987, 258 S., 6 Abb., £ 30.25, ISSN 0271-6232. *Biom. J*. 1989;31(1):131-132.

28. Guan W-J, Ni Z-Y, Hu Y, et al. Clinical characteristics of coronavirus disease 2019 in China. *N Engl J Med*. 2020;382(18):1708-1720.
29. Fogarty H, Townsend L, Ni Cheallaigh C, et al. COVID19 coagulopathy in Caucasian patients. *Br J Haematol*. 2020;189(6):1044-1049.
30. Ranucci M, Ballotta A, Di Dedda U, et al. The procoagulant pattern of patients with COVID-19 acute respiratory distress syndrome. *J Thromb Haemost*. 2020;18(7):1747-1751.
31. Nassiri M, Liu J, Kulak S, et al. Repressors NFI and NFY participate in organ-specific regulation of von Willebrand factor promoter activity in transgenic mice. *Arterioscler Thromb Vasc Biol*. 2010;30(7):1423-1429.
32. Shirodkar AV, St Bernard R, Gavryushova A, et al. A mechanistic role for DNA methylation in endothelial cell (EC)-enriched gene expression: relationship with DNA replication timing. *Blood*. 2013;121(17):3531-3540.
33. Mojiri A, Nakhai-Nejad M, Phan W-L, et al. Hypoxia results in upregulation and de novo activation of von Willebrand factor expression in lung endothelial cells. *Arterioscler Thromb Vasc Biol*. 2013;33(6):1329-1338.
34. Pinsky DJ, Naka Y, Liao H, et al. Hypoxia-induced exocytosis of endothelial cell Weibel-Palade bodies. A mechanism for rapid neutrophil recruitment after cardiac preservation. *J Clin Invest*. 1996;97(2):493-500.
35. Mojiri A, Alavi P, Lorenzana Carrillo MA, et al. Endothelial cells of different organs exhibit heterogeneity in von Willebrand factor expression in response to hypoxia. *Atherosclerosis*. 2019;282:1-10.
36. Guo T, Fan Y, Chen M, et al. Cardiovascular implications of fatal outcomes of patients with coronavirus disease 2019 (COVID-19). *JAMA Cardiol*. 2020;5(7):811.
37. Henry BM, de Oliveira MHS, Benoit S, Plebani M, Lippi G. Hematologic, biochemical and immune biomarker abnormalities associated with severe illness and mortality in coronavirus disease 2019 (COVID-19): a meta-analysis. *Clin Chem Lab Med*. 2020;58(7):1021-1028.
38. Assiri A, Al-Tawfiq JA, Al-Rabeeh AA, et al. Epidemiological, demographic, and clinical characteristics of 47 cases of Middle East respiratory syndrome coronavirus disease from Saudi Arabia: a descriptive study. *Lancet Infect Dis*. 2013;13(9):752-761.
39. Wang D, Hu B, Hu C, et al. Clinical characteristics of 138 hospitalized patients with 2019 novel coronavirus-infected pneumonia in Wuhan, China. *JAMA*. 2020;323(11):1061.
40. Rietveld IM, Lijfering WM, le Cessie S, et al. High levels of coagulation factors and venous thrombosis risk: strongest association for factor VIII and von Willebrand factor. *J Thromb Haemost*. 2019;17(1):99-109.
41. Sabater-Lleal M, Huffman JE, de Vries PS, et al. Genome-wide association transethnic meta-analyses identifies novel associations regulating coagulation factor VIII and von Willebrand factor plasma levels. *Circulation*. 2019;139(5):620-635.
42. Marini JJ, Gattinoni L. Management of COVID-19 respiratory distress. *JAMA*. 2020;323(22):2329.
43. Vincent J-L, Taccone FS. Understanding pathways to death in patients with COVID-19. *Lancet Resp Med*. 2020;8(5):430-432.

SUPPORTING INFORMATION

Additional supporting information may be found online in the Supporting Information section.

How to cite this article: Rauch A, Labreuche J, Lassalle F, et al. Coagulation biomarkers are independent predictors of increased oxygen requirements in COVID-19. *J Thromb Haemost*. 2020;18:2942-2953. <https://doi.org/10.1111/jth.15067>

Arterial Pulsatility and Circulating von Willebrand Factor in Patients on Mechanical Circulatory Support



Flavien Vincent, MD,^{a,b,c,*} Antoine Rauch, MD, PhD,^{b,c,d,*} Valentin Loobuyck, MD,^{b,c,e} Emmanuel Robin, MD, PhD,^{b,c,f} Christoph Nix, MSc,^g André Vincentelli, MD, PhD,^{b,c,e} David M. Smadja, PHARM, PhD,^{h,i} Pascal Leprince, MD, PhD,^j Julien Amour, MD, PhD,^k Gilles Lemesle, MD, PhD,^{a,b,c} Hugues Spillemaeker, MD,^{a,b,c} Nicolas Debry, MD,^a Christian Latremouille, MD, PhD,^l Piet Jansen, MD, PhD,^m Antoine Capel, PhD,^m Mouhamed Moussa, MD,^{b,c,f} Natacha Rousse, MD,^e Guillaume Schurtz, MD,^a Cédric Delhaye, MD,^a Camille Paris, MD,^d Emmanuelle Jeanpierre, PHARM, PhD,^d Annabelle Dupont, PHARM, PhD,^{b,c,d} Delphine Corseaux, PhD,^{b,c} Mickaël Rosa, PhD,^{b,c} Yoann Sottejeau, PhD,^{b,c} Svenja Barth, MSc,^g Claudia Mourran, PhD,^g Valérie Gomane, BSc,^d Augustin Coisne, MD,^{a,b,c} Marjorie Richardson, MD,^a Claudine Caron, MD, PhD,^d Cristian Preda, PhD,ⁿ Alexandre Ung, BSc,^{b,c,d} Alain Carpentier, MD,^{l,m} Thomas Hubert, DVM, PhD,^o Cécile Denis, PhD,^p Bart Staels, PhD,^{b,c} Peter J. Lenting, PhD,^p Eric Van Belle, MD, PhD,^{a,b,c,*} Sophie Susen, MD, PhD,^{b,c,d,*}

ABSTRACT

BACKGROUND The main risk factor for bleeding in patients with continuous-flow mechanical circulatory support (CF-MCS) is the acquired von Willebrand factor (VWF) defect related to the high shear-stress forces developed by these devices. Although a higher bleeding rate has been reported in CF-MCS recipients who had reduced pulsatility, the relation between pulsatility and the VWF defect has never been studied.

OBJECTIVES The purpose of this study was to investigate the relation between pulsatility and VWF under CF-MCS.

METHODS We assessed the effect of 2 CF-MCS on VWF multimer degradation in a mock circulatory loop (model 1). Using these devices, we investigated in a dose-effect model (model 2) 3 levels of pulsatility in 3 groups of swine. In a cross-over model (model 3), we studied the effects of sequential changes of pulsatility on VWF. We reported the evolution of VWF multimerization in a patient undergoing serial CF-MCS and/or pulsatile-MCS.

RESULTS We demonstrated the proteolytic degradation of VWF multimers by high shear CF-MCS in a circulatory loop without pulsatility. We observed both in swine models and in a patient that the magnitude of the VWF degradation is modulated by the pulsatility level in the high shear-stress level condition, and that the restoration of pulsatility is a trigger for the endothelial release of VWF.

CONCLUSIONS We demonstrated that the VWF defect reflects the balance between degradation induced by the shear stress and the endothelial release of new VWF triggered by the pulsatility. This modulation of VWF levels could explain the relationship between pulsatility and bleeding observed in CF-MCS recipients. Preservation of pulsatility may be a new target to improve clinical outcomes of patients. (J Am Coll Cardiol 2018;71:2106-18) © 2018 by the American College of Cardiology Foundation.



Listen to this manuscript's audio summary by JACC Editor-in-Chief Dr. Valentin Fuster.



From the ^aCHU Lille, Cardiology, Lille, France; ^bUniversity of Lille, INSERM U1011-EGID, Lille, France; ^cInstitut Pasteur de Lille, Lille, France; ^dCHU Lille, Hematology Transfusion, Lille, France; ^eCHU Lille, Cardiac Surgery, Lille, France; ^fCHU Lille, Department of Anesthesia and Intensive Care, Lille, France; ^gAbiomed Europe GmbH, Aachen, Germany; ^hHematology Department, Hôpital Européen Georges Pompidou, Assistance Publique-Hôpitaux de Paris, University Paris Descartes, Sorbonne Paris Cité, Paris, France; ⁱInserm UMR-S1140, Paris, France; ^jSorbonne Université, UMR INSERM 1166, IHU ICAN, Assistance Publique-Hôpitaux de Paris (AP-HP), Department of Thoracic and Cardiovascular Surgery, Pitié-Salpêtrière Hospital, Paris, France; ^kSorbonne Université, UMR INSERM 1166, IHU ICAN, Assistance Publique-Hôpitaux de Paris (AP-HP), Department of Anesthesiology and Critical Care Medicine, Pitié-Salpêtrière Hospital, Paris, France; ^lDepartment of Cardiovascular Surgery, Hôpital Européen Georges Pompidou, Assistance Publique-Hôpitaux de Paris, University Paris Descartes-Sorbonne Paris Cité, Paris, France; ^mCarmat SA, Vélizy-Villacoublay, France; ⁿLaboratoire de Mathématiques, Paul Painlevé, UMR CNRS 8524, Université de Sciences et Technologies de Lille, Lille, France; ^oINSERM U1190-EGID, Lille, France; and the ^pINSERM U1176, University Paris-Sud, University Paris-Saclay, Le Kremlin-Bicêtre, France. *Drs. Vincent, Rauch, Van Belle, and Susen contributed equally to the study. This work was supported by Lille-II University and

Continuous flow (CF) mechanical circulatory support (MCS) devices have been developed to treat end-stage heart failure in patients waiting for heart transplant or as a destination therapy. Bleeding is currently the most frequent adverse event observed in patients with CF-MCS and represent a major source of morbidity. Gastrointestinal bleeding occurs in $\leq 50\%$ of patients and impact their management, quality of life, and ultimately survival (1-3).

The acquired von Willebrand factor (VWF)-defect related to the high shear-stress forces developed by these devices has been shown to be 1 of the main risk factors of bleeding (4-6). VWF is a multimeric glycoprotein synthesized and released by the endothelial cells involved in hemostasis and angiogenesis. The supra-physiological shear stress induced by CF-MCS promotes the proteolytic degradation of the high molecular weight (HMW) multimers of VWF into smaller protein complexes with less hemostatic potential (7).

SEE PAGE 2119

CF-MCS also decreases arterial pulsatility to a various extent depending on the balance between the residual native left ventricle (LV) contractility and the flow rate of the device. Several studies have reported a higher bleeding rate in CF-MCS-supported patients who had reduced pulsatility (8-10). However, the direct relationship between pulsatility and multimeric profile of VWF has never been studied. This question is of major clinical importance to understand whether preservation of pulsatility under CF-MCS could reduce the incidence of bleeding and affect patient management (11,12).

We hypothesized that the defect of VWF observed under MCS could be modulated by the endothelial response to the level of pulsatility. One in vitro endothelial-free mock circulatory loop model and 2 experimental swine models with CF-MCS were used to investigate the relationship between pulsatility and VWF multimerization. We further investigated the evolution of VWF parameters in a patient with

cardiogenic shock requiring MCS with successively 3 serial pulsatile and CF devices.

METHODS

STUDY DESIGN. To assess the effect of changes of pulsatility as a modulator of VWF defect under CF-MCS, we developed 3 experimental models and we investigated a patient undergoing sequential changes of pulsatility. The results obtained in this patient are part of the “first clinical use of a bioprosthetic total artificial heart” CARMAT study (Figure 1, Online Table 1).

For the experimental part, we used 2 percutaneous micro-axial catheter-mounted high shear rotary pumps adapted from Impella-CP (MCS-A) and Impella-5.0 (MCS-B) and using a dedicated cannula adapted to pig anatomy constraints (Abiomed Europe-GmbH, Aachen, Germany). The 2 pumps were designed to induce very similar shear with a tip velocity of 9.5 and 10.0 $\text{m} \cdot \text{s}^{-1}$ for MCS-A and -B, respectively. During all of the experiments, the pumps were used at a constant and maximal speed with a maximum flow of 3.2 l/min (MCS-A) and 4.5 l/min (MCS-B).

For the in vitro model, we used an endothelial-free mock circulatory loop (without pulsatility) to investigate the intrinsic capacity of these 2 high-shear CF-MCS to induce a loss of HMW multimers after proteolytic degradation of VWF (Figure 1A). For the in vivo experimental part, we developed 2 swine models with normal heart function to study the relationship between pulsatility and the intensity of VWF defect (Figures 1B and 1C).

We further investigated the evolution of multimeric profile in a patient with cardiogenic shock requiring MCS with successively 3 serial pulsatile and CF devices: 1) CF-MCS with venoarterial

ABBREVIATIONS AND ACRONYMS

ADAMTS13 = A disintegrin and metalloprotease with thrombospondin type 1 repeats-13

CF = continuous flow

ECMO = extracorporeal membrane oxygenation

FVIIIc = Factor VIII coagulant activity

HMW = high molecular weight

LDH = lactate dehydrogenase

LV = left ventricle/ventricular

MCS = mechanical circulatory support

PF = pulsatile flow

PP = pulse pressure

VWF = von Willebrand factor

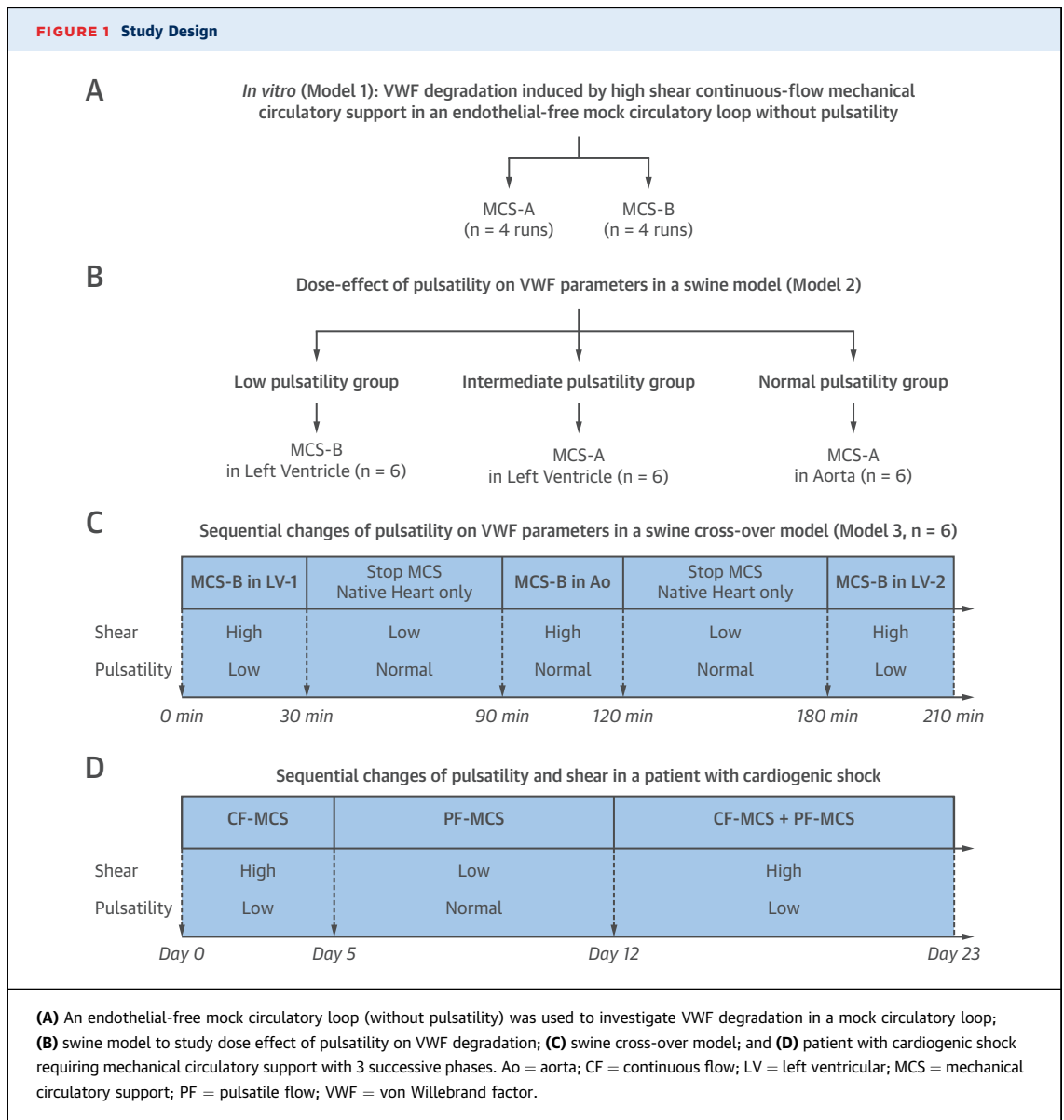
VWF:Ag = von Willebrand factor antigen

VWF:CB = von Willebrand factor collagen-binding activity

WPB = Weibel Palade body

by the National Research Agency (Programme d'Investissement d'Avenir), ANR-17-RHUS-0011. The clinical study of feasibility and safety of CARMAT pulsatile total artificial heart implantation is registered to French government health authorities with number 2001-A00972-39 and financed by Carmat. Dr. Vincent has received a research grant from the Fédération Française de Cardiologie. Drs. Nix, Barth, and Mourran are full-time employees of Abiomed. Dr. Carpentier is cofounder and shareholder of Carmat. Drs. Smadja, Latremouille, Leprince, and Susen have received consulting fees from Carmat. Dr. Leprince has served as a proctor for St. Jude/Abbott, Medtronic, and Syncardia. Dr. Lemesle has received fees for lectures or consulting from Amgen, AstraZeneca, Bayer, Biopharma, Bristol-Myers Squibb, Boehringer Ingelheim, Daiichi-Sankyo, Eli Lilly, Merck Sharp & Dohme, Novartis, Pfizer, Sanofi, Servier, and The Medicines Company. Drs. Jansen and Capel are employed by Carmat. Dr. Susen has received consulting fees from LFB, HemaBiologics, Roche, Shire, Sobi, and Carmat; has received research support from CSL-Behring, LFB, Stago, and Carmat; and has received travel fees from CSL-Behring, LFB, Bayer, Novo, Shire, Siemens, Sobi, Stago, and Bristol-Myers Squibb-Pfizer. All other authors have reported that they have no relationships relevant to the contents of this paper to disclose.

Manuscript received July 30, 2017; revised manuscript received January 25, 2018, accepted February 25, 2018.



extracorporeal membrane oxygenation (ECMO); 2) pulsatile-flow (PF) MCS with experimental CARMAT total artificial heart; and 3) the association of both (CF-MCS + PF-MCS) (Figure 1D).

The assessment of arterial pulsatility *in vivo* was based on the invasive measurement of pulse pressure (PP) defined by the difference between systolic and diastolic arterial pressure.

IN VITRO STUDY: VWF DEGRADATION INDUCED BY HIGH-SHEAR CF-MCS IN AN ENDOTHELIAL-FREE MOCK CIRCULATORY LOOP WITHOUT PULSATILITY. The endothelium-independent effects of these 2 CF-MCS on VWF degradation were assessed *in vitro* in a

mock circulatory loop perfused with human whole blood (12). This loop allowed for the investigation of the direct effect of the device on VWF without the potential release of new VWF from the endothelial cells (Figure 1A, Online Appendix). Each experiment lasted 30 min for both pumps (MCS-A and -B) and for a total of 4 runs for each. Four more runs were performed in the presence of an unspecific inhibitor of VWF proteolysis (ethylene diamine tetra acetic acid [EDTA] at 10 mmol/l).

DOSE-EFFECT OF PULSATILITY ON VWF PARAMETERS IN A SWINE MODEL. A swine model was designed to investigate VWF parameters in 3 distinct groups of

animals (18 animals, 6 in each condition) defined by 3 degrees of pulsatility depending on the combination of the maximum flow of the device and its localization: 1) low pulsatility group: implantation of the MCS-B inside the LV to achieve a strong decrease of PP (i.e., PP <10 mm Hg); 2) intermediate pulsatility group: implantation of the MCS-A inside the LV to achieve a mild decrease of PP (i.e., PP between 10 and 25 mm Hg); and 3) normal pulsatility group: implantation of the MCS-B inside the aorta to preserve the PP generated by the heart (i.e., PP >25 mm Hg) (Figure 1B).

In all animals, irrespective of the group, the pump was inserted via an introducer in the aorta after laparotomy (Online Appendix).

CONSEQUENCES OF SEQUENTIAL CHANGES OF PULSATILITY ON VWF PARAMETERS IN A SWINE CROSS-OVER MODEL. We investigated the time course of changes of VWF parameters in a swine cross-over model (6 animals) allowing acute variations of pulsatility under high-shear conditions in the same animal (Figure 1C).

For this dynamic model in 5 phases, we implanted the MCS-B as described previously successively inside of the LV and inside of the aorta to achieve the largest variations of PP:

- Phase 1: The MCS was first implanted and initiated inside of the LV for 30 min (LV-1; low pulsatility and high shear).
- Phase 2: The MCS was stopped and retrieved inside the aorta for 60 min (native heart only-1; normal pulsatility and low shear).
- Phase 3: The MCS operated for 30 min inside the aorta (aorta; normal pulsatility and high shear).
- Phase 4: The MCS was stopped again and remained inside the aorta for 60 min (native heart only-2; normal pulsatility and low shear).
- Phase 5: The MCS was reinserted inside the LV for the remaining 30 min of the experiment (LV-2; low pulsatility and high shear).

The MCS was operating at the same maximal rotational speed during the LV and the aorta phases to maintain a constant shear-stress level.

SEQUENTIAL CHANGES OF PULSATILITY AND SHEAR IN A PATIENT WITH CARIOGENIC SHOCK REQUIRING MCS. A 58-year-old man with dilated cardiomyopathy was admitted to the cardiac intensive care unit for a severe biventricular dysfunction refractory to vasopressive and inotropic drugs (INTERMACS class I) and underwent successively 3 phases of MCS with different hemodynamic and shear patterns (Figure 1D):

1. First, a peripheral CF-MCS with venoarterial ECMO was rapidly implanted as a bridge to decision

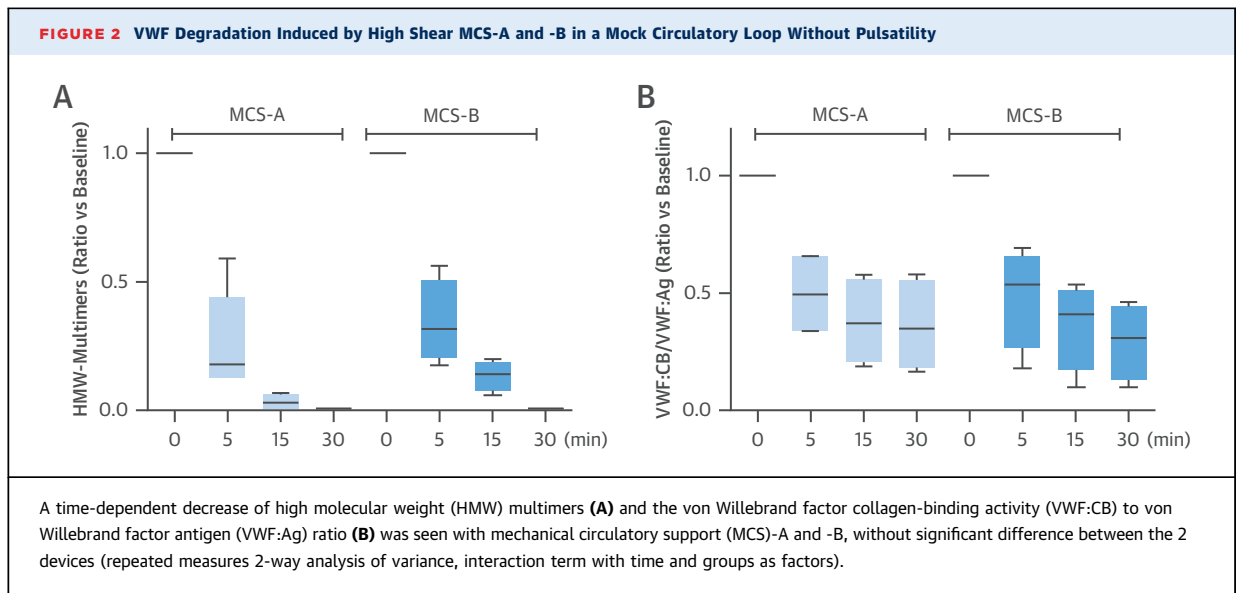
therapy (phase 1: low pulsatility and high shear; CF-MCS). The patient was considered neither as a suitable candidate for heart transplantation nor for usual long-term ventricular assist device implantation, but fulfilled the criteria to be included in a clinical trial investigating PF-MCS with CARMAT total artificial heart (13).

2. Thus, after informed consent, the patient was implanted with the PF-MCS (phase 2: low shear and normal pulsatility; PF-MCS).
3. Seven days after implantation, because of hemodynamic and respiratory failure, a CF-MCS with venoarterial ECMO was added to provide both oxygenation and hemodynamic support (phase 3: high shear and low pulsatility; CF-MCS + PF-MCS) (14).

BLOOD SAMPLING AND VWF ANALYSES. Blood sampling was performed before and after initiation (at 5, 15, and 30 min) of MCS to assess the time course of the VWF collagen-binding activity over VWF antigen ratio (VWF:CB/VWF:Ag ratio), HMW multimers, and VWF:Ag (7). The same time course was used for blood sampling in the 3 models. This time course was derived from our observation of the kinetics of VWF degradation/restoration in humans (4).

In the patient, blood samples were collected for VWF analysis during each phase of support. The biological exploration of VWF was performed on platelet-poor plasma. Platelet-poor plasma was frozen at -80°C until analysis.

VWF AND OTHER BIOLOGICAL PARAMETER ANALYSES IN SWINE BLOOD SAMPLES. VWF antigen levels were evaluated by immunoturbidimetry (VWF:Ag, Siemens, Marburg, Germany). VWF activity was assessed by an enzyme-linked immunosorbent assay (ELISA) collagen-binding assay (VWF:CB) (Horm, Nycomed, Oslo, Norway). VWF multimeric analysis was adapted for the swine model (Online Appendix) and as previously described (7). Factor VIII (FVIIIc) activity was measured by a 1-stage assay, on a Sysmex CA1500 analyzer with the use of commercial reagents (Triniclot aPTT and FVIII deficient, Siemens). A disintegrin and metalloprotease with thrombospondin type I repeats-13 (ADAMTS13) activity was measured using a chromogenic assay, Technozym ADAMTS13 activity ELISA (Technoclone, Vienna, Austria). Angiotensin-2 (Ang-2) levels were measured by ELISA (R&D Systems, Minneapolis, Minnesota). Plasma lactate dehydrogenase (LDH) was measured with a fluorimetric assay (Roche Diagnostics, Mannheim, Germany).



VWF ANALYSIS IN HUMAN BLOOD SAMPLES. VWF:Ag and VWF:CB levels were measured as described in the previous text. The multimeric structure of plasma VWF was quantified after electrophoresis as previously described (7). The von Willebrand factor propeptide (VWFpp) (VWF & Propeptide Assay, Immucor GTI Diagnostics, Waukesha, Wisconsin) was measured by ELISA.

STATISTICAL ANALYSIS. Time points were compared with a Wilcoxon signed-rank test for paired or Mann-Whitney *U* test for unpaired groups. Correlation was performed with Spearman rank correlation coefficient. Multiple time comparisons were performed using repeated measures of 1-way analysis of variance (ANOVA). To compare the dynamic of HMW multimers between the groups, we have fitted a repeated measures 2-way ANOVA model with time and groups as factors. The interaction term between the 2 factors is tested to assess the difference between the dynamics of the groups. Statistical analysis was performed using SPSS (IBM, Armonk, New York) and the R software with the nlme package (R Foundation for Statistical Computing, Vienna, Austria). Results are expressed as median (interquartile range [IQR]). All *p* values <0.05 were considered statistically significant.

RESULTS

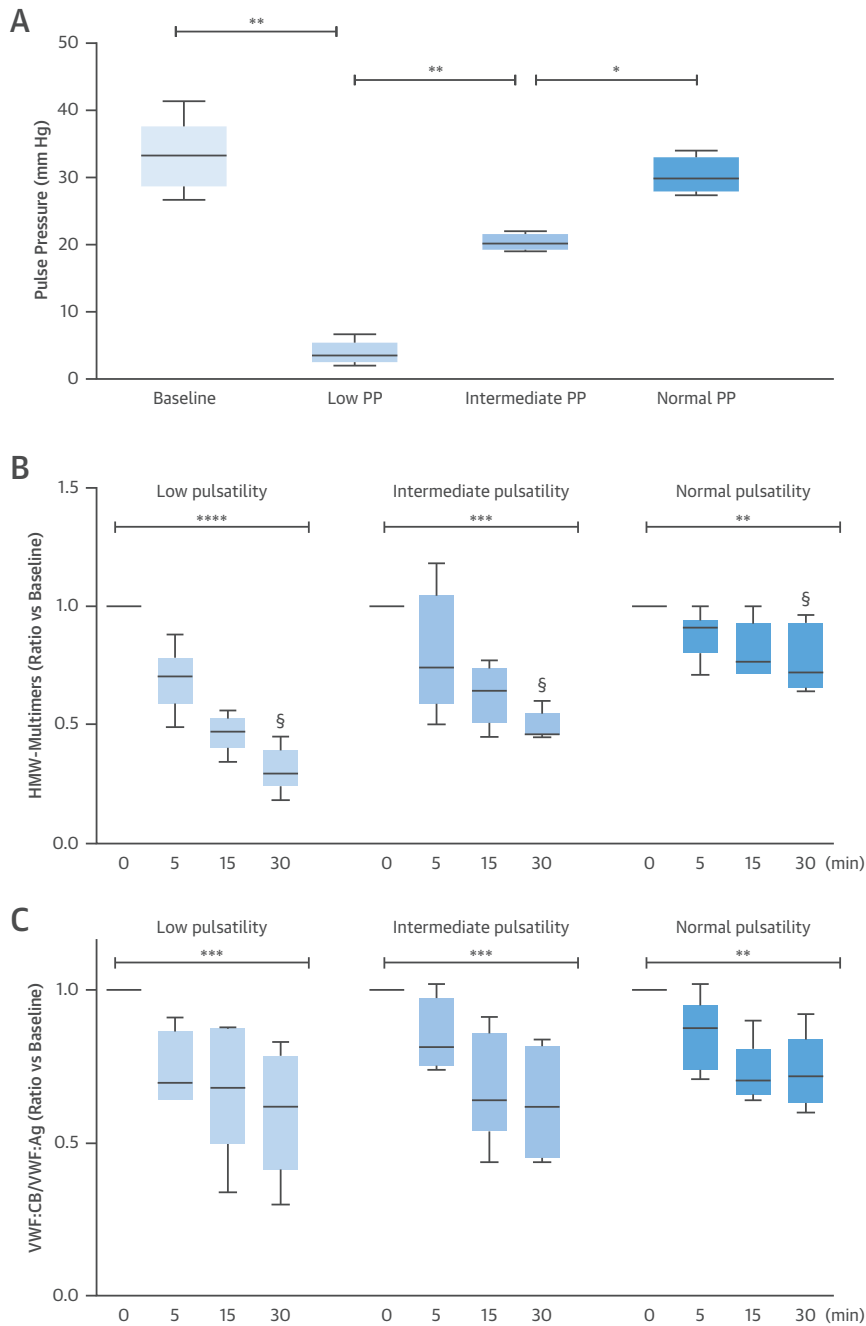
IN VITRO STUDY: VWF DEGRADATION INDUCED BY HIGH-SHEAR CF-MCS IN AN ENDOTHELIAL-FREE MOCK CIRCULATORY WITHOUT PULSATILITY (MODEL 1). A rapid time-dependent loss of HMW

multimers (>60% after 5 min and >90% after 30 min) was observed in both MCS-A and -B experiments (Figure 2A). The loss of HMW multimers coincided with a loss of collagen-binding activity (Figure 2B). Loss of HMW multimers and collagen-binding activity followed a similar time course in MCS-A and -B (*p* = 0.578 and *p* = 0.771 for HMW multimers and VWF:CB/VWF:Ag, respectively). This time-dependent degradation of VWF was inhibited when spiking EDTA before initiating the experiments with both devices (Online Figure 1).

DOSE-EFFECT OF PULSATILITY ON VWF PARAMETERS IN A SWINE MODEL (MODEL 2). The aim of this experiment was first to analyze the effect of MCS-A and -B on PP in 3 animal groups: 1 group with expected low pulsatility, 1 group with expected intermediate pulsatility, and 1 group in which placement of MCS-B was supposed to maintain normal pulsatility (Figure 3A, Online Figure 2). The baseline PP was 32 mm Hg (IQR: 26.9 to 37.6 mm Hg). In the low-pulsatility group, the implantation of the MCS-B inside the LV induced a drop of the PP (PP = 4 mm Hg [IQR: 2 to 6 mm Hg]; *p* < 0.01 vs. baseline). In the intermediate-pulsatility group, the implantation of the MCS-A inside the LV induced a mild decrease in PP (PP = 20 mm Hg [IQR: 19 to 22 mm Hg]; *p* < 0.01 vs. low and *p* < 0.05 vs. normal-pulsatility group). The placement of the MCS-B inside the aorta preserved a normal PP (PP = 26 mm Hg [IQR: 24 to 33 mm Hg]). This suggests that placement of the MCS influences changes in pulsatility upon changes in PP.

We next analyzed how MCS affected VWF parameters in each group (Figures 3B and 3C). A significant

FIGURE 3 Dose Effect of Pulsatility on VWF Parameters



(A) Changes of pulse pressure (PP) within the 3 groups of pulsatility: baseline (PP = 32 mm Hg [interquartile range (IQR): 26.9 to 37.6 mm Hg]; low-pulsatility group (PP = 4 mm Hg [IQR: 2 to 6 mm Hg]; ** $p < 0.01$ vs. baseline); intermediate-pulsatility group (PP = 20 mm Hg [IQR: 19 to 22 mm Hg]; ** $p < 0.01$ vs. low-pulsatility group); and normal-pulsatility group (PP = 26 mm Hg [IQR: 24 to 33 mm Hg]; * $p < 0.05$ vs. intermediate-pulsatility group). **(B)** A significant loss of HMW multimers was observed in the 3 conditions when compared with baseline (analysis of variance [ANOVA] $p < 0.01$). A significant effect of pulsatility on the dynamic of HMW-multimer loss was observed ($p < 0.0001$; 2-way ANOVA). *** $p < 0.001$; **** $p < 0.0001$. §At 30 min, HMW multimers were significantly lower under low pulsatility (0.30 [IQR: 0.24 to 0.39]) compared with intermediate (0.46 [IQR: 0.45 to 0.54]; $p < 0.05$) and normal pulsatility (0.72 [IQR: 0.75 to 0.93]; $p < 0.01$). This difference was also significant between intermediate and normal pulsatility ($p < 0.01$). **(C)** A significant decrease of VWF:CB/VWF:Ag was observed in the 3 conditions of pulsatility when compared with baseline (ANOVA $p < 0.01$). Abbreviations as in [Figure 2](#).

loss of HMW multimers was observed in each of the 3 conditions of pulsatility when compared with baseline values (ANOVA $p < 0.01$). However, the dynamics of HMW multimer loss was significantly dependent on the pulsatility regimen (low, intermediate, and normal; $p < 0.0001$; for the interaction term in the 2-way ANOVA with group and time as factors). As a result, at the end of the experiment, the HMW-multimer ratio was significantly lower in the low-pulsatility group (0.30 [IQR: 0.24 to 0.39]) compared with both the intermediate- (0.46 [IQR: 0.45 to 0.54]; $p < 0.05$) and normal-pulsatility groups (0.72 [IQR: 0.75 to 0.93]; $p < 0.01$). This difference was also significant between the intermediate- and normal-pulsatility groups ($p < 0.01$). Mirroring HMW-multimer ratio results, the same trend was observed with the VWF:CB/VWF:Ag ratio (Figure 3C). When combining all data points, a strong correlation was observed between arterial pulsatility and HMW-multimer ratio ($r = 0.73$; $p < 0.01$). Of note, no significant increase in LDH was observed during the time of the experiment (30 min), with no difference between the 2 devices (MCS-A or -B) in any of the locations (LV or aorta) (Online Figure 3).

CONSEQUENCES OF SEQUENTIAL CHANGES OF PULSATILITY ON VWF PARAMETERS IN A SWINE CROSS-OVER MODEL (MODEL 3). The aim of this experiment was to analyze the effect of MCS-B on changes in PP by placing it at various positions (LV or aorta) over time while using different speeds of rotation (Figure 4A). The baseline PP was 39 mm Hg [IQR: 32 to 46 mm Hg]. After initiating MCS-B support in the LV (phase 1), a drop in PP was observed (PP = 5.8 mm Hg [IQR: 2.9 to 10.8 mm Hg]; $p < 0.01$). PP returned to normal (PP = 28.5 mm Hg [IQR: 26 to 33 mm Hg]) when MCS-B was replaced to the aorta in the absence of rotation speed (phase 2). After restarting rotation speed in the aorta (phase 3, in which normal functioning of the LV ensures normal pulsatility), PP levels remained close to baseline values (PP = 30.6 mm Hg [IQR: 25.5 to 35.5 mm Hg]; $p = 0.92$ vs. baseline). Again, no changes in PP occurred when terminating rotation speed with the MCS-B being placed in the aorta (phase 4; PP = 35 mm Hg [IQR: 28 to 46 mm Hg]). Finally, reinstallation of MCS-B into the LV with full rotation speed (phase 5) once more resulted in a significant drop in PP (PP = 5 mm Hg [IQR: 2.7 to 7.7 mm Hg]; $p < 0.01$). Thus, this series of experiments demonstrates that in this model, PP can be significantly and easily manipulated by relocating the same device (MCS-B) from one position to another (LV vs. aorta and vice versa).

CHANGES IN VWF PARAMETERS. Changes in VWF parameters are shown in Figures 4B to 4D and Online Figures 4 and 5.

The first low-pulsatility phase (phase 1: MCS in LV-1) was associated with a rapid and significant loss of HMW multimers (0.74 [IQR: 0.58 to 0.88], 0.51 [IQR: 0.38 to 0.60], and 0.39 [IQR: 0.22 to 0.48] at 5, 15, and 30 min, respectively vs. 0.90 [IQR: 0.84 to 1.10] at baseline; ANOVA $p < 0.0001$). After stopping the pump for 60 min (phase 2: native heart only-1) and restoring a low shear and a normal pulsatility, a complete recovery of HMW-multimer ratio (at 1.0 [IQR: 0.89 to 1.26]) was obtained. During the normal PP phase (phase 3: MCS in aorta), a decrease of HMW-multimer ratio was also observed (0.87 [IQR: 0.69 to 1.04], 0.76 [IQR: 0.73 to 0.88], and 0.74 [IQR: 0.62 to 0.82] at 5, 15, and 30 min, respectively; ANOVA $p < 0.0001$). However, this effect was less pronounced when compared to the first low-pulsatility phase (HMW-multimer ratio = 0.74 [IQR: 0.62 to 0.82] at 120 min vs. 0.39 [IQR: 0.22 to 0.48] at 30 min; $p < 0.05$ for phases 3 and 1, respectively).

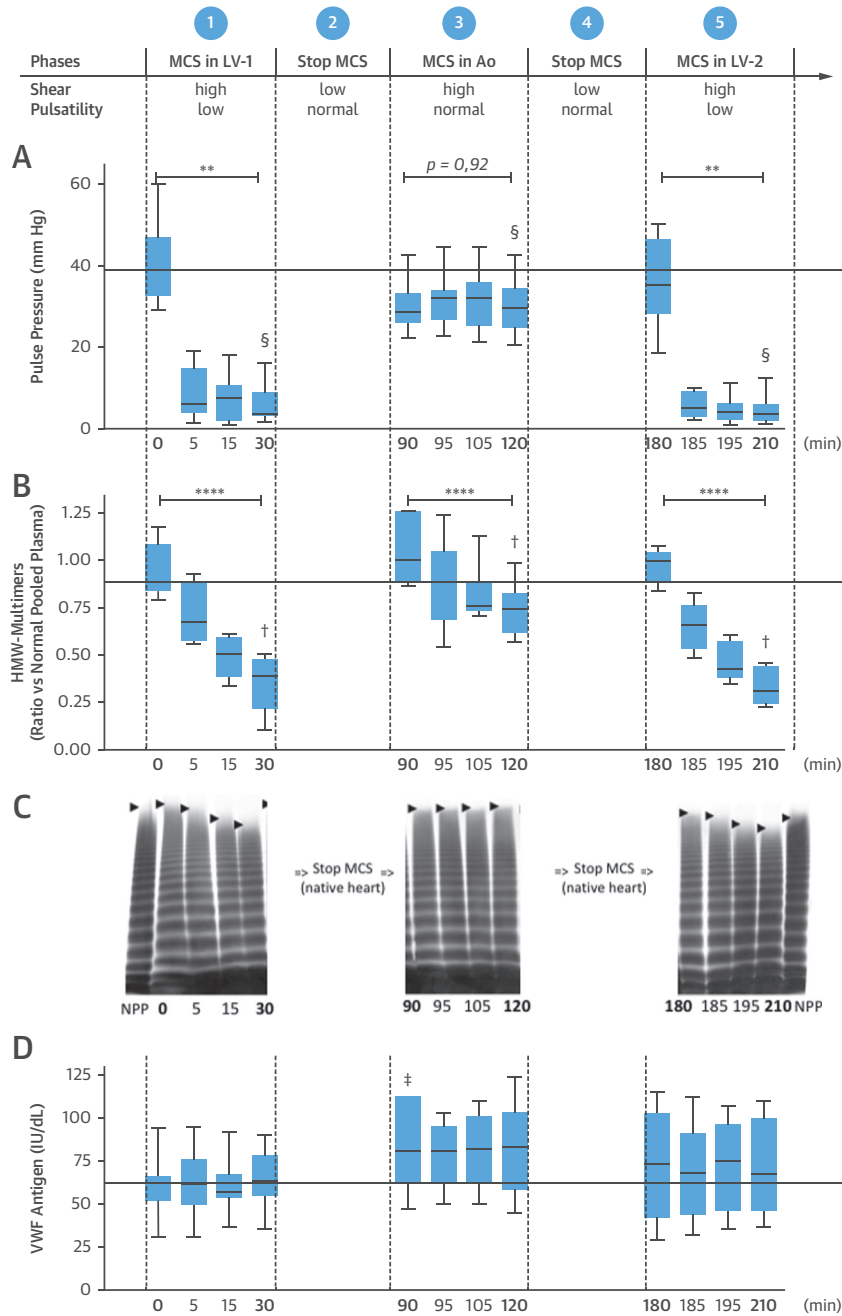
After stopping the pump for 60 min (phase 4: second phase of native heart only-2), a complete recovery of VWF was again observed (HMW-multimer ratio at 1.0 [IQR: 0.87 to 1.05]). In the second low-pulsatility phase (phase 5: MCS in LV-2), a rapid loss of HMW multimers similar to the first low-pulsatility phase was observed.

To elucidate whether the recovery of VWF multimers could originate from endothelial VWF release in response to pulsatility, the evolution of VWF:Ag levels was analyzed.

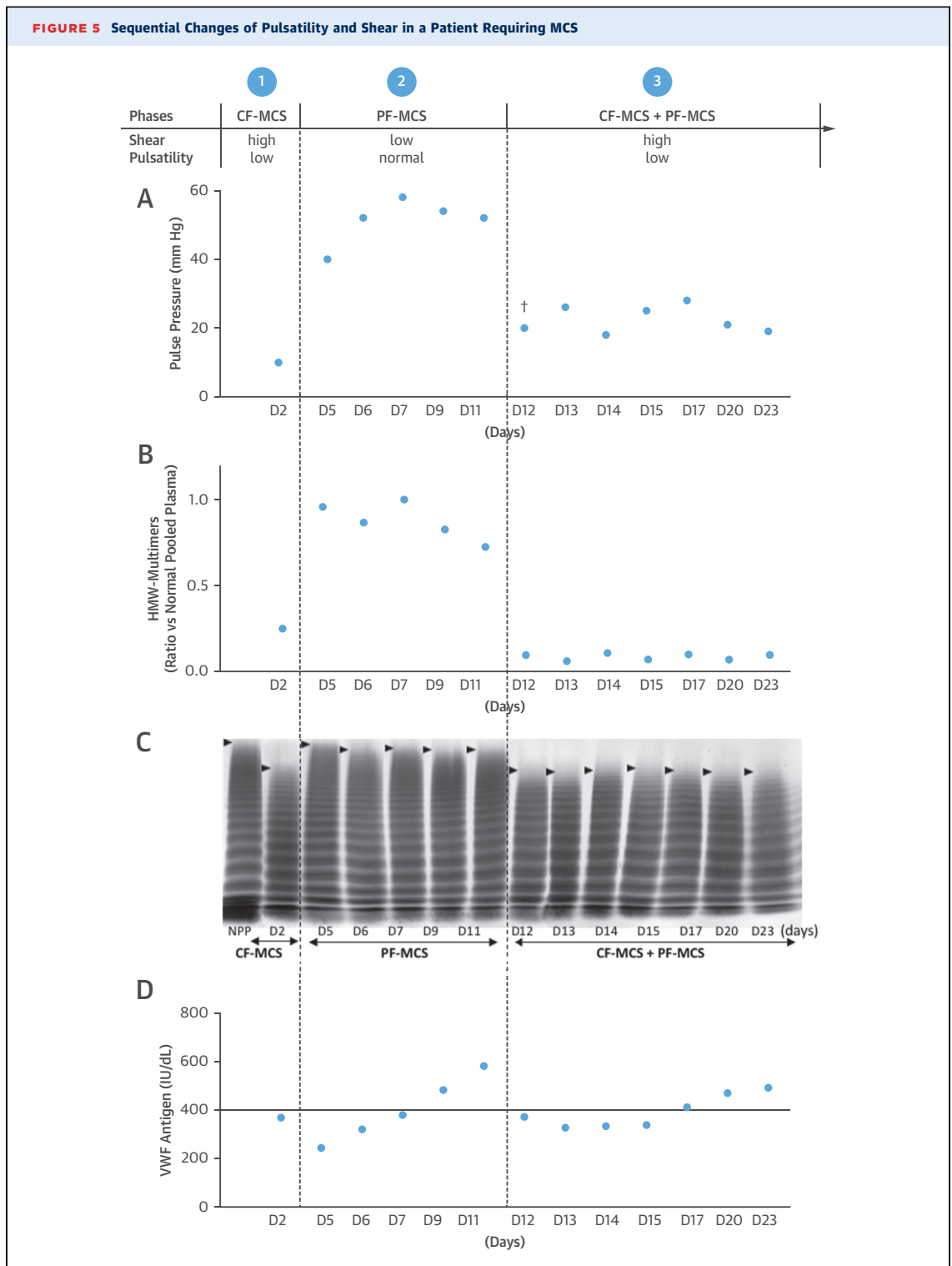
A raise of VWF:Ag was only observed after a sudden increase in PP (between phases 1 and 2) with an increase of 29% of the VWF:Ag level ($p = 0.03$). The increase in VWF:Ag in the phase 1 to 2 transition was accompanied by a concomitant increase in FVIIIc ($p = 0.03$) and Ang-2 levels ($p = 0.03$), suggesting the release of these 3 proteins from endothelial Weibel-Palade bodies (WPBs). No changes in levels of the VWF-cleaving protease ADAMTS13 were detected.

SEQUENTIAL CHANGES OF PULSATILITY AND SHEAR IN A PATIENT WITH CARDIOGENIC SHOCK REQUIRING MCS. Changes in PP during the different phases. Figure 5A shows the changes in PP during the different phases. The PP during the first phase of CF-MCS was very low (<10 mm Hg). In the second phase, after PF-MCS implantation occurred, a high increase of PP (51 mm Hg [IQR: 42.5 to 54 mm Hg]). Then, during the last phase of dual support (CF-MCS + PF-MCS), we observed a significant drop of

FIGURE 4 VWF Parameters in a Swine Cross-Over Model Associated With Sequential Changes of Pulsatility



(A) Baseline PP = 39 mm Hg (IQR: 32 to 46 mm Hg). Decrease during low-pulsatility phases (1 and 5): 5.8 mm Hg (IQR: 2.9 to 10.8 mm Hg; $p < 0.01$) and 5 mm Hg (IQR: 2.7 to 7.7 mm Hg; $p < 0.01$). PP in the normal range in native heart phases (2 and 4): 28.5 mm Hg (IQR: 26 to 33 mm Hg); 35 mm Hg (IQR: 28 to 46 mm Hg). There was no significant decrease in phase 3 (30.6 mm Hg [IQR: 25.5 to 35.5 mm Hg]; $p = 0.92$). §PP was reduced in the LV phases compared with the aortic phase ($p < 0.01$). **(B)** Phase 1: rapid loss of HMW multimers (0.74 [IQR: 0.58 to 0.88 mm Hg], 0.51 [IQR: 0.38 to 0.60 mm Hg], and 0.39 [IQR: 0.22 to 0.48 mm Hg] at 5, 15, and 30 min vs. 0.90 [IQR: 0.84 to 1.10 mm Hg] at baseline; ANOVA $p < 0.0001$). Recovery of HMW multimers in phases 2 and 4 at 1.0 (IQR: 0.89 to 1.26) and 1.0 (IQR: 0.87 to 1.05). Phase 3: decrease of HMW multimers: 0.87 (IQR: 0.69 to 1.04), 0.76 (IQR: 0.73 to 0.88), and 0.74 (IQR: 0.62 to 0.82) at 5, 15, and 30 min; ANOVA $p = 0.0001$. †Lower decrease of HMW multimers within normal pulsatility (phase 3) than within low pulsatility (phase 1): HMW multimers = 0.74 (IQR: 0.62 to 0.82) at 120 min versus 0.39 (IQR: 0.22 to 0.48) at 30 min. ** $p < 0.01$; **** $p < 0.0001$. **(C)** VWF multimeric profile. **(D)** Increase in VWF:Ag (+29%; $p = 0.03$) after PP increase between phases 1 (30 min) and 2 (at 120 min), † $p < 0.05$. Abbreviations as in [Figures 1 to 3](#).



PP (25 mm Hg [IQR: 20 to 30 mm Hg] vs. 51 mm Hg [IQR: 42.5 to 54 mm Hg], $p < 0.01$).

Changes in VWF parameters. Figures 5B to 5D and Online Figure 6 show the changes in VWF parameters. Under CF-MCS (high shear and low pulsatility), a marked decrease of both VWF:Act/VWF:Ag and HMW-multimer ratio (0.6 and 0.3, respectively) were observed. Three hours after implantation, the PF-MCS support provided a rapid restoration of functional VWF with a complete normalization of both VWF:Act/VWF:Ag and HMW multimers (Online Figure 3) and a parallel increase in VWFpp/VWF:Ag ratio from 1.0 to 2.2. During the 7 days of PF-MCS (low shear and normal pulsatility), VWF:Act/VWF:Ag and HMW multimers remained into the normal range (VWF:Act/VWF:Ag ratio = 1.11 [IQR: 1.04 to 1.22], HMW-multimers ratio = 0.87 [IQR: 0.78 to 0.98]). The hemodynamic and respiratory failure during PF-MCS required the addition of CF-MCS to PF-MCS (phase 3: high shear and low pulsatility). Upon initiation of PF-MCS, we noted a recurrence of a functional VWF defect that remained stable over time (VWF:Act/VWF:Ag ratio = 0.51 [IQR: 0.47 to 0.55], HMW-multimers ratio = 0.10 [IQR: 0.07 to 0.10]). Under single PF-MCS support, a continuous increase in VWF:Ag occurred from 295 IU/dl just after implantation to 581 IU/dl after completing 7 days of PF-MCS. After implantation of additional CF to PF-MCS, VWF:Ag dropped to 369 IU/dl within the first day of dual support. Then, a progressive and milder rise of VWF:Ag was observed from 326 IU/dl in the second day to 491 IU/dl after completing 11 days of dual support. A progressive rise of VWFpp was noted under PF-MCS from 385 to 660 IU/dl between day 6 and day 12. After the addition of CF-MCS to PF-MCS, a progressive decrease of VWFpp occurred, from 660 IU/dl at day 13 to 363 IU/dl at day 23.

DISCUSSION

In the present study, we investigated for the first time the potential relationship between arterial pulsatility under CF-MCS and VWF physiology. Using a specifically developed sequential swine model, we demonstrated that the degree of pulsatility is a key modulator of circulating VWF in CF-MCS. These results were further confirmed in the clinical scenario of a patient with cardiogenic shock supported sequentially with pulsatile and CF devices.

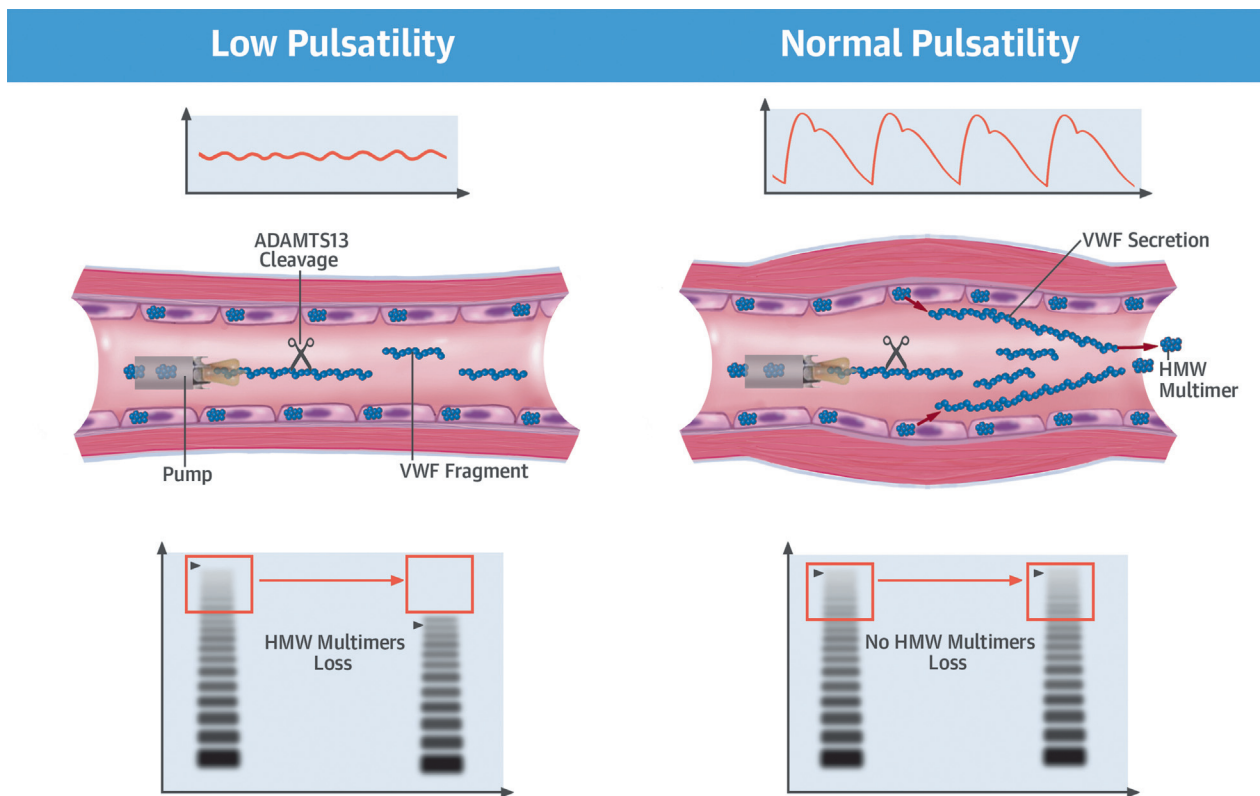
LOSS OF HMW MULTIMERS WITH CF-MCS IN THE ABSENCE OF VASCULAR BED. The VWF degradation signature of 2 MCS devices generating distinct blood flow levels was assessed in vitro in a mock circulatory loop. This loop allowed for the assessment of the effect of the device geometry and shear characteristics

on VWF degradation in the absence of endothelium response. VWF degradation was prevented by EDTA validating the enzymatic nature of degradation under this type of support. As expected and previously reported by our group (4), both devices were generating very similar high shear and were associated with a very fast and equivalent loss of HMW multimers. We took advantage of these similar characteristics to design the swine series of experiments.

PULSATILITY MODULATES THE HMW MULTIMERS LOSS UNDER STEADY-STATE OR DURING SEQUENTIAL CHANGES IN FLOW REGIMEN: RESULTS FROM A CROSS-OVER SWINE MODEL OF CF-MCS. We first investigated the effect of 3 “steady-state” pulsatility conditions, all obtained at similar high shear, on VWF multimerization. Three distinct levels of pulsatility—low, intermediate, or normal—could be obtained by the implantation of 1 of the 2 devices, MCS-A or -B, in either the LV or the aorta of our swine model. These 3 conditions were achieved with the same high level of shear as demonstrated by the results of the in vitro experiments and by the measurements of LDH in vivo disclosing a similar increase of LDH in the 3 conditions. Loss of HMW multimers was faster and more pronounced in animals supported in conditions of low pulsatility compared with animals supported with intermediate or normal pulsatility. This series of experiments demonstrated that the level of arterial pulsatility is a strong modulator of VWF degradation.

We next investigated whether sequential and dynamic changes of pulsatility could modulate VWF multimerization over time. This was done by designing a swine cross-over model using 1 given MCS at 2 different locations, LV or aorta, in the same animal in a sequential fashion. As in the previous set of experiments, the HMW-multimer defect was more pronounced in conditions of low pulsatility than in conditions of preserved pulsatility. This cross-over model confirms the occurrence of dynamic variations of the VWF multimeric profile in response to acute changes in pulsatility levels. It further demonstrates that changes in pulsatility regimen can be pivotal to modulate VWF multimerization in high shear conditions.

ENDOTHELIUM AS A SENSOR OF PULSATILE FLOW. Our findings suggest that the link between the acute change of pulsatility and the restoration of the HMW multimer profile originates from an acute release of VWF, stored in the WPBs of the endothelial cells of the vascular wall. The acute release of VWF was demonstrated by the significant increase in VWF:Ag observed in the swine cross-over model as soon as the vascular endothelium is exposed to a high pulsatility-flow regime.

CENTRAL ILLUSTRATION Pulsatility as a Modulator of Circulating von Willebrand Factor

Vincent, F. *et al.* *J Am Coll Cardiol.* 2018;**71**(19):2106-18.

In case of low pulsatility (**left**) the high shear conditions induce a proteolytic cleavage of von Willebrand factor (VWF) and a loss of high molecular weight (HMW) multimers, which is not compensated by the release of new VWF. In the case of normal pulsatility (**right**), the change in pulse pressure induces a release of new VWF from Weibel Palade bodies (WPBs), which preserves HMW multimers. ADAMTS13 = A disintegrin and metalloprotease with thrombospondin type 1 repeats-13.

Because WPBs store other bioactive compounds, such as FVIIIc and Ang-2, the concomitant increase of VWF:Ag, FVIIIc, and Ang-2 upon high-pulsatility conditions is highly suggestive of an acute release of new VWF multimers from WPBs (**Central Illustration**).

These results were further confirmed in a patient. After the implantation of PF-MCS, a rise in VWFpp and in VWF:Ag was observed, suggesting a release from WPBs. The addition of CF-MCS and the subsequent nonpulsatile flow pattern was associated with a decrease in VWF:Ag and the reappearance of the VWF defect.

Numerous physiological functions of endothelial cells are directly affected by physical changes in blood flow. *In vitro*, an increase in the arterial luminal pressure induces an acute release of VWF from endothelial WPBs (15). Exposition of endothelial cells to laminar flow of varying shear-stress magnitude has been shown to modulate the VWF release (16).

In vivo, CF-MCS and aortic stenosis are 2 clinical conditions associated with a VWF HMW-multimer defect and a reduced PP. We recently reported a nearly immediate recovery of the HMW-multimer defect upon the acute reversion of aortic stenosis (associated with recovery of normal PP) in a rabbit model and in patients undergoing transcatheter or surgical aortic valve implantation (7,17,18). As in the present situation, the early correction of VWF defect after transcatheter aortic valve implantation was associated with a simultaneous increase in VWFpp, demonstrating the release of new HMW multimers from the endothelial cells (7).

CLINICAL RELEVANCE OF VASCULAR BED RESPONSE TO RESTORATION OF PULSATILITY TO PREVENT THE VWF DEFECT UNDER CF-MCS. Our findings suggest that the VWF defect associated with CF-MCS devices could be dependent not only on the

pump geometry itself (shear stress) but also on the nature of the flow (pulsatile or not) delivered by the combination of the pump and the LV.

In patients with CF devices, the pulsatility is related both to the residual LV function and the flow capacity of the pump (11,19). Under long-term support, the magnitude of the protective effect of pulsatility on VWF defect could therefore depend on the LV residual function. The importance of the level of pulsatility under CF pumps was first established by Wever-Pinzon et al. (8) who reported less bleeding events in HeartMate-II (Thoratec, Pleasanton, California) recipients with a high pulsatility index than in patients with a low pulsatility index. However, no VWF analysis was performed in this study.

In line with these findings, it has been described that a CF-MCS with intrinsic pulsatility features seems to prevent VWF deficiency (20) and improve hemocompatibility, without evidence establishing a link with the different flow pattern or to the different shear-stress condition of this centrifugal flow pump (9,12).

TOWARD A BETTER PREVENTION OF ACQUIRED VWF DEFECT UNDER CF-MCS. According to our findings, a promising approach to reduce the intensity of HMW-multimer defect under CF-MCS could be to restore a high degree of residual pulsatility. Thus, flow-modulation algorithms allowing an increase of pulsatility are currently under evaluation to be implemented in CF devices (21,22). Overall, the next generation of devices will need an optimal balance between low-shear and high-pulsatility properties to reduce the VWF defect and avoid bleeding complications.

STUDY LIMITATIONS. Although most of our findings were obtained in a swine model of short-term MCS with normal cardiovascular function, the observation made in a patient with cardiogenic shock over the course of several days suggests a strong clinical relevance of our results. This observation further demonstrates the potential of PF-MCS to preserve VWF from excessive degradation (23).

Further research is needed, however, to extend the benefit of pulsatility to long-term MCS. In addition, whether our data could translate to next generation of CF-MCS with speed modulation algorithms providing pulsatile flow variations is unknown.

CONCLUSIONS

The present study demonstrated that the VWF defect under CF-MCS reflects the balance between

degradation induced by high shear stress and the endothelial release triggered by the pulsatile flow.

The role of pulsatility in the direct modulation of VWF defect could explain the relationship between low residual arterial pulsatility and high bleeding rate in patients receiving MCS with CF devices (8). These data support the concept of developing new MCS devices with pulsatility properties to reduce the bleeding burden and improve the safety of patients.

ACKNOWLEDGMENTS The authors thank the technicians from the National Reference Center for von Willebrand Disease, Lille, and from the hematology department of Pitié Salpêtrière and Georges Pompidou hospital for their help. The authors are also very grateful to the animal laboratory staff of the University and Hospital Department for Experimental Research of Lille 2, headed by Thomas Hubert (Martin Fourdrinier, Arnold Dive, and Michel Potier), and to César Belin and Cassandre Vincent for their technical support during the experiments. Finally, the authors also thank the nursing staff of the cardiac intensive care unit and surgery departments.

ADDRESS FOR CORRESPONDENCE: Dr. Eric Van Belle, Department of Cardiology, Institut Cœur Poumon, Centre Hospitalier Universitaire de Lille, Boulevard du Pr. Jules Leclercq, 59037 Lille Cedex, France. E-mail: ericvanbelle@aol.com. OR Dr. Sophie Susen, Centre Hospitalier Universitaire de Lille, Département d'hématologie et transfusion, Boulevard du Pr. Jules Leclercq, 59037 Lille Cedex, France. E-mail: sophiesusen@aol.com.

PERSPECTIVES

COMPETENCY IN PATIENT CARE AND PROCEDURAL

SKILLS: Bleeding is the most frequent adverse event during CF-MCS. The acquired VWF defect observed during support with these devices has been attributed mainly to high shear forces, but low arterial pulsatility also contributes to the risk of bleeding.

TRANSLATIONAL OUTLOOK: Further research is needed to determine whether restoration of pulsatile arterial flow could mitigate the acquired VWF defect, reduce bleeding, and improve clinical outcomes for patients requiring MCS.

REFERENCES

1. Katz JN, Adamson RM, John R, et al. Safety of reduced anti-thrombotic strategies in HeartMate II patients: a one-year analysis of the US-TRACE Study. *J Heart Lung Transplant* 2015;34:1542-8.
2. Crow S, John R, Boyle A, et al. Gastrointestinal bleeding rates in recipients of nonpulsatile and pulsatile left ventricular assist devices. *J Thorac Cardiovasc Surg* 2009;137:208-15.
3. Starling RC, Naka Y, Boyle AJ, et al. Results of the Post-U.S. Food and Drug Administration-approval study with a continuous flow left ventricular assist device as a bridge to heart transplantation. *J Am Coll Cardiol* 2011;57:1890-8.
4. Susen S, Rauch A, Van Belle E, Vincentelli A, Lenting PJ. Circulatory support devices: fundamental aspects and clinical management of bleeding and thrombosis. *J Thromb Haemost* 2015;13:1757-67.
5. Meyer AL, Malehsa D, Budde U, Bara C, Haverich A, Strueber M. Acquired von Willebrand Syndrome in patients with a centrifugal or axial continuous flow left ventricular assist device. *J Am Coll Cardiol HF* 2014;2:141-5.
6. Uriel N, Pak S-W, Jorde UP, et al. Acquired von Willebrand Syndrome after continuous-flow mechanical device support contributes to a high prevalence of bleeding during long-term support and at the time of transplantation. *J Am Coll Cardiol* 2010;56:1207-13.
7. Van Belle E, Rauch A, Vincentelli A, et al. Von Willebrand factor as a biological sensor of blood flow to monitor percutaneous aortic valve interventions. *Circ Res* 2015;116:1193-201.
8. Wever-Pinzon O, Selzman CH, Drakos SG, et al. Pulsatility and the risk of nonsurgical bleeding in patients supported with the continuous-flow left ventricular assist device HeartMate II. *Circ Heart Fail* 2013;6:517-26.
9. Muthiah K, Connor D, Ly K, et al. Longitudinal changes in hemostatic parameters and reduced pulsatility contribute to non-surgical bleeding in patients with centrifugal continuous-flow left ventricular assist devices. *J Heart Lung Transplant* 2016;35:743-51.
10. Jabbar HR, Abbas A, Ahmed M, et al. The incidence, predictors and outcomes of gastrointestinal bleeding in patients with left ventricular assist device (LVAD). *Dig Dis Sci* 2015;60:3697-706.
11. Patel SR, Jorde UP. Creating adequate pulsatility with a continuous flow left ventricular assist device: just do it! *Curr Opin Cardiol* 2016;31:329-36.
12. Uriel N, Colombo PC, Cleveland JC, et al. Hemocompatibility-related outcomes in the MOMENTUM 3 trial at 6 months. *Circulation* 2017;135:2003-12.
13. Carpentier A, Latrémouille C, Cholley B, et al. First clinical use of a bioprosthetic total artificial heart: report of two cases. *Lancet* 2015;386:1556-63.
14. Banfi C, Pozzi M, Siegenthaler N, et al. Venovenous extracorporeal membrane oxygenation: cannulation techniques. *J Thorac Dis* 2016;8:3762-73.
15. Xiong Y, Hu Z, Han X, et al. Hypertensive stretch regulates endothelial exocytosis of Weibel-Palade bodies through VEGF receptor 2 signaling pathways. *Cell Res* 2013;23:820-34.
16. Galbusera M, Zoja C, Donadelli R, et al. Fluid shear stress modulates Von Willebrand factor release from human vascular endothelium. *Blood* 1997;90:1558-64.
17. Vincentelli A, Susen S, Le Tourneau T, et al. Acquired von Willebrand syndrome in aortic stenosis. *N Engl J Med* 2003;349:343-9.
18. Van Belle E, Rauch A, Vincent F, et al. Von Willebrand factor multimers during transcatheter aortic-valve replacement. *N Engl J Med* 2016;375:335-44.
19. Soucy KG, Koenig SC, Giridharan GA, Sobieski MA, Slaughter MS. Defining pulsatility during continuous-flow ventricular assist device support. *J Heart Lung Transplant* 2013;32:581-7.
20. Netuka I, Kvasnička T, Kvasnička J, et al. Evaluation of von Willebrand factor with a fully magnetically levitated centrifugal continuous-flow left ventricular assist device in advanced heart failure. *J Heart Lung Transplant* 2016;35:860-7.
21. Soucy KG, Giridharan GA, Choi Y, et al. Rotary pump speed modulation for generating pulsatile flow and phasic left ventricular volume unloading in a bovine model of chronic ischemic heart failure. *J Heart Lung Transplant* 2015;34:122-31.
22. Mehra MR, Naka Y, Uriel N, et al. A fully magnetically levitated circulatory pump for advanced heart failure. *N Engl J Med* 2017;376:440-50.
23. Smadja DM, Susen S, Rauch A, et al. Carmat bioprosthetic total artificial heart is associated with an early hemostatic recovery and no acquired von Willebrand syndrome in calves. *J Cardiothorac Vasc Anesth* 2017;31:1595-602.

KEY WORDS arterial pulsatility, bleeding, blood flow, extracorporeal membrane oxygenation, mechanical circulatory support, von Willebrand factor

APPENDIX For an expanded Methods section as well as supplemental figures and a table, please see the online version of this paper.

ORIGINAL ARTICLE

Von Willebrand Factor Multimers during Transcatheter Aortic-Valve Replacement

E. Van Belle, A. Rauch, F. Vincent, E. Robin, M. Kibler, J. Labreuche, E. Jeanpierre, M. Levade, C. Hurt, N. Rousse, J.-B. Dally, N. Debry, J. Dallongeville, A. Vincentelli, C. Delhaye, J.-L. Auffray, F. Juthier, G. Schurtz, G. Lemesle, T. Caspar, O. Morel, N. Dumonteil, A. Duhamel, C. Paris, A. Dupont-Prado, P. Legendre, F. Mouquet, B. Marchant, S. Hermoire, D. Corseaux, K. Moussa, A. Manchuelle, J.-J. Bauchart, V. Loobuyck, C. Caron, C. Zawadzki, F. Leroy, J.-C. Bodart, B. Staels, J. Goudemand, P.J. Lenting, and S. Susen

ABSTRACT

BACKGROUND

Postprocedural aortic regurgitation occurs in 10 to 20% of patients undergoing transcatheter aortic-valve replacement (TAVR) for aortic stenosis. We hypothesized that assessment of defects in high-molecular-weight (HMW) multimers of von Willebrand factor or point-of-care assessment of hemostasis could be used to monitor aortic regurgitation during TAVR.

METHODS

We enrolled 183 patients undergoing TAVR. Patients with aortic regurgitation after the initial implantation, as identified by means of transesophageal echocardiography, underwent additional balloon dilation to correct aortic regurgitation. HMW multimers and the closure time with adenosine diphosphate (CT-ADP), a point-of-care measure of hemostasis, were assessed at baseline and 5 minutes after each step of the procedure. Mortality was evaluated at 1 year. A second cohort (201 patients) was studied to validate the use of CT-ADP in order to identify patients with aortic regurgitation.

RESULTS

After the initial implantation, HMW multimers normalized in patients without aortic regurgitation (137 patients). Among the 46 patients with aortic regurgitation, normalization occurred in 20 patients in whom additional balloon dilation was successful but did not occur in the 26 patients with persistent aortic regurgitation. A similar sequence of changes was observed with CT-ADP. A CT-ADP value of more than 180 seconds had sensitivity, specificity, and negative predictive value of 92.3%, 92.4%, and 98.6%, respectively, for aortic regurgitation, with similar results in the validation cohort. Multivariable analyses showed that the values for HMW multimers and CT-ADP at the end of TAVR were each associated with mortality at 1 year.

CONCLUSIONS

The presence of HMW-multimer defects and a high value for a point-of-care hemostatic test, the CT-ADP, were each predictive of the presence of aortic regurgitation after TAVR and were associated with higher mortality 1 year after the procedure. (Funded by Lille 2 University and others; ClinicalTrials.gov number, NCT02628509.)

The authors' full names, academic degrees, and affiliations are listed in the Appendix. Address reprint requests to Dr. Susen at Centre de Biologie Pathologie, Centre Hospitalier Regional, 59037 Lille CEDEX, France, or at sophiesusen@aol.com.

Drs. Van Belle and Rauch contributed equally to this article.

N Engl J Med 2016;375:335-44.

DOI: 10.1056/NEJMoa1505643

Copyright © 2016 Massachusetts Medical Society.

POSTPROCEDURAL AORTIC REGURGITATION, usually due to paravalvular leak, occurs in 10 to 20% of patients with aortic stenosis who undergo transcatheter aortic-valve replacement (TAVR).^{1,3} Patients with aortic regurgitation that is more than mild after TAVR have poorer outcomes than those without aortic regurgitation, including increased rates of rehospitalization, death from cardiac causes, and death from any cause at 1 year.⁴ Ideally, aortic regurgitation after TAVR should be detected at the time of the procedure, because correction maneuvers can be undertaken immediately. However, despite the combined use of angiography, echocardiography, and hemodynamic evaluation, it is very difficult to identify and grade aortic regurgitation accurately before the patient leaves the catheterization laboratory. There is therefore an unmet clinical need for a quick and reliable screening method.

Previous studies have shown that a loss of high-molecular-weight (HMW) multimers of von Willebrand factor, hereafter referred to as HMW-multimer defects, is observed in patients with clinically significant aortic stenosis⁵ or valvular regurgitation⁶ and is corrected after surgical valve replacement⁵ (see animation, available with the full text of this article at NEJM.org). We recently reported that HMW-multimer defects resolve within minutes during TAVR but not after balloon valvuloplasty procedures.⁷

The Platelet Function Analyzer 100 (PFA-100, Siemens Healthcare Diagnostics) is a testing device for the evaluation of hemostasis. The device aspirates blood from a sample into a test cartridge containing a membrane coated with collagen and adenosine diphosphate (ADP). Platelet aggregation occludes an aperture in the membrane; the time necessary for aperture occlusion is termed the closure time with ADP (CT-ADP). The CT-ADP, as assessed with the use of the PFA-100, is highly sensitive to HMW-multimer defects^{5,7-10} and can be used in point-of-care testing. We evaluated point-of-care CT-ADP to identify aortic regurgitation occurring after TAVR.

METHODS

STUDY DESIGN, OVERSIGHT, AND SUPPORT

The study was designed by the first and last authors, with approval from the ethics committee at each participating institution. It was supported by Lille 2 University and Lille University Hospi-

tal. No external funding was obtained to support the study. All devices and consumable items for this research were purchased at full market price. All authors attest to the completeness and accuracy of the data and the analyses. All patients in the primary and validation cohorts provided written informed consent before enrollment.

PRIMARY STUDY COHORT

The primary cohort consisted of patients at Lille University Hospital with aortic stenosis who were undergoing implantation of the SAPIEN XT valve (Edwards Lifesciences) through femoral arterial access. Participation included clinical data collection, serial blood sampling during the procedure, and follow-up. Transthoracic echocardiography (TTE) and multidetector-row computed tomography (CT)^{11,12} were performed in all patients before the procedure (see the Methods section in the Supplementary Appendix, available at NEJM.org).

TAVR PROCEDURE

Technical aspects of transfemoral TAVR with the SAPIEN XT valve have been reported previously.^{1,2} To facilitate transesophageal echocardiography (TEE) monitoring, procedures were conducted while the patients were under general anesthesia. TEE was used to assess valve function at baseline and to quantify the severity of paravalvular aortic regurgitation approximately 5 minutes after implantation was completed (time T1) (Fig. 1). Paravalvular aortic regurgitation that was more than mild was defined as a circumferential extent of regurgitation that was greater than 10%.¹³ If paravalvular aortic regurgitation was detected after valve implantation, additional dilation was performed to attempt to eliminate or reduce the regurgitant leak or a second valve was implanted. TEE was repeated after additional dilation or implantation of a second valve (time T2) if a corrective procedure was performed, or approximately 15 minutes after valve implantation if no corrective procedure was performed. TEE was repeated again at the end of the entire procedure (time T3).

All patients received aspirin before the procedure, with ongoing aspirin therapy after the procedure. Clopidogrel was not administered unless the patient was already receiving long-term clopidogrel treatment. No clopidogrel loading was performed.



An animation showing VWF synthesis is available at NEJM.org

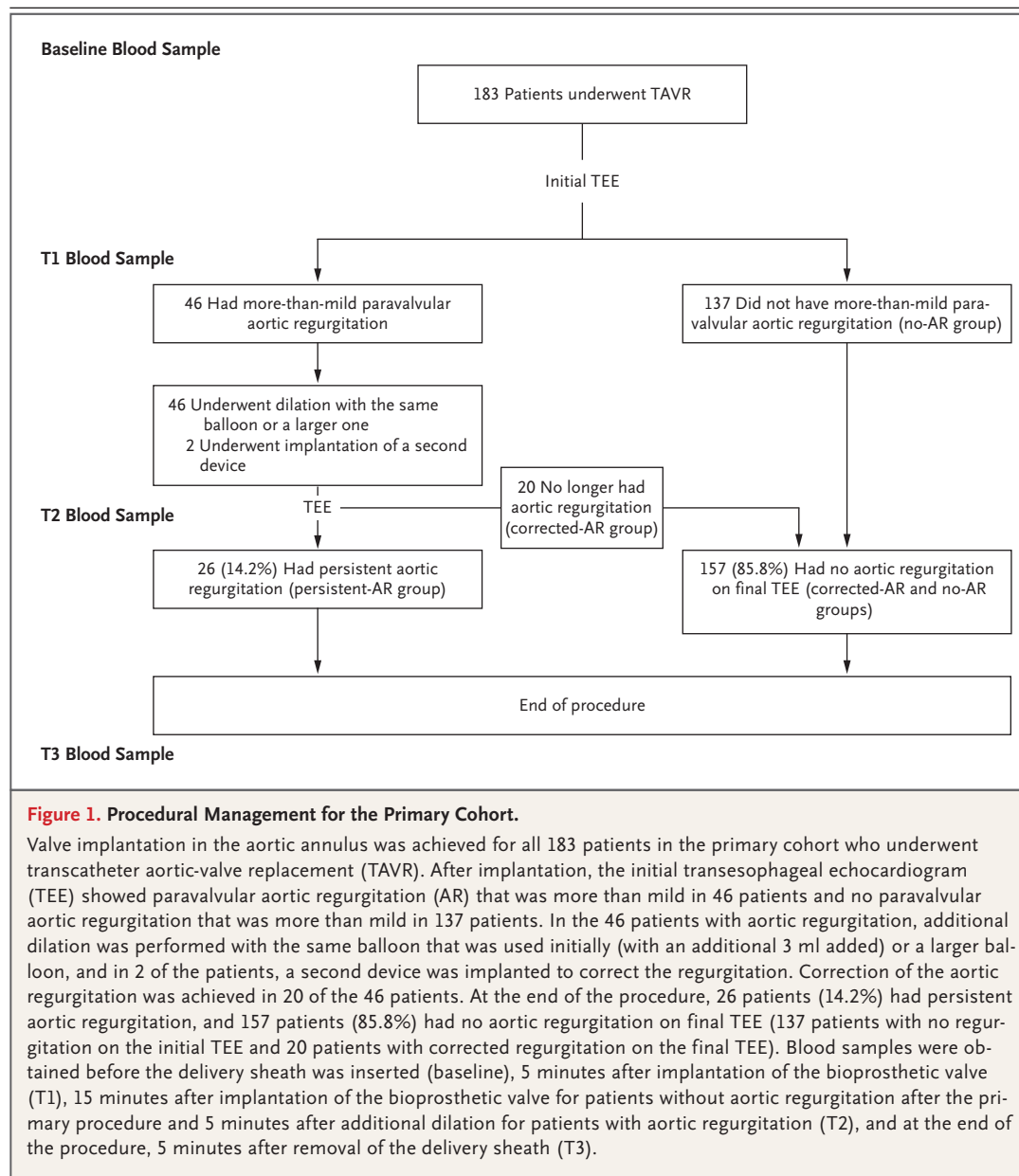


Figure 1. Procedural Management for the Primary Cohort.

Valve implantation in the aortic annulus was achieved for all 183 patients in the primary cohort who underwent transcatheter aortic-valve replacement (TAVR). After implantation, the initial transesophageal echocardiogram (TEE) showed paravalvular aortic regurgitation (AR) that was more than mild in 46 patients and no paravalvular aortic regurgitation that was more than mild in 137 patients. In the 46 patients with aortic regurgitation, additional dilation was performed with the same balloon that was used initially (with an additional 3 ml added) or a larger balloon, and in 2 of the patients, a second device was implanted to correct the regurgitation. Correction of the aortic regurgitation was achieved in 20 of the 46 patients. At the end of the procedure, 26 patients (14.2%) had persistent aortic regurgitation, and 157 patients (85.8%) had no aortic regurgitation on final TEE (137 patients with no regurgitation on the initial TEE and 20 patients with corrected regurgitation on the final TEE). Blood samples were obtained before the delivery sheath was inserted (baseline), 5 minutes after implantation of the bioprosthetic valve (T1), 15 minutes after implantation of the bioprosthetic valve for patients without aortic regurgitation after the primary procedure and 5 minutes after additional dilation for patients with aortic regurgitation (T2), and at the end of the procedure, 5 minutes after removal of the delivery sheath (T3).

HMW-MULTIMER AND CT-ADP ANALYSIS

Blood was obtained through contralateral femoral arterial access for use in three different quantitative measures of von Willebrand factor function at four time points (see the Methods section in the Supplementary Appendix). These quantitative measures included the HMW-multimer ratio (a measure of the amount of the largest multimers in the sample as compared with the amount in normal pooled human plasma) and the ratio of von Willebrand factor collagen-binding activity (a measure of the binding of von

Willebrand factor to collagen, which is a function of the quantity of HMW multimers) to von Willebrand factor antigen (a measure of the quantity of von Willebrand factor, regardless of the size of the multimers). In addition, the CT-ADP assay was performed with the use of the PFA-100. Samples were collected before valve implantation (baseline) and at times T1, T2, and T3 (Fig. 1). Samples obtained at times T1 and T2 were collected after TEE confirmation that no central aortic regurgitation was induced by the delivery wire.

CLINICAL FOLLOW-UP

Clinical follow-up data, including stroke during the first 30 days after TAVR and vital status at 1 year, were obtained for all patients. Events were assessed according to the Valve Academic Research Consortium 2 (VARC-2) classification.¹³ The primary outcome was overall mortality at 1 year.

VALIDATION COHORT

A second patient cohort was studied to validate the threshold value on the CT-ADP test for identifying patients with aortic regurgitation at the end of TAVR. Patients in the validation cohort underwent transfemoral valve implantation at Lille University Hospital, Strasbourg University Hospital, or Toulouse University Hospital. Procedural management and blood testing are described in detail in the Methods section in the Supplementary Appendix.

STATISTICAL ANALYSIS

In the primary cohort and the validation cohort, three subgroups of patients were identified on the basis of the TEE findings (Fig. 1). These subgroups consisted of patients who did not have aortic regurgitation that was more than mild after valve implantation (the no-regurgitation group), patients who had more than mild aortic regurgitation after valve implantation but no aortic regurgitation after additional dilation or a second valve implantation (the corrected-regurgitation group), and patients who had more than mild aortic regurgitation that persisted after additional dilation or a second implantation (the persistent-regurgitation group). Analysis of variance for repeated measures was used to compare the changes in the HMW-multimer ratio and in the CT-ADP among these three groups. Multivariable linear regression was used to study the relationship between the HMW-multimer ratio or the CT-ADP at final evaluation and the presence of aortic regurgitation on TEE, adjusted for age, sex, trans-aortic gradient, clopidogrel treatment (yes or no), and mitral regurgitation at baseline (yes or no).

We used receiver-operating-characteristic (ROC) curves to determine whether the HMW-multimer ratio and the CT-ADP could be used to identify patients with aortic regurgitation on TEE. The area under the ROC curve (AUC) was calculated, and the threshold that was optimal (in terms of sensitivity and specificity) in the primary study co-

hort was determined on the basis of the Youden Index that maximizes the sum of sensitivity and specificity. External validation of CT-ADP for the detection of aortic regurgitation was performed in the validation cohort.

We used Kaplan–Meier analysis to estimate the risk of death at 1 year according to the presence or absence of aortic regurgitation on TEE, the optimal threshold of the HMW-multimer ratio, and the optimal threshold of CT-ADP. Cox proportional-hazards models were used to calculate hazard ratios for death. Statistical analyses were performed with SAS software, version 9.1 (SAS Institute). A P value of less than 0.05 (two-sided) was considered to indicate statistical significance. Further details of the statistical analyses are provided in the Methods section in the Supplementary Appendix.

RESULTS**TAVR IN THE PRIMARY STUDY COHORT**

A total of 183 patients undergoing TAVR were enrolled in the primary study cohort between August 2012 and April 2014. Baseline characteristics of the patients are presented in Table 1. After implantation, TEE revealed the presence of paravalvular aortic regurgitation that was more than mild in 46 patients at time T1 (Fig. 1). Correction of the aortic regurgitation by additional dilation or a second implantation was achieved in 20 of the 46 patients, leaving 26 patients (14.2%) with aortic regurgitation at the end of the procedure.

ASSOCIATION OF HMW-MULTIMER RATIO AND CT-ADP WITH AORTIC REGURGITATION

Among the 137 patients in the no-regurgitation group, the HMW-multimer ratio increased from a mean (\pm SD) value of 0.62 ± 0.19 at baseline to 0.91 ± 0.21 at T1 and 1.09 ± 0.21 at T2 (a 76% relative increase from baseline to T2) (Fig. 2A). In the corrected-regurgitation group (20 patients), the HMW-multimer ratio did not change markedly from baseline (0.61 ± 0.19) to T1 (0.67 ± 0.11) but increased after the corrective procedure to 1.07 ± 0.09 at T2 (a 60% relative increase from T1). In the persistent-regurgitation group (26 patients), the HMW-multimer ratio remained relatively low throughout the procedure (0.58 ± 0.17 at baseline and 0.74 ± 0.20 at T2, a 28% relative increase

Table 1. Baseline Characteristics of the Patients in the Primary and Validation Cohorts.*

Characteristic	Primary Cohort (N=183)	Validation Cohort (N=201)
Age — yr	81.7±7.0	83.0±7.0
Male sex — no. (%)	87 (47.5)	100 (49.7)
Logistic EuroSCORE — %†	21.7±13.8	23.3±15.6
NYHA functional class — no. (%)‡		
II	62 (34.2)	63 (31.3)
III	92 (50.8)	121 (60.2)
IV	27 (14.9)	17 (8.5)
Body-mass index§	27.6±5.8	27.2±6.1
Clopidogrel use — no. (%)	40 (21.9)	47 (23.4)
Computed tomographic preprocedural measurements		
Aortic annulus diameter — mm	24.4±2.9	24.5±2.5
Aortic annulus area — mm ²	467±110	474±95
TTE preprocedural measurements		
Aortic annulus diameter — mm	22.7±1.9	22.8±2.5
LVEF — %	54.5±11.5	52.0±13.3
Aortic-valve area — cm ²	0.68±0.19	0.71±0.19
Maximum aortic-valve velocity — m/sec	4.18±0.64	4.20±0.70
Mean aortic-valve gradient — mm Hg	45.3±15.5	45.5±15.3
Aortic insufficiency grade ≥2 — no. (%)¶	22 (12.0)	24 (11.9)
Mitral regurgitation grade ≥2 — no. (%)¶	37 (20.2)	35 (17.4)
Pulmonary hypertension — no. (%)	50 (27.3)	59 (29.3)
Procedural device — no. (%)		
SAPIEN XT	183 (100.0)	97 (48.2)
CoreValve	—	55 (27.4)
SAPIEN 3	—	49 (24.4)
VWF and hemostasis assays		
VWF HMW-multimer ratio	0.61±0.19	NA
Ratio of VWF CB activity to VWF antigen	0.80±0.19	NA
CT-ADP	239±61	228±69

* Plus–minus values are means ±SD. Percentages may not total 100 because of rounding. CB denotes collagen binding, CT-ADP closure time with adenosine diphosphate, HMW high molecular weight, LVEF left ventricular ejection fraction, NA not available, TTE transthoracic echocardiography, and VWF von Willebrand factor.

† The logistic EuroSCORE (European System for Cardiac Operative Risk Evaluation), calculated by means of a logistic-regression equation, ranges from 0 to 100%, with higher scores indicating greater surgical risk and a score of more than 20% indicating high surgical risk.

‡ New York Heart Association (NYHA) functional classes range from I to IV, with higher classes indicating worse condition. Data were missing for two patients in the primary cohort.

§ The body-mass index (BMI) is the weight in kilograms divided by the square of the height in meters.

¶ Aortic insufficiency and mitral regurgitation were assessed with the use of a color-flow Doppler signal, according to guidelines from the European Association of Echocardiography.

|| The ratio is a measure of the amount of the largest multimers in the sample as compared with the amount in normal pooled human plasma.

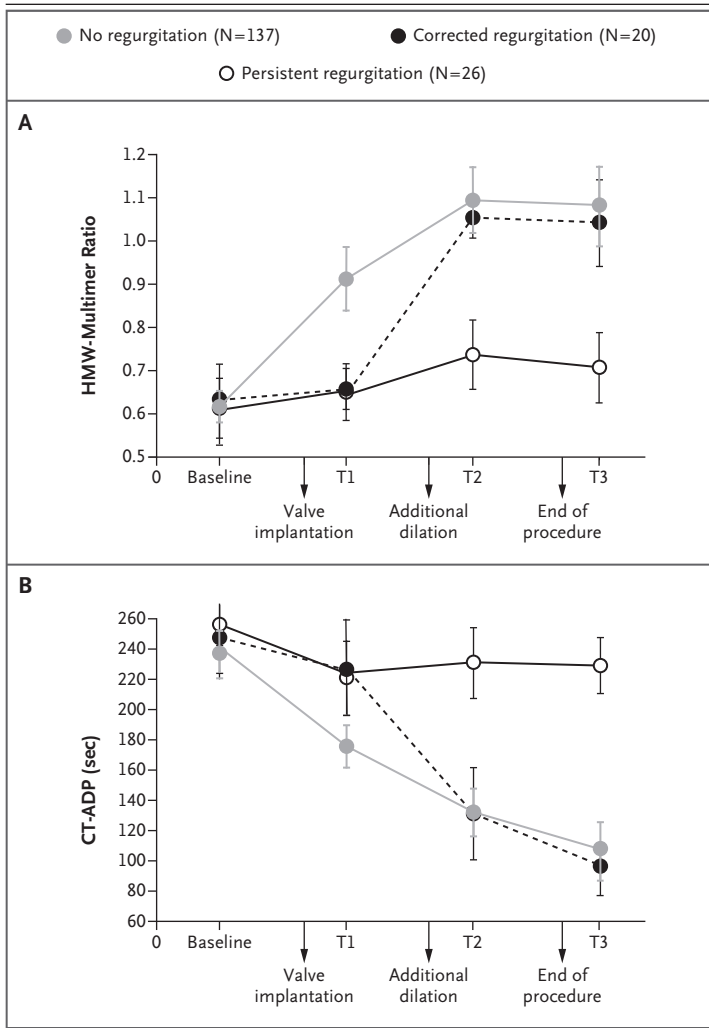


Figure 2. Sequence of Changes in the von Willebrand Factor High-Molecular-Weight (HMW)–Multimer Ratio and Closure Time with Adenosine Diphosphate (CT-ADP) in the Primary Cohort, According to Status with Respect to Aortic Regurgitation.

Panel A shows the sequence of changes in the HMW-multimer ratio (a measure of the amount of the largest multimers in the sample as compared with the amount in normal pooled human plasma), which differed significantly among the three groups ($P < 0.001$ for time–group interaction). At baseline, there was no significant difference in the HMW-multimer ratio among the three groups ($P = 0.54$). After 5 minutes, the mean HMW-multimer ratio was higher in the no-regurgitation group than in the other two groups ($P < 0.001$ for both comparisons). At time T2, the mean HMW-multimer ratio was similar in the no-regurgitation group and the corrected-regurgitation group ($P = 0.59$), and these values were both higher than that in the persistent-regurgitation group ($P < 0.001$ for both comparisons). The results observed at time T3 were similar to those observed at time T2. Panel B shows the sequence of changes in CT-ADP, which differed significantly among the three groups ($P < 0.001$ for time–group interaction). At baseline, there were no significant between-group differences ($P = 0.29$). After 5 minutes, the mean CT-ADP in the no-regurgitation group was lower than that in the corrected-regurgitation group ($P = 0.004$) and the persistent-regurgitation group ($P < 0.001$). At time T2, the mean CT-ADP was similar in the no-regurgitation and corrected-regurgitation groups ($P = 0.63$), and these values were lower than that in the persistent-regurgitation group ($P < 0.001$ for both comparisons). Note that the x axis is not a true time scale and the arrow markers for clinical procedures are not meant to indicate the exact timing of the events. These differences between the persistent-regurgitation group and the two other groups were greater at time T3. 1 bars indicate ± 1 SD.

from baseline). The results observed at T3 were similar to those at T2. The sequence of mean values for the HMW-multimer ratio from baseline through T3 differed significantly among the three groups ($P < 0.001$).

The changes in the CT-ADP were similar to those seen in the HMW-multimer ratio. In the no-regurgitation group, the CT-ADP decreased from 235 ± 62 seconds at baseline to 174 ± 62 seconds at T1 and 129 ± 54 seconds at T2 (a 45% relative decrease from baseline) (Fig. 2B). In the corrected-regurgitation group, the CT-ADP did not change markedly from baseline (250 ± 53 seconds) to T1 (223 ± 49 seconds) but decreased after the corrective procedure to 124 ± 59 seconds at T2 (a 44% relative decrease from T1). In the persistent-regurgitation group, the CT-ADP remained high throughout the procedure (253 ± 59 seconds

at baseline and 231 ± 55 seconds at T2, an 8% relative decrease from baseline). The results observed at T3 were similar to those at T2. The sequence of mean values for the CT-ADP from baseline through T3 differed significantly among the three groups ($P < 0.001$).

The sequence of changes in the mean values for the HMW-multimer ratio and the CT-ADP from baseline to times T1, T2, and T3 were similar for patients who were taking clopidogrel and those who were not, and for patients who had mitral regurgitation at baseline and those who did not (see the Results section in the Supplementary Appendix). In patients with mitral regurgitation at baseline, the HMW-multimer ratio was lower and the CT-ADP was higher than in those without mitral regurgitation. In a multivariable anal-

ysis that included status with respect to aortic regurgitation at the final evaluation, age, sex, transaortic gradient, and status with respect to clopidogrel use and mitral regurgitation at baseline, the HMW-multimer ratio at T3 and the CT-ADP at T3 were significantly associated only with the presence or absence of aortic regurgitation at the final evaluation and of mitral regurgitation at baseline (see the Results section in the Supplementary Appendix).

PREDICTIVE VALUE OF HMW-MULTIMER RATIO AND CT-ADP IN THE PRIMARY COHORT

ROC analysis of the HMW-multimer ratio at T3 to discriminate between patients with and those without aortic regurgitation on TEE showed an AUC of 0.94 (95% confidence interval [CI], 0.89 to 0.99) (Fig. 3A). The optimal threshold value for the HMW-multimer ratio was 0.8, which had a sensitivity, specificity, and negative predictive value of 92.3%, 94.9%, and 98.7%, respectively. When the 37 patients with mitral regurgitation were excluded, the sensitivity decreased to 90.5%, the specificity increased to 97.6%, and the negative predictive value was 98.4%.

ROC analysis of the CT-ADP at T3 to discriminate between patients with and those without aortic regurgitation on TEE showed an AUC of 0.93 (95% CI, 0.87 to 0.98) (Fig. 3B). The optimal threshold of 180 seconds had a sensitivity, specificity, and negative predictive value of 92.3%, 92.4%, and 98.6%, respectively. When the 37 patients with mitral regurgitation were excluded, the sensitivity decreased to 90.5%, the specificity increased to 96.0%, and the negative predictive value was 98.4%.

PREDICTIVE VALUE OF CT-ADP IN THE VALIDATION COHORT

A total of 201 patients undergoing TAVR were enrolled in the validation cohort. Baseline characteristics are presented in Table 1. After TAVR, aortic regurgitation was observed on TEE in 14.9% of the patients (30 of 201). The CT-ADP at the end of the procedure was significantly higher in patients with aortic regurgitation than in those without regurgitation (244±64 seconds vs. 118±53 seconds, $P<0.001$).

ROC analysis of the CT-ADP to discriminate between patients with and those without aortic regurgitation on TEE at the end of the procedure showed an AUC of 0.92 (95% CI, 0.86 to 0.97)

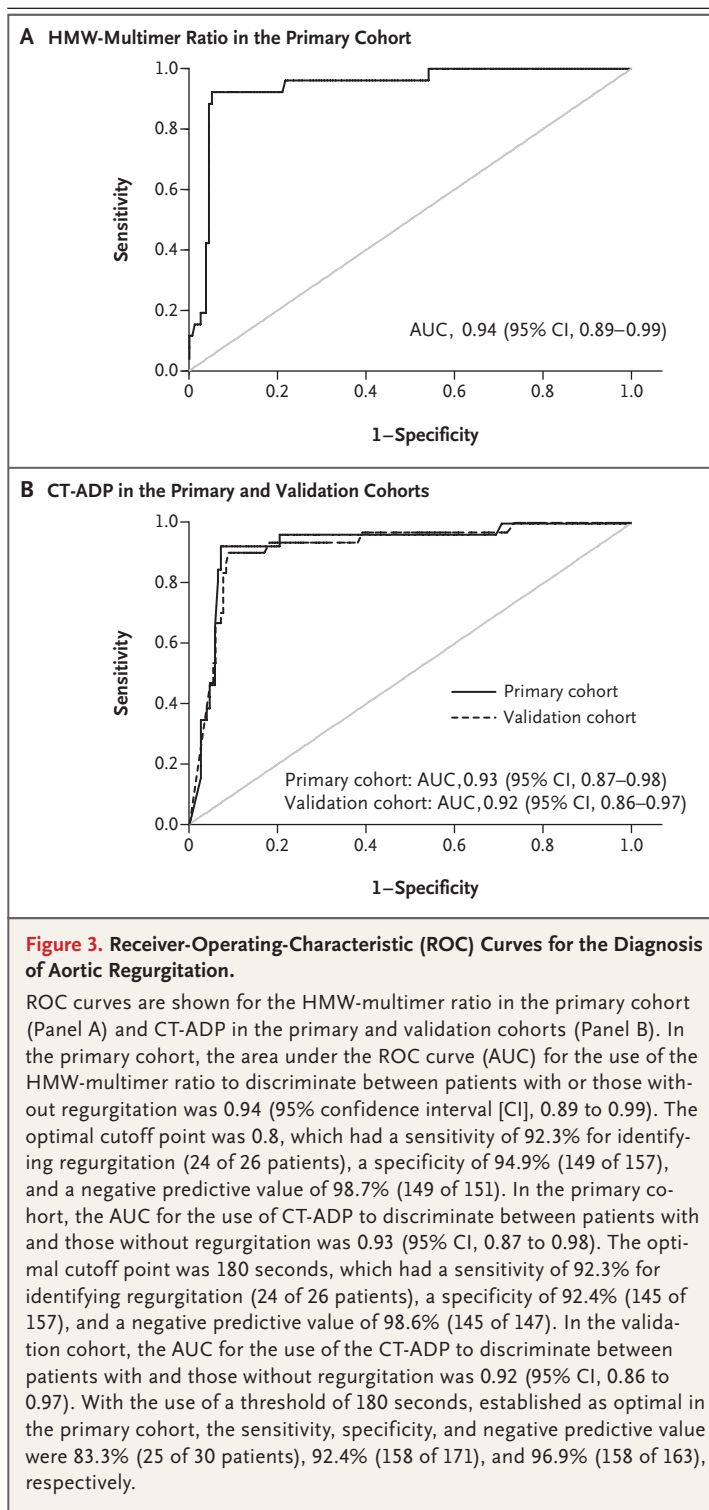


(Fig. 3B). With the use of a threshold of 180 seconds, established as optimal in the primary study cohort, the sensitivity, specificity, and negative

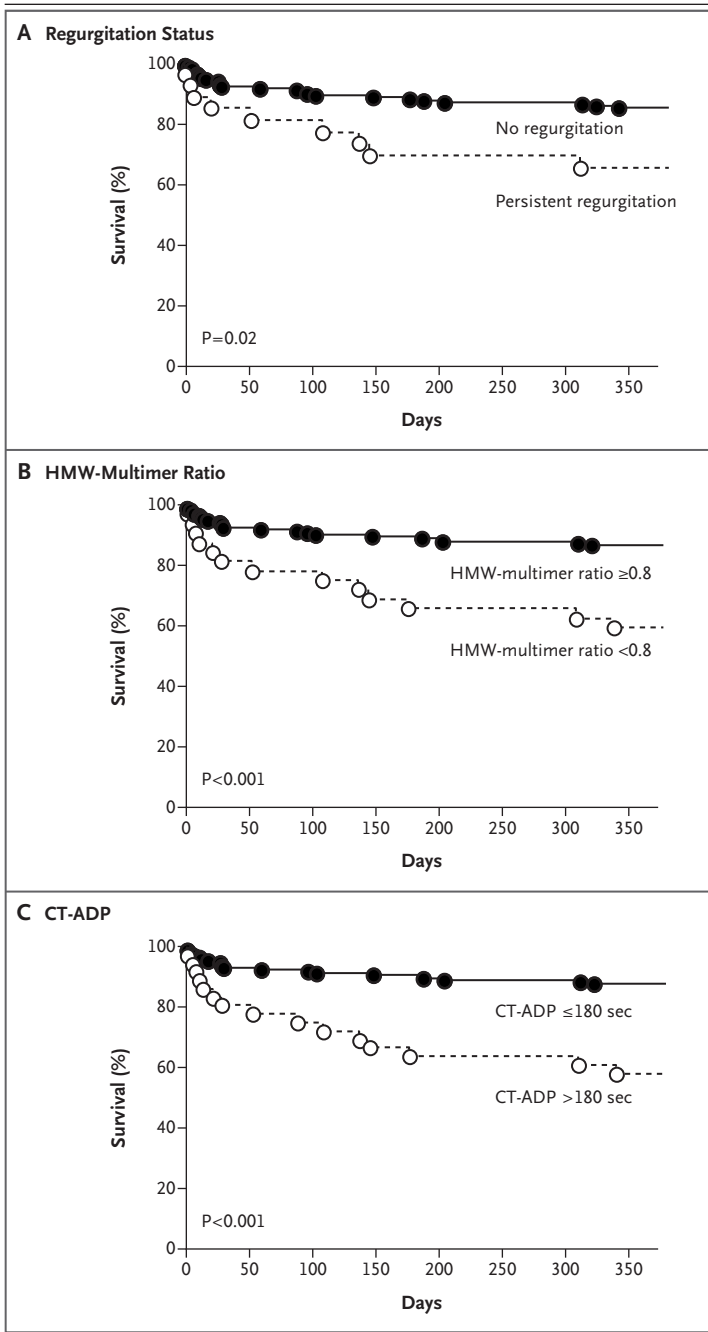


Figure 4. Time-to-Event Curves for Overall Survival at 1 Year in the Primary Cohort, According to Aortic Regurgitation Status, HMW-Multimer Ratio, and CT-ADP.

Panel A shows that mortality at 1 year was increased by a factor of more than 2 among the 26 patients with persistent regurgitation on TEE at the end of the procedure, as compared with the 157 patients without regurgitation (34.6% vs. 15.3%, $P=0.02$ by the log-rank test). Panel B shows that among the 32 patients with an HMW-multimer ratio of less than 0.8 at time T3, mortality at 1 year was increased by a factor of more than 3, as compared with patients who had an HMW-multimer ratio of 0.8 or higher (40.6% vs. 13.2%, $P<0.001$ by the log-rank test). Panel C shows that among the 36 patients with a CT-ADP that was longer than 180 seconds, mortality at 1 year was increased by a factor of 3.5, as compared with patients who had a CT-ADP of 180 seconds or less (41.7% vs. 12.2%, $P<0.001$ by the log-rank test).

During 1 year of follow-up, 33 patients (18.0%) died. Among the 26 patients with aortic regurgitation on TEE at T3, the rate of death at 1 year was more than twice the rate among those without regurgitation at T3 (34.6% vs. 15.3%, $P=0.02$ by the log-rank test) (Fig. 4A). In a multivariable model that included the logistic EuroSCORE (European System for Cardiac Operative Risk Evaluation) and status with respect to mitral regurgitation at baseline (model 1), only aortic regurgitation at the end of the procedure and mitral regurgitation at baseline were associated with an increased risk of death (see the Results section in the Supplementary Appendix).

Among the 32 patients with a final HMW-multimer ratio of less than 0.8, the rate of death was three times as high as the rate among the 151 patients with an HMW-multimer ratio of 0.8 or higher (40.6% vs. 13.2%, $P<0.001$ by the log-rank test) (Fig. 4B). Model 2 involved the addition of the HMW-multimer ratio to model 1, significantly improving model fit ($P=0.01$) (see the Results section in the Supplementary Appendix). In model 2, an HMW-multimer ratio of less than 0.8 at T3 was associated with increased mortality, whereas aortic regurgitation at T3 and mitral regurgitation at baseline were not.

Among the 36 patients with a final CT-ADP of more than 180 seconds, the rate of death was increased by a factor of 3.5, as compared with the rate among the 147 patients with a CT-ADP of 180 seconds or less (41.7% vs. 12.2%, $P<0.001$ by the log-rank test) (Fig. 4C). Model 3 involved

predictive value were 83.3%, 92.4%, and 96.9%, respectively.

STROKE AND DEATH IN THE PRIMARY COHORT

During the 30 days after the TAVR procedure, 6 of the 183 patients in the primary cohort (3.2%) had a clinical stroke: 2 of the 46 patients (4.3%) who underwent additional dilation and 4 of the 137 patients (2.9%) who did not ($P=0.63$).

the addition of CT-ADP to model 1, significantly improving model fit (see the Results section in the Supplementary Appendix) ($P < 0.001$). In model 3, a CT-ADP of more than 180 seconds at T3 was associated with increased mortality, whereas aortic regurgitation at T3 and mitral regurgitation at baseline were not.

DISCUSSION

In the present study, we found that a point-of-care hemostatic test, the CT-ADP, was predictive of the presence or absence of paravalvular aortic regurgitation after TAVR. The CT-ADP test is highly sensitive to defects in von Willebrand factor HMW multimers. Such defects occur in patients with paravalvular aortic regurgitation, because turbulent blood flow through the paravalvular leak alters the conformation of the HMW multimer, unfolding the molecule and exposing it to proteolytic cleavage (see animation).^{7,14} The loss of HMW multimers reduces the hemostatic competence of von Willebrand factor and causes a prolongation of the CT-ADP.

Two recent studies involving a total of six patients with aortic regurgitation who underwent TAVR suggested a relationship between postprocedural aortic regurgitation and HMW-multimer defects.^{7,15} The present report, based on the findings in two independent cohorts, with a total of 76 cases of aortic regurgitation detected on TEE, confirms this relationship. Furthermore, the present study shows the dynamic relationship between correction of aortic regurgitation and recovery of HMW multimers. When aortic regurgitation occurred after TAVR, the preexisting HMW-multimer defect (due to the presence of aortic stenosis) did not resolve; when aortic regurgitation was corrected by additional dilation, normalization of HMW multimers occurred within minutes and within the time frame of the procedure.

A further finding of our study is that a rapid correction in CT-ADP, reflecting the recovery of HMW multimers, occurs during the TAVR procedure in patients without clinically significant aortic regurgitation, whereas in patients with persistent aortic regurgitation, this correction is not observed. A value for CT-ADP of more than 180 seconds discriminated between patients with aortic regurgitation and those without regurgitation, with negative predictive values of 98.6%

in the primary (derivation) cohort and 96.9% in the validation cohort. These findings suggest that measurement of CT-ADP, which can be performed as a point-of-care test, could be used for monitoring during TAVR procedures to identify a subgroup of patients for whom TEE or other imaging methods may be appropriate.

Finally, the present study confirms the finding that among patients undergoing TAVR, mortality at 1 year is twice as high among those with more-than-mild aortic regurgitation as among those without regurgitation.^{2,3} Both the final CT-ADP and the final HMW-multimer ratio are better predictors of 1-year mortality than TEE. This suggests that flow-related biologic markers provide an integrated assessment of valve function that is distinct from, and perhaps more accurate than, the assessment obtained with imaging.

Several limitations of our study should be considered. First, the primary cohort was from a single center, and the results may therefore have been influenced by clinical practice at this institution. It would be desirable to evaluate larger samples of patients from multiple institutions in order to determine whether our findings are broadly generalizable. Second, the study was not designed to evaluate the potential effect of clopidogrel therapy on the testing strategy, although no such effect was detected. Finally, other drugs or medical conditions that influence hemostasis could also alter the ability of the CT-ADP test to detect post-TAVR aortic regurgitation.

In conclusion, the present study showed that a point-of-care hemostatic test, the CT-ADP, was predictive of the presence or absence of paravalvular aortic regurgitation after TAVR. The test was also predictive of the rate of death 1 year after the procedure.

Supported by Lille 2 University, Lille University Hospital, and the Institut Universitaire de France (to Dr. Staels).

Disclosure forms provided by the authors are available with the full text of this article at NEJM.org.

We thank Brigitte Jude for supporting the development of the present translational program and for advice regarding the conduct of this study; Anne Bauters, Isabelle Grit, Pauline Guyon, Pascale Renom, Bruno Rossetti, Veronique Tintillier, Nathalie Trillot, Alexandre Ung, and Bénédicte Wibaut (Lille University Hospital) for their contribution to the study, and the members of the catheterization laboratory and cardiac operating room teams in the Department of Cardiology at Lille University Hospital, represented by their chief nurses (Catherine Desormeaux, Fabienne Delesalle, and Bernard Collet), for their commitment to the project.

APPENDIX

The authors' full names and academic degrees are as follows: Eric Van Belle, M.D., Ph.D., Antoine Rauch, M.D., Ph.D., Flavien Vincent, M.D., Emmanuel Robin, M.D., Ph.D., Marion Kibler, M.D., Julien Labreuche, B.S.T., Emmanuelle Jeanpierre, Pharm.D., Marie Levade, M.D., Christopher Hurt, M.D., Natacha Rousse, M.D., Jean-Baptiste Dally, M.D., Nicolas Debry, M.D., Jean Dallongeville, M.D., Ph.D., Andre Vincentelli, M.D., Ph.D., Cedric Delhay, M.D., Jean-Luc Auffray, M.D., Francis Juthier, M.D., Ph.D., Guillaume Schurtz, M.D., Gilles Lemesle, M.D., Ph.D., Thibault Caspar, M.D., Olivier Morel, M.D., Ph.D., Nicolas Dumonteil, M.D., Alain Duhamel, M.D., Ph.D., Camille Paris, M.D., Annabelle Dupont-Prado, Pharm.D., Ph.D., Paulette Legendre, B.Sc., Frederic Mouquet, M.D., Ph.D., Berenice Marchant, B.Sc., Sylvie Hermoire, B.Sc., Delphine Corseaux, Ph.D., Karim Moussa, M.D., Aurelie Manchuelle, M.D., Jean-Jacques Bauchart, M.D., Valentin Loobuyck, M.D., Claudine Caron, Pharm.D., Christophe Zawadzki, Pharm.D., Ph.D., Fabrice Leroy, M.D., Jean-Christophe Bodart, M.D., Bart Staels, Ph.D., Jenny Goudebrand, M.D., Ph.D., Peter J. Lenting, Ph.D., and Sophie Susen, M.D., Ph.D.

The authors' affiliations are as follows: the Departments of Cardiology (E.V.B., F.V., C.H., J.-B.D., N. Debry, C.D., J.-L.A., G.S., G.L., B.M., K.M., A.M., J.-J.B., F.L., J.-C.B.), Hematology and Transfusion (A.R., E.J., C.P., A.D.-P., S.H., C.C., C.Z., B.S., J.G., S.S.), and Cardiac Surgery (E.R., N.R., A.V., F.J., V.L.), Centre Hospitalier Universitaire (CHU) Lille, INSERM Unité 1011 (E.V.B., A.R., F.V., E.R., N.R., A.V., F.J., C.P., A.D.-P., F.M., B.M., D.C., C.Z., B.S., J.G., S.S.), Université Lille, INSERM Unité 1011 — European Genomic Institute for Diabetes (E.V.B., A.R., F.V., E.R., N.R., A.V., F.J., C.P., A.D.-P., F.M., B.M., D.C., C.Z., J.G., S.S.), INSERM Unité 1167 (J.D.), Institut Pasteur de Lille (E.V.B., A.R., F.V., E.R., N.R., J.D., A.V., F.J., C.P., A.D.-P., F.M., B.M., D.C., C.Z., J.G., S.S.), and Université Lille, CHU Lille, Equipe d'accueil 2694 — Santé Publique: Epidemiologie et Qualité des Soins (J.L., A.D.), Lille, Pole d'Activité Médico-chirurgicale Cardio-vasculaire, Nouvel Hôpital Civil, CHU, Université de Strasbourg, Strasbourg (M.K., T.C., O.M.), INSERM Unité 1048 and Université Toulouse III (J.L., A.D.), Institut des Maladies Métaboliques et Cardiovasculaires (M.L., N. Dumonteil), and Laboratoire d'Hématologie (M.L.), and Service de Cardiologie (N. Dumonteil), CHU de Toulouse, Toulouse, Unité Mixte de Recherche (UMR), Centre Nationale de la Recherche Scientifique 7213, Laboratoire de Biophotonique et Pharmacologie, Faculté de Pharmacie, Université de Strasbourg, Illkirch (O.M.), and INSERM UMR-S Unité 1176, Université Paris-Sud, Université Paris-Saclay, Le Kremlin-Bicêtre (P.L., P.J.L.) — all in France.

REFERENCES

- Gilard M, Eltchaninoff H, Iung B, et al. Registry of transcatheter aortic-valve implantation in high-risk patients. *N Engl J Med* 2012;366:1705-15.
- Van Belle E, Juthier F, Susen S, et al. Postprocedural aortic regurgitation in balloon-expandable and self-expandable transcatheter aortic valve replacement procedures: analysis of predictors and impact on long-term mortality: insights from the FRANCE2 Registry. *Circulation* 2014;129:1415-27.
- Kodali SK, Williams MR, Smith CR, et al. Two-year outcomes after transcatheter or surgical aortic-valve replacement. *N Engl J Med* 2012;366:1686-95.
- Kodali S, Pibarot P, Douglas PS, et al. Paravalvular regurgitation after transcatheter aortic valve replacement with the Edwards sapien valve in the PARTNER trial: characterizing patients and impact on outcomes. *Eur Heart J* 2015;36:449-56.
- Vincentelli A, Susen S, Le Tourneau T, et al. Acquired von Willebrand syndrome in aortic stenosis. *N Engl J Med* 2003;349:343-9.
- Blackshear JL, Wysokinska EM, Safford RE, et al. Shear stress-associated acquired von Willebrand syndrome in patients with mitral regurgitation. *J Thromb Haemost* 2014;12:1966-74.
- Van Belle E, Rauch A, Vincentelli A, et al. Von Willebrand factor as a biological sensor of blood flow to monitor percutaneous aortic valve interventions. *Circ Res* 2015;116:1193-201.
- Fressinaud E, Veyradier A, Truchaud F, et al. Screening for von Willebrand disease with a new analyzer using high shear stress: a study of 60 cases. *Blood* 1998;91:1325-31.
- Blackshear JL, Wysokinska EM, Safford RE, et al. Indexes of von Willebrand factor as biomarkers of aortic stenosis severity (from the Biomarkers of Aortic Stenosis Severity [BASS] study). *Am J Cardiol* 2013;111:374-81.
- Le Tourneau T, Susen S, Caron C, et al. Functional impairment of von Willebrand factor in hypertrophic cardiomyopathy: relation to rest and exercise obstruction. *Circulation* 2008;118:1550-7.
- Samim M, Stella PR, Agostoni P, et al. Automated 3D analysis of pre-procedural MDCT to predict annulus plane angulation and C-arm positioning: benefit on procedural outcome in patients referred for TAVR. *JACC Cardiovasc Imaging* 2013;6:238-48.
- Samim M, Juthier F, Van Belle C, et al. Automated 3D analysis of multislice computed tomography to define the line of perpendicularity of the aortic annulus and of the implanted valve: benefit on planning transcatheter aortic valve replacement. *Catheter Cardiovasc Interv* 2014;83(1):E119-27.
- Kappetein AP, Head SJ, Généreux P, et al. Updated standardized endpoint definitions for transcatheter aortic valve implantation: the Valve Academic Research Consortium-2 consensus document. *Eur Heart J* 2012;33:2403-18.
- Lippok S, Radtke M, Obser T, et al. Shear-induced unfolding and enzymatic cleavage of full-length VWF multimers. *Biophys J* 2016;110:545-54.
- Spangenberg T, Budde U, Schewel D, et al. Treatment of acquired von Willebrand syndrome in aortic stenosis with transcatheter aortic valve replacement. *JACC Cardiovasc Interv* 2015;8:692-700.

Copyright © 2016 Massachusetts Medical Society.

A novel ELISA-based diagnosis of acquired von Willebrand disease with increased VWF proteolysis

Antoine Rauch^{1,2}; Claudine Caron¹; Flavien Vincent^{2,3}; Emmanuelle Jeanpierre¹; Catherine Ternisien⁴; Pierre Boisseau⁵; Christophe Zawadzki^{1,2}; Edith Fressinaud¹; Annie Borel-Derlon⁶; Sylvie Hermoire¹; Camille Paris¹; Cécile Lavenu-Bombled⁷; Agnès Veyradier⁸; Alexandre Ung¹; André Vincentelli^{2,3}; Eric Van Belle^{2,3}; Peter J. Lenting⁹; Jenny Goudemand^{1,2}; Sophie Susen^{1,2}

¹Département d'Hématologie Transfusion, CHU Lille, Lille, France; ²INSERM UMR 1011, Univ Lille 2, Institut Pasteur de Lille, Lille, France; ³Département de Cardiologie, CHU Lille, Lille, France; ⁴Hématologie Biologique, CHU Nantes, Nantes, France; ⁵Laboratoire de génétique moléculaire, CHU Nantes, Nantes, France; ⁶Hématologie Biologique, Hôpital de la côte de Nacre, CHU Caen, Caen, France; ⁷Hématologie Biologique, Hôpital Lariboisière, AP-HP, Paris, France; ⁸Inserm, UMR_S 1176, Univ. Paris-Sud, Université Paris-Saclay, Le Kremlin-Bicêtre, France; ⁹INSERM Unit 770, Le Kremlin-Bicêtre, Val-de-Marne, France

Summary

Von Willebrand disease-type 2A (VWD-2A) and acquired von Willebrand syndrome (AVWS) due to aortic stenosis (AS) or left ventricular assist device (LVAD) are associated with an increased proteolysis of von Willebrand factor (VWF). Analysis of VWF multimeric profile is the most sensitive way to assess such increased VWF-proteolysis. However, several technical aspects hamper a large diffusion among routine diagnosis laboratories. This makes early diagnosis and early appropriate care of increased proteolysis challenging. In this context of unmet medical need, we developed a new ELISA aiming a quick, easy and reliable assessment of VWF-proteolysis. This ELISA was assessed successively in a LVAD-model, healthy subjects (n=39), acquired TTP-patients (n=4), VWD-patients (including VWD-2A(IIA), n=22; VWD-2B, n=26; VWD-2A(IIE), n=21; and VWD-1C, n=8) and in AVWS-patients (AS, n=9; LVAD, n=9; and MGUS, n=8). A standard of VWF-proteolysis was specifically developed. Extent of VWF-proteolysis was expressed as relative percentage and as VWF proteolysis/VWF:Ag ratio. A speed-

dependent increase in VWF-proteolysis was assessed in the LVAD model whereas no proteolysis was observed in TTP-patients. In VWD-patients, VWF-proteolysis was significantly increased in VWD-2A(IIA) and VWD-2B and significantly decreased in VWD-2A(IIE) versus controls (p<0.0001). In AVWS-patients, VWF-proteolysis was significantly increased in AS- and LVAD-patients compared to controls (p<0.0001) and not detectable in MGUS-patients. A significant increase in VWF-proteolysis was detected as soon as three hours after LVAD implantation (p<0.01). In conclusion, we describe a new ELISA allowing a rapid and accurate diagnosis of VWF-proteolysis validated in three different clinical situations. This assay represents a helpful alternative to electrophoresis-based assay in the diagnosis and management of AVWS with increased VWF-proteolysis.

Keywords

von Willebrand disease, acquired von Willebrand syndrome, proteolysis, aortic stenosis, circulatory support device

Correspondence to:

Sophie Susen
Centre de Biologie Pathologie
Centre Hospitalier Régional
59037 Lille Cedex, France
Tel.: +33 3 20 44 59 37, Fax: +33 3 20 44 69 89
E-mail: sophiesusen@aol.com

Received: August 10, 2015

Accepted after major revision: January 5, 2016

Epub ahead of print: January 21, 2016

<http://dx.doi.org/10.1160/TH15-08-0638>

Thromb Haemost 2016; 115: 950–959

Supplementary Material to this article is available online at www.thrombosis-online.com.

Introduction

von Willebrand factor (VWF) proteolysis by ADAMTS13 (A Disintegrin And Metalloprotease with Thrombospondin domains-13) is a physiological process that regulates the size of circulating multimers in plasma. Shear stress provokes an unfolding of the globular VWF conformation and once unfolded, VWF becomes sensitive to proteolysis by the VWF-cleaving protease ADAMTS13. Mutations within VWF A2 domain or exposure of native VWF to pathological high shear stress can enhance this physiological proteolysis. Excess of VWF proteolysis is the central mechanism of the loss of high-molecular-weight multimers (HMW-multimers) observed in most cases of von Willebrand disease type 2A (VWD-2A) and in acquired von Willebrand syndrome (AVWS) associated with aortic stenosis (AS) or left ventricular assist device (LVAD) therapy (1–4).

In patients with AS or LVAD therapy, AVWS is frequently (but inconstantly) observed and is considered to be one of the main risk-factor of bleeding occurring in these high-risk populations (5, 6). Accumulated evidence demonstrates that early identification of AVWS, in particular in patients with LVAD, is of major clinical importance as it can modify the medical management and improve the clinical outcome of these patients (7).

An early positive diagnosis of increased proteolysis still remains challenging most of the time, since current electrophoresis-based and immuno-precipitation assays are time-consuming and very difficult to implement in “routine” due to the fact that they need to be performed in small batches by dedicated technicians specifically trained to these techniques. This sometimes makes VWD-typing and AVWS positive diagnosis cumbersome processes, and the use of these diagnostic methods is of little help when a rapid clinical decision is needed.

In this context, there is therefore an emerging need for an easy, rapid, quantitative and reproducible diagnostic tool to determine the extent of VWF proteolysis. Our purpose was 1) to develop an enzyme-linked immunosorbent assay (ELISA)-based diagnosis of increased VWF-proteolysis; 2) to validate its ability to identify and discriminate different forms of constitutive VWD and AVWS according to their mechanisms and to their quantified impact on VWF proteolysis.

Material and methods

Patients and controls

All patients provided informed written consent according to the Declaration of Helsinki. Healthy subjects from the laboratory staff (► Table 1, n=39) were sampled as controls. Patients with acquired Thrombotic Thrombocytopenic Purpura (TTP) (n=4) were selected from the French reference centre of TTP.

Patients with VWD were selected from the French cohort multicentric database of VWD according to their mutations and the mechanism of the reduction in HMW-multimers (8). The study was approved by the North of France ethical committee. The database and biobank (plasma and DNA) of the French VWD cohort (Centre de Référence Maladie de Willebrand, CRMW) were declared to the French data protection authority. Mutations characterised by an increase (2A (IIA) group 2 mutations, n=22; and 2B patients, n=26), or no increase (2A (IIE), n=21) in VWF-proteolysis (1) were included in the study (► Table 2). For a sub-analysis, VWD2B-patients were classified according to the multimeric pattern as previously described (A=partial loss of HMW multimers; B=complete loss of HMW multimers; C= loss also of intermediate multimers) (9). VWD2B patients with a normal multimeric pattern (Malmö or New York) were excluded from the study. We also included patients with VWD-Vicenza (n=8) as a reference of increased clearance of VWF.

After approval from the North of France ethical committee, patients with AVWS associated with high shear-induced VWF proteolysis (severe AS, n=9; and after implantation of LVAD-, n=9) or due to increased VWF clearance associated with monoclonal gammopathy of uncertain significance (MGUS-IgG, n=8) were included in the study (► Table 3). In the seven AS-patients who underwent a Transcatheter Aortic Valve Implantation (TAVI),

samples were also collected after procedure. Samples were collected from patients with LVAD before and 3 hours (h) after initiation of HeartMate-II®-LVAD support at 9000 rpm. For all the patients and healthy controls included, the phenotypic data are summarised in ► Tables 1-3. Patients with TTP were selected on the basis of an undetectable ADAMTS13 activity (<5%) associated with the presence of ultralarge (UL) VWF multimers in plasma.

LVAD-perfusion model

In a previously described LVAD-model, we induced an excess of VWF proteolysis in whole blood obtained from healthy subjects, which reproduces the biological phenotype of AVWS (4, 10). This model is associated with a time-related loss of HMW-multimers, except in the presence of EDTA, a non specific inhibitor of ADAMTS13, and in the presence of an anti-VWF antibody (mAb508) reducing ADAMTS13 proteolysis (10).

In this model we evaluated the effect of the pump speed (3000, 6000 and 9000 rpm) and the inhibition of VWF proteolysis under high shear conditions (9000 rpm) in the presence of EDTA; (10 mM final concentration) or mAb508; (50 µg/ml final concentration) (10). Blood was sampled at baseline and 180 minutes (min) after onset of perfusion. Platelet-rich plasma (PRP) was obtained from baseline samples by centrifugation of citrated whole blood at 100 g for 15 min at 20°C and then incubated in Triton-PBS (phosphate-buffered saline) buffer to obtain platelet lysates. Poor-platelet plasma (PPP) was obtained from either unprocessed or processed-whole blood by further centrifugation at 2000 g for 15 min. Platelet lysates and PPP samples were analysed for VWF multimeric analysis as previously described (3) and for VWF-proteolysis by ELISA. HMW-multimers was measured and quantified as previously described (4).

Laboratory assessment of VWF

All samples were collected on citrate 0.109M BD Vacutainer® 5ml tubes. VWF antigen levels were measured by immunoturbidimetry (VWF: Ag, Siemens®). VWF activity was evaluated by a gain-of-function mutant GPIb binding assay (VWF: GPIbM, Innovance® VWF Ac; Siemens Healthcare Diagnostics, Marburg, Germany) or an ELISA collagen-binding assay (VWF: CB) with the use of equine type I/III collagen (Horm; Nycomed, Oslo,

Table 1: Phenotypic data of healthy controls (median ± SD and range).

Controls	Number of controls	VWF-proteolysis (%)	VWF-proteolysis / VWF:Ag ratio	VWF:Ag (IU dl ⁻¹)	VWF:GPIbM (IU dl ⁻¹)	VWF: GPIbM / VWF:Ag ratio	VWFpp / VWF:Ag ratio
O group	19	4.5 ± 1.4 (2.9–9.1)	0.07 ± 0.02 (0.03–0.10)	63 ± 21.7 (41–120)	66 ± 26.5 (37–127)	0.96 ± 0.16 (0.66–1.18)	1.32 ± 0.26 (1–1.85)
Non-O group	20	5.6 ± 1.6 (3–9.2)	0.06 ± 0.02 (0.03–0.09)	108 ± 21.8 (76–150)	95 ± 28.4 (50–151)	0.91 ± 0.14 (0.64–1.04)	1.15 ± 0.28 (0.85–1.83)
All	39	5.2 ± 1.6 (2.9–9.2)	0.06 ± 0.02 (0.03–0.10)	93 ± 27.7 (41–150)	75 ± 29.7 (37–151)	0.92 ± 0.15 (0.64–1.18)	1.24 ± 0.28 (0.85–1.85)

Type	Mutation	Number of families	Number of patients	VWF-proteolysis (%)	VWF-proteolysis / VWF:Ag ratio	VWF:Ag (IU dl ⁻¹)	VWF:GPIbM (IU dl ⁻¹)
2A (IIA)	p.Ala1500Glu	1	1	20	0.72	28	10
	p.Arg1597Trp	3	11	32 ± 23 (15–86)	0.84 ± 0.24 (0.30–1.13)	40 ± 21 (24–89)	11 ± 4 (7–20)
	p.Gly1609Arg	2	6	35 ± 13 (32–68)	0.71 ± 0.13 (0.63–1)	53 ± 7 (46–68)	14 ± 3 (11–18)
	p.Ile1628Thr	2	2	48.5 (45–52)	1.12 (1.11–1.14)	43 (41–45)	6.5 (3–10)
	p.Glu1638Lys	1	2	46.6	0.78 (0.75–0.81)	62	10
	All	9	22	33 ± 18 (15–86)	0.77 ± 0.21 (0.30–1.14)	45 ± 16 (24–89)	11 ± 4 (3–20)
2B	p.Arg1306Gln*	1	2	12.5 (11–14)	0.42 (0.3–0.44)	36 (24–48)	26 (21–31)
	p.Arg1308Cys***	1	4	19 (19–25.7)	0.62 (0.47–0.88)	34 (29–49)	8.5 (5–11)
	p.Val1316Met***	2	2	24.4 (23.7–25.1)	0.61 (0.46–0.76)	43 (31–55)	29 (10–48)
	p.Pro1337Leu*	1	1	14	0.25	56	27
	p.Arg1341Gln**	5	15	13 ± 5 (7.4–22)	0.34 ± 0.13 (0.09–0.56)	47 ± 18 (27–89)	27 ± 12 (10–45)
	p.Ala1461Val*	1	2	9	0.14 (0.11–0.16)	68.5 (52–85)	56 (29–83)
	All	11	26	14.1 ± 6 (7.4–25.7)	0.36 ± 0.19 (0.09–0.88)	50 ± 22 (24–89)	28 ± 23 (5–83)
2A(III)	p.Cys1130Phe	2	3	<2%	nc	20 (16–42)	14 (8–22)
	p.Cys1130Trp	2	2	<2%	nc	26 (15–37)	10
	p.Cys1130Tyr	1	3	<2%	nc	12 (11–17)	10
	p.Tyr1146Cys	4	5	<2%	nc	17 (10–28)	11 (10–28)
	p.Cys1173Phe	1	2	<2%	nc	26.5 (21–32)	19.5 (12–27)
	p.Cys1196Arg	1	6	<2%	nc	23.5 ± 8 (16–38)	20 ± 7 (10–28)
	All	11	21	<2%	nc	21 ± 9 (10–42)	17 ± 7 (8–28)
1C	p.Arg1205Leu	1	2	<2%	nc	10.5 (7–14)	6 (5–7)
	p.Arg1205His	2	6	<2%	nc	12 ± 2 (9–15)	10 ± 2 (5–13)

Classification of 2B patients according to the multimeric pattern as previously described (9); *A=partial loss of HMW multimers; **B=complete loss of HMW multimers; ***C= loss also of intermediate multimers – nc: not calculable – na: not available.

Norway) (11). The proportion of VWF in its GPIb- α -binding conformation ('active VWF') was assessed on VWD-2B samples with a nanobody-based ELISA as previously described (12). VWF propeptide (VWFpp) was assessed with a commercially available kit (VWF & Propeptide Assay, Lifecodes®). VWF multimeric analysis was performed as previously described (3). Loss of HMW-multimers was measured and calculated as previously described

(10). ADAMTS13 activity was performed using fluorescence resonance energy transfer (FRETs) (13).

Determination of VWF proteolysis by ELISA

A 96-well microplate (Immulon® 4HBX) was coated with a monoclonal antibody (mAb27642, R&D Systems, Minneapolis, MN,

Table 3: Phenotypic data of AVWS-patients* (median ± SD and range).

	Number of patients	VWF- proteolysis (%)	VWF- proteolysis ratio	VWF:Ag (IU dl ⁻¹)	VWF:CB (IU dl ⁻¹)	VWF:CB / VWF:Ag ratio	VWFpp / VWF:Ag ratio
Aortic stenosis	9	16 ± 19 (8–64)	0.11 ± 0.05 (0.04–0.22)	167 ± 132 (67–449)	97 ± 109 (60–381)	0.66 ± 0.13 (0.58–0.97)	1.2 ± 0.2 (0.8–1.5)
LVAD	9	99 ± 33 (15–179)	0.31 ± 0.10 (0.10–0.75)	275 ± 106 (126–384)	200 ± 113 (109–456)	0.70 ± 0.24 (0.55–1.19)	2.5 ± 0.6 (1.7–3.5)
MGUS-IgG	8	<2%	nc	12 ± 7 (4–25)	10 ± 5 (4–16)	Nc	11.7 ± 9.2 (7.5–33)

*All patients with loss of HMW-multimers.

VWF:GPIbM / VWF:Ag ratio	VWF:CB (IU dl ⁻¹)	VWF:CB	VWFpp/VWF:Ag ratio
0.36	2	0.07	na
0.30 ± 0.07 (0.22–0.45)	5 ± 4 (3–16)	0.11 ± 0.06 (0.01–0.24)	na
0.26 ± 0.05 (0.20–0.33)	2 ± 3 (2–8)	0.04 ± 0.05 (0.03–0.16)	na
0.16 (0.07–0.24)	1	0.02	na
0.16	2 (1–3)	0.05 (0.02–0.08)	na
0.29 ± 0.08 (0.07–0.45)	3 ± 3 (1–16)	0.09 ± 0.06 (0.01–0.24)	na
0.76 (0.65–0.88)	8.5 (2–15)	0.19 (0.08–0.31)	na
0.21 (0.16–0.30)	3.2 (2.5–4)	0.11 (0.07–0.12)	na
0.59 (0.32–0.87)	11 (2–20)	0.21 (0.06–0.36)	na
0.48	18	0.32	na
0.51 ± 0.23 (0.27–0.81)	12 ± 8 (4–33)	0.31 ± 0.11 (0.13–0.47)	na
0.77 (0.56–0.97)	21 (6–36)	0.27 (0.12–0.42)	na
0.53 ± 0.26 (0.16–0.97)	10.5 ± 9 (2–36)	0.22 ± 0.12 (0.06–0.47)	na
0.52 (0.28–0.87)	8.5 (6–20)	0.42 (0.37–0.48)	na
0.76 (0.46–1.06)	13 (5–21)	0.45 (0.33–0.57)	na
0.83 (0.59–0.91)	5 (4–6)	0.36 (0.35–0.42)	na
0.85 (0.61–1)	8 (4–15)	0.47 (0.4–0.62)	na
0.70 (0.57–0.83)	12 (11–13)	0.46 (0.40–0.52)	na
0.77 ± 0.10 (0.63–0.90)	13.5 ± 7 (7–26)	0.57 ± 0.10 (0.44–0.58)	na
0.72 ± 0.20 (0.28–1.06)	12 ± 6 (4–26)	0.43 ± 0.10 (0.19–0.68)	na
0.5 (0.3–0.7)	na	na	10.8 (7.7–14)
0.75 ± 0.26 (0.56–1.30)	na	na	14.8 ± 7 (12.3–32)

Table 2: Phenotypic and genotypic data of VWD-patients (median ± SD and range).

USA) targeting an epitope on VWF adjacent to the cleavage site Y¹⁶⁰⁵-M¹⁶⁰⁶ within VWF A2 domain. Such epitope was previously reported to be cryptic on native VWF and unmasked after ADAMTS13-mediated cleavage. Furthermore, the affinity of the antibody directed against cleaved VWF was reported to be similar for monomeric and dimeric VWF fragments (14). To determine sample activity, optical density at 450 nm (OD_{450nm}) was recorded. The calibration curve was performed using serial dilution of partially proteolysed VWF obtained after ADAMTS13-cleavage of purified plasma-derived VWF (pdVWF) concentrate (Wilfactin®, LFB Les Ulis France) under denaturing conditions. A semi-quantitative analysis of VWF degradation was performed as control on this standard (see Suppl. Material, available online at www.thrombosis-online.com). Three different standard preparations were tested (see Suppl. Material, available online at www.thrombosis-online.com). OD_{450nm} obtained in samples from patients and controls were plotted against the calibration curve. VWF proteolysis rate was thus expressed as a relative percentage with the 100% of proteolysis arbitrary set for the OD_{450nm} value obtained at standard dilution 1/8. Inner assays performances were evaluated as described in additional data.

Statistical analysis

Data are expressed as mean ± SD. Statistical analysis was performed with SPSS software. When appropriate, time points were compared with a Wilcoxon rank test for paired or Mann Whitney for unpaired groups. P-values <0.05 were considered statistically significant.

Results

Assay performance

The partial proteolysis of VWF in the standard used as a calibrator was confirmed by: 1) a loss of HMW-multimers in SDS-agarose electrophoresis 2) a decrease of 225 kDa bands (uncleaved VWF) and an increase in 140 kDa and 176 kDa bands (cleaved-VWF) by immunoprecipitation /western blotting (Suppl Figure 1, available online at www.thrombosis-online.com). Three independent standard preparations were tested with reproducible results (Suppl. Figure 2, available online at www.thrombosis-online.com).

The lower detection limit (LDL) of the assay was calculated using the equation $LDL = \text{mean} + 3SD$ of the blank OD_{450nm} value. The mean OD_{450nm} value of standard's replicates diluted 1/512 was significantly higher than the mean blank OD_{450nm} value more 3 SD ($p < 0.01$, Mann Whitney test). The coefficient of variation (CV) of OD_{450nm} values of standard's replicates diluted 1/512 was 3.3%. According that the 100% of proteolysis was arbitrary set for the OD_{450nm} value obtained for standard dilution 1/8, LDL and lower quantification limit (LQL) were therefore set at 2%. Intra-assay CVs for the low and high rate of VWF proteolysis were at 7.7% and 2.3%, respectively. Inter-assay CVs for the low and high rate of VWF proteolysis were at 13.1% and 12%, respectively. The coefficient of correlation R^2 was 0.99 over the concentrations range tested for linearity experiments.

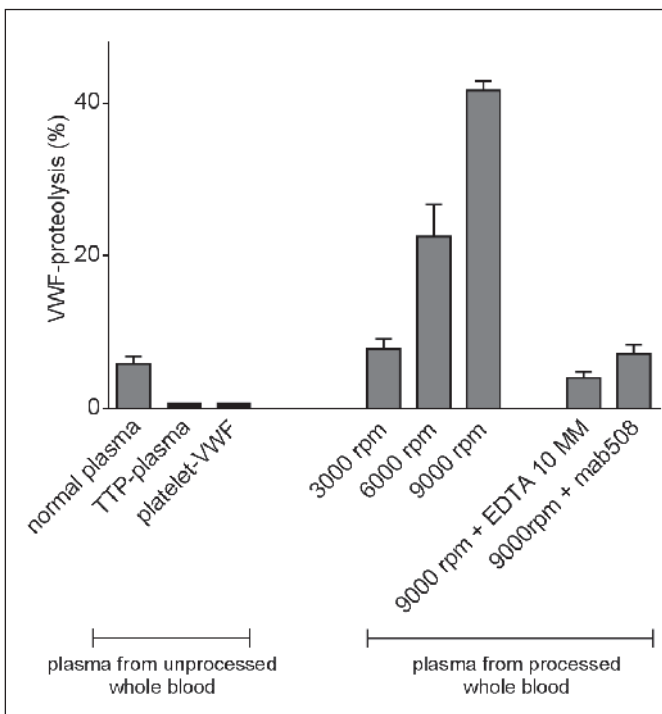


Figure 1: ELISA assessment in the LVAD-perfusion model. Whole blood from healthy donors was perfused in a mock circulatory loop model using Heartmate-II® pump at different rotor speeds (3000, 6000 and 9000 rpm, each in triplicate). Further experiments were performed at 9000 rpm in the presence of EDTA (10 mM final concentration) or an anti-VWF antibody (mAb508, 50 µg/ml final concentration), each in triplicate. Blood was sampled at baseline and 180 min after onset of perfusion. Platelet-rich plasma (PRP) was isolated from baseline samples by centrifugation (150g for 15 min) and then incubated in Triton-PBS buffer to obtain platelet lysates. Platelet-VWF was quantified using a latex-enhanced immunoturbidimetric assay (Hemosil VWF activity). All samples were centrifugated (2,000g for 15 min) for platelet-poor plasma (PPP). Platelet-VWF (range: 0.5 to 2 UI/ml final concentration) and PPP-samples (normal plasma) were assayed for VWF-proteolysis by ELISA. Data (mean ± SD of 3 independent experiments) are expressed as a percentage of VWF-proteolysis. In addition, four PPP-samples from acquired TTP-patients with severe ADAMTS13 deficiency (FRETS ADAMTS13 activity < 5%) and UL multimers of VWF in plasma were assayed for VWF-proteolysis (mean ± SD) by ELISA (TTP-plasma).

VWF-proteolysis in controls

At baseline, as expected, a low grade of VWF-proteolysis was observed in PPP-samples (plasma-VWF), whereas no proteolysis was detected in platelet lysates obtained from baseline PRP-samples (platelet-VWF) (► Figure 1). A significant relationship between VWF: Ag levels and VWF-proteolysis (%) was observed ($r=0.45$; $p < 0.001$; ► Figure 2A). Accordingly, the VWF-proteolysis (%) was lower in group-O patients when compared to non-O patients (► Table 1, ► Figure 2B) and this difference was not longer observed when results were expressed as a ratio between VWF-proteolysis (%) and VWF: Ag (VWF-proteolysis/VWF: Ag ratio; ► Table 1, ► Figure 2C).

Under shear conditions, we observed a speed-related increase in VWF-proteolysis (%) (3000 rpm: 8.6 ± 2.1 < 6000 rpm: 22.5 ± 7.3 < 9000 rpm: 41.6 ± 2.1) in PPP control samples obtained from processed whole blood of three healthy donors. This increase in VWF proteolysis rate was related to the intensity of HMW-multimers defect (3000 < 6000 < 9000 rpm, data not shown) observed on plasma samples obtained from blood used in the Heart-Mate-II® perfusion experiments. This increased proteolysis under high shear conditions (9000 rpm) was blunted by both EDTA and mAb508 (► Figure 1). No VWF-proteolysis was detected in the four acquired TTP-patients with severe ADAMTS13 deficiency (ADAMTS13 activity below 5% for all patients) (► Figure 1).

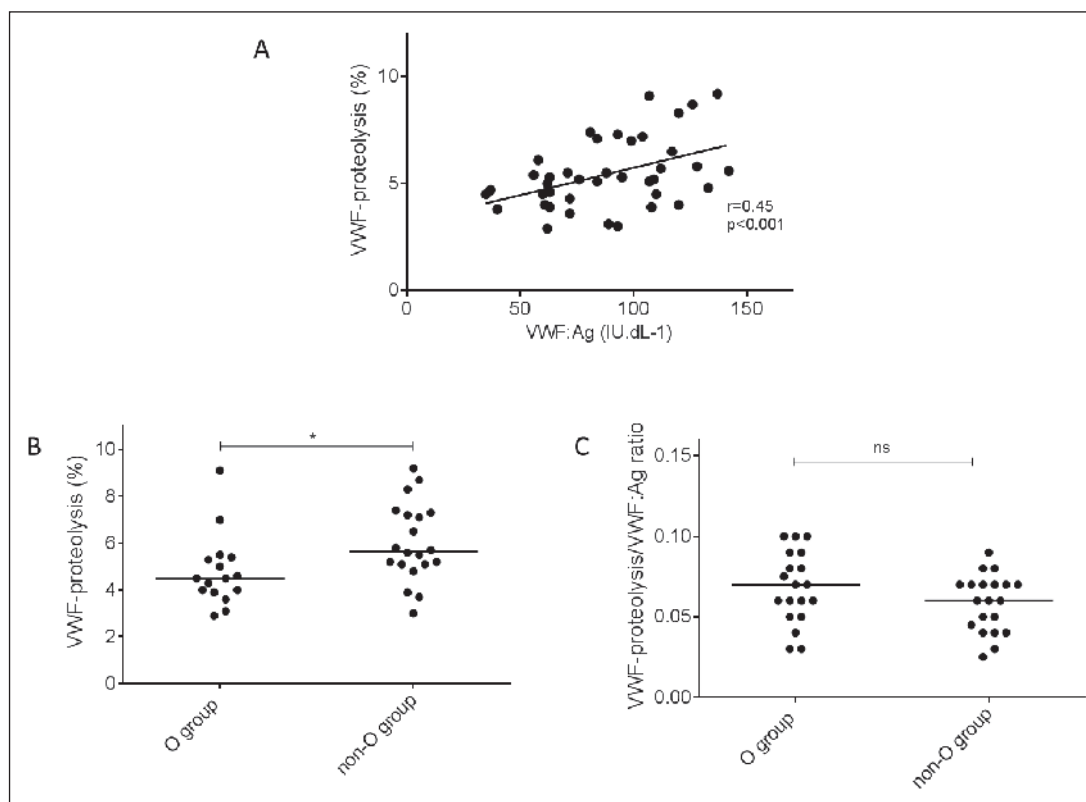
Discrimination of the different types of VWD according to the VWF-proteolysis status

A significant relation between VWF-proteolysis (%) or VWF-proteolysis/VWF: Ag ratio and the mechanism of the disease was observed in selected patients with type 2 VWD. An increase in VWF-proteolysis (%) was observed in VWD-2A(IIA) and VWD-2B when compared to control or to VWD-2A(IIE) patients (► Table 2, ► Figure 3A). The extent of VWF-proteolysis was significantly higher in these 2A(IIA) patients when compared to VWD-2B patients ($p < 0.0001$). In VWD-2B, the extent of VWF-proteolysis increased with the intensity of HMW-multimers loss ($A < B < C$) (► Figure 3C) regardless of the VWF activation state (data not shown). VWF-proteolysis was below the LQL of the assay in VWD-2A(IIE) patients. A similar discrimination between VWD-patients was obtained with VWF-proteolysis/VWF: Ag ratio (► Figure 3B, D).

Diagnosis of the mechanism in AVWS

In high shear-associated cardiovascular disorders, the extent of VWF-proteolysis (%) was significantly increased when compared to controls ($p < 0.0001$; ► Table 3, ► Figure 4A). This increase was even more pronounced for LVAD-patients when compared to AS patients ($p < 0.01$; ► Table 3, ► Figure 4A). Again, this difference remained when the data were expressed as VWF-proteolysis/VWF: Ag ratio (► Table 3, ► Figure 4B). In patients with constitutional or acquired increased clearance of VWF, VWD-Vicenza (VWFpp/VWF: Ag = 15.7 ± 7.2) and MGUS (VWFpp/VWF:

Figure 2: ELISA assessment in controls. VWF-proteolysis was assessed by ELISA in 39 healthy subjects including 19 O-group and 20 non O-group. Results are expressed as percentage of VWF-proteolysis (2A, B) and as VWF-proteolysis/VWF:Ag ratio (2C). Correlation between VWF-proteolysis and VWF:Ag was assessed by Pearson coefficient. Inter-group comparison was performed using a Mann Whitney test. $p < 0.05$ was considered as significant (*).



Ag = 15.5 ± 9.2), respectively, VWF-proteolysis (%) was dramatically reduced, when compared to controls ($p < 0.001$; ► Table 3, ► Figure 4A). A similar discrimination between AVWS-patients was observed with VWF-proteolysis/VWF: Ag ratio which was significantly increased in LVAD- and AS-patients when compared to patients with increased clearance (VWD-Vicenza and MGUS). The VWFpp/VWF: Ag mirrored the VWF-proteolysis/VWF: Ag with values significantly lower in LVAD- and AS-patients when compared to patients with increased VWF clearance (VWD-Vicenza and MGUS) (► Figure 4C).

In LVAD-patients, the extent of VWF-proteolysis assessed by the VWF-proteolysis/VWF: Ag ratio was significantly increased when analysed 3 h after implantation. This increase was observed in all patients with a six-fold increase when compared to baseline (0.27 ± 0.09 after implantation vs 0.05 ± 0.09 at baseline, $p=0.009$; ► Figure 5A). This paralleled the loss of HMW-multimers observed in all LVAD-patients. The correction of AS in patients who underwent a TAVI procedure was associated with a significant decrease in VWF-proteolysis/VWF: Ag ratio (0.06 ± 0.02 vs 0.15 ± 0.04 before TAVI, $p < 0.05$; ► Figure 5B).

Discussion

The present study aimed to develop and validate a novel ELISA-based assay to quantify VWF-proteolysis in AVWS. We present here the validation of this ELISA in a LVAD model and in a se-

lected cohort of VWD-patients according to their mutation and related mechanism. We have demonstrated in this study that this ELISA discriminates AVWS characterised by an increased VWF-proteolysis and allows a rapid quantification of proteolysis and could help to overcome some limitations of electrophoresis-based assays.

Validation of the assay

Assay validation was made both methodologically and biologically. We demonstrated an apparent consistency of the assay when using three independent standard preparations. Such reliability was further confirmed when assessing inner assay performances with acceptable ranges for intra- ($< 10\%$) and inter-assay CVs ($< 15\%$). By using appropriate controls, we demonstrated in controls that our assay is well suited to detect VWF-proteolysis.

This “physiological” proteolysis was related to the VWF: Ag level and varied according to the blood group, but was similar when expressed relatively as VWF-proteolysis/VWF: Ag ratio. No VWF-proteolysis was detected in acquired TTP-patients with severe ADAMTS13 deficiency and UL VWF multimers in plasma, used as controls. In our LVAD *ex vivo* experiments we confirmed that VWF-proteolysis was related to the shear and prevented by non-specific and specific inhibition of ADAMTS13-mediated proteolysis. Indeed, both EDTA and mAb508, an anti-VWF D4 domain, were previously reported to prevent the degradation of VWF HMW-multimers in the LVAD model (10).

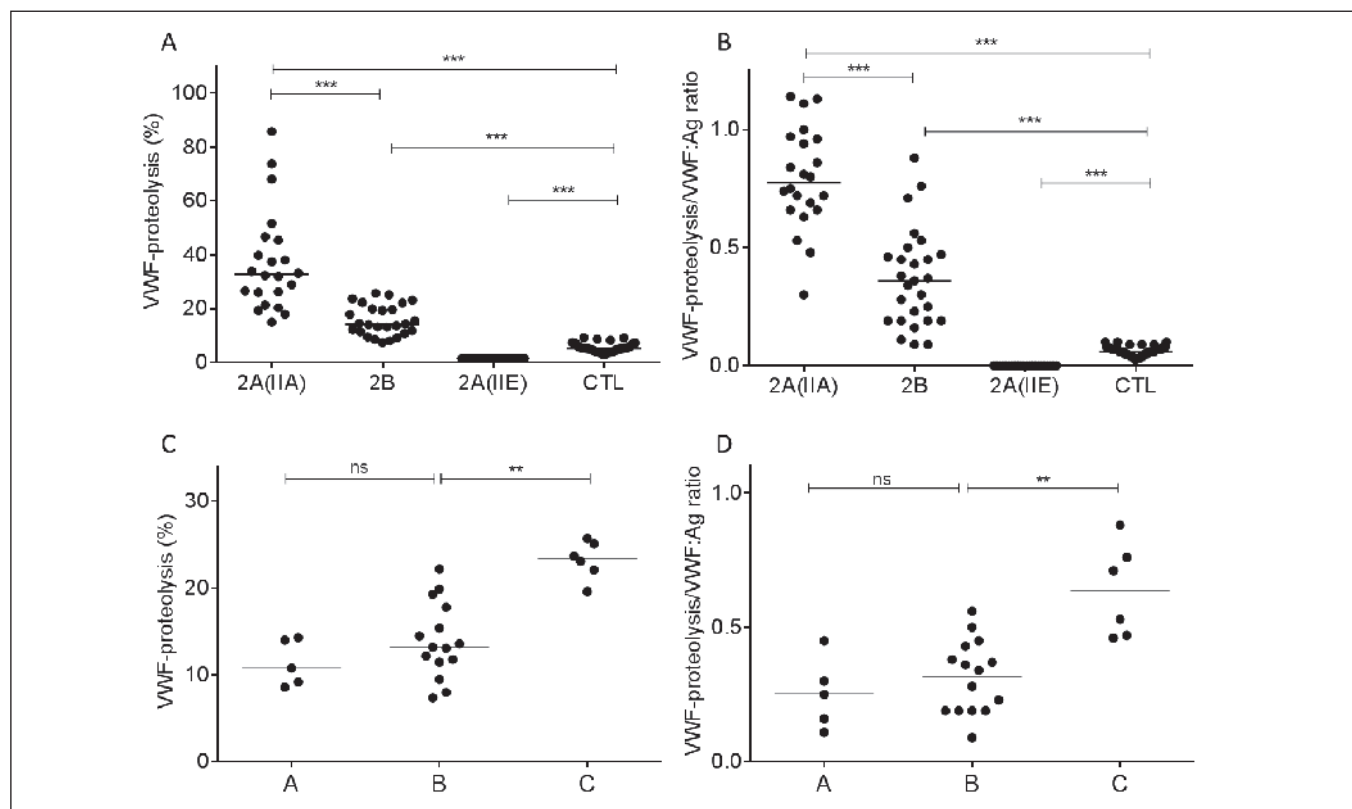


Figure 3: ELISA assessment in VWD patients. VWF-proteolysis was assessed by ELISA in VWD variants type 2A (IIA) (n=22), 2B (n=26), 2A (IIE) (n=21). Healthy subjects were used as control (n=39) (3A, 3B). VWF-proteolysis was further analysed in VWD variants type 2B according to the severity of VWF multimeric defect (3C, 3D): pattern A (partial loss of the HMW-multimers; including p. Arg1306Gln/ p.Pro1337Leu and p.Ala1461Val mutations), pattern B (complete loss of HMW-multimers; including

p.Arg1341Gln mutation) and pattern C (loss also of intermediate multimers, including p. Arg1308Cys and p.Val1316Met mutations). Results are expressed for each group as percentage of VWF-proteolysis (3A, 3C) and as VWF-proteolysis/VWF:Ag ratio (3B, 3D). Inter-group comparisons were performed using a Mann Whitney test. $p < 0.05$ was considered as significant. (* $p < 0.05$; ** $p < 0.01$; *** $p < 0.001$).

Discrimination of patients with selected forms of VWD

As expected in VWD-patients, VWF-proteolysis was significantly increased in VWD-2B and even more in VWD-2A(IIA) compared to controls. In this study, we have selectively included VWD-2A(IIA) patients with group 2 mutations, as increased VWF-proteolysis is the central pathological mechanism underlying HMW-multimers loss in these patients (15).

In VWD-2B, an increased ADAMTS13-mediated proteolysis accounts for the loss of HMW-multimers observed with some mutations (16). Indeed, a lower shear stress threshold might be required for ADAMTS13-mediated cleavage when VWF is bound to platelets compared to free VWF molecules (17, 18). We observed no correlation between VWF-proteolysis and VWF activation state in VWD-2B in accordance with a recent report showing no relationship between the level of 'active VWF' and the extent of HMW-multimers defect in VWD-2B (19). This suggests that the proportion of VWF in its platelet-binding conformation is not predictive of VWF susceptibility to ADAMTS13 proteolysis in VWD-2B. Alternatively, VWF-proteolysis was significantly de-

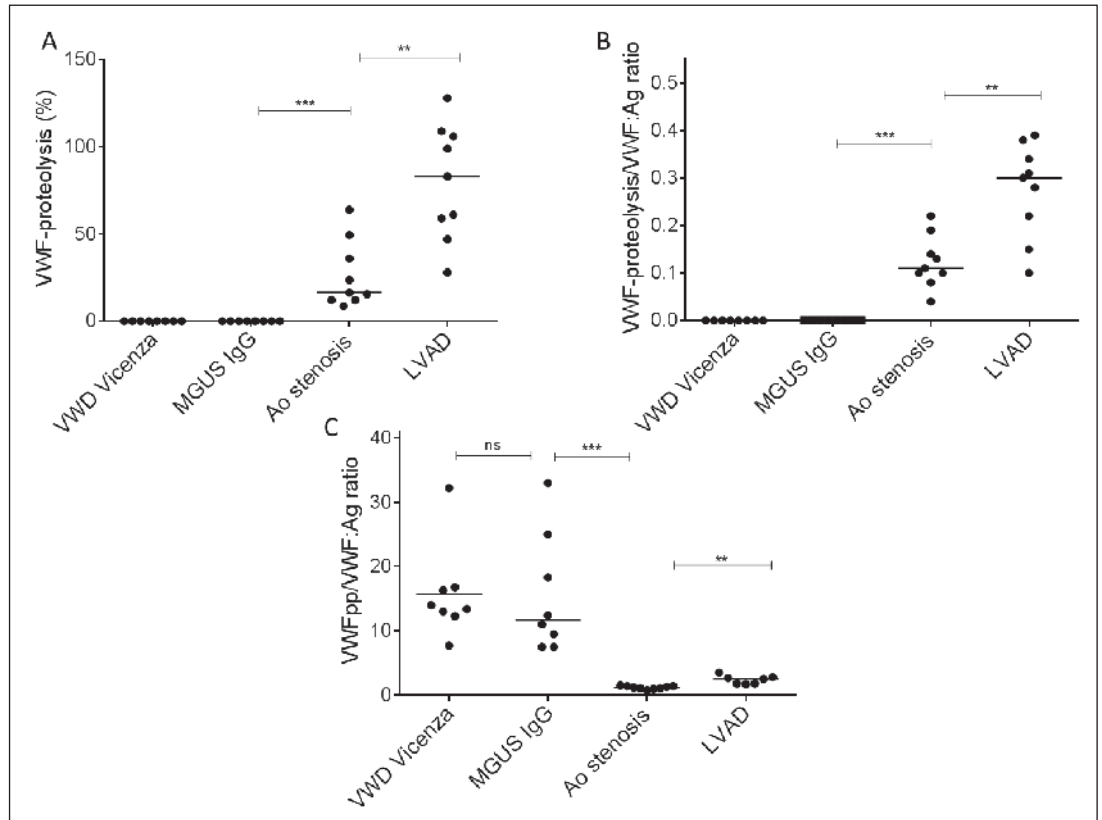
creased in VWD-2A(IIE) patients compared to controls in accordance with the decreased susceptibility of VWD-2A(IIE) variant to proteolysis reported previously (20).

Current electrophoresis-based assays are necessary to differentiate VWD subtypes 2A and 2M, after exclusion of VWD-2B and VWD-2N. In the flow-chart diagnosis of VWD, an ELISA-based assessment of VWF-proteolysis could be used, after exclusion of VWD-2B and VWD-2N, to provide an easier and rapid identification of most VWD-2A patients, i.e. VWD-2A(IIA) and VWF-2A(IIE) variants with autosomal inheritance. This point may be clinically relevant since a higher bleeding incidence was recently reported in VWD-2A patients compared to others type 2 variants (21). However, a larger prospective study on unselected VWD-patients will be required before assay implementation to determine the cut-off values allowing a good discrimination of VWD variants based on modification of VWF-proteolysis.

Diagnosis of AVWS

This ELISA provides a rapid identification of AVWS associated with aortic stenosis and LVAD therapy, two conditions associated

Figure 4: ELISA assessment in AVWS-patients. VWF-proteolysis was assessed by ELISA in AS-patients (n=9), LVAD-patients (n=9) and MGUS IgG-patients (n=8). VWD-Vicenza patients were included as controls of increased clearance. Results are expressed for each group as percentage of VWF-proteolysis (4A) and as VWF-proteolysis/VWF:Ag ratio (4B). Inter-group comparisons were performed using a Mann Whitney test. $p < 0.05$ was considered as significant (* $p < 0.05$; ** $p < 0.01$; *** $p < 0.001$).



with an increased VWF-proteolysis. VWF impairment through proteolysis of its HMW-multimers is a common finding in severe aortic stenosis (3) and LVAD therapy (6), and is also observed in other high shear cardiac disorders (22, 23) reported to induce the unfolding of circulating VWF molecules and their proteolysis by the specific VWF protease ADAMTS13.

This enhanced proteolysis of the largest VWF multimers is thought to account for the increased prevalence of gastrointestinal bleedings (GI) from angiodysplasia in these high shear cardiac disorders (24). The classical management of GI bleeding occurring in this setting of Heyde's syndrome is challenging as illustrated by the high rate of bleeding recurrence after endoscopic therapy. The treatment of the underlying cardiac lesion might represent the op-

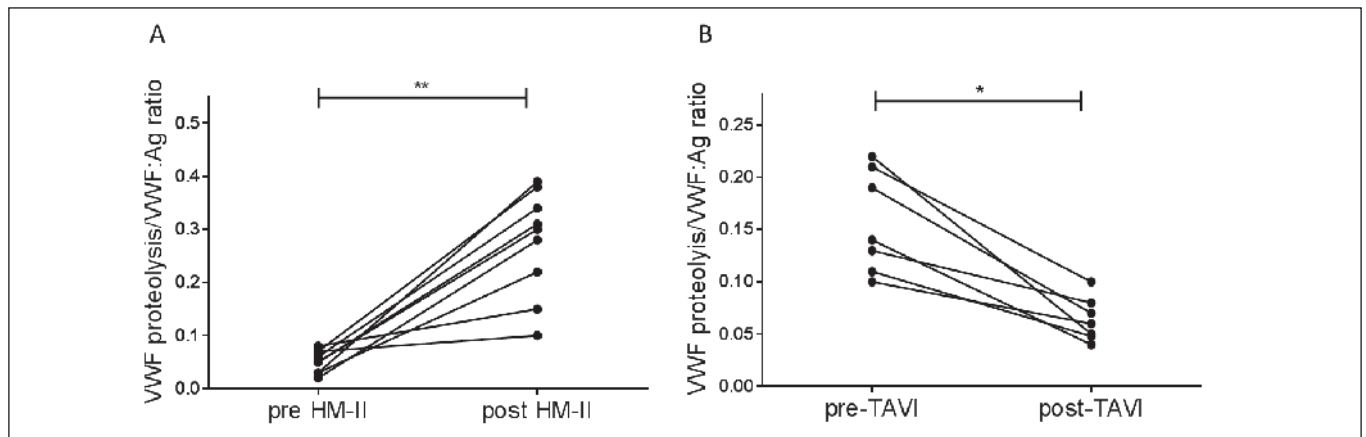


Figure 5: Dynamic assessment of VWF-proteolysis in HeartMate-II® LVAD-patients before and early after device implantation and in AS-patients undergoing TAVI procedure. Nine consecutive LVAD-patients were evaluated before and 3 h after LVAD HeartMate-II® implantation for HMW-multimers by SDS-agarose 1.4% electrophoresis and for VWF-pro-

teolysis by ELISA (5A). Seven AS-patients were assayed for VWF-proteolysis by ELISA before and after correction of aortic valve stenosis with TAVI procedure (5B). Results are expressed for each group as VWF-proteolysis/VWF:Ag ratio. Statistical analysis was performed using two-tailed Wilcoxon rank test. $p < 0.05$ was considered as significant (* $p < 0.05$; ** $p < 0.01$).

What is known about this topic?

- Electrophoresis is currently essential for VWD typing and AVWS diagnosis.
- Electrophoresis-based assays are sometimes not adapted to medical needs in these settings.

What does this paper add?

- We report a new ELISA for a simplified and reliable diagnosis of VWD and AVWS with increased VWF-proteolysis
- Such assay might improve the diagnosis and management of AVWS potentially in a time frame acceptable for emergency situations.

timal management to stop GI bleedings in this subset of patients (25, 26), but the diagnosis of Heyde's syndrome is challenging in the absence of a widespread biological assay. In the setting of recurrent GI bleeding refractory to endoscopic therapy, we speculate that an ELISA-based assessment of an increased VWF-proteolysis could reflect the presence of a high shear cardiac disorder associated with Heyde's syndrome.

The diagnosis and management of AVWS under mechanical circulatory support often remains an unmet medical need. Whereas HMW-multimers proteolysis seems to occur in all patients with continuous-flow devices (6), little is known about its real prevalence under ECMO support or pulsatile biventricular support (27). Furthermore, this ELISA represents a real standardised quantification tool of VWF-proteolysis in comparison with electrophoresis-based assessment of HMW-multimers. Our assay might help to screen more rapidly for AVWS under mechanical circulatory support, given the potential of such an ELISA method to be more widely used than current VWF electrophoresis-based assays. Such early diagnosis of AVWS could improve the medical management of bleeding complications observed under LVAD therapy. It seems also that, in patients undergoing a TAVI-procedure for AS, this

Abbreviations

ADAMTS13=a disintegrin and metalloproteinase with a thrombospondin type 1 motif, member 13; AS=aortic stenosis; AVWS=acquired von Willebrand syndrome; CV=coefficient of variation; ECMO=extracorporeal membrane oxygenation; EDTA=Ethylenediaminetetraacetic acid; ELISA=enzyme-linked immunosorbent assay; HMW-multimers=high molecular weight multimers; LDL=lower detection limit; LQL=lower quantification limit; LVAD=left ventricular assist device; MGUS=Monoclonal gammopathy of undetermined significance; OD=optical density; PBS=phosphate buffered saline; PPP=platelet-poor plasma; PRP=platelet-rich plasma; SD=standard deviation; VWD=von Willebrand disease; VWF=von Willebrand factor.

assay could provide a potential useful tool to monitor the success of valve implantation. First-line management of GI bleedings in LVAD patients, relying on adaptation of antithrombotic therapy and digestive endoscopic revision for local haemostasis (28), is often inefficient to prevent bleeding recurrence (29). Strategies based on the reduction of the speed of the LVAD rotor and/or off-label use of pure VWF concentrates have been reported as effective to control severe bleedings (28, 30). These strategies are, however, at potential risk (haemodynamic instability, thrombosis) for LVAD patients (31) and should only be considered once the diagnosis of AVWS is confirmed. Moreover, this ELISA assay might be of interest to tailor LVAD speed or VWF concentrates infusion in LVAD carriers with GI bleedings.

Clinical implications

This ELISA proteolysis assay allows to identify and to discriminate different forms of VWD and AVWS according to their mechanisms and their impact on VWF proteolysis. Although we can not completely exclude that the affinity of the antibody directed against cleaved VWF may be reduced for the largest multimers, the ELISA provides a reliable quantitative analysis of VWF proteolysis, potentially in a time frame acceptable for emergency situations. An early diagnosis of AVWS could improve the medical management of bleeding complications observed under LVAD therapy. Alternatively, the documentation of correction of VWF proteolysis at an individual level might be also of major area of interest in particular after correction of aortic stenosis. The implementation of this ELISA could open the door for a biological and "real-time" monitoring of TAVI-procedure and mechanical circulatory support.

Acknowledgements

We would like to thank Sophie Capdenat (Hôpital Lariboisière, APHP, Paris), Hélène Mandard (Hôpital Bicêtre, APHP, Paris) and Catherine Marichez (CHU de Lille, Lille) for their assistance in collecting the data. We would also like to thank Pascale Renom, Véronique Tintillier, Nathalie Trillot and Bénédicte Wibaut (CHU Lille, Lille) for their assistance in recruiting AVWS. We would like to thank Paulette Legendre (Inserm U1176, Kremlin Bicêtre) who performed the nanobody experiments.

Author contributions

AR designed research, performed the experiments, analysed data, wrote and reviewed the manuscript. CC, FV and EJ designed research, performed the experiments and analysed data. CT, PB, CZ, EF, ABD, CLB, AV included patients and analysed data. AVi, EVB, PJJ and JG designed research and reviewed the manuscript. SS supervised and designed research, analysed data, wrote and reviewed the manuscript.

Conflicts of interest

C.T has received support for attending scientific meetings and honoraria (consultant in advisory boards) from Baxalta, Bayer HealthCare, LFB, Novo Nordisk, BMS/Pfizer, CSL-Behring (none

of these relate to this study). J.G. has received support for attending scientific meetings and honoraria (speaker fees/consultant in advisory boards) from Baxalta, Bayer HealthCare, LFB, Novo Nordisk, Pfizer and Sobi; has been an investigator in studies sponsored by Baxter, LFB, Novo Nordisk, and Pfizer; and has received research support from Novo Nordisk and CSL Behring (none of these relate to this study). S.S. has received support for attending scientific meetings and honoraria (speaker fees/consultant in advisory boards) from Baxalta, Bayer HealthCare, LFB, Novo Nordisk, BMS-Pfizer; Boehringer, CSL-Behring, Stago and Carmat and has been an investigator in studies sponsored by LFB and Boehringer (none of these relate to this study). The remaining authors declare no competing financial interests.

References

- Zimmerman TS, Dent JA, Ruggeri ZM et al. Subunit composition of plasma von Willebrand factor. Cleavage is present in normal individuals, increased in IIA and IIB von Willebrand disease, but minimal in variants with aberrant structure of individual oligomers (types IIC, IID, and IIE). *J Clin Invest* 1986; 77: 947–951.
- Hassenpflug WA, Budde U, Obser T et al. Impact of mutations in the von Willebrand factor A2 domain on ADAMTS13-dependent proteolysis. *Blood* 2006; 107: 2339–2345.
- Vincentelli A, Susen S, Le Tourneau T, et al. Acquired von Willebrand syndrome in aortic stenosis. *N Engl J Med* 2003; 349: 343–349.
- Van Belle E, Rauch A, Vincentelli A et al. Von Willebrand factor as a biological sensor of blood flow to monitor percutaneous aortic valve interventions. *Circ Res* 2015; 116: 1193–1201.
- Crow S, John R, Boyle A et al. Gastrointestinal bleeding rates in recipients of nonpulsatile and pulsatile left ventricular assist devices. *J Thorac Cardiovasc Surg* 2009; 137: 208–215.
- Meyer AL, Malehsa D, Budde U et al. Acquired von Willebrand syndrome in patients with a centrifugal or axial continuous flow left ventricular assist device. *JACC Heart Fail* 2014; 2: 141–145.
- Goldstein DJ, Aaronson KD, Tatoes AJ et al. Gastrointestinal bleeding in recipients of the HeartWare Ventricular Assist System. *JACC Heart Fail* 2015; 3: 303–313.
- Boisseau P, Ternisien C, Caron C et al. Incidence of large VWF gene deletions and duplications in the french cohort of 1182 patients with von Willebrand disease (VWD). *Journal of thrombosis and haemostasis: J Thromb Haemost* 2013; 11 (Suppl 2): 116.
- Federici AB, Mannucci PM, Castaman G et al. Clinical and molecular predictors of thrombocytopenia and risk of bleeding in patients with von Willebrand disease type 2B: a cohort study of 67 patients. *Blood* 2009; 113: 526–534.
- Rauch A, Legendre P, Christophe OD et al. Antibody-based prevention of von Willebrand factor degradation mediated by circulatory assist devices. *Thromb Haemost* 2014; 112: 1014–1023.
- Favaloro EJ, Henniker A, Facey D et al. Discrimination of von Willebrand disease (VWD) subtypes: direct comparison of von Willebrand factor: collagen binding assay (VWF: CBA) with monoclonal antibody (MAB) based VWF-capture systems. *Thromb Haemost* 2000; 84: 541–547.
- Hulstein JJ, De Groot PJ, Silence K et al. A novel nanobody that detects the gain-of-function phenotype of von Willebrand factor in ADAMTS13 deficiency and von Willebrand disease type 2B. *Blood* 2005; 106: 3035–3042.
- Kato S, Matsumoto M, Matsuyama T et al. Novel monoclonal antibody-based enzyme immunoassay for determining plasma levels of ADAMTS13 activity. *Transfusion* 2006; 46: 1444–1452.
- Moatti-Cohen M, Garrec C, Wolf M et al. Unexpected frequency of Upshaw-Schulman syndrome in pregnancy-onset thrombotic thrombocytopenic purpura. *Blood* 2012; 119: 5888–5897.
- Jacobi PM, Gill JC, Flood VH et al. Intersection of mechanisms of type 2A VWD through defects in VWF multimerization, secretion, ADAMTS-13 susceptibility, and regulated storage. *Blood* 2012; 119: 4543–4553.
- Rayes J, Hollestelle MJ, Legendre P et al. Mutation and ADAMTS13-dependent modulation of disease severity in a mouse model for von Willebrand disease type 2B. *Blood* 2010; 115: 4870–4877.
- Shim K, Anderson PJ, Tuley EA et al. Platelet-VWF complexes are preferred substrates of ADAMTS13 under fluid shear stress. *Blood* 2008; 111: 651–657.
- Springer TA. von Willebrand factor, Jedi knight of the bloodstream. *Blood* 2014; 124: 1412–1425.
- Casonato A, Pontara E, Morpurgo M et al. Higher and lower active circulating VWF levels: different facets of von Willebrand disease. *Br J Haematol* 2015; Epub ahead of print.
- Schneppenheim R, Michiels JJ, Obser T et al. A cluster of mutations in the D3 domain of von Willebrand factor correlates with a distinct subgroup of von Willebrand disease: type 2A/IIIE. *Blood* 2010; 115: 4894–4901.
- Federici AB, Bucciarelli P, Castaman G et al. The bleeding score predicts clinical outcomes and replacement therapy in adults with von Willebrand disease. *Blood* 2014; 123: 4037–4044.
- Blackshear JL, Wysokinska EM, Safford RE et al. Shear stress-associated acquired von Willebrand syndrome in patients with mitral regurgitation. *J Thromb Haemost* 2014; 12: 1966–1974.
- Le Tourneau T, Susen S, Caron C et al. Functional impairment of von Willebrand factor in hypertrophic cardiomyopathy: relation to rest and exercise obstruction. *Circulation* 2008; 118: 1550–1557.
- Loscalzo J. From clinical observation to mechanism--Heyde's syndrome. *N Engl J Med* 2012; 367: 1954–1956.
- Jackson CS, Gerson LB. Management of gastrointestinal angiodysplastic lesions (GIADs): a systematic review and meta-analysis. *Am J Gastroenterol* 2014; 109: 474–483.
- Blackshear JL, Stark ME, Agnew RC et al. Remission of recurrent gastrointestinal bleeding after septal reduction therapy in patients with hypertrophic obstructive cardiomyopathy-associated acquired von Willebrand syndrome. *J Thromb Haemost* 2015; 13: 191–196.
- Heilmann C, Geisen U, Beyersdorf F et al. Acquired von Willebrand syndrome in patients with ventricular assist device or total artificial heart. *Thromb Haemost* 2010; 103: 962–967.
- Feldman D, Pamboukian SV, Teuteberg JJ et al. The 2013 International Society for Heart and Lung Transplantation Guidelines for mechanical circulatory support: executive summary. *J Heart Lung Transplant* 2013; 32: 157–187.
- Bunte MC, Blackstone EH, Thuita L et al. Major bleeding during HeartMate II support. *J Am Coll Cardiol* 2013; 62: 2188–2196.
- Fischer Q, Huisse MG, Voiriot G et al. Von Willebrand factor, a versatile player in gastrointestinal bleeding in left ventricular assist device recipients? *Transfusion* 2014; 55: 51–54.
- Starling RC, Moazami N, Silvestry SC et al. Unexpected abrupt increase in left ventricular assist device thrombosis. *N Engl J Med* 2014; 370: 33–40.

von Willebrand Factor as a Biological Sensor of Blood Flow to Monitor Percutaneous Aortic Valve Interventions

Eric Van Belle,* Antoine Rauch,* André Vincentelli, Emmanuelle Jeanpierre, Paulette Legendre, Francis Juthier, Christopher Hurt, Carlo Banfi, Natacha Rousse, Anne Godier, Claudine Caron, Ahmed Elkalioubie, Delphine Corseaux, Annabelle Dupont, Christophe Zawadzki, Cédric Delhaye, Frédéric Mouquet, Guillaume Schurtz, Dominique Deplanque, Giulia Chinetti, Bart Staels, Jenny Goudemand, Brigitte Jude, Peter J. Lenting, Sophie Susen

Rationale: Percutaneous aortic valve procedures are a major breakthrough in the management of patients with aortic stenosis. Residual gradient and residual aortic regurgitation are major predictors of midterm and long-term outcome after percutaneous aortic valve procedures. We hypothesized that (1) induction/recovery of high molecular weight (HMW) multimers of von Willebrand factor defect could be instantaneous after acute changes in blood flow, (2) a bedside point-of-care assay (platelet function analyzer-closure time adenine DI-phosphate [PFA-CADP]), reflecting HMW multimers changes, could be used to monitor in real-time percutaneous aortic valve procedures.

Objective: To investigate the time course of HMW multimers changes in models and patients with instantaneous induction/reversal of pathological high shear and its related bedside assessment.

Methods and Results: We investigated the time course of the induction/recovery of HMW multimers defects under instantaneous changes in shear stress in an aortic stenosis rabbit model and in patients undergoing implantation of a continuous flow left ventricular assist device. We further investigated the recovery of HMW multimers and monitored these changes with PFA-CADP in aortic stenosis patients undergoing transcatheter aortic valve implantation or balloon valvuloplasty. Experiments in the aortic stenosis rabbit model and in left ventricular assist device patients demonstrated that induction/recovery of HMW multimers occurs within 5 minutes. Transcatheter aortic valve implantation patients experienced an acute decrease in shear stress and a recovery of HMW multimers within minutes of implantation which was sustained overtime. In patients with residual high shear or with residual aortic regurgitation, no recovery of HMW multimers was observed. PFA-CADP profiles mimicked HMW multimers recovery both in transcatheter aortic valve implantation patients without aortic regurgitation (correction) and transcatheter aortic valve implantation patients with aortic regurgitation or balloon valvuloplasty patients (no correction).

Conclusions: These results demonstrate that variations in von Willebrand factor multimeric pattern are highly dynamic, occurring within minutes after changes in blood flow. It also demonstrates that PFA-CADP can evaluate in real time the results of transcatheter aortic valve procedures. (*Circ Res.* 2015;116:1193-1201. DOI: 10.1161/CIRCRESAHA.116.305046.)

Key Words: aortic valve stenosis ■ blood flow velocity ■ von Willebrand factor

Percutaneous aortic valve procedures, including transcatheter aortic valve implantation (TAVI) and balloon aortic valvuloplasty (BAV), are recent major breakthrough in the management of patients with aortic stenosis (AS).^{1,2} In some circumstances their results can still be inadequate, whereas

their evaluation in real-time may remain difficult with current techniques.³ Among examples are the cases of balloon valvuloplasty procedures and valve-in-valve TAVI procedures, where an insufficient opening of the valve and a high residual gradient can still be observed or the cases of periprocedural

Original received August 18, 2014; revision received February 2, 2015; accepted February 10, 2015. In January 2015, the average time from submission to first decision for all original research papers submitted to *Circulation Research* was 14.7 days.

From the Department of Cardiology, Lille University Hospital, Lille, France (E.V.B., A.V., F.J., C.H., C.B., N.R., C.D., G.S., D.D.); INSERM UMR 1011, Univ Lille 2, Institut Pasteur de Lille, EGID, Lille, France (E.V.B., A.R., A.V., E.J., F.J., C.B., N.R., C.C., A.E., D.C., A.D., C.Z., G.C., B.S., J.G., B.J., S.S.); Department of Hematology, Transfusion Lille University Hospital, Lille, France (A.R., E.J., C.C., A.E., C.Z., F.M., J.G., B.J., S.S.); INSERM U1176 and UMR_S1176, Univ Paris-Sud, Le Kremlin Bicêtre, France (P.L., P.J.L.); and INSERM UMR 1140, Paris, France (A.G.).

*These authors contributed equally to this article.

The online-only Data Supplement is available with this article at <http://circres.ahajournals.org/lookup/suppl/doi:10.1161/CIRCRESAHA.116.305046/-/DC1>.

Correspondence to Sophie Susen, MD, PhD, Centre de Biologie Pathologie, Centre Hospitalier Régional, 59037 Lille Cedex, France. E-mail sophiesusen@aol.com
© 2015 American Heart Association, Inc.

Circulation Research is available at <http://circres.ahajournals.org>

DOI: 10.1161/CIRCRESAHA.116.305046

Nonstandard Abbreviations and Acronyms

AR	aortic regurgitation
AS	aortic stenosis
BAV	balloon aortic valvuloplasty
HMW	high molecular weight
IMW	intermediate molecular weight
LMW	low molecular weight
LVAD	left ventricular assist device
PFA-CADP	platelet function analyzer-closure time adenine DI-phosphate
TAVI	transcatheter aortic valve implantation
VWF	von Willebrand factor
VWF:Ag	VWF antigen
VWFpp	VWF propeptide

aortic regurgitation (AR) observed in 10% to 30% of TAVI procedures with current techniques.^{1,2}

Acquired deficiency of von Willebrand factor (VWF), characterized by a loss of high molecular weight (HMW) multimers, is associated with cardiovascular disorders in which the entire blood volume is exposed to high shear stress.⁴⁻⁹ It has been demonstrated that acquired VWF deficiency can be detected within days after implantation of an axial continuous flow left ventricular assist device (LVAD).¹⁰ We and others^{11,12} also demonstrated that the VWF deficiency present in patients with AS is corrected within days after its surgical treatment. Based on *in vitro* studies, it was inferred that unfolding and cleavage of the VWF A2 domain *in vivo* could occur within 200 seconds in response to acute changes in shear conditions.¹³ However, the initial time course of loss/recovery of VWF HMW multimers after acute changes in blood flow *in vivo* has not yet been studied.

PFA-closure time ADP (CADP) is a highly sensitive way to screen for HMW multimers defects¹⁴ and has been shown to be prolonged in patients with high shear-cardiovascular disorders including those with AS.^{6,11,15} As PFA-CADP can be assessed by a small whole blood analyzer (PFA-100) it has the potential to be used as a bedside monitor of HMW multimers changes.

We hypothesized that induction/recovery of HMW multimers defect could occur within minutes of acute changes in blood flow induced by cardiac interventions and we further investigated the potential underlying mechanisms. We also hypothesized that HMW multimers recovery, as assessed by PFA-CADP, could be used to monitor in real time the results of transcatheter aortic valve procedures, including the presence of a high postprocedural aortic gradient and the presence of a significant postprocedural AR. To evaluate these hypotheses *in vivo*, we investigated the time course of HMW multimers loss/recovery in an animal model of reversible AS specifically developed for that purpose. We further investigated the time course of HMW multimers loss/recovery and its related bedside whole blood assessment (PFA-100 analyzer) in 38 patients included in a prospective registry and undergoing (1) implantation of an axial continuous flow LVAD (HeartMate-II, n=8) for heart failure and (2) transcatheter aortic valve procedures, either BAV (n=10) or TAVI (n=20), to treat AS.

Methods**Instantaneous Induction and Reversion of High Shear Stress in a Rabbit Model of Reversible AS**

We developed a new rabbit model of instantaneous, reversible, calibrated supra-AS, adapted from Assad et al¹⁶ and Godier et al¹⁷ (see Methods in the Online Data Supplement). This model allowed the evaluation in the same rabbit, of the dynamic time course of loss and recovery of HMW multimers. In each rabbit (n=17), blood was sampled, before (T0) and after the induction of AS (5 and 30 minutes). Then the stenosis was reversed 30 minutes after its induction and blood was sampled 5 and 30 minutes after reversion (35 and 60 minutes).

Prospective Patients Registry

After approval from the local ethics committee, we performed a prospective registry of patients undergoing HeartMate-II implantation or percutaneous aortic valve intervention, including clinical data collection and blood sampling during the procedure. All patients provided informed written consent and were included in the Willebrand TAVI registry.

Induction of High Shear Stress in Patients Undergoing Implantation of HeartMate-II LVAD

HeartMate-II (Thoratec Corp, Pleasanton, CA) is an axial continuous flow LVAD. A time course of VWF multimeric analysis was performed *in vivo* in 8 consecutive patients at the time of initiation of HeartMate-II support. Samples were collected before (T0) and after initiation of HeartMate-II support at 9000 rpm (5, 30, and 180 minutes).

Reversion of High Shear Stress in Patients With AS Undergoing Transcatheter Aortic Valve Procedure

A time course of HMW multimers analysis and its related whole blood assessment (PFA-CADP) was performed *in vivo* in 30 patients with severe aortic valve stenosis in stable clinical condition, with a clinical need for either TAVI (n=20) or BAV (n=10) procedures. Both procedures were performed through a percutaneous transfemoral approach according to standard practice, whereas TAVI was performed with the Edwards-Sapien XT device.^{2,3,18} Samples were collected before (0) and after the procedure (5, 30, and 180 minutes and week 4).

Evaluation of shear stress conditions, including aortic velocity and gradient and postprocedural AR, was performed by a transthoracic echocardiography performed before and 24 hours after the procedure. The presence of a significant postprocedural AR was defined as the presence of an AR moderate or greater according to the VARC2 (valve academic research consortium) classification.¹⁹

Induction of High Shear Stress *In Vitro* Using a HeartMate-II Assist Device Model

Using an *in vitro* HeartMate-II model, we first investigated the kinetics of HMW multimers loss and recovery in the absence of endothelium. For each experiment, human blood (either heparinized or citrated) from healthy donors was perfused in a tubing system using a circulatory flowing pump device in which the HeartMate-II was the pump. Because the results of the experiments performed using heparinized or citrated blood were similar, they are presented together. The HeartMate-II rotor was set to high shear (9000 rpm), as achieved in patients implanted with HeartMate-II or to low shear (3000 rpm).

We further assessed the role of VWF proteolysis as a mechanism underlying the loss of HMW multimers in this model (see Methods in the Online Data Supplement).

Laboratory Assessment

VWF antigen (VWF:Ag; Sta Liatest, Diagnostica Stago, Inc) and VWF propeptide (VWFpp; Lifecodes VWF & Propeptide Assay, Gen-probe) levels were measured by ELISA. VWF activity was assessed by a latex immunoturbidimetric assay (Innovance VWF Ac; Siemens Healthcare Diagnostics, Marburg, Germany). As our aim was to detect changes in HMW multimers, we chose to perform

experiments using gels with low agarose concentrations.^{20,21} VWF multimeric analysis was performed as previously described.¹¹ The results are expressed as a ratio to normal pooled plasma (standard human plasma Siemens Healthcare Diagnostics, Marburg, Germany). Immunoprecipitation/Western blot analysis was performed to measure VWF proteolysis fragments (176 and 140 kDa; see Methods in the Online Data Supplement).

PFA-CADP was assessed by platelet-function analyzer PFA-100, (Siemens Healthcare Diagnostics, Marburg, Germany) using ADP cartridges (PFA-CADP, normal range, 68–121 seconds) as previously described.^{11,14}

VWF:Ag and VWF multimeric analysis were newly developed for rabbits. Loading of the electrophoretic gels was normalized for VWF:Ag content. The results are expressed as relative to baseline values determined for each animal.

Statistical Analysis

Data were expressed as mean (\pm SD), unless indicated otherwise. Multiple time comparisons were performed using repeated measures of 1-way ANOVA. When appropriate, time points were compared with a Wilcoxon rank test for paired or Mann–Whitney for unpaired groups. *P* values <0.05 were considered statistically significant.

Results

Instantaneous Induction and Reversion of High Shear Stress in a Rabbit Model of Reversible AS

In the AS-rabbit model, a significant decrease in HMW multimers was observed 5 minutes (0.76 ± 0.13 ; $P<0.01$) and further 30 minutes (0.74 ± 0.07 ; $P<0.01$) after stenosis induction when compared with baseline values (Figure 1). Conversely, a significant increase in HMW multimers was already observed 5 minutes after reversion of the stenosis (0.89 ± 0.12 ; $P<0.01$). Thirty minutes after the reversion, a complete recovery of HMW multimers was observed (0.98 ± 0.10 ; Figure 1).

Rapid Loss of HMW Multimers After Induction of High Shear Stress in Patients Undergoing HeartMate-II Implantation

The kinetics of HMW multimers loss in human blood was studied at the time of HeartMate-II implantation in 8 consecutive patients (6 men and 2 women, aged 59 ± 12 years). A significant time-dependent loss of HMW multimers was observed after initiating the pump (rotor set ≈ 9000 rpm) reaching 0.86 ± 0.37 , 0.69 ± 0.32 , and 0.48 ± 0.18 at 5, 30, and 180 minutes, respectively ($P<0.01$; Figure 2C and 2D). A significant time-dependent increase in intermediate (I) plus low (L) MW mirroring the loss of HMW multimers was observed reaching 1.11 ± 0.11 at 180 minutes compared with 1.01 ± 0.08 at baseline ($P<0.05$). Consistent with the loss of HMW multimers, a time-dependent decrease in VWF collagen-binding activity/VWF:Ag ratio was also observed reaching 0.75 ± 0.22 at 180 mm versus 0.88 ± 0.18 at baseline ($P<0.05$).

These findings were further investigated in the in vitro HeartMate-II model. In the in vitro HeartMate-II-model, when whole human blood was submitted to high shear stress (rotor set at 9000 rpm), a progressive and time-dependent loss of HMW multimers was also observed. The loss of HMW multimers was more pronounced after 5 minutes than in LVAD patients and was complete after 180 minutes ($P<0.0001$; Figure 2A and 2B). The role of VWF proteolysis was verified by (1) a time-dependent increase in specific VWF proteolytic fragments (140 and 176 kDa) in patients (Online Figure IA) and (2) an absence of time-dependent loss of HMW multimers when spiking EDTA before pump initiation in vitro (Online Figure IB). The shear dependency of HMW multimers loss was also verified by setting the rotor of HeartMate-II at 3000 rpm (Online Figure IC).

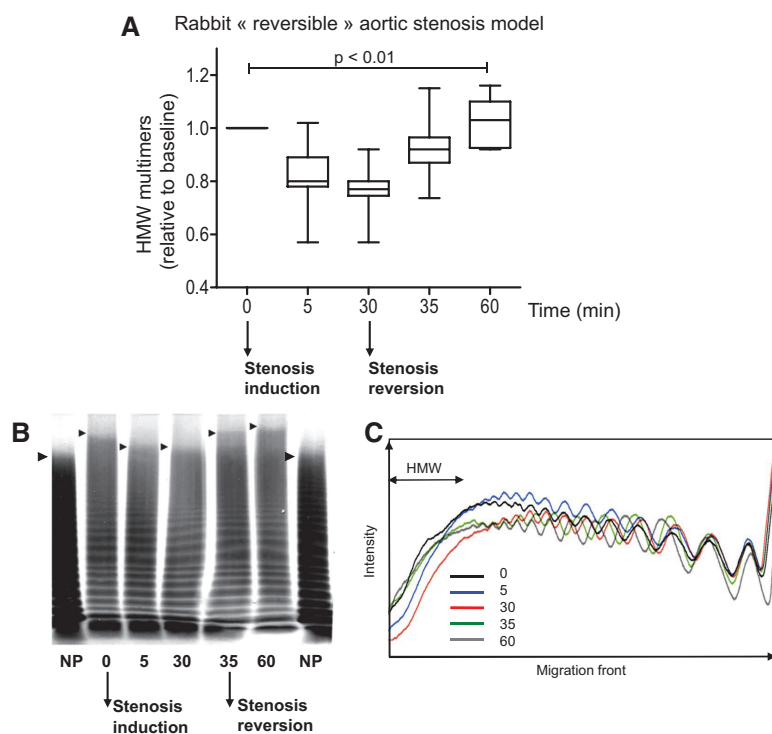


Figure 1. Dynamic loss and recovery of high molecular weight (HMW) multimers in a rabbit reversible aortic stenosis model. **A**, Quantitative analysis of HMW multimers (relative to baseline) after induction and reversion of aortic stenosis (repeated ANOVA, $P<0.01$ overall; $n=17$). Significant loss of HMW multimers 5 and 30 minutes after induction of stenosis ($P<0.01$ vs baseline) and immediate recovery 5 minutes and 30 minutes after reversion of stenosis ($P<0.01$ vs 30 minutes after induction) were observed. **B**, Representative profile of von Willebrand factor multimeric patterns at the different time points after induction and reversion of stenosis in 1 rabbit. **C**, Densitometric analysis of electrophoretic gel image (black arrows indicate the front of migration). NP indicates normal human pooled plasma.

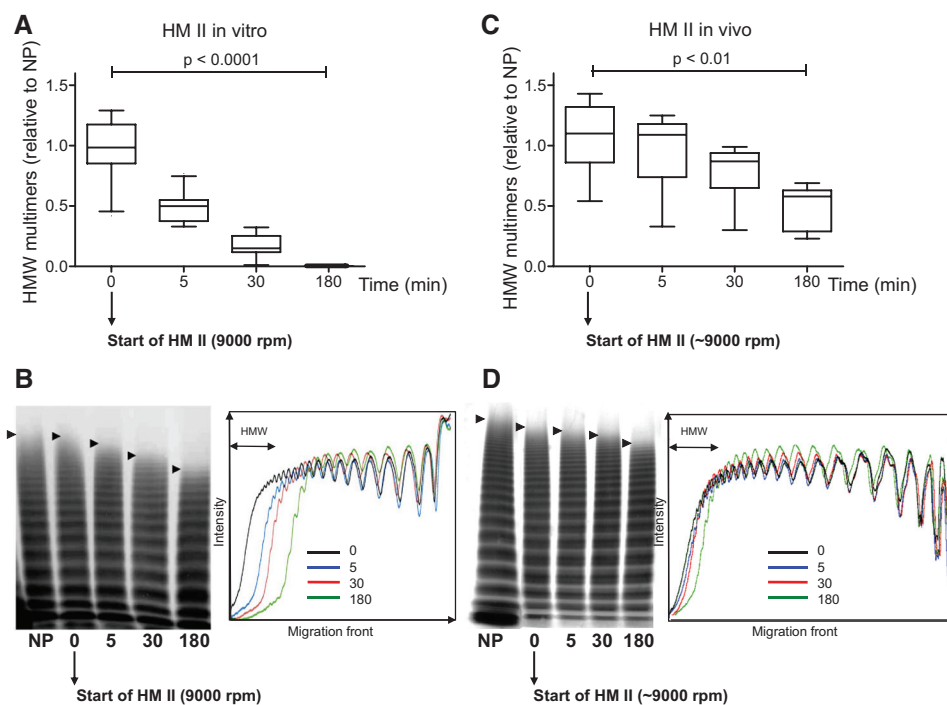


Figure 2. Immediate loss of high molecular weight (HMW) multimers on high shear stress at initiation of axial continuous flow HeartMate-II (HM II) device. **A**, Quantitative analysis of HMW multimers (relative to normal human pooled plasma) after perfusion of human whole blood under high shear conditions (9000 rpm) in the HM II in vitro model (repeated ANOVA, $P < 0.0001$ overall; $n = 10$). A significant loss of HMW multimers occurred overtime, already significant 5 minutes after HM II start ($P < 0.01$ vs baseline) and complete at 180 minutes. **B**, Representative time course of HMW multimers loss (with densitometric analysis) after initiating the HM II in vitro. **C**, Quantitative analysis of HMW multimers (relative to normal human pooled plasma) in patients undergoing initiation of HM II support (repeated ANOVA, $P < 0.01$ overall; $n = 8$). A significant loss of HMW multimers occurred overtime, already significant 30 minutes after initiating the HM II support ($P < 0.01$ vs baseline). **D**, Representative time course of HMW multimers loss (with densitometric analysis) after initiating the HM II support in vivo (**B** and **D**, black arrows indicate the front migration). NP indicates normal human pooled plasma.

In patients undergoing HeartMate-II implantation, a time-dependent increase in VWFpp was observed. This VWFpp increase, already significant 5 minutes after initiating the pump (528 ± 184 versus 259 ± 139 UI/dL at baseline; $P = 0.01$), was still apparent after 30 minutes (538 ± 139 UI/dL) and 180 minutes (560 ± 140 UI/dL). In vitro, no change in VWFpp was observed overtime (89 ± 27 at 180 minutes versus 89 ± 32 at baseline, ns).

HMW Multimers Increase Rapidly After Reversion of Pathological High Shear Stress in Patients Undergoing TAVI Procedure

The effect of the reversion of high shear on the VWF multimeric pattern was studied in 30 patients with AS requiring to undergo either BAV ($n = 10$; 5 men and 5 women; aged 82 ± 6 years; LVEF = $53\% \pm 10\%$) or TAVI ($n = 20$; 9 men and 11 women; aged 82 ± 6 years, LVEF = $53\% \pm 10\%$). All patients had New York Heart Association class 3 or 4 and no patient had decompensated heart failure.

As expected, in patients with AS a HMW multimers defect was observed at baseline (0.50 ± 0.19 compared with normal pooled plasma), whereas increased levels of IMW+LMW multimers (1.07 ± 0.04) were present.

In patients treated with TAVI, the procedure resulted in a near normalization of maximal transvalvular velocity (from 4.44 ± 0.47 m/s at baseline to 2 ± 0.56 m/s after valve replacement; $P < 0.0001$) inducing a marked reduction in mean transvalvular gradient (50.6 ± 12.5 to 9.6 ± 5.1 mmHg; $P < 0.0001$), whereas in 4 of them (20%) a postprocedural AR moderate or greater was

observed. Those treated with BAV experienced a modest improvement in shear conditions (max transvalvular velocity from 4.47 ± 0.25 m/s at baseline to 3.88 ± 0.65 m/s after BAV; $P < 0.05$) and, as a consequence, a modest decrease in mean transvalvular gradient (49.6 ± 3.8 to 35.6 ± 13.4 mmHg; $P < 0.05$).

In the 20 patients undergoing TAVI, the amount of HMW multimers dramatically increased 5 minutes after valve implantation (from 0.51 ± 0.18 at baseline to 0.75 ± 0.24 ; $P < 0.001$). An almost complete recovery was observed after 180 minutes (0.97 ± 0.25 ; $P < 0.0001$; Figure 3A and 3B) which was sustained by 4 weeks (0.91 ± 0.15). Together with the HMW multimers recovery, a significant time-dependent decrease of IMW+LMW multimers already significant at 5 minutes (1.03 ± 0.05) and peaking at 180 minutes (0.99 ± 0.04) was observed ($P < 0.01$). A time-dependent correction of VWF collagen-binding activity/VWF:Ag ratio was also observed (from 0.76 ± 0.14 at baseline to 0.94 ± 0.30 at 180 minutes; $P < 0.01$).

BAV procedures did not increase significantly the amount of HMW multimers (0.58 ± 0.2 , 0.66 ± 0.25 , 0.64 ± 0.15 , and 0.65 ± 0.21 at 5, 30, 180 minutes, and 4 weeks after BAV, respectively; $P = 0.59$; Figure 3C and 3D). No significant time-dependent changes in IMW+LMW multimers nor in VWF:Act/VWF:Ag ratio were observed.

Of note, as part of the TAVI procedure a balloon predilatation was performed before valve implantation. This predilatation had no significant impact on HMW multimers (0.54 ± 0.11 at 5 minutes; $P = 0.61$ versus baseline).

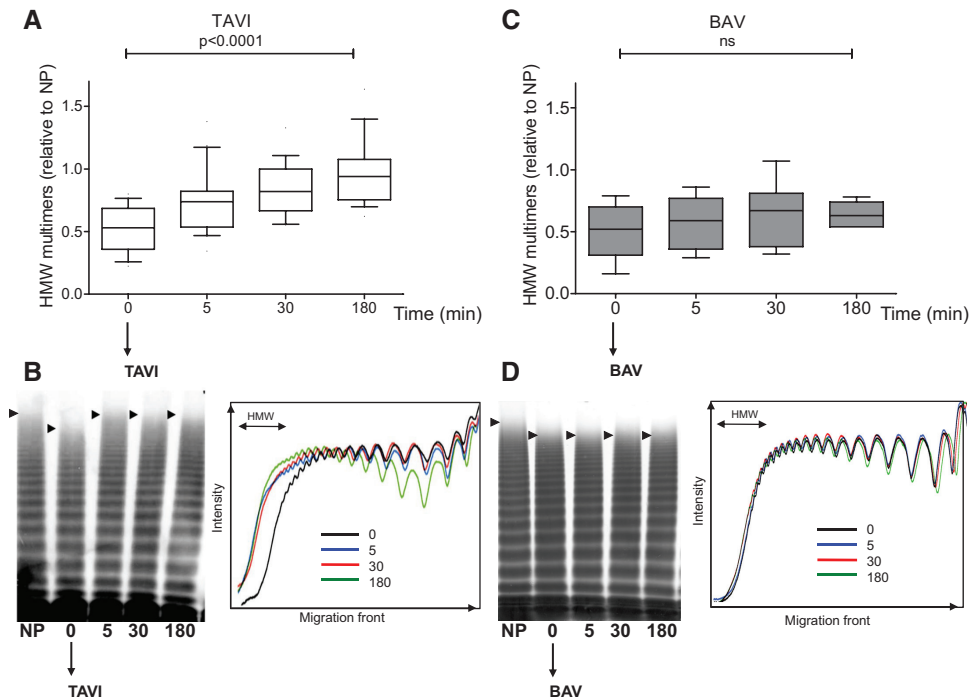


Figure 3. Time course of high molecular weight (HMW) multimers recovery in patients with severe aortic stenosis undergoing transcatheter aortic valve interventions. **A**, Quantitative analysis of HMW multimers in patients undergoing correction of aortic stenosis by transcatheter aortic valve implantation (TAVI; repeated ANOVA, $P < 0.0001$ overall; $n = 20$). HMW multimers recovery was significant 5 minutes after valve implantation ($P < 0.05$) and completed at 180 minutes ($P < 0.01$). **B**, Representative time course of von Willebrand factor (VWF) multimeric pattern (with densitometric analysis) in a patient undergoing TAVI procedure. **C**, Quantitative analysis of HMW multimers in patients undergoing balloon valvuloplasty (BAV) procedure (repeated ANOVA, $P = 0.21$ overall; $n = 10$). No significant changes in VWF multimeric pattern occurred after valve dilatation. **D**, Representative time course of VWF multimeric pattern (with densitometric analysis) in a patient undergoing BAV procedure. NP indicates normal human pooled plasma.

When all TAVI and BAV patients were analyzed together ($n = 30$), a significant and inverse relation between postprocedural mean transvalvular gradient and postprocedural HMW multimers was observed ($r = -0.68$; $P < 0.0001$; Figure 4).

After TAVI, despite a consistently low residual gradient (9.6 ± 5.1 mm Hg), a relatively large standard deviation in HMW multimer values was observed. This was mainly related to the occurrence of a significant postprocedural AR in 4 patients in whom the HMW multimers increased to a lesser extent and in whom HMW multimer at 180 minutes was significantly lower than in the 16 TAVI patients without postprocedural AR (0.74 ± 0.10 versus 1.02 ± 0.25 ; $P = 0.04$).

Acute Endothelial Release of VWF in Patients Undergoing TAVI Procedures

A potential role of the vascular endothelium in the HMW multimers recovery was investigated by evaluating the secretion of VWF by the endothelium after reversion of high shear in TAVI and BAV procedures. It was further investigated by studying the recovery of HMW multimers after reversion of high shear in a model free of endothelium (in vitro HeartMate-II).

In TAVI procedures, VWFpp significantly increased 5 minutes after valve implantation (190 ± 85 UI/dL), and further after 30 (240 ± 111 UI/dL) and 180 minutes (394 ± 191 UI/dL) when compared with baseline (171 ± 84 UI/dL; $P < 0.01$). In BAV procedures, VWFpp did not increase significantly overtime (275 ± 136 UI/dL at 180 minutes versus 199 ± 107 UI/dL at baseline, ns).

In the in vitro HeartMate-II model, high shear was induced for 3 hours (9000 rpm), then the blood flow was submitted to low shear (by switching the speed from 9000 to 3000 rpm) for the next 3 hours, mimicking reversal of pathological high shear. In the absence of endothelium, no recovery of HMW multimers was observed in this model (Figure 5).

Real-Time Monitoring of Percutaneous Aortic Valve Procedures by PFA-CADP Closure Time

As expected and mimicking the VWF multimeric profile, characterized by reduced HMW multimers, PFA-CADP was prolonged in AS patients (243 ± 65 seconds). In TAVI patients, a time-dependent correction of PFA-CADP was observed (195 ± 74 , 165 ± 75 , 139 ± 73 , 141 ± 73 seconds at 5, 30, 180 minutes, and 4

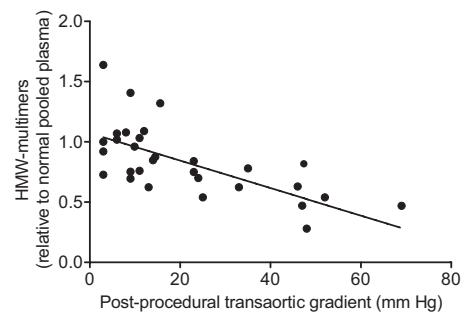


Figure 4. Relation between postprocedural gradient and postprocedural high molecular weight (HMW) multimers. The mean postprocedural gradient is plotted against the postprocedural HMW multimers values (180 minutes, $r = -0.68$; $P < 0.0001$).

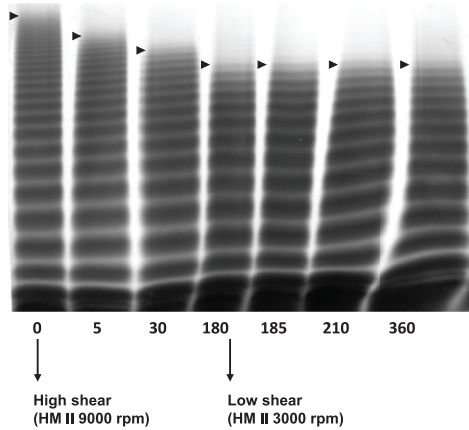


Figure 5. Absence of high molecular weight (HMW) multimers recovery after reversion of pathological high shear in the HeartMate-II (HM II) assist device model. Whole human blood was submitted to high shear (9000 rpm) during 3 hours and then to low shear for the next 3 hours (3000 rpm) by switching the pump. The von Willebrand factor multimeric profile remained unchanged after the offset of high shear stress.

weeks respectively, $P < 0.0001$; Figure 6). By contrast, in BAV patients no significant change in PFA-CADP was observed overtime (212±61, 204±71, 219±76, 221±75 seconds at 5, 30, 180 minutes, and 4 weeks; $P = 0.82$; Figure 6). Mirroring the observation made with HMW multimers, patients with a prolonged PFA-CADP value had a higher final residual gradient than patients with a normal PFA-CADP value (29.2±5.1 versus 7.85±1.12; $P < 0.001$). Importantly all patients with a normal final PFA-CADP had final residual gradient <15 mm Hg.

After TAVI, and similar to the heterogeneity observed with HMW multimer values, a relatively large SD in PFA-CADP measurement was observed. This was mainly related to the occurrence of a significant postprocedural AR in 4 patients in whom PFA-CADP measurements were significantly higher than in the 16 patients without AR (225±41 versus 100±23 seconds; $P < 0.01$; Figure 7). In all patients with a residual AR the PFA-CADP at the

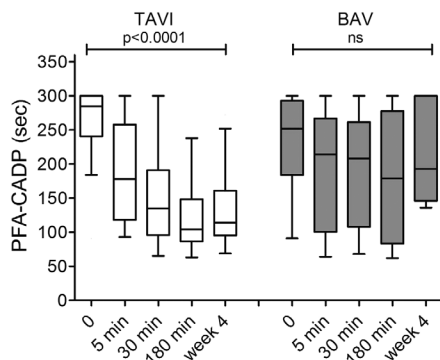


Figure 6. Real-time assessment of changes in von Willebrand factor (VWF) multimeric pattern with platelet function analyzer-closure time adenine DI-phosphate (PFA-CADP) in patients undergoing transcatheter aortic valve interventions. In transcatheter aortic valve implantation (TAVI) patients, a time-dependent correction of PFA-CADP was observed (repeated ANOVA, $P < 0.0001$). In balloon valvuloplasty (BAV) patients, no significant time-dependent change of PFA-CADP was observed. In TAVI patients this correction was still present 4 weeks after the procedure and conversely PFA-CADP remained prolonged at this time point in BAV patients.

end of the procedure was >180 seconds, whereas of those without any residual AR the final PFA-CADP was <140 seconds.

Conversely, in patients undergoing implantation of a HeartMate-II device, a sudden increase in PFA-CADP was observed as soon as 5 minutes after initiation of the support (246±63 versus 106±40 seconds; $P = 0.01$).

Discussion

The present study, performed in 3 clinical conditions and 1 animal model in which the entire blood volume is exposed to high shear stress, demonstrates that acute changes in blood flow are associated with highly dynamic consequences on the VWF multimeric profile, occurring within minutes and then remaining steady overtime. It demonstrates the key roles of HMW multimers proteolysis and VWF multimers release by the vascular endothelium in those acute changes of VWF multimeric profile. It further demonstrates that bedside whole blood assessment (PFA-CADP), reflecting HMW multimers changes, could be used in clinical practice to monitor in real time the quality of the results of percutaneous aortic valve procedures, in particular, to detect the occurrence of postprocedural AR. Altogether these results provide the first integrated demonstration that VWF can be considered as a biological sensor of blood flow in vivo.

Dynamic Variations in HMW Multimers in Response to Acute Changes in Blood Flow

The present study is the first one to demonstrate that variations in VWF multimeric profile in response to acute changes in blood flow in vivo are highly dynamic.

Although it has been demonstrated that the loss of HMW multimers could be observed the day after the initiation of LVAD support,¹⁰ the initial response of VWF multimers after induction of high shear in vivo was unknown. The dynamic onset of shear-induced proteolysis of HMW multimers has been extensively described in vitro.^{13,20,22} Hence, when subjecting VWF to high shear forces, unfolding of large VWF multimers has been shown to occur in <1 second in vitro and VWF cleavage was inferred to be effective within 200 seconds in vivo.¹³ The present study confirms that the loss of HMW

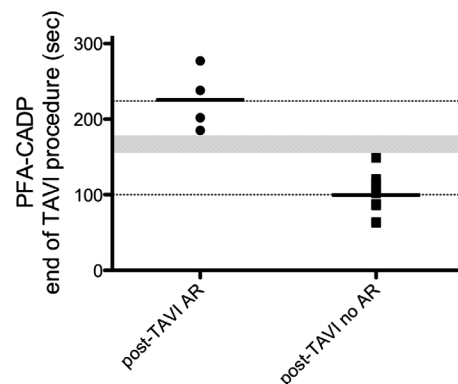


Figure 7. Impact of a significant postprocedural aortic regurgitation (AR) on platelet function analyzer-closure time adenine DI-phosphate (PFA-CADP) at the end of the transcatheter aortic valve implantation (TAVI) procedure. In patients with a significant postprocedural AR (n=4) the postprocedural PFA-CADP was significantly higher than in patients without AR (n=16, $P < 0.01$) and remained as prolonged as in patients with aortic stenosis.

multimers follows a similar time frame *in vivo* and occurs almost immediately after the induction of high shear stress. Indeed, a significant decrease in HMW multimers was observed 5 minutes after induction of high shear, both in rabbits submitted to an acute AS and after initiation of HeartMate-II support at high speed (9000 rpm). Additional experiments performed in the HeartMate-II LVAD model further confirmed the shear dependency of HMW multimers loss; a rapid loss of HMW multimers was observed at high speed (9000 rpm), whereas no loss was observed at low speed (3000 rpm).

Although HMW multimers recovery has been observed within days after aortic valve surgical replacement in AS patients,^{11,12} no information was available on the initial phase of correction of AS. A major finding of this study is to demonstrate a nearly immediate recovery of the HMW multimers on reversion of the high-shear conditions, whereas no recovery was observed in the absence of correction. In the rabbit model and in AS patients undergoing TAVI, HMW multimers recovery was observed 5 minutes after correction of AS and was sustained overtime. In AS patients undergoing a percutaneous procedure but in whom only a weak reduction in shear forces was achieved, as those undergoing BAV or those undergoing TAVI with a significant postprocedural AR, no consistent HMW multimers recovery was observed.

HMW Multimers Proteolysis as a Shear-Dependent Process

VWF shear-induced proteolysis is considered the main mechanism underlying the acquired HMW multimers defect observed in high-shear cardiovascular conditions, such as AS or continuous axial flow LVAD support.^{4,23} The present study provides new experimental evidence that proteolysis links the induction of high shear to the nearly immediate loss of HMW multimers. First, in the HeartMate-II LVAD patients, the loss of HMW multimers was associated with an increase in VWF proteolytic fragments. Second, the loss of HMW multimers at initiation of high shear conditions was blunted when a protease inhibitor (EDTA) was added to the *in vitro* device model. Finally, the increase in IMW and LMW multimers as seen in HeartMate-II LVAD patients and the decrease of IMW and LMW multimers seen in TAVI patients are also consistent with this hypothesis. Altogether these results further re-enforce that shear-induced proteolysis is the major mechanism underlying the acquired HMW multimers loss observed in high-shear cardiovascular disorders.

Vascular Endothelium and Recovery of HMW Multimers Defect

The inhibition of the proteolysis of HMW multimers is not sufficient to explain alone their sudden rise in TAVI patients, unless newly secreted VWF circulate in the blood. This question was investigated by measuring VWFpp in patients undergoing TAVI. In these patients the increase of VWFpp was indicative of an acute release of VWF by the vascular endothelium.²⁴ This demonstrates that in combination with the acute inhibition of HMW multimers proteolysis, an acute release of VWF multimers by the endothelium is requested for the acute recovery of the HMW multimers defect. The absence of recovery of the HMW multimers in a model of acute shear recovery but without endothelium is also consistent with this hypothesis.

Recent studies have demonstrated that an increase in the arterial luminal pressure is able to induce an acute release of VWF by the vascular endothelium.²⁵ In our study, the observations of a sudden rise in VWFpp in situations where an increase of arterial luminal pressure is observed (such as TAVI or HeartMate-II LVAD patients), and the lack of VWFpp increase in a model without endothelium, is consistent with this hypothesis.

Altogether this suggests that in TAVI patients, the multimers newly provided by the endothelium in response to the increased arterial luminal pressure are no longer submitted to local abnormal high shear and proteolysis when passing through the valve, thus resulting in an ultimate increase in the proportion of HMW multimers (Figure 8).

PFA-CADP to Monitor in Real Time the Result of Aortic Percutaneous Interventions

Periprocedural evaluation of the result of percutaneous aortic interventions, while important because corrective measures can be undertaken at that time, remains a challenging issue. In particular, the occurrence of postprocedural AR after TAVI is a vexing clinical problem observed in 10% to 30% of cases. Although it has been associated with an increased long-term mortality,² its detection and accurate evaluation in the catheterization laboratory remain difficult.¹⁹ There is therefore a critical need for a quick and reliable method of evaluation of the results of these interventions.

PFA-100, which is a whole blood functional test of primary hemostasis, has been shown to be highly sensitive to HMW multimers defects.¹⁴ A major finding is that a rapid correction in PFA-CADP, reflecting HMW multimers recovery, was observed in patients undergoing TAVI, whereas no significant change was observed in those undergoing BAV. Furthermore in TAVI patients with a clinically significant AR, an incomplete correction of PFA-CADP was also observed and PFA-CAP values were able to segregate perfectly patients with (<180 seconds) or without (<140 seconds) residual AR. This demonstrates that PFA-100 can reflect in real-time acute shear modification and evaluate the quality of the results of transcatheter aortic valve procedures.

PFA-CADP could therefore be used to monitor TAVI procedures in some critical patients such as those with a high risk of mortality in case of AR, for example, patients with atrial fibrillation, renal failure, or pure AS without AR,² and those with conflicting results about the significance of postprocedural AR by other investigatory means (angiography, echocardiography, etc). In such circumstances, it has been shown that balloon postdilatation could decrease the magnitude of AR but at the price of an increased risk of stroke or bioprosthesis damages.²⁶ The lack of improvement of PFA-CADP measured in real time could provide additional informations and be integrated in the decision process. Similarly, although TAVI is often performed in patients with a degenerated biological prosthesis in the so-called valve-in-valve procedure, the result can be hampered by the high residual transvalvular gradient because of a prosthesis/prosthesis mismatch. The development of a broader size choice and fully retrievable devices will provide the opportunity to adapt the initial choice during the procedure pending that prosthesis/prosthesis mismatch can be accurately and quickly recognized. In this situation also, the lack of improvement

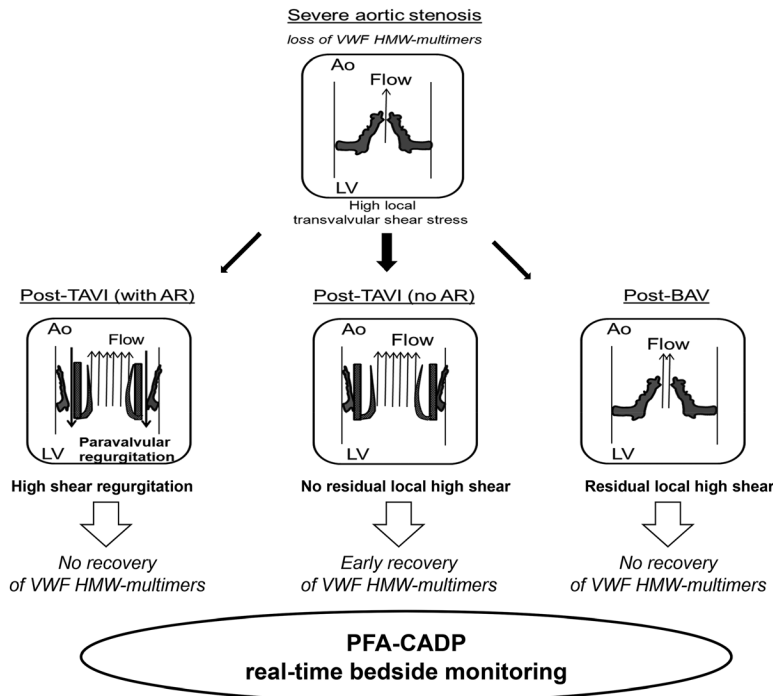


Figure 8. von Willebrand factor (VWF) as a biomarker of transcatheter aortic valve interventions. A loss of VWF high molecular weight (HMW) multimers is observed in severe aortic stenosis consecutive to an increase in shear-induced proteolysis of VWF through the pathological aortic valve. A recovery of VWF HMW multimers is observed early after a transcatheter aortic valve implantation (TAVI)-mediated new aortic valve implantation excepted in case of postprocedural aortic regurgitation (AR), whereas VWF multimeric profile remains unchanged after a balloon valvuloplasty (BAV)-mediated aortic valve dilatation associated with high residual mean transaortic gradient. We proposed that the time course of HMW multimers recovery after TAVI procedure is mediated by 2 mechanisms dependent on the correction of aortic stenosis: (1) a normalization in local aortic transvalvular shear stress conditions preventing the proteolysis of circulating HMW multimers through the implanted aortic valve. (2) An increase of HMW multimers release by the vascular endothelium secondary to an increase in arterial luminal pressure. Finally platelet function analyzer (PFA)-bedside assessment reflecting HMW multimers changes could be used clinically to monitor in real time the results of transcatheter aortic valve interventions. Ao indicates aorta; CADP, closure time adenine Diphosphate; and LV, left ventricle.

of PFA-CADP could help the medical decision while the patient is still in the catheterization laboratory.

Such approach has also the potential to be helpful in tuning a ventricular assist system.

Study Limitations

The number of patients included in this study could be considered as limited. This was largely a consequence of the translational approach of our study and of our goal to provide a real-time assessment of the processes involved. We think that such an approach favoring multiple clinical situations and the assessment of multiple time points in each clinical situation rather than a high number of subjects in each clinical situation was more adapted to our research. It did not preclude the detection of significant differences, while the findings obtained in one situation allowed further validation of the findings from another.

Although the rabbit model allowed us to investigate onset/offset of loss of HMW multimers, the underlying mechanisms could not be investigated in the same model because of the lack of specific reagents for rabbits. However, these mechanisms were investigated using the HeartMate-II LVAD model and in patients undergoing transcatheter aortic valve procedures.

The use of multimeric analysis of VWF as a biomarker of blood flow is potentially limited by the fact that it is a time-consuming technique. This issue was offset, however, by the use of a point-of-care PFA-CADP assay, which renders our observation clinically relevant.

Finally, we have to acknowledge that the mechanistic arguments for rapid recovery of VWF multimers, involving pressure-related endothelium-release of VWpp, while consistent with our study findings, are partly speculative. Similarly, our study does not allow drawing any definite conclusion on the impact of pulsatile versus continuous blood flow on the release of VWpp. These 2 important issues will require further and dedicated investigations.

Conclusions: VWF as a Biological Sensor of Blood Flow

Although this was previously speculated based on in vitro findings,¹³ our results provide the first integrated demonstration that circulating VWF acts as a biological mechanosensor and a dynamic marker of changes in blood flow in vivo. This observation, together with the recently described²⁷ pleiotropic function of VWF, suggests a key role of VWF as a biological transducer of changes in blood flow (Figure 8).

In addition, the mechanosensor property of VWF, as assessed by a point-of-care assay, could be useful in clinical practice to monitor in real-time TAVI procedures, detect key procedural complications with a deleterious impact on clinical outcome (high residual gradient, postprocedural AR), and assist the clinical decision.

Acknowledgments

We thank Alexandre Ung (Lille university Hospital), Bérénice Marchant (Lille University Hospital), Marion Durand (Private Hospital of Anthony), Pauline Guyon (Lille University Hospital), Flavien Vincent (Lille university Hospital), Karim Moussa (Lille University Hospital) for their important contribution. We also thank all the members of the catheterization laboratory and cardiac operating room teams of the Department of Cardiology of the Lille University Hospital represented by their chief nurses (Catherine Desormeaux, Fabienne Delesalle and Bernard Collet) for their commitment to the project.

Sources of Funding

This work was supported by Lille-II University.

Disclosures

None.

References

1. Leon MB, Smith CR, Mack M, et al; PARTNER Trial Investigators. Transcatheter aortic-valve implantation for aortic stenosis in patients

who cannot undergo surgery. *N Engl J Med.* 2010;363:1597–1607. doi: 10.1056/NEJMoa1008232.

2. Van Belle E, Juthier F, Susen S, et al; FRANCE 2 Investigators. Postprocedural aortic regurgitation in balloon-expandable and self-expandable transcatheter aortic valve replacement procedures: analysis of predictors and impact on long-term mortality: insights from the FRANCE2 Registry. *Circulation.* 2014;129:1415–1427. doi: 10.1161/CIRCULATIONAHA.113.002677.
3. Khawaja MZ, Sohal M, Valli H, et al. Standalone balloon aortic valvuloplasty: indications and outcomes from the UK in the transcatheter valve era. *Catheter Cardiovasc Interv.* 2013;81:366–373. doi: 10.1002/ccd.24534.
4. Loscalzo J. From clinical observation to mechanism—Heyde’s syndrome. *N Engl J Med.* 2012;367:1954–1956. doi: 10.1056/NEJMcibr1205363.
5. Geisen U, Heilmann C, Beyersdorf F, Benk C, Berchtold-Herz M, Schlensak C, Budde U, Zieger B. Non-surgical bleeding in patients with ventricular assist devices could be explained by acquired von Willebrand disease. *Eur J Cardiothorac Surg.* 2008;33:679–684. doi: 10.1016/j.ejcts.2007.12.047.
6. Le Tourneau T, Susen S, Caron C, et al. Functional impairment of von Willebrand factor in hypertrophic cardiomyopathy: relation to rest and exercise obstruction. *Circulation.* 2008;118:1550–1557. doi: 10.1161/CIRCULATIONAHA.108.786681.
7. Meyer AL, Malehsa D, Bara C, Budde U, Slaughter MS, Haverich A, Strueber M. Acquired von Willebrand syndrome in patients with an axial flow left ventricular assist device. *Circ Heart Fail.* 2010;3:675–681. doi: 10.1161/CIRCHEARTFAILURE.109.877597.
8. Uriel N, Pak SW, Jorde UP, Jude B, Susen S, Vincentelli A, Ennezat PV, Cappelman S, Naka Y, Mancini D. Acquired von Willebrand syndrome after continuous-flow mechanical device support contributes to a high prevalence of bleeding during long-term support and at the time of transplantation. *J Am Coll Cardiol.* 2010;56:1207–1213. doi: 10.1016/j.jacc.2010.05.016.
9. Federici AB, Rand JH, Bucciarelli P, Budde U, van Genderen PJ, Mohri H, Meyer D, Rodeghiero F, Sadler JE; Subcommittee on von Willebrand Factor. Acquired von Willebrand syndrome: data from an international registry. *Thromb Haemost.* 2000;84:345–349.
10. Heilmann C, Geisen U, Beyersdorf F, Nakamura L, Trummer G, Berchtold-Herz M, Schlensak C, Zieger B. Acquired Von Willebrand syndrome is an early-onset problem in ventricular assist device patients. *Eur J Cardiothorac Surg.* 2011;40:1328–1333; discussion 1233. doi: 10.1016/j.ejcts.2011.03.021.
11. Vincentelli A, Susen S, Le Tourneau T, Six I, Fabre O, Juthier F, Bauters A, Decoene C, Goudemand J, Prat A, Jude B. Acquired von Willebrand syndrome in aortic stenosis. *N Engl J Med.* 2003;349:343–349. doi: 10.1056/NEJMoa022831.
12. Solomon C, Budde U, Schneppenheim S, Czaja E, Hagl C, Schoechl H, von Depka M, Rahe-Meyer N. Acquired type 2A von Willebrand syndrome caused by aortic valve disease corrects during valve surgery. *Br J Anaesth.* 2011;106:494–500. doi: 10.1093/bja/aeq413.
13. Zhang X, Halvorsen K, Zhang CZ, Wong WP, Springer TA. Mechanoenzymatic cleavage of the ultralarge vascular protein von Willebrand factor. *Science.* 2009;324:1330–1334. doi: 10.1126/science.1170905.
14. Fressinaud E, Veyradier A, Truchaud F, Martin I, Boyer-Neumann C, Trossaert M, Meyer D. Screening for von Willebrand disease with a new analyzer using high shear stress: a study of 60 cases. *Blood.* 1998;91:1325–1331.
15. Blackshear JL, Wysokinska EM, Safford RE, Thomas CS, Stark ME, Shapiro BP, Ung S, Johns GS, Chen D. Indexes of von Willebrand factor as biomarkers of aortic stenosis severity (from the Biomarkers of Aortic Stenosis Severity [BASS] study). *Am J Cardiol.* 2013;111:374–381. doi: 10.1016/j.amjcard.2012.10.015.
16. Assad RS, Cardarelli M, Abduch MC, Aiello VD, Maizato M, Barbero-Marcial M, Jatene A. Reversible pulmonary trunk banding with a balloon catheter: assessment of rapid pulmonary ventricular hypertrophy. *J Thorac Cardiovasc Surg.* 2000;120:66–72.
17. Godier A, Mazoyer E, Cymbalista F, Cupa M, Samama CM. Recombinant activated factor VII efficacy and safety in a model of bleeding and thrombosis in hypothermic rabbits: a blind study. *J Thromb Haemost.* 2007;5:244–249. doi: 10.1111/j.1538-7836.2007.02320.x.
18. Ben-Dor I, Pichard AD, Satler LF, et al. Complications and outcome of balloon aortic valvuloplasty in high-risk or inoperable patients. *JACC Cardiovasc Interv.* 2010;3:1150–1156. doi: 10.1016/j.jcin.2010.08.014.
19. Kappetein AP, Head SJ, Généreux P, et al. Updated standardized endpoint definitions for transcatheter aortic valve implantation: the Valve Academic Research Consortium-2 consensus document. *J Am Coll Cardiol.* 2012;60:1438–1454. doi: 10.1016/j.jacc.2012.09.001.
20. Tsai HM, Sussman II, Nagel RL. Shear stress enhances the proteolysis of von Willebrand factor in normal plasma. *Blood.* 1994;83:2171–2179.
21. Ott HW, Griesmacher A, Schnapka-Koepf M, Guderer G, Sieberer A, Spannagl M, Scheibe B, Perkhof S, Will K, Budde U. Analysis of von Willebrand factor multimers by simultaneous high- and low-resolution vertical SDS-agarose gel electrophoresis and Cy5-labeled antibody high-sensitivity fluorescence detection. *Am J Clin Pathol.* 2010;133:322–330. doi: 10.1309/AJCPZSBTD2BWOMVL.
22. Dong JF. Cleavage of ultra-large von Willebrand factor by ADAMTS-13 under flow conditions. *J Thromb Haemost.* 2005;3:1710–1716. doi: 10.1111/j.1538-7836.2005.01360.x.
23. Pareti FI, Lattuada A, Bressi C, Zanobini M, Sala A, Steffan A, Ruggeri ZM. Proteolysis of von Willebrand factor and shear stress-induced platelet aggregation in patients with aortic valve stenosis. *Circulation.* 2000;102:1290–1295.
24. van Mourik JA, Boertjes R, Huisveld IA, Fijnvandraat K, Pajkrt D, van Genderen PJ, Fijnheer R. von Willebrand factor propeptide in vascular disorders: A tool to distinguish between acute and chronic endothelial cell perturbation. *Blood.* 1999;94:179–185.
25. Xiong Y, Hu Z, Han X, Jiang B, Zhang R, Zhang X, Lu Y, Geng C, Li W, He Y, Huo Y, Shibuya M, Luo J. Hypertensive stretch regulates endothelial exocytosis of Weibel-Palade bodies through VEGF receptor 2 signaling pathways. *Cell Res.* 2013;23:820–834. doi: 10.1038/cr.2013.56.
26. Nombela-Franco L, Rodés-Cabau J, DeLarochelière R, et al. Predictive factors, efficacy, and safety of balloon post-dilation after transcatheter aortic valve implantation with a balloon-expandable valve. *JACC Cardiovasc Interv.* 2012;5:499–512. doi: 10.1016/j.jcin.2012.02.010.
27. Lenting PJ, Casari C, Christophe OD, Denis CV. von Willebrand factor: the old, the new and the unknown. *J Thromb Haemost.* 2012;10:2428–2437. doi: 10.1111/jth.12008.

Novelty and Significance

What Is Known?

- Acquired defect of von Willebrand factor (VWF) has been reported in various cardiovascular disorders associated with high shear, in particular, with aortic valve stenosis.
- Correction of the pathological condition has been associated with reversion of the VWF defect.
- In vitro data suggest that changes in VWF multimeric could be highly dynamic in response to changes in shear.

What New Information Does This Article Contribute?

- In response to in vivo changes in shear, the VWF multimer can change within minutes.
- VWF can be used as a biomarker of change in blood flow to evaluate percutaneous aortic valve interventions.
- Point-of-care assay could be implemented in the catheterization laboratory as part of a real-time monitoring strategy of the result of percutaneous aortic valve interventions.

Based on in vitro findings, it has been previously speculated that the multimeric pattern of VWF could change dynamically in response to high shear. Our results show that circulating VWF acts as a biological mechanosensor and a dynamic marker of changes in blood flow in vivo. We describe a highly dynamic recovery of HMW multimers along with the sudden changes in blood flow after a complete correction of aortic stenosis during percutaneous aortic valve procedures. We document that the failure of percutaneous aortic valve procedures, because of a high residual gradient and a post-procedural aortic regurgitation, is detected by a point-of-care assay sensitive to HMW multimers defect. These results provide the basis for a per-procedural evaluation of percutaneous aortic valve interventions, using VWF as a biomarker of complete aortic stenosis reversion/acute change in blood flow. We suggest that such point-of-care assay could be implemented in the catheterization laboratory as part of a real-time monitoring strategy for the early detection of transcatheter aortic valve implantation procedural failure.

Antibody-based prevention of von Willebrand factor degradation mediated by circulatory assist devices

Antoine Rauch^{1,2,3,4}; Paulette Legendre^{1,2}; Olivier D. Christophe^{1,2}; Jenny Goudemand^{3,4}; Eric van Belle^{4,5}; André Vincentelli^{4,5}; Cécile V. Denis^{1,2}; Sophie Susen^{3,4}; Peter J. Lenting^{1,2}

¹INSERM Unit 770, Le Kremlin-Bicêtre, France; ²UMR_S 770, Univ Paris-Sud, Le Kremlin-Bicêtre, France; ³Department of Hematology & Transfusion, Lille University Hospital, Lille, France; ⁴Equipe d'Accueil 2693, Lille-II University, Lille, France; ⁵Department of Cardiology, Lille University Hospital, Lille, France

Summary

Haemorrhagic episodes in patients carrying circulatory assist devices represent a severe life-threatening clinical complication. These bleeding episodes may originate from a reduced functionality of von Willebrand factor (VWF), a multimeric protein pertinent to the formation of a haemostatic plug. It has been reported that the reduced functionality is due to increased proteolytic degradation by the enzyme ADAMTS13, a phenomenon that is facilitated by device-induced increases in shear stress to which VWF is exposed. Here, we have tested a series of VWF-derived protein fragments and monoclonal murine anti-VWF antibodies for their capacity to reduce shear stress-dependent degradation of VWF. Via direct binding experiments, we identified an anti-VWF antibody that partially blocked VWF-ADAMTS13 interactions ($46 \pm 14\%$). Epitope mapping experiments revealed that the antibody, designated mAb508, is directed against the distal portion of the VWF D4-domain (residues 2134–2301) and recognises a synthetic peptide encompassing residues 2158–2169. Consistent with its partial

inhibition of VWF-ADAMTS13 interactions in binding assays, mAb508 reduced ADAMTS13-mediated VWF degradation in a vortex-based degradation assay by $48 \pm 10\%$. In a HeartMateII-based whole blood-perfusion system, mAb508 was able to reduce degradation of high-molecular-weight (HMW)-VWF-multimers dose-dependently, with a maximal inhibition ($83 \pm 8\%$) being reached at concentrations of 10 $\mu\text{g/ml}$ or higher. In conclusion, we report that partial inhibition of VWF-ADAMTS13 interactions using an anti-VWF antibody can prevent excessive degradation of HMW-VWF multimers. This strategy may be used for the development of therapeutic options to treat bleeding episodes due to shear stress-dependent VWF degradation, for instance in patients carrying circulatory assist devices.

Keywords

von Willebrand factor, ADAMTS13, circulatory assist devices, acquired von Willebrand syndrome, antibody therapy

Correspondence to:

Peter J. Lenting
INSERM U770
80 rue du General Leclerc
94276 Le Kremlin-Bicêtre, France
Tel.: +33 149595651, Fax: +33 146719472
E-mail: peter.lenting@inserm.fr

Financial support:

This study was supported by the Institute Nationale de la Santé et de la Recherche Médicale (Inserm) and Lille-II University.

Received: February 18, 2014
Accepted after major revision: May 30, 2014
Epub ahead of print: July 17, 2014

<http://dx.doi.org/10.1160/TH14-02-0148>
Thromb Haemost 2014; 112: 1014–1023

Introduction

Von Willebrand factor (VWF) is a multimeric glycoprotein that plays an essential role in the formation of platelet-rich thrombi, particularly under conditions of high shear stress. The main source of circulating VWF are the endothelial cells, where it is synthesised as a single chain pro-subunit with a discrete domain architecture, which was recently re-annotated: D1-D2-D'-D3-A1-A2-A3-D4-C1-C2-C3-C4-C5-C6-CK (1). Intra-cellular processing results in the removal of the propeptide (D1-D2 domains), and multimerisation of the protein via amino- and carboxy-terminal disulfide bonding (2). These processes generate a heterologous pool of differentially sized multimers that may contain as many as 60 subunits, which are stored in the endothelial Weibel-Palade bodies and secreted into plasma via constitutive and agonist-induced pathways (3).

The multimer size of VWF is pertinent to its platelet-recruiting function, with the larger multimers displaying the highest haemostatic potential. In normal plasma, the multimers may contain between 2 and 40 subunits (1–20 bands when analysed by SDS-agarose electrophoresis [4]), which are shorter than those found in the endothelial storage organelles. Indeed, mechanisms are in place regulating VWF multimer size in the circulation, including proteolysis by the VWF-cleaving protease ADAMTS13 (A Disintegrin And Metalloprotease with Thrombospondin domains-13) (5).

The molecular basis of VWF proteolysis by ADAMTS13 has been extensively studied (6). A number of interactive sites have been identified, including the A2- and D4-domains of VWF, which are important for the proper alignment of the ADAMTS13 active site (7–9). This active site attacks the Tyr1605-Met1606 peptide bond that is located within the VWF A2 domain (10). Interestingly, access to this peptide bond relies on the shear stress-

induced unfolding of the substrate (for review see [11]), thereby protecting it against degradation while circulating normally, and limiting proteolysis to specific conditions. One of these conditions occurs when multiple VWF multimers assemble into large stretched bundles attached to the endothelial surface upon agonist-induced secretion. These bundles are not only capable of catching platelets, but their stretched conformation allows proteolysis by ADAMTS13 thereby preventing the release of platelet-binding ultra-large VWF multimers into the circulation (12, 13). Another condition favouring proteolysis occurs when VWF binds to platelets within the growing thrombus. This opens the ADAMTS13 cleavage site, and subsequent proteolysis results in reduction of VWF multimer size (14). Consequently, the platelet-binding capacity is diminished, avoiding excessive thrombus growth that could occlude the vessel.

The physiological relevance of ADAMTS13-mediated proteolysis of VWF is apparent from the severe thrombotic micro-angiopathy that is associated with the functional deficiency of ADAMTS13, a disorder known as thrombotic thrombocytopenic purpura (TTP) (15). In contrast, increased proteolysis of VWF by ADAMTS13 leads to a bleeding diathesis, as is exemplified by von Willebrand disease (VWD)-type 2A. VWD-type 2A is caused by mutations (mostly in the VWF A2 domain) that result in excessive proteolysis of the VWF by ADAMTS13, with a concomitant loss of the higher haemostatically active multimers (16). Another example relates to acquired von Willebrand syndrome (aVWS), where increased VWF proteolysis has been associated with various clinical settings, like aortic stenosis (17, 18) and ventricular assist devices (VADs) therapy (19, 20). Both conditions are characterised by an increased incidence of bleedings, especially gastrointestinal (GI) bleedings (20, 21), in association with a selective loss of high-molecular-weight (HMW)-multimers and an increase in VWF degradation products (18, 22). aVWS usually resolves after aortic valve replacement or discontinuation of VAD support (18, 20, 23, 24). However, the latter is limited by graft availability and GI bleeding represents thus the most challenging complication under VAD support.

Overall there is a clear unmet medical need for a treatment targeting specifically excessive degradation of HMW-VWF multimers, for instance induced by circulatory assist devices. Ideally, such treatment should only partially interfere with VWF degradation in order to prevent drug-induced TTP-like symptoms. We hypothesised that interfering with VWF-ADAMTS13 binding exosites might subsequently provide a partial inhibition of VWF proteolysis. Here, we describe a monoclonal anti-VWF D4 domain antibody supporting this proof of concept. Biochemical analysis revealed a potent partial inhibitory effect on VWF-ADAMTS13 interactions. Its potential to diminish VWF proteolysis was confirmed using a recently developed *ex vivo* model of increased VWF degradation in whole blood induced by a circulatory assist device, which faithfully reproduces the biological phenotype of aVWS.

Materials and methods

Proteins

Purified plasma-derived (pd)-VWF and recombinant (r)-VWF were obtained as described previously (25, 26). All r-VWF fragments were produced using stably transfected BHK-cell lines. Transfection was performed using pNUT- or pFUSE-plasmids that contained synthetic cDNA sequences. cDNAs cloned into pNUT contained a 5'-sequence encoding the VWF signal peptide to allow secretion and a 3'-sequence encoding the HPC4 recognition motif (amino acid sequence EDQVDPRLIDGK). D'D3-HPC4 was obtained via the expression of a pNUT-plasmid encoding VWF-residues 1-1247. The purified protein lacks the VWF propeptide (residues 1-763) and is dimeric. A1A2A3-HPC4 and D4-HPC4 include VWF-residues 1261-1872 and 1947-2301, respectively. HPC4-tagged proteins were purified to homogeneity using HPC4-immuno affinity chromatography as instructed by the manufacturer (Roche Diagnostics, Meylan, France). A1-Fc, A2-Fc, A3-Fc and D4-Fc include VWF residues 1261-1478, 1480-1672, 1681-1878 and 1947-2301, respectively. A13-1-685-Fc includes residues 1-685 of ADAMTS13. All proteins expressed using the pFUSE contained a C-terminal Fc sequence of human IgG1 and were dimeric. Fc-tagged proteins were purified to homogeneity using protein A-Sepharose as instructed by the manufacturer (VWR International, Fontenay-sous-Bois, France). A panel of 29 monoclonal murine antibodies against human VWF was established in the 1980s (27, 28). Monoclonal antibodies were purified to homogeneity as described (27). Recombinant wild-type ADAMTS13 (wt-rADAMTS13) containing a V5- and a His-tag was produced as described (29). Conditioned medium enriched in wt-rADAMTS13 that was concentrated five-fold using an Amicon Ultra-15 centrifugal filter unit with a Ultracel-30K membrane (Millipore, Molsheim, France) and extensively dialysed against 50 mM Tris, pH 7.4 was used throughout the study. Bovine Serum Albumin (BSA) was obtained from Sigma-Aldrich (Saint-Quentin Fallavier, France).

Binding of wt-rADAMTS13 to VWF

pd-VWF (2 µg/ml) was adsorbed to microtitre wells. After blocking with BSA-containing buffer, immobilised VWF was incubated with supernatant containing wt-rADAMTS13 (3 µg/ml) supplemented with EDTA (10 mM) and Pefabloc (10 mM) for 3 hours (h) at 37°C. Bound wt-rADAMTS13 was probed using a peroxidase-labelled monoclonal anti-V5 tag antibody (Abcys, Paris, France) for 2 h at 37°C and detected via peroxidase-mediated hydrolysis of tetramethylbenzidine (TMB). VWF fragments (10 nM final concentration, unless indicated otherwise) or anti-VWF antibodies (0.1 mg/ml final concentration, unless indicated otherwise) were pre-incubated with wt-rADAMTS13 for 30 minutes (min) at room temperature before addition to VWF containing microtiter wells.

Vortex-based VWF degradation assay

Vortex-based degradation of VWF was essentially performed as described (30). Briefly, purified pd-VWF (30 µg/ml), wt-rADAMTS13 (3 µg/ml) and Pefabloc (2.5 mM; Sigma-Aldrich) were incubated in a volume of 40 µl and exposed to constant vortexing (2500 rpm; Vortex Genie 2T; VWR International) for the indicated

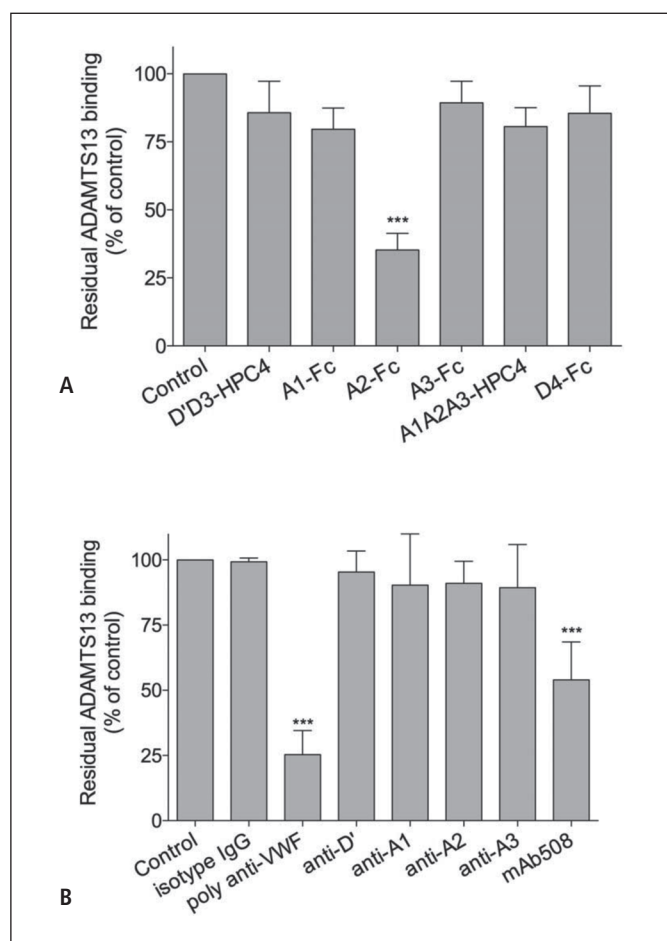


Figure 1: Screening for competitive inhibitors of VWF-ADAMTS13 binding. Candidate inhibitors were tested in an immuno-sorbent assay evaluating the binding of V5-tagged wt-rADAMTS13 (3 µg/ml) to immobilised pd-VWF (2 µg/ml) in the presence of EDTA (10 mM). A) Fc- or HPC4-tagged VWF fragments (10 nM) were incubated for 30 min at 37°C with wt-rADAMTS13 before addition to immobilised full-length VWF in microtitre wells for 3 h. Bound ADAMTS13 was probed using a peroxidase-labelled monoclonal anti-V5 tag antibody for 2 h at 37°C and detected via peroxidase-mediated hydrolysis of TMB. B) mAbs targeting VWF was evaluated for their effect on ADAMTS13 binding to VWF as described for panel A using polyclonal antibodies as negative (mouse IgG) and positive (rabbit anti-VWF IgG) controls (all antibodies were tested at a concentration of 0.1 mg/ml). Data represent the mean \pm SD of 3–5 experiments and are expressed as residual ADAMTS13 binding compared to incubation in the absence of VWF-fragments or antibodies for panel A and B, respectively. For panel B, data representing antibodies recognising different VWF domains (D', A1, A2, A3) are depicted. ***: $p < 0.0001$ as calculated via one-way ANOVA with Dunnett-multiple comparison test.

time. Where indicated, samples were supplemented with EDTA (10 mM), polyclonal goat anti-ADAMTS13 antibodies (50 µg/ml), A2-Fc (1 µg/ml) or mAb508 (0.1 mg/ml). VWF degradation was assessed via Western blot analysis, which was preceded by immuno-precipitation using anti-VWF antibodies where indicated. VWF was immuno-precipitated using rabbit polyclonal anti-VWF antibodies (50 µg/ml beads; Dako, Glostrup, Denmark) adsorbed onto Protein-G-coated magnetic beads (Dynabeads Protein G, Invitrogen, Saint Aubin, France) for 2 h at room temperature. After extensive washing in PBS/0.1 % Tween-20, immunoprecipitated VWF was released from the beads via a 5 min incubation at 100°C in 30 µl PBS/10 µl NuPAGE-LDS 4x sample buffer (Life Technologies, Saint Aubin, France) in the presence of 2 mM dithiothreitol. Samples were separated via discontinuous 4–12% SDS-page (Invitrogen) and transferred to an Immobilon P membrane (Millipore, Molsheim, France). The presence of VWF or degradation fragments was revealed via incubation with a pool of 10 distinct monoclonal antibodies recognising distinct epitopes of VWF (10 µg/ml). Bound antibodies were probed using peroxidase-labelled goat anti-mouse antibodies (dilution 1:500; Santa Cruz, Heidelberg, Germany) and visualised with SuperSignal West-Pico Enhanced Chemiluminescence Substrate (Thermo-Fischer Scientific, Villebon-sur-Yvette, France). Blots were analysed via ImageJ 1.44 software (<http://rsbweb.nih.gov/ij/index.html>) in order to quantify increase in VWF degradation products (represented by the presence of 140 kDa and 176 kDa bands) relative to untreated VWF.

Antibody binding to synthetic peptides

A series of nine highly purified (>95%) synthetic peptides overlapping various hydrophilic motifs of the D4 domain region 2140–2277 containing a N-terminal biotin tag were obtained from EZBiolab (Carmel, IN, USA). Peptides were solubilised in H₂O, eventually supplemented with one-sixth volume of 10% NH₄OH to improve solubility if necessary. Peptides were immobilised onto streptavidin-coated microtitre plates (SigmaScreen Streptavidin High Capacity, Sigma-Aldrich) at a concentration of 50 µg/ml. Peptide-coated wells were incubated with mAb508 or mouse isotype IgG (5 µg/ml) in PBS containing 3% BSA. Bound antibody was probed using peroxidase-labelled polyclonal anti-mouse IgG and detected via peroxidase-mediated hydrolysis of TMB.

Bilayer interferometry-analysis

Equilibrium binding assays were performed via bilayer interferometry (BLI)-analysis using Octet-QK equipment (ForteBio, Reading, UK) essentially as described (26). Protein A-coated biosensors were incubated with mAb508 (0.5 mg/ml) in BLI-buffer (PBS / 2% BSA) for 7 min allowing saturation of the sensor. Biosensors were then incubated for 5 min in BLI-buffer to achieve stable baseline, and subsequently incubated with various concentrations of pd-VWF in BLI-buffer for 10 min. All incubations were performed at room temperature under continuous shaking (1000 rpm). Data were analysed using Octet Software version 4.0.

Ex vivo whole blood perfusion

The perfusion system consisted of a circulatory flowing pump device in which the HeartMateII® (Thoratec Corp., Pleasanton, CA, USA) was the pump. Two cylindrical tubings (1×2×3/32 xs; Sorin group Implant®) were used to connect the device. The inlet and outlet ducts of the HeartMateII® were connected with these two tubings to obtain a closed circuit, which further contained a sampling device. The distribution volume was approximately 250 ml. The system was filled with citrate-anticoagulated whole blood (Blood group O) provided by the local blood bank (Etablissement Français du Sang, Lille, France). Where indicated, blood was supplemented with EDTA (10 mM final concentration) or antibody mAb508 (0.5–50 µg/ml final concentration). The pump rotor was set at 9000 rpm, a speed that is normally applied upon patient use (31). Blood was sampled 5 min before onset of perfusion (T0) and 5, 30 and 180 min after onset of perfusion (T5, T30 and T180, respectively). Blood samples were analysed for multimeric profile via 1.4% SDS-agarose electrophoresis as described (18). Analysis of loss of HMW-multimers was measured and calculated as described (18).

Results

Selection of candidates inhibiting VWF-ADAMTS3 interactions

To select potential inhibitors of VWF proteolysis, we first tested candidate molecules in an immunosorbent assay assessing binding of ADAMTS13 to immobilised VWF in the presence of EDTA. In this assay, immobilised VWF is elongated and exposes its interactive sites for ADAMTS13, including those localised within the VWF A2 domain (8). Two distinct types of potential inhibitors were evaluated. First, the potential of several monomeric or dimeric VWF-derived fragments (C-terminally tagged with either the HPC4-recognition sequence or with Fc) to block VWF-ADAMTS13 interactions was tested (►Figure 1A). When analysed at a concentration of 10 nM, the majority of them (D'D3-HPC4, A1-Fc, A3-Fc, A1A2A3-HPC4 and D4-Fc) exhibited minor inhibition ($\leq 20\%$), whereas dimeric A2-Fc displayed substantial inhibition at this concentration ($65 \pm 6\%$; $n=5$; $p<0.001$). We next assessed a panel of murine monoclonal antibodies (0.1 mg/ml) directed either against VWF or ADAMTS13 (►Figure 1B). Control experiments showed that ADAMTS13 binding was markedly inhibited in the presence of polyclonal anti-VWF antibodies ($75 \pm 9\%$; $n=3$; $p<0.0001$), whereas binding was unaffected in the presence of control mouse IgG. None of our three monoclonal anti-ADAMTS13 antibodies proved inhibitory (data not shown). Among the 29 monoclonal anti-VWF antibodies tested, 18 mAbs were unable to inhibit VWF-ADAMTS13 interactions, whereas 10 antibodies displayed mild inhibition ($<15\%$). In ►Figure 1B, representative data for antibodies recognising different VWF domains (D', A1, A2, A3) are depicted. The strongest inhibitor was antibody mAb508, which reduced binding of ADAMTS13 to VWF by $46 \pm 14\%$ ($n=5$; $p<0.0001$). Taken to-

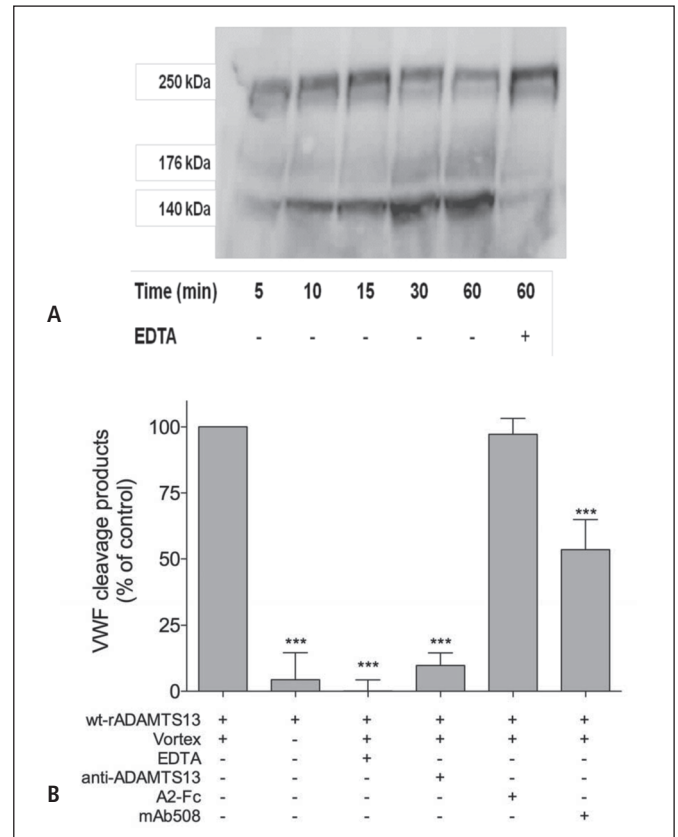


Figure 2: Functional evaluation of mAb508 and A2-Fc in a vortex-based degradation assay. A) pd-VWF (30 µg/ml), wt-rADAMTS13 (3 µg/ml) and Pefabloc (2.5 mM) were incubated in a volume of 40 µl and exposed to constant vortexing (Vortex Genie 2T; 2500 rpm) for different periods of time (5–60 min). As a control, a 60-min incubation under vortexing was performed in the presence of EDTA (10 mM). VWF degradation was assessed via Western blot analysis. Panel A represents a typical experiment showing time-dependent degradation of VWF. B) pd-VWF, wt-rADAMTS13 and Pefabloc were exposed to constant vortexing for 60 min as described under panel A in the absence or presence of one the following components: EDTA (10 mM), polyclonal anti-ADAMTS13 antibodies (50 µg/ml), A2-Fc (1 µg/ml) or mAb508 (0.1 mg/ml). VWF and ADAMTS13 were also incubated for 60 min in the absence of vortexing (no shear). VWF degradation was semi-quantified via integration of immuno-precipitated VWF degradation bands (140 & 176 kDa) using ImageJ software. Data represent mean \pm SD of four experiments and are expressed as percentage VWF degradation. Degradation after 60 min vortexing in the absence of additional components added was set at 100%. ***: $p<0.0001$ as calculated via one-way ANOVA with Dunnett-multiple comparison test.

gether, these data identify the A2-Fc fragment and antibody mAb508 as potential inhibitors of the VWF-ADAMTS13 interaction.

mAb508 reduces vortex shear stress-induced VWF proteolysis

Fluid shear stress plays a critical role in regulating ADAMTS13-mediated proteolytic cleavage of soluble VWF by ADAMTS13. Therefore, we tested the inhibitory effect of mAb508

(0.1 mg/ml) and A2-Fc (1 µg/ml), under conditions of increased shear stress, using a vortex-based degradation assay (30). VWF degradation was monitored using densitometric integration of VWF cleavage products (140 and 176 kDa) obtained after immunoprecipitation and western-blot analysis. In our experimental conditions, proteolytic cleavage of pd-VWF (30 µg/ml) by recombinant ADAMTS13 (3 µg/ml) increases as a function of incubation time, with maximal degradation obtained after 30 min (► Figure 2A). In subsequent experiments, we incubated for 60 min to ensure maximal degradation. Importantly, degradation of VWF by the metalloprotease ADAMTS13 was inhibited by the addition of

the chelator EDTA (10mM) or polyclonal goat anti-human ADAMTS13 antibodies (residual proteolysis <10% compared to control; ► Figure 2B). Furthermore, no VWF proteolysis was observed in the absence of shear stress. Unexpectedly, VWF proteolysis was unaffected (residual proteolysis 96 ± 5%; n=3) by the addition of A2-Fc (1 µg/ml), despite the notion that this fragment interferes with VWF-ADAMTS13 interactions under static conditions. In contrast, degradation of VWF was markedly reduced (residual proteolysis 52 ± 10% compared to control; n=4; p<0.0001) in the presence of mAb508 (0.1 mg/ml). This indicates that the monoclonal anti-VWF antibody mAb508 is able to partially

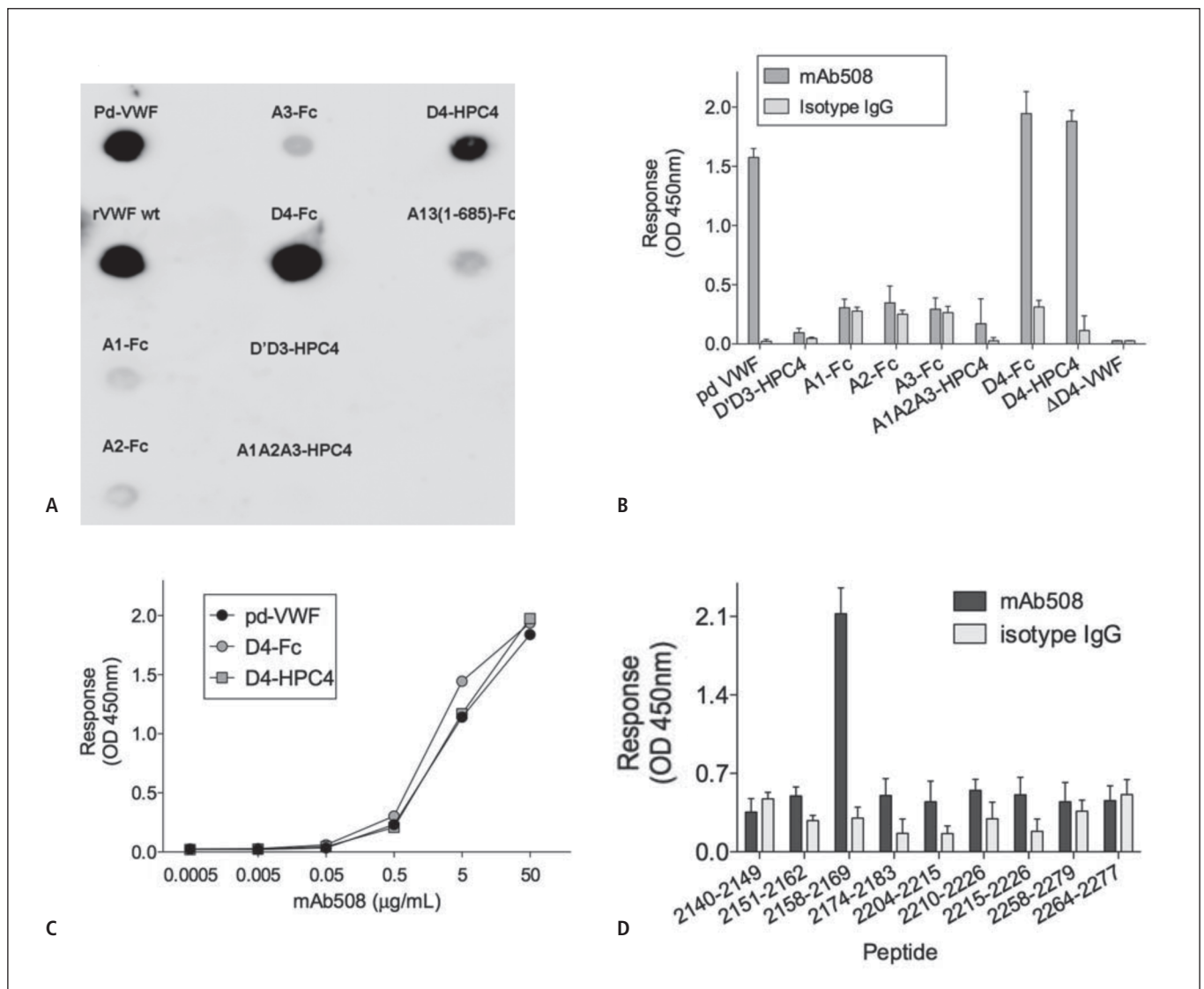


Figure 3: mAb508 interacts with D4 domain of VWF. A) Purified proteins (all 10 nM) were immobilised onto a blotting membrane and incubated with mAb508 (5 µg/ml) for 16 h at room temperature. Bound mAb508 was probed with peroxidase-labelled goat-anti-mouse antibodies and detected via luminal-based enhanced chemiluminescence. B and C) Purified proteins (10 nM) were immobilised onto microtitre wells for 16 h at 4°C. After washing, wells were incubated with mAb508 (B: 5 µg/ml; C: 0.5 ng/ml-50 µg/ml) or an isotype mouse IgG control (B: 5 µg/ml) for 1 h at 37°C. Bound anti-

bodies were probed using peroxidase-labelled polyclonal goat anti-mouse IgG antibodies and detected via peroxidase-mediated TMB hydrolysis. D) Biotinylated-peptides were immobilised onto streptavidin-coated microtitre wells and incubated with mAb508 or isotype mouse IgG (both 5 µg/ml). Bound antibodies were probed and detected as described for panels B and C. Data in panels B and D represent mean ± SD of 3–5 experiments. For panel C, data from a single experiment are shown.

interfere with ADAMTS13-mediated proteolysis under conditions of increased shear stress.

The epitope for mAb508 is located in the VWF D4 domain

To identify the epitope of mAb508, we first evaluated binding of the antibody to distinct VWF fragments in an immuno dot-blot assay, in which bound antibody was probed using peroxidase-conjugated polyclonal goat anti-mouse antibodies (► Figure 3A). As expected, mAb508 interacted with both r-VWF and pd-VWF that were used as positive controls. No signal was observed for HPC4-tagged constructs D'D3-HPC4 and A1A2A3-HPC4, whereas a weak signal was present for Fc-tagged variants A1-Fc, A2-Fc and A3-Fc. A similar weak signal was observed with a control Fc-fragment containing residues 1-685 of ADAMTS13, suggesting a minor cross-reaction of the anti-mouse IgG with human Fc fragments. Conversely, mAb508 strongly bound to two different fragments that contained the D4 sequence (VWF residues 1947-2301; ► Figure 3A), i.e. monomeric D4-HPC4 and dimeric D4-Fc. A similar specificity for VWF D4 domain was observed in an immuno-sorbent assay (► Figure 3B). Indeed, no binding was observed with VWF fragments lacking the D4 domain, including a D4 domain-deleted VWF variant. In contrast, a strong positive signal was observed for the binding of mAb508 to pd-VWF and both D4 fragments (► Figure 3B). Moreover, similar dose-response curves were observed for the binding of mAb508 to immobilised D4 fragments and pd-VWF, suggesting that the D4 domain contains the full epitope for mAb508 (► Figure 3C). In order to define the mAb508 epitope in the VWF D4 domain, we next tested binding of the antibody to VWF fragments obtained via proteolysis by *Staphylococcus aureus* V-8 protease, which cleaves within the D4 domain between residues 2133 and 2134 (32). mAb508 reacted exclusively with the SPII fragment (residues 2134-2813) but not with the SPIII fragment (764-2133) (data not shown), narrowing the antibody's epitope to the distal part of the D4 domain, i.e. residues 2134-2301. To obtain more detailed information on the epitope localisation, we used a series of nine biotinylated-peptides encompassing hydrophilic regions of the distal D4 domain. Using this approach, we observed that mAb508 bound to a single peptide covering residues 2158 to 2169 (► Figure 3D). In conclusion, the epitope of mAb508 appears to be located within the VWF D4 domain, a region previously found to be of relevance for the VWF-ADAMTS13 interaction (6, 8).

mAb508 is a partial inhibitor of VWF-ADAMTS13 interactions

To further characterise the mAb508-VWF interaction, the apparent binding affinity was determined. Interactions between mAb508 and globular full-length VWF were assessed via bio-layer interferometry analysis using Octet-QK-equipment. Increasing concentrations of purified pd-VWF (0 to 0.2 mg/ml) were incubated with mAb508 immobilised onto protein A-biosensor tips. A time- and dose-dependent association of pd-VWF to mAb508 was

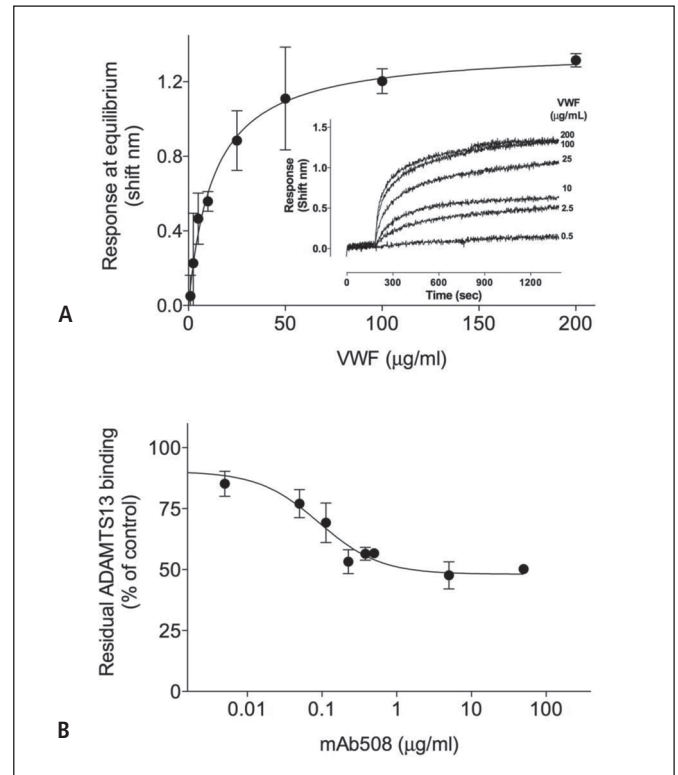


Figure 4: Biochemical analysis of VWF-mAb508 interaction. A) Protein A-coated biosensors were saturated with mAb508 (0.5 mg/ml) during a 7 min incubation using Octet-QK equipment. Subsequently, biosensors were incubated with various concentrations purified pd-VWF (0–0.2 mg/ml) and association of VWF was monitored real-time for a 10-min period until equilibrium was reached. Data represent mean \pm SD of four independent associations and depicted are the calculated responses (shift in nm) at equilibrium versus VWF concentration. The drawn line represents the best fit using a model describing the interaction of a single class of binding sites. Inset panel A: representative association curves of different concentrations of VWF. B) Binding of ADAMTS13 to immobilised VWF was performed as described for Figure 1 in the absence or presence of various concentrations mAb508 (0.05 ng/ml – 50 µg/ml). Data represent the mean \pm SD of four experiments and are expressed as % of residual ADAMTS13 binding compared to the absence of mAb508. Drawn line represents the best fit using a sigmoidal dose-response.

observed (► Figure 4A, inset). In order to calculate the apparent affinity, responses at equilibrium (B_{max}) were plotted versus VWF concentrations. Best fitting of the data was obtained using a model describing the interaction of a single class of binding sites (► Figure 4A), which revealed a $K_{D,app}$ of 13 ± 3 µg/ml (mean \pm SD), corresponding to 52 ± 11 nM based on VWF monomer concentrations. We next investigated the inhibitory potential of mAb508 for the VWF-ADAMTS13 interaction in a competitive VWF-ADAMTS13 inhibition binding assay. VWF was directly coated (2 µg/ml) into a microtitre plate and increasing concentrations of mAb508 (range: 0 to 50 µg/ml) were used as competitor of ADAMTS13 (4 µg/ml). A dose-dependent inhibition was observed (► Figure 4B). mAb508 inhibited the binding of soluble ADAMTS13 to immobilised VWF with an estimated IC_{50} of $0.09 \pm$

0.03 µg/ml. Maximal inhibition was obtained using 0.5 µg/ml of antibody and did not exceed 50% even when using antibody concentrations up to 50 µg/ml (► Figure 4B). In conclusion, mAb508 binds to VWF with moderate affinity, and its binding to VWF partially inhibits the interaction between VWF and ADAMTS13.

Mab508 leaves haemostatic potential of VWF unaffected

We next tested if mAb508 modulates VWF function, and two different tests were performed. First, VWF-ristocetin cofactor (VWF:RCo) activity was determined in the presence or absence of antibody mAb508 (50 µg/ml). A similar VWF:RCo activity was determined in the absence or presence of mAb508, when tested in plasma of three separate individuals ($72.7 \pm 7\%$ vs $71.0 \pm 10.6\%$, respectively). Second, the effect of Ab508 on the haemostatic activity using the whole-blood platelet function analyser (PFA)-100 was assessed. The closure time of this test is highly dependent on functional VWF. No differences in PFA-100 closure times were observed, irrespective whether collagen/epinephrine (Col/Epi) or collagen/ADP (Col/ADP) cartridges were used. Closure times were: Col/Epi: 139 ± 29 seconds [sec] vs 131 ± 72 sec & Col/ADP: 83 ± 9 vs 83 ± 4 sec in the absence and presence of mAb508, respectively. This data indicate that mAb508 leaves VWF function unaffected.

mAb508 reduces shear stress-induced VWF proteolysis under conditions of flow

To evaluate whether mAb508 could represent a potential tool to inhibit degradation of HMW-multimers in patients with VAD, we used an *ex vivo* perfusion system incorporating the circulatory support pump Heartmate II[®]. Perfusion of citrated whole blood

using this device results in a time-dependent loss of HMW-multimers (defined as >15 bands; ► Figure 5A), a phenomenon also observed in patients carrying this device (19). Densitometric analysis revealed a 50% loss of HMW-multimers was observed at 5 min after initiation of the perfusion, and a >95% loss of HMW-multimers occurred after 3 h of perfusion (► Figure 5A-D). In the presence of the chelator EDTA, HMW-multimers remained stable, with only a marginal loss ($7 \pm 3\%$) observed after 3 h of perfusion under pathological high shear stress (► Figure 5B). Using increasing concentrations of mAb508 (range: 0.5-50 µg/ml; n=3 for each concentration), a dose-dependent mAb-based inhibition of VWF proteolysis was observed at each of the time points analysed (► Figure 5A and B). Representative densitometric scans of multimer patterns at time points 0 and 3 h for the control and 3 h for mAb508 (0.5 and 10 µg/ml) are presented in ► Figure 5C and D. A similar extent of inhibition was observed for antibody concentrations of 10 and 50 µg/ml, indicating that maximal inhibition was achieved at 10 µg/ml. Importantly, inhibition was partial in both cases, as a 20% loss of HMW-multimers was detected after 3 h perfusion for each of these antibody concentrations (► Figure 5B), consistent with the partial inhibitory potential of mAb508 in the binding experiments. We considered the possibility that the kinetics of ADAMTS13-mediated VWF degradation or the action of mAb508 could be modulated by the use of citrate as an anticoagulant. Therefore, similar perfusion experiments were performed using blood that was heparin-anticoagulated (5.7 U unfractionated heparin/ml blood, corresponding to a dose of 400 U/kg body-weight assuming 70 ml blood/kg bodyweight). As presented in ► Figure 5E, the kinetics of VWF degradation in heparin-anticoagulated blood was similar to that in citrate-anticoagulated blood. In addition, Mab508 (10 µg/ml) inhibited VWF degradation to a similar extent in heparin- and citrate-anticoagulated blood, indicating that its mode of action is independent of the anticoagulant used. In conclusion, our findings describe the identification of antibody mAb508 as a partial inhibitor of ADAMTS13-mediated degradation of VWF, preventing excessive VWF proteolysis in whole blood under flowing conditions.

Figure 5: Evaluation of mAb508 on shear-induced VWF proteolysis in flowing blood. Citrated whole human blood (200 ml) was perfused in an *ex vivo* perfusion system incorporating a HeartMateII[®] pump. The pump rotor was set to 9000 rpm. Perfusions were performed in the absence (closed black circles) or presence of EDTA (10 mM; closed black squares) or various concentrations of mAb508 (0.5 µg/ml, grey circles; 2 µg/ml grey squares; 10 µg/ml, grey triangles up; 50 µg/ml, grey triangles down). Samples were taken 5 min before the onset of perfusion (T0) and after 5 min (T5), 30 min (T30) or 180 min (T180). Samples were subsequently tested for multimer patterns via 1.4% SDS-agarose electrophoresis and the presence of HMW-multimers (>15-mers) was determined. A) Representative multimer pattern of samples taken in the absence or presence of mAb508 (10 µg/ml). Normal plasma (NP) is added as reference. B) Presence of HMW-multimers (percentage of HMW-multimers compared to T0, which was set at 100%) as a function of time. C, D) Overlays obtained by densitometric scanning of VWF multimeric patterns showing the relative amount of HMW-multimers (>15 bands) at T180 vs T0. Presented patterns in the absence of mAb508 (T180) or in the presence of mAb508 (T180 and T180 & mAb508) either at 10 µg/ml (C) or 0.5 µg/ml (D). E) Representative multimer pattern of samples taken during perfusion of heparin-anticoagulated blood (5.7 U unfractionated heparin/ml blood) in the absence or presence of mAb508 (10 µg/ml). Normal plasma (NP) is added as reference.

Discussion

Bleeding secondary to increased VWF degradation is currently the leading complication in patients undergoing left ventricular assist device (LVAD) support (33) and points to an emerging medical need for a treatment preventing proteolysis of VWF. The most likely candidate responsible for shear stress-induced VWF degradation is ADAMTS13, although a contribution of other proteases cannot be fully excluded (34). Given that a lack of ADAMTS13 activity is associated with TTP, it is further important to consider that blocking VWF proteolysis should be incomplete in order to avoid TTP-like complications. In search for proteolysis inhibitors, we evaluated distinct candidates aiming to disrupt binding of ADAMTS13 to the VWF A2 or D4 domain, two interactive sites necessary to allow VWF proteolysis (6). Among these candidates, one mAb targeting the VWF D4 domain was identified to com-

bine the desired properties of a potential therapeutic candidate, as it partially inhibited VWF-ADAMTS13 binding and reduced but not fully inhibited loss of HMW multimers under conditions of high shear stress.

As expected, our screening of inhibitors of ADAMTS13-mediated proteolysis revealed that a recombinant A2-Fc variant was efficient in interfering with VWF-ADAMTS13 binding, achieving 65% inhibition while a two-fold molar excess of ADAMTS13 over A2-Fc was present (► Figure 1). This inhibitory action fits with the localisation of the Tyr1605-Met1606 scissile bond and additional interactive sites within the VWF A2-domain. The exposure of these A2-domain interactive sites is shear stress-dependent for full-length VWF, but appears to be constitutive for the tested A2-Fc fragment. However, A2-Fc (used at a concentration of 1 µg/ml, corresponding to 10 nM) was unable to prevent VWF degradation under conditions of increased shear stress, suggesting that the scissile bond within the A2-Fc fragment is rapidly cleaved under these conditions thereby reducing the inhibitory potential of this fragment (► Figure 2). Indeed, it has previously been reported that peptides overlapping the C-terminal part of VWF A2 domain interfere with VWF proteolysis at micromolar concentrations, indicating that such fragments are relatively weak inhibitors (35). Additional experiments would therefore be needed to test the inhibitory effect of A2-Fc at higher concentrations. An alternative approach could be to block A2 domain-ADAMTS13 interactions using anti-A2 domain antibodies, as was described elsewhere (36) or antibodies targeting ADAMTS13 epitopes that overlap the A2-interactive site, including the ADAMTS13 spacer domain. However, this ADAMTS13 spacer domain contains the core antigenic epitope of anti-ADAMTS13 auto-antibodies known to be associated with acquired autoimmune TTP (37, 38). Hence, such approach might be associated with an increased risk of drug-induced TTP.

Besides the VWF A2 domain, the VWF D4 domain is also an attractive target to block ADAMTS13-mediated proteolysis. Indeed, the VWF D4 domain contains an exosite accessible on globular VWF, mediating the initial step in the association be-

tween VWF and ADAMTS13 (8, 9). However, opposite to the A2-Fc fragment, no inhibition of VWF-ADAMTS13 binding was observed using a D4-Fc fragment (► Figure 1). We considered the possibility that D4-Fc was folded incorrectly. However, D4-Fc displayed similar binding as full-length VWF to three distinct anti VWF D4-domain Abs (► Figure 3 & data not shown), indicating that its folding was within the normal range. More likely, D4-Fc is simply inefficient in its interaction with ADAMTS13. This possibility is consistent with the low affinity ($K_{D,app} = 0.7 \mu\text{M}$) that was previously reported for the interaction between the isolated VWF D4 domain and ADAMTS13 (8).

Unlike the D4-Fc fragment, binding was efficiently inhibited in the presence of a murine mAb directed against VWF D4 domain (designated as mAb508). The epitope for mAb508 is localised between residues 2134 and 2301 and seems to involve the sequence 2158-2169 (► Figure 3). mAb508 binds the VWF D4 domain with a moderate affinity ($K_{D,app} = 52 \text{ nM}$; ► Figure 4A). This value should be considered as an estimate in view of the multimeric structure of VWF and the dimeric nature of the mAb, which complicate an accurate assessment of the true affinity constant. Despite its moderate affinity, mAb508 was particularly efficient to block VWF-ADAMTS13 binding under the conditions employed. Additional experiments are needed to reveal the nature of the inhibitory mechanism, whether inhibition is allosteric or involves direct competition for overlapping binding sites.

In order to assess the clinical potency of the use of anti-D4 domain antibodies to prevent excessive VWF degradation under LVAD support, we implemented a novel LVAD-perfusion model (► Figure 5). This model faithfully mimics the clinical setting, since all experiments are performed in citrated whole blood in the presence of physiological concentrations of VWF and ADAMTS13. Furthermore, unlike vortex-based degradation assays (30), there is no volume limitation allowing more flexibility with regard to spiking experiments with inhibitors and allowing time-course studies with several blood samplings. Using this LVAD-based perfusion model, a dose-dependent inhibition of HMW-multimer degradation was obtained with mAb508, consistent with the marked inhibition obtained in the vortex-based degradation assay (► Figure 2 and ► Figure 5). Antibody mAb508 shares its specificity for the D4 domain with antibody RU8, which was recently reported to interfere with ADAMTS13-mediated degradation of VWF in a vortex-based degradation assay (8). However, degradation of HMW-multimers was fully repressed in the presence of 25 µg/ml of antibody RU8, whereas residual VWF proteolysis was still detectable at mAb508 concentrations of 45 µg/ml, indicating fundamental differences in their mode of action. The inability of mAb508 to fully inhibit VWF proteolysis, even in the presence of a vast molar excess, not only fits the requirement for partial inhibition in order to avoid TTP-like symptoms, but also allows for a wide therapeutic window.

In conclusion, we provide an *ex vivo* proof-of-concept for an antibody-based therapy for the treatment of VWF degradation induced by circulatory assist devices. Such antibody-based treatment could be of benefit not only in VAD, but also in other pathologies characterised by increased VWF proteolysis like aortic stenosis or

What is known about this topic?

- It is known that patients carrying circulatory assist devices have an increased risk of bleeding due to dysfunctional VWF.
- These devices induce high shear stress-conditions, favouring ADAMTS13-mediated degradation of VWF.

What does this paper add?

- We describe monoclonal anti-VWF antibody mAb508, which is directed against the VWF D4-domain.
- mAb508 prevents excessive VWF degradation in a HeartMatell whole blood-perfusion model.
- Our results may provide the basis for an antibody-based therapy to prevent VWF-dependent bleeding episodes in patients carrying circulatory assist devices.

hypertrophic obstructive cardiomyopathy complicated by Heyde syndrome (18, 39), VWD-type 2A (40), essential thrombocytemia (41) or extracorporeal membrane oxygenation support (42). Additional studies including humanisation of mAb508 and extensive pre-clinical studies to evaluate the *in vivo* efficacy and safety of this approach are warranted to further assess its therapeutic potential. One issue that requires particular attention concerns the combination of this antibody-based approach in combination with the anticoagulant used by the patient. Often, patients carrying LVADs are given vitamin K-antagonists and/or heparin (rather than direct thrombin- or factor Xa-inhibitors). Combining anti-VWF antibodies with these anticoagulants could potentially increase the bleeding risk in these patients. However, our analyses demonstrated that antibody mAb508 leaves VWF function unaffected (as determined in VWF:RCO and PFA-100 assays). Moreover, the action of mAb508 was independent of the anticoagulant used, suggesting that the antibody could be used in combination with current anticoagulants without increasing the bleeding risk.

Conflicts of interest

None declared.

References

- Zhou YF, et al. Sequence and structure relationships within von Willebrand factor. *Blood* 2012; 120: 449-458.
- Sadler JE. von Willebrand factor assembly and secretion. *J Thromb Haemost* 2009; 7 (Suppl 1): 24-27.
- Valentijn KM, et al. Functional architecture of Weibel-Palade bodies. *Blood* 2011; 117: 5033-5043.
- Groot E, et al. The active conformation of von Willebrand factor in patients with thrombotic thrombocytopenic purpura in remission. *J Thromb Haemost* 2009; 7: 962-969.
- De Ceunynck K, et al. Unwinding the von Willebrand factor strings puzzle. *Blood* 2013; 121: 270-277.
- Crawley JT, et al. Unraveling the scissile bond: how ADAMTS13 recognizes and cleaves von Willebrand factor. *Blood* 2011; 118: 3212-3221.
- Gao W, et al. Exosite interactions contribute to tension-induced cleavage of von Willebrand factor by the antithrombotic ADAMTS13 metalloprotease. *Proc Natl Acad Sci USA* 2006; 103: 19099-19104.
- Zanardelli S, et al. A novel binding site for ADAMTS13 constitutively exposed on the surface of globular VWF. *Blood* 2009; 114: 2819-2828.
- Feys HB, et al. Multi-step binding of ADAMTS-13 to von Willebrand factor. *J Thromb Haemost* 2009; 7: 2088-2095.
- Xiang Y, et al. Mechanism of von Willebrand factor scissile bond cleavage by a disintegrin and metalloproteinase with a thrombospondin type 1 motif, member 13 (ADAMTS13). *Proc Natl Acad Sci USA* 2011; 108: 11602-11607.
- Tsai HM. von Willebrand factor, shear stress, and ADAMTS13 in haemostasis and thrombosis. *ASAIO J* 2012; 58: 163-169.
- Dong JF, et al. ADAMTS-13 rapidly cleaves newly secreted ultralarge von Willebrand factor multimers on the endothelial surface under flowing conditions. *Blood* 2002; 100: 4033-4039.
- De Ceunynck K, et al. Local elongation of endothelial cell-anchored von Willebrand factor strings precedes ADAMTS13 protein-mediated proteolysis. *J Biol Chem* 2011; 286: 36361-36367.
- Shim K, et al. Platelet-VWF complexes are preferred substrates of ADAMTS13 under fluid shear stress. *Blood* 2008; 111: 651-657.
- Levy GG, et al. Mutations in a member of the ADAMTS gene family cause thrombotic thrombocytopenic purpura. *Nature* 2001; 413: 488-494.
- Sadler JE, et al. Update on the pathophysiology and classification of von Willebrand disease: a report of the Subcommittee on von Willebrand Factor. *J Thromb Haemost* 2006; 4: 2103-2114.
- Warkentin TE, et al. Aortic stenosis and bleeding gastrointestinal angiodysplasia: is acquired von Willebrand's disease the link? *Lancet* 1992; 340: 35-37.
- Vincentelli A, et al. Acquired von Willebrand syndrome in aortic stenosis. *N Engl J Med* 2003; 349: 343-349.
- Geisen U, et al. Non-surgical bleeding in patients with ventricular assist devices could be explained by acquired von Willebrand disease. *Eur J Cardiothorac Surg* 2008; 33: 679-684.
- Uriel N, et al. Acquired von Willebrand syndrome after continuous-flow mechanical device support contributes to a high prevalence of bleeding during long-term support and at the time of transplantation. *J Am Coll Cardiol* 2010; 56: 1207-1213.
- Crow S, et al. Gastrointestinal bleeding rates in recipients of nonpulsatile and pulsatile left ventricular assist devices. *J Thorac Cardiovasc Surg* 2009; 137: 208-215.
- Pareti FI, et al. Proteolysis of von Willebrand factor and shear stress-induced platelet aggregation in patients with aortic valve stenosis. *Circulation* 2000; 102: 1290-1295.
- Meyer AL, et al. Acquired von Willebrand syndrome in patients with an axial flow left ventricular assist device. *Circ Heart Fail* 2010; 3: 675-681.
- Thompson JL, 3rd, et al. Risk of recurrent gastrointestinal bleeding after aortic valve replacement in patients with Heyde syndrome. *J Thorac Cardiovasc Surg* 2012; 144: 112-116.
- Lenting PJ, et al. An experimental model to study the *in vivo* survival of von Willebrand factor. Basic aspects and application to the R1205H mutation. *J Biol Chem* 2004; 279: 12102-12109.
- Pegon JN, et al. Factor VIII and von Willebrand factor are ligands for the carbohydrate-receptor Siglec-5. *Haematologica* 2012; 97: 1855-1863.
- Meyer D, et al. Hybridoma antibodies to human von Willebrand factor. I. Characterisation of seven clones. *Br J Haematol* 1984; 57: 597-608.
- Meyer D, et al. Hybridoma antibodies to human von Willebrand factor. II. Relative role of intramolecular loci in mediation of platelet adhesion to the sub-endothelium. *Br J Haematol* 1984; 57: 609-620.
- Rayes J, et al. Effect of von Willebrand disease type 2B and type 2M mutations on the susceptibility of von Willebrand factor to ADAMTS-13. *J Thromb Haemost* 2007; 5: 321-328.
- Han Y, et al. A shear-based assay for assessing plasma ADAMTS13 activity and inhibitors in patients with thrombotic thrombocytopenic purpura. *Transfusion* 2011; 51: 1580-1591.
- Frazier OH, et al. First clinical use of the redesigned HeartMate II left ventricular assist system in the United States: a case report. *Tex Heart Inst J* 2004; 31: 157-159.
- Layet S, et al. Evidence that a secondary binding and protecting site for factor VIII on von Willebrand factor is highly unlikely. *Biochem J* 1992; 282: 129-137.
- Eckman PM, John R. Bleeding and thrombosis in patients with continuous-flow ventricular assist devices. *Circulation* 2012; 125: 3038-3047.
- Lancellotti S, et al. Proteolytic Processing of Von Willebrand Factor by Adamts13 and Leukocyte Proteases. *Mediterr J Hematol Infect Dis* 2013; 5: e2013058.
- Wu JJ, et al. Characterisation of a core binding site for ADAMTS-13 in the A2 domain of von Willebrand factor. *Proc Natl Acad Sci USA* 2006; 103: 18470-18474.
- Zhang J, et al. A conformation-sensitive monoclonal antibody against the A2 domain of von Willebrand factor reduces its proteolysis by ADAMTS13. *PLoS One* 2011; 6: e22157.
- Klaus C, et al. Epitope mapping of ADAMTS13 autoantibodies in acquired thrombotic thrombocytopenic purpura. *Blood* 2004; 103: 4514-4519.
- Luken BM, et al. The spacer domain of ADAMTS13 contains a major binding site for antibodies in patients with thrombotic thrombocytopenic purpura. *Thromb Haemost* 2005; 93: 267-274.
- Blackshear JL, et al. Hypertrophic obstructive cardiomyopathy, bleeding history, and acquired von Willebrand syndrome: response to septal myectomy. *Mayo Clin Proc* 2011; 86: 219-224.
- Favaloro EJ, et al. Different bleeding risk in type 2A and 2M von Willebrand disease: a 2-year prospective study in 107 patients: a rebuttal. *J Thromb Haemost* 2012; 10: 1455-1458.
- Rolf N, et al. Essential thrombocythaemia in a teenage girl resulting in acquired von Willebrand syndrome with joint haemorrhage and menorrhagia. *Thromb Haemost* 2010; 103: 1272-1274.
- Heilmann C, et al. Acquired von Willebrand syndrome in patients with extracorporeal life support (ECLS). *Intensive Care Med* 2012; 38: 62-68.